

LEEB HARDNESS TEST FOR ROCK JOINT WALL COMPRESSIVE STRENGTH
EVALUATION

by

Brock Jeans

Submitted in partial fulfilment of the requirements
for the degree of Master of Applied Science

at

Dalhousie University

Halifax, Nova Scotia

July 2021

© Copyright by Brock Jeans, 2021

TABLE OF CONTENTS

LIST OF TABLES v

LIST OF FIGURES vi

1 INTRODUCTION 1

 1.1 BACKGROUND 1

 1.2 AIM AND OBJECTIVES..... 4

 1.3 ASSUMPTIONS AND LIMITATIONS 7

 1.4 STRUCTURE OF THE THESIS..... 8

2 LITERATURE REVIEW 9

 2.1 ROCK DISCONTINUITY SHEAR STRENGTH 9

 2.1.1 EARLY DEVELOPMENTS MADE IN THE FIELD OF ROCK
 MECHANICS 9

 2.1.2 DEVELOPMENT OF PARAMETERS 11

 2.2 ROCK WALL MATERIAL RESEARCH USING CONVENTIONAL
 METHODS 19

 2.2.1 METHODS USED TO FIND JCS..... 20

 2.2.2 QUANTIFICATION OF WEATHERING..... 24

 2.3 THE VIABILITY OF THE LEEB DEVICE ON ROCK 25

 2.3.1 INTRODUCTION TO THE LEEB DEVICE FOR USE ON ROCK 28

 2.3.2 EVOLUTIONAL TIMELINE OF THE LEEB DEVICE IN ROCK
 ENGINEERING 33

3 RESEARCH METHODOLOGY 61

 3.1 LABORATORY WORK 63

 3.1.1 ARTIFICIAL MATERIAL AND ROCK..... 64

 3.1.1.1 STEADY STATE CURING BEHAVIOUR SPECIMENS 67

 3.1.1.2 ARITIFICAL COMPOSITE SPECIMENS 70

3.1.1.3	TESTING – ARTIFICIAL MATERIAL STRENGTH.....	74
3.1.1.4	HARDNESS TESTING	74
3.1.2	NATURAL ROCK OF DIFFERING ROCK PROPERTIES.....	76
3.1.2.1	COLLECTION OF NATURAL ROCK SAMPLES.....	77
3.1.2.2	SPECIMEN PREPARATION - BLOCKS.....	82
3.1.2.3	SPECIMEN PREPARATION – CYLINDRICAL CORES.....	91
3.1.2.4	TESTING.....	94
4	RESULTS	100
4.1	ARTIFICIAL MATERIAL SPECIMENS.....	100
4.1.1	STEADY STATE CURING AGE.....	101
4.1.2	SS SPECIMENS	102
4.1.3	SH SPECIMENS	107
4.2	NATURAL ROCK TRANSITION SPECIMENS	111
4.2.1	SS SPECIMENS	114
4.2.2	SH SPECIMENS	116
4.2.3	UM SPECIMENS	117
4.3	WEATHERED/ ALTERED ROCK SPECIMENS	120
4.4	NUMERICAL MODELING	122
4.5	SURFACE TREATMENT EVALUATION	128
4.6	JRC AND JCS PREDICTIONS.....	131
4.6.1	JRC DETERMINATION.....	132
4.6.2	JCS DETERMINATION	139
5	CONCLUSION.....	145
	REFERENCES	148
	APPENDIX A – ARTIFICIAL MATERIAL SPECIMEN DATA PART 1	151

APPENDIX B – ARTIFICIAL MATERIAL SPECIMEN DATA PART 2	159
APPENDIX C - HARDNESS VS DEPTH: NATURAL ROCK DATA PART 1	170
APPENDIX D - HARDNESS VS DEPTH: NATURAL ROCK DATA PART 2.....	177
APPENDIX E – JRC SURVEY	209

LIST OF TABLES

Table 2-1: Summary of physical properties of Plaster of Paris specimens (Patton, 1966).....	12
Table 2-2: Predictions of classes and descriptions and their corresponding peak shear strength criterion (Barton, 1973b).	15
Table 2-3: Estimated reductions in density for various degrees of relative alteration (Barton and Choubey, 1977).....	22
Table 2-4: Manual index test criteria (ISRM, 1978).	23
Table 2-5: Suggested methods for the quantitative description of discontinuities (ISRM, 1978).....	24
Table 2-6: Weathering grade of rock material (ISRM, 1978).	25
Table 2-7: Statistical summary based on 100 impacts per rock type (Corkum et al., 2018).....	44
Table 2-8: Standard error, coefficient of determination and fitting parameters for power function (Corkum et al., 2018).	47
Table 2-9: ISRM R Grades and corresponding ranges of σ_c and LD predicted from correlation curves from Eq. 16 and Table 2-8 (Corkum et al., 2018).	48
Table 2-10: Summary information on the four sandstone types (modified from Desarnaud et al., 2019).	49
Table 2-11: Digitized data from Figure 2-22b and Figure 2-22c for type D probe (after Desarnaud et al., 2019).....	57
Table 3-1: Artificial mix designs to produce the rock categories of R0, R1, and R2 described in Table 2-4 which shows a table reproduced from the ISRM Suggested Methods (1978).	67
Table 4-1: Table showing JRC survey results showing min, max, median, and standard deviation for both the X- and Y-direction profiles. The mean of the combined X- and Y-direction results is shown on the far right.	135
Table 4-2: The difference in standard deviation found in the hardness data received on the natural surface in comparison to the average standard deviation found in the subsequent, secondary material surfaces for that specimen.	138

LIST OF FIGURES

Figure 2-1: Failure envelopes for specimens with irregular surfaces (reproduced from Patton, 1966).....	13
Figure 2-2: Roughness profiles showing the typical range of JRC values (reproduced from Barton and Choubey, 1977)	18
Figure 2-3: Non-linear shear strength envelope based on a range of JCS values as a percentage of σ_c ($\sigma_c = 50 \text{ MPa}$, $\phi_r = 25^\circ$).....	20
Figure 2-4: Rock strength chart based on Schmidt hardness (Deere and Miller, 1966).....	21
Figure 2-5: Measurement ranges of cone penetrometer (model YH62, Yamanaka, Tokyo), needle-type penetrometer (model SH-70, Maruto, Tokyo), Schmidt hammer, and the Equotip hardness tester (Modified after Aoki and Matsukura, 2007).....	26
Figure 2-6: Relationship (a) between R_{max} - and R_s -values and (b) between L_{max} - and L_s -values (From Aoki and Matsukura, 2007).	27
Figure 2-7: TIME 5100 (Leeb) hardness tester used in this research program with labelled features (Modified from TIME Group Inc., n.d.).....	29
Figure 2-8: First three level of prompts in the Leeb hardness tester (reproduced from TIME Group Inc., n.d.).....	30
Figure 2-9: Hardness values on weathered sandstone and limestone walls ground down progressively to fresh rock (Modified from Hack et al., 1993).	34
Figure 2-10: Unconfined Compressive Strength against Equotip values: + artificial; \circ clastic limestone; \square crystalline; and Δ sandstone. (Verwaal and Mulder, 1993).	35
Figure 2-11: 'UCS' (MPa) plotted against k-value (Aoki and Matsukura, 2008)..	40
Figure 2-12: 'UCS' (MPa) plotted against L_s (Aoki and Matsukura, 2008).....	41
Figure 2-13: 'UCS' (MPa) plotted against porosity (%) for three rebound-value ranges (Aoki and Matsukura, 2008).....	42
Figure 2-14: Measured 'UCS' (MPa) against Calculated 'UCS' (MPa) found with Eq. 15 (Aoki and Matsukuri, 2008).	42

Figure 2-15: Accuracy gain associated with increased number of impacts (Corkum et al., 2018).....	44
Figure 2-16: Specimen size effects on <i>LD</i> found with TM12 approach (Corkum et al., 2018).....	46
Figure 2-17: Entire database plotted by rock type category with correlation curves corresponding to Eq. 16 with Table 2-8 coefficients (Corkum et al., 2018).....	47
Figure 2-18: Hardness for different thicknesses with both C and D probes (Desarnaud et al., 2019).....	51
Figure 2-19: Hardness versus volume – specimens stored at $48 \pm 2\%$ RH and $20 \pm 2^\circ\text{C}$ (Desarnaud et al., 2019).....	51
Figure 2-20: Hardness of the four sandstone types at different moisture conditions (Desarnaud et al., 2019).....	52
Figure 2-21: Hardness against surface roughness (<i>Sz</i>) found with type D probe (Desarnaud et al., 2019).....	54
Figure 2-22: Hardness and deformation after 1, 5, 10, 15, and 20 repeated impacts with the probe type C (a) and type D (b) on OH, LB, SM, and PS. (c) Deformation (depth of indentation) against 'UCS' (Desarnaud et al., 2019).....	55
Figure 2-23: 3D microscope representations of 1, 10, and 20 probe type D impacts for (A) SM and (B) PS. The vertical scale bars show the variation in heights in μm (Desarnaud et al., 2019).....	56
Figure 2-24: 3D microscope representations of 1, 10, and 20 probe type C impacts for (A) SM and (B) PS. The vertical scale bars show the variation in heights in μm (Desarnaud et al., 2019).....	56
Figure 2-25: 'UCS' (MPa) versus hardness x density for probe type D and type C on all eight sandstone types. Results of SIM are shown in the left illustration while results of RIM are shown in the right (Desarnaud et al., 2019).	58
Figure 2-26: Hardness on all 8 sandstone types of varying porosities using SIM and RIM and both probes (Desarnaud et al., 2019).	59

Figure 3-1: Three categories of specimens created in the laboratory: a) artificial composite material (plaster and rock), b) natural rock with a clear primary and secondary material interface, and c) naturally weathered rock (gradient).	64
Figure 3-2: Objects used to create artificial material UCS specimens. From left to right: stainless steel dual specimen cast, cured artificial material specimen, and a thin sandstone disk.....	68
Figure 3-3: Two artificial specimens made to ISRM, 1978 standards for UCS testing.....	70
Figure 3-4: Interactive sample collection map (Google, 2021).	80
Figure 3-5: Photo showing the assigned front of Sample 1 together with a 10 cm scale bar.	81
Figure 3-6: Example of boulders with two different procedures for block extraction: a) Category 1: blocks can only be taken from one side of the secondary rock; b) Category 2: blocks can be taken from both sides of the secondary rock.	83
Figure 3-7: Paper template showing the dimensions of the surface of a cube with 50 mm side length positioned on the secondary rock surface of a boulder.	84
Figure 3-8: Cut line displaying arrow indicating the final dimension of the cut-off piece is to be taken to edge of the line indicated with a black arrow. Photo shows a boulder fastened in the cutting machine vise with the cut line aligned with the cutting wheel and the guide marks aligned with the edges of the upright vise components.....	86
Figure 3-9: First vertical cut made perpendicular to the primary rock specimen bottom and secondary to primary rock contact line.	90
Figure 3-10: Photo of vise secured to drill platform with two clamps.	93
Figure 3-11: Three rock type transition block specimens aligned in the v-notch block on the grinder. On all specimens, the Leeb strikes can be seen on the visible face (method 1, Section 3.1.2.4) as well as the marked line aligned with the top of the v-notch block.	97

Figure 4-1: Steady state curing behaviour of the 3:1 mix.	101
Figure 4-2: Steady state curing behaviour of the 3:2 mix.	102
Figure 4-3: TM20 hardness versus secondary material thickness found on the artificial SS specimens using the first testing methodology (specimens with no secondary material thickness reduction) identified in Section 3.1.1.4.....	104
Figure 4-4: TM20 hardness versus secondary material thickness found on the artificial SS specimens using the second testing methodology (specimens with secondary material thickness reduction) identified in Section 3.1.1.4.....	106
Figure 4-5: TM20 hardness versus secondary material thickness found on the artificial SH specimens using the first testing methodology (specimens with no secondary material thickness reduction) identified in Section 3.1.1.4.....	108
Figure 4-6: TM20 hardness versus secondary material thickness found on the artificial SH specimens using the second testing methodology (specimens with secondary material thickness reduction) identified in Section 3.1.1.4.....	110
Figure 4-7: Geology classification, extraction location, image, and hardness results for two of the six natural rock transition SS specimens.	114
Figure 4-8: Geology classification, extraction location, image, and hardness results for one of two natural rock transition SH specimens.	116
Figure 4-9: Geology classification, extraction location, image, and hardness results for three of five natural rock transition UM specimens.	117
Figure 4-10: Geology classification, extraction location, image, and hardness results for four of the 14 weathered natural rock specimens.	121
Figure 4-11: Axisymmetric model of a tungsten carbide (Leeb) ball on the surface of a sandstone produced using RS2 by Rocscience.....	124
Figure 4-12: Influence zone depth into sandstone beneath the impact location of the Leeb device using the finite element code RS2.	127

Figure 4-13: Surface treatment evaluation on Wallace Sandstone cylinder surfaces saw cut and ground.....	130
Figure 4-14: JRC evaluation survey results for all of the specimens tested in this study.	133
Figure 4-15: JRC value plotted against standard deviation increase.....	139
Figure 4-16: Simple linear regression of the representative LD values in the weathered gradient. The value found on the natural surface was influenced by roughness and resulted in a larger standard deviation and lower TM20 value. A more representative <i>LDS</i> value could be 642 rather than 563. Data was produced on Specimen 39 Block 1: The Box and Whisker plot and data can be seen in Appendix C and D.	142
Figure 4-17: A dual axis chart showing box and whisker plots for the TM20 data found on each surface of Specimen 61 Block 1. The <i>LD</i> results, displayed via the right axis is the upper plot while the <i>JCSLD</i> results, displayed via the left axis is the lower plot.	143

ABSTRACT

The Joint Wall Compressive Strength (JCS) parameter introduced by Nick Barton significantly influences predictions of rock discontinuity shear strength but current methods in obtaining this parameter are insufficient. A correlation equation for laboratory prepared intact rock specimens of sufficient size produced by Corkum et al. in 2018 has the capability of predicting the JCS value from a hardness value obtained with the Leeb hardness device. This device has the sensitivity required to predict the hardness of a weathered rock joint wall which makes it the ideal tool for this function. However, the methodology for application on rock surfaces of various conditions required consideration and study. To understand the validity of the strength value predicted, a thorough examination of what the hardness readings consist of was considered as being of paramount importance. This study examines the effects of roughness, the effects from the surface preparation method used, and the size and the associated effects of the zone beneath the impact that influences the hardness readings (influence zone). Moreover, methods are developed and presented to determine a representative hardness value exempt of these effects to consist solely of the hardness of the tested material. An example is presented of how to predict the JCS value using this representative surface hardness value. Using a grinding/ hardness testing technique employed by Hack et al. in 1993, roughness effects were identified through evaluation of the difference in standard deviation between the natural surface and the additional surfaces tested. It was also observed that hardness testing results depend on how the surface was prepared and on the moisture conditions of the tested surface. Finally, it was found that an influence zone 1.7 mm thick exists below the impacted surface for the Leeb hardness device.

LIST OF ABBREVIATIONS AND SYMBOLS USED

This list includes the key abbreviations and symbols seen in the forthcoming thesis. Because there are numerous abbreviations and symbols associated with the literature review section (the work of others), this list is not entirely comprehensive. All abbreviations and symbols are introduced and explained within the text.

UCS	Unconfined compressive strength (test name)
'UCS'	Unconfined compressive strength not conforming to ISRM or ASTM standards (quotations indicate non-conformance)
σ_c	Unconfined compressive strength (peak stress)
HL	A single Leeb hardness value
VB	Rebound velocity
VA	Impact velocity
GSI	Geological Strength Index
JCS	Joint wall compressive strength
JRC	Joint roughness coefficient
$MeanL_D$	The mean of the L_D values found in the secondary material of a rock specimen exempt of the natural surface if deemed too rough
L_D	Hardness value chosen to represent surface, obtained with a type D Leeb device
L_{DS}	Hardness value deemed representative of a natural surface for correlation with JCS. The 'S' is a denotation for 'secondary material'
L_{DP}	Hardness value deemed representative of the unweathered, intact rock for correlation with σ_c . The 'P' is a denotation for 'primary material'
JCS_{LD}	Joint wall compressive strength derived from L_{DS}
σ_{CLD}	Unconfined compressive strength derived from L_{DP}
SD	Standard deviation
TM20	20-impact trimmed mean
NX Size	54 mm diameter rock core
α	Fitting parameter
β	Fitting parameter

ACKNOWLEDGEMENTS

I would like to acknowledge Dr. Andrew Corkum, my thesis supervisor and mentor for my graduate studies at Dalhousie University for his efforts in helping me complete this achievement. I feel fortunate for his guidance in the completion of this thesis, and for providing me with many valuable skills that I will take with me, from writing to tunneling and everything in between.

I would also like to acknowledge the Swedish Nuclear Fuel and Waste Management Co (SKB) for providing the funding to make this research possible. My thanks are extended to Dr. Diego Mas Ivars of SKB for being on my research committee and for sharing his invaluable insights as I conducted this research program. I also want to address my thanks to Dr. Navid Bahrani of Dalhousie University for serving on my research committee, for providing invaluable insights as I conducted this research program and for teaching me numerical modeling in geomechanics. I want to also acknowledge Jesse Keane, Jordan Maerz, and Brian Kennedy for their assistance in the laboratories for which I worked.

I want to express gratitude to my wife Sarah for her involvement in me completing this graduate degree. Her willingness to uproot our life, time and time again for me to fulfill my career ambitions, all the while providing encouragement and taking care of everything else in our life, is something that I am truly thankful for. Additional gratitude is extended to my children Theodore and Aubrey for providing me with the motivation to succeed. I feel fortunate for the time that we were able to spend together throughout this degree. My gratitude is also extended to my parents Kirk and Laura Jeans for the moral support they provide in everything I do. They have given me the confidence required to tackle any goal that I have, and I am fortunate for this.

My special thanks are extended to Yalin Li, Soheil Sanipour, Subharajit Roy, Ryan Ziebarth, Mehdi Ghasemi, and Luis Fernando Gomez de Alba for their assistance throughout this degree. I wish you all terrific success in your life and careers.

1 INTRODUCTION

Predicting whether a rock mass will remain stable during and after excavation depends predominantly on the accurate selection of parameters that describe the true characteristics of the features present in the rock mass. This is particularly important for projects requiring consideration of rock slopes, planar failures, or tunnel ground support. A thorough understanding of the conditions of a rock discontinuity and its ability to resist shearing forces is of great significance in accurately predicting the stability of the mass. The enclosed study focuses particularly on weathered rock discontinuities and aims to improve the current methods of predicting the occurrences that can be expected on these discontinuities.

1.1 BACKGROUND

Nick Barton in 1973 introduced the Peak Shear Strength Criterion which predicts the shear stress required to cause a rock joint to slip and depends on four parameters: a) the amount of normal stress present on the joint, b) the roughness of the walls, c) the residual friction angle of the two mated walls, and d) the strength of the wall rock material present. The first three parameters mentioned can be predicted currently with relative certainty while the final parameter mentioned (wall rock strength) remains highly subjective as there has been little advancement in a true quantification methodology that can be applicable to all rock types and infill materials encountered. Barton termed this parameter the Joint Wall Compressive Strength (JCS) and as the name suggests, it is the compressive strength of the rock wall material present in the joint. On a fresh joint with no weathering or alteration, the JCS is said to equal that of the unconfined compressive strength (σ_c) of the intact rock, whereas, if there is weathering and/or alteration, the JCS value is often a value different than the σ_c of the intact rock. It is the latter scenario which requires a quantification methodology as simply doing a UCS test on a graded or layered specimen would not produce indicative results of strength at the surface.

Regardless of whether a methodology existed or not, the influence of the JCS value chosen to represent the joint on the final shear strength result is substantial. Thus, it is not uncommon for consulting engineers to use an unrealistically low value of JCS to produce a seemingly safe lower bound shear strength failure envelope to be used in their design.

Producing safe designs in this manner, for the most part, renders JCS determined by traditional methods meaningless and are likely not conducted, or the results are not used in producing engineered designs. For a parameter of such substantial influence on the overall shear strength prediction, a methodology that can actually be used and trusted is of high necessity.

Recognized methods do currently exist to predict a JCS parameter through correlation from hardness; particularly, through the use of a common Schmidt hammer. In general, the use of any hardness testing device on any material, let alone the Schmidt hammer on rock, requires a thorough understanding of what the hardness result is really showing. By understanding the applicability of the hardness findings relative to the characteristics of the material being tested, one can then pursue correlation to JCS with more certainty of the prediction's accuracy. Without an understanding of what the hardness result really consists of is cause for potential errors in the prediction of JCS, and consequently, shear strength on the rock joint. The Schmidt hammer for example, works well in certain applications on rock, whereas its use in other applications produces results that are inaccurate. In the latter case, an inexperienced user or a user with limited understanding of the result is likely to believe the hardness result to be valid even though it is incorrect, or they could be skeptical of the result and discard it, likely to make a guess.

The traditional Schmidt hammer has an impact force that is quite large and when tested on smooth, adequate-sized intact rock specimens consisting of certain properties, it has the ability to produce accurate results. However, due to the large impact magnitude, the influence zone is large, limiting it to producing results that derived from deep within the material tested. This is particularly troublesome in applications where a thin material overlies another material of differing properties, such as that seen on a weathered rock surface or on a thin rock deposit. In these cases, the hardness result found will not be solely of the surfacing material but a combination of this material and that of the underlying material. Thus, this high-powered device is not able to produce hardness results that reflect a weathered or thinly layered rock surface if the surfacing material is too thin. This renders it incapable of producing viable results on such surfaces, meaning

that a valid, correlated JCS value of a weathered rock joint in nearly all cases, would not be achievable if hardness found on this device was used to predict it.

On weathered rock surfaces, Aoki and Matsukura (2008) compared the Schmidt hammer to the Leeb Hardness device: a device with $1/67^{\text{th}}$ of the impact magnitude of the Schmidt hammer being tested in their study. They found that the Leeb device was much more capable of producing a hardness value of the rock's weathered surface than the Schmidt hammer. Essentially, the main method of predicting the JCS value of a weathered joint surface was proven by these authors as being much less capable of doing this as compared to the Leeb device; a device that is hardly known in the rock mechanics industry.

The Leeb hardness device saw its introduction into the rock mechanics industry in the early part of the 1990s. Specifically, the Leeb device has the ability to predict quantifiable and repeatable hardness values to a reasonable level of accuracy. Similar to the Schmidt hammer, the hardness values found with this device can be correlated with JCS and the strength of the wall rock material for all rock types encountered and, in all scenarios, can be found; something that is not able to be done by the Schmidt hammer, or any other known hardness device.

Some of the earliest works with the Leeb device was on natural weathered rock surfaces and attempts were made to better understand what is referred to as the "influence zone" of this device by examining the hardness change with depth into the rock through the weathered profile. An "influence zone" is a term used to describe a certain volume (zone) of material beneath the impact location that influences the hardness readings captured on the device. While testing weathered rock surfaces of three rock types, Hack et al. in 1993 found that a maximum material thickness of 5 mm was an appropriate representation of this respective influence zone. The influence zone determination made by these authors was found by grinding and testing on surfaces through the weathered profile of a rock. Their results showed that at approximately 5 mm thickness away from the depth of unweathered rock, that an increasing trend in hardness could be seen for the subsequent surfaces in the remainder of the weathered profile. Further, a correlation equation was developed by these authors to find the JCS parameter and was based on a limited database made from specimens with laboratory-prepared, flat surfaces consisting

of a small variety of rock types. From this, these authors were successful in predicting a JCS value for rock; the first researchers to do this with this device.

Research was conducted with the Leeb device in the 1990s following the work of Hack et al. by Asef (1995). This author produced an expansive database of rock type data and more refined correlation equations that could better predict JCS using a few different types of Leeb devices. Asef found that roughness of a natural weathered surface greatly impacted the hardness results found on the device and thus suggested that a natural rock surface be polished in the field with a handheld device prior to testing. He also determined that a different impact quantity and technique is required for gathering field testing results as opposed to that in the laboratory to achieve the best correlation with JCS. It was found that of the devices used in his research, Asef found that the Leeb ‘type D with ball’ device produced the best fitting correlations between hardness and JCS.

Following the work of Hack et al. and Asef, the efforts of numerous researchers produced many Leeb hardness, L_D to Unconfined Compressive Strength, σ_c correlation equations on laboratory-prepared, flat-surfaced rock specimens. In 2018, a large database was merged together by Corkum et al. for the Leeb ‘type D with ball’ device consisting of all the data making up these correlation equations and an all-encompassing correlation equation was developed.

1.2 AIM AND OBJECTIVES

The only outstanding task for the viable use of the Leeb device on rock joints is a quantification methodology which can only be developed after a thorough understanding is gained of the device and the results it produces. It is this understanding that forms the primary scope of this study: to understand what the hardness results found on the Leeb device comprise of and in what scenarios can the device be used in to produce viable hardness results that can be correlated to JCS.

To understand what a hardness testing result consists of, an examination of the influence zone must occur. When testing the surface of a material that is underlain by a material of differing characteristics, if the influence zone exists solely in the overlying material, then the hardness readings on the device will reflect that of the overlying material. If the influence zone extends into the underlying material, then the hardness

values captured on the device will reflect that of both materials. In this case, the magnitude of the influence of the underlying material hardness on the captured result is dependent on the volume of the overlying material. Specifically, the lesser the volume of overlying material, the greater the magnitude of influence will be present in the readings from the underlying material. Understanding the influence zone for the specific device is therefore essential to be able to validate the findings found on the device when testing a surface; especially for weathered surfaces or on surfaces of rock featuring thin rock layers.

A method was developed to examine the influence zone on materials that do not increase in strength with depth to rule out strength gradient effects in the results. In an attempt to understand the influence zone and how it affects hardness readings, this current study examines the influence zone based on a one-dimensional material thickness rather than based on volume, identical to Hack et al. in 1993. Rather than basing the influence zone on the examination of a point of trending hardness increase inside a rock's weathered profile, this study uses artificial material composite specimens to make this determination. The influence zone of the Leeb device (type D) was determined successfully in this study to be slightly under 2 mm in thickness. With this result, for the first time in the literature, a thickness of weathered material in exceedance of 2 mm, when tested, was proven to produce hardness values that are uninfluenced by the underlying, unweathered rock and can be correlated to produce arguably the most accurate JCS value to date.

Apart from the influence zone, another measurable characteristic that influences the hardness findings on the device is the roughness of material. Thus, another primary objective of this study was to find the effects of roughness on the hardness results and to determine how best to predict JCS with respect to natural roughness. The aim was to develop an easy and practical method to determine JCS with the Leeb device: one correlation equation, one device, and one impact technique that could be applied in all situations. The focus was also to provide a couple of methods to rule out discrepant data such as from roughness effects. Following the recommendations of Asef, a slight polishing of the surface is considered in this study to be advantageous if this is of interest

to the person performing the evaluation. However, this study suggests methods for the case that the end user is not interested in removing natural roughness to find JCS.

If the grinding and testing method used in this study is employed on some samples of the rock type under investigation, a wealth of understanding can be gained, be it for a particular project or study. The value gained from this exercise provides the evaluator with a) the weathering depth, b) the standard deviation information per surface, and c) the hardness gradient. With the understanding of the impacts of the influence zone, the weathered depth gives the evaluator the understanding of the magnitude (if any) of the underlying, unweathered rock influence on the readings: if it is thicker than 2 mm, hardness values irrespective of roughness are solely of the weathered surface material. The standard deviation information allows the evaluator to process out the roughness effects seen on the natural surface. The standard deviation is understood from the results of this study to be higher on the natural surface than that found on the subsequent surfaces found in the weathered profile. A method in this study is mentioned to eliminate the effects of roughness by refining the data to match the average standard deviation of the subsequent surfaces. The hardness gradient found on the non-natural surfaces in the weathered profile can be interpolated following the trend of the data (this study primarily seen a linear trend) to the surface. An evaluation can then be made on the significance of the underlying material influence or roughness. If the evaluation leads to the conclusion that the hardness results on the surface are much too low (roughness effect issue), the interpolated value may be used to represent the surface hardness.

In addition, Nick Barton's other parameter used in the prediction of rock joint shear stress, the Joint Roughness Coefficient, JRC is examined in this study. Using a laser scanner, the surface of all rock specimens examined in this study was completed. The profiles of the scans in the x and y axes were prepared and put into an evaluation package. This package was sent out to 11 rock mechanics consulting engineers for their predictions of JRC based on Barton and Choubey's JRC chart (1977). A secondary aim of this study was to determine if JRC could be associated with hardness effects seen in the results on the device. The average JRC value for each specimen was compared to the standard deviation increase seen on the natural surface (in comparison to the other surfaces in the weathered profile). This was examined to see if JRC magnitude could be

correlated with data scatter indicative of roughness effects. More work needs to be done in the future to further develop this understanding; however, this study shows that no real correlation can be seen linking roughness effects determined by standard deviation and JRC selected manually.

In this study, the iterative grinding and hardness testing process by Hack et al. (1993) was adopted using the Leeb ‘type D with ball’ device. Processes are discussed to determine the most suitable weathered surface hardness value given the findings of this iterative exercise. This hardness value is next submitted into Corkum et al.’s all-encompassing L_D to σ_c correlation equation to find JCS. It is believed by the author that the processes used in this study produce the most accurate JCS value to ever exist and can be used on any rock type. Additionally, this process is believed to be a solid foundation for further improvements on this topic.

1.3 ASSUMPTIONS AND LIMITATIONS

For Hack et al.’s 5 mm thickness to be truly an influence zone, the authors mention that an assumption was made that the rock material in the weathered profile consists of ‘more or less uniform strength overlying stronger backing rock’. The author of this current study believes that this assumption is not yet fully supported by findings or adequately quantified as the entire process of the formation of weathering on a rock surface means that the surface needs to increasingly degrade for the weathered depth to increase. This results in the weakest material locating at the surface with an increase in strength with depth until it reaches an unweathered state at the point of termination of the weathered profile. This current study proceeds with the understanding that the weathered profile is a gradient, with the strength increasing with depth.

With the understanding that natural heterogeneity exists in natural rock, attempts in this study were made to reduce the amount of heterogeneity in the specimens being tested for evaluation of the influence zone. Composite specimens consisting of sandstone and Plaster of Paris were made for the purposes of eliminating unexplainable results that could arise from heterogeneities. Both of these two materials were assumed in this study to represent materials of a relatively homogeneous and isotropic nature. With one of these materials overlying the other in a fixed fashion, it was believed that any deviation in

hardness found on the top surface to the hardness of this same overlying material tested independently would be the effect of the influences of the underlying material. To validate the findings on a rock mechanics level, natural rock specimens hosting a transition of rock types within the specimen were then used to verify the results.

Finally, despite the suggestion of Asef to find JCS from L_D found using a correlation derived from natural rock surfaces, it was considered in this current study as not being as controlled and practical for the end user as a laboratory-derived correlation. The reason for this is because the amount of weathering present on a rock surface differs depending on its geological location and the conditions it is subjected to. A single rock type could have different amounts of weathering on it and therefore different properties. Thus, the all-encompassing L_D to σ_c correlation equation of Corkum et al. in 2018 was considered as being the best suited to achieve the goals of this study.

1.4 STRUCTURE OF THE THESIS

Included herein is a thesis document discussing the findings of a literature review of the work considered pertinent to the research described in this document. Following this is a detailed section on the methodology used in this study and finalizes with a section discussing the associated results. Appendix documents are included at the end of the thesis and contain the collected Leeb hardness data found on the specimens in this study as well as a JRC evaluation survey package which was sent out to consulting engineers for their input.

2 LITERATURE REVIEW

In this section, a literature review focused on the work of many of the key researchers that built the knowledge base leading to the work conducted in this research program is outlined. It starts with a section showing an identifiable need for research on rock discontinuities and transitions into the establishment of the pertinent parameters associated with the shear strength of a rock discontinuity. At this stage, the JCS parameter is identified as being of paramount importance to the prediction of a realistic shear strength value. From this point, the qualitative and quantitative methodologies to date, and the tool recommended for use to obtain this parameter are identified. An obvious need is identified here for a more capable methodology and tool for the adequate prediction of the JCS parameter. The Leeb device, also known as the Equotip, is identified as being a possible solution for this obvious need. This section concludes with a discussion of the literature on the use of the Leeb device in rock mechanics as it pertains to this research program.

2.1 ROCK DISCONTINUITY SHEAR STRENGTH

Many great researchers over the past century have worked towards developing a quantifiable system to predict the shear strength of rock joints. It can be observed that in the early beginnings that predictions of the occurrences on projects involving rock were solely from construction observations of past projects or during the current project. In time this shifted to analytical theory together with field and laboratory observation. This section herein divides these predominant two categories discussing first the early establishments which identified a need for future advancement and then discusses next, the main, successful works that developed the parameters pertinent to the work of this research program.

2.1.1 EARLY DEVELOPMENTS MADE IN THE FIELD OF ROCK MECHANICS

In the early part of the 1900s, discontinuities in rock masses were not considered as having any structural significance to the whole mass (Müller, 1979). But, an individual by the name of Joseph Stini, who is linked to the founding of the field of rock mechanics (Hoek, 2007), was one of the few at that time that viewed rock joints as being important

and he took the lead in trying to understand them (Müller, 1979). Stini, a director of research at Vienna's Technical University, originated the 'Kluftkörper', which translates in English as 'joint body': a conceptual model illustrating jointed rock mass properties such as the degree and the kind of rock jointing, engineering difficulties to be expected in underground excavations and information on water percolation. In addition to his 333 publications, Stini taught his students with real data that he obtained himself through construction observations in the field and attempted to use these to develop a quantitative geological analysis. Apart from Stini, and perhaps Stini's aspiring students such as Müller, little rock discontinuity quantification headway had been made for many decades.

In North America, Karl Terzaghi (Terzaghi, 1946) in the 1940's described varying discontinuities seen in rock and tried his hand at establishing a quantification guideline to predict the amount of overbreak to be expected in tunnels being constructed in rock. In a similar fashion to Stini, this quantification guideline was developed based on real-world construction observation, in this case from various tunnels constructed in jointed rock and considered the amount of rock load and unsupported tunnel standup time.

It was not until 1963 when the lack of understanding of rock discontinuity behaviour proved fatal, and an obvious need for this understanding was the cause for many great researchers to emerge and start developing this better understanding. The fatal disaster was the result of a rockslide at the Vajont Dam in Italy in 1963; the second of two major rockslides occurred into the storage basin above a dam at the toe of Monte Toc. The displacement of water devastated the town below, killing approximately 2500 people. Stini's former student Müller began working on this project in 1957 in an owner's consultant role and as well, in a hired investigator role after the disaster. Müller mentioned in detail (Müller 1964) that this lack of understanding was clearly present on this project. His post-disaster report provides an excellent example of where this discipline was in the late 1950s: multiple consultants providing opinions based on their own expertise gathered from limited geological observations; most of which being entirely contradictory to that of another consultant involved. Essentially, the level of water behind the dam would be raised, and then the displacement of the adjacent mountainous rock would be monitored as the joints in the mass would be filled with

water and parts of the mass would subtly slip on a chief plane. Some consultants involved would argue that the sliding rock mass will slide eventually while others would argue that an equilibrium will be reached if the water was gradually raised. Regardless of the opinions of the consultants, a target height of head was expected to be met. To get the water to this height, they would fill the dam with water and stop it at certain heights. They would then monitor the downward movement of the mountainous rock and when it eventually ceased to move, they would then repeat the process. When there appeared to be movement that was not reaching equilibrium, they would reduce the water for a certain duration of time and then increase it again or figure out ways to stabilize the sliding mass. The time of the disaster followed a large amount of rainfall while the dam had a high level of head and a relatively recent display of stability in the walls. In a similar way to their predecessors, construction observation was the current standard: a ‘when we do this, this seems to happen’ approach but in this case, it was backed by a clear political pressure to deliver. No analysis conducted prior to the slide was believable enough to stop the raising of water. Innocent people lost their lives and people taking responsibility went to prison over this one; but, it was an era in rock mechanics in which decisions needed to be made with no methods of quantification available to make sound decisions. An unfortunate event that sparked the prosperous advance of knowledge to prevent events such as this to happen again.

2.1.2 DEVELOPMENT OF PARAMETERS

In the mid to late 1960s and 1970s, several authors made huge leaps towards the establishment of a quantitative system in rock mechanics. Of these authors, probably the first researcher to gain some ground in rock discontinuity research was Patton in 1966. Patton built artificial specimen pairs made primarily of Plaster of Paris featuring discontinuities of differing material strengths (Table 2-1) and asperity geometries. With each pair mated, he tested these in direct shear; he varied the loading normal to the pair and measured how much force would be required to shear the pair. Then for each outcome, the amount of normal load was then plotted against the determined shearing strength. First, he tested pairs with flat surfaces for each mix type in direct shear and found that in all cases, the shear failure envelope passed through the origin and that the

inclination of the failure envelope, which he denoted as being the frictional sliding resistance, φ_u , increased with increasing specimen strength.

Table 2-1: Summary of physical properties of Plaster of Paris specimens (Patton, 1966).

Filler	Sand	Sand	Kaolinite	Kaolinite
Ratio Filler: Plaster by weight	3:1	3:2	1:1	1:2
Weight Mixing Water lbs/100lbs Plaster	148	85	127	96
Unit weight at testing lbs/cu ft	88.9	94.3	64.5	66.9
φ_r degrees ⁽¹⁾	34 – 36	35 – 39	27 – 28	29 – 30
Tests on Cylinders				
Av. Unconfined comp. strength psi	248	1240	601	988
Av. Point-load tensile strength psi	53	120	70	90
Average $E_t \times 10^6$ psi ⁽²⁾	.65	1.15	.22	.45
(1) Obtained from direct shear tests after large displacements				
(2) E_t is the tangent modulus of elasticity at 50% ultimate strength				

Next, he tested the specimen pairs with inclined asperities under low normal loading and found that the residual shearing resistance, φ_r at large displacement closely matched that of φ_u of that mix type. A typical plot of the two failure envelopes performed on specimens with asperities sheared at low normal loads is illustrated in Figure 2-1. Line A shows the maximum failure envelope while Line B shows the residual failure envelope of these same specimens after a long shearing displacement.

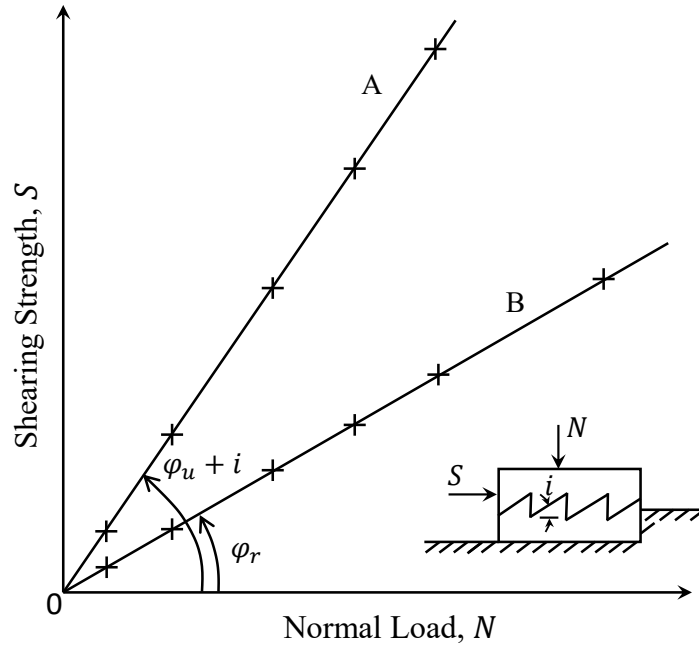


Figure 2-1: Failure envelopes for specimens with irregular surfaces (reproduced from Patton, 1966).

Patton found from the plotted results, that the maximum strength envelope had no cohesion intercept even though intact material had been sheared. He recognized that the asperities still contributed, by way of increased surface frictional resistance, to the overall internal cohesive strength; a value equal to the strength difference between the maximum and residual strength envelopes at any given normal load.

An equation for the maximum shear strength envelope was developed:

$$S = N \tan(\varphi_u + i) \quad \text{Eq. 1}$$

And the residual envelope equation as:

$$S = N \tan \varphi_r \quad \text{Eq. 2}$$

Where:

N = the total normal load

S = the total shearing strength

i = is the angle of inclination of the failure surfaces with respect to the direction of application of the shearing force

Additionally, he found that with asperities steeper than 25° , the failure envelope changes from linear to bi-linear with the lower part of the envelope inclining at $\varphi_u + i$ while the upper portion of the envelope inclines at φ_r . Patton determined that the surface frictional resistance of the asperities contributed solely to the maximum shear strength; thereby creating the lower portion of the curve. After the failure envelope slope transition, the maximum shear strength is unrelated to the surface frictional properties of the asperities.

The work of Nick Barton is arguably the next most influential contribution to rock discontinuity research as it pertains to shear strength. Some of his early works included the topic of soil fillings in joints where he not only compiled all of the known shear strength data from the literature for different types of rock and filling combinations, but he also developed a qualification system for filled discontinuities (Barton, 1973a). He examined dilation, shear displacement rate, porosity, actions about asperities, drainage condition, and clay “adhesion” and provided recommendations as to how to reduce errors in laboratory testing the filling material. Also, in 1973, Barton produced a paper (Barton, 1973b) on the subject of shear strength on rock joints absent of soil fillings. In particular, he focused his attention on rough, undulating, non-planar joints, exclusive of filling material formed by tensile failure; a brilliant methodology to determine a criterion for non-weathered joints representing the roughest end of the joint roughness spectrum. It was his plan to receive this information and then look at strength reducing characteristics and determine criterion to analyze the peak strength of these, such as weathered joints and joints with less roughness. He created specimens that were made of realistic, low strength, brittle model materials, representing large surfaces (2 to 30 m) at a much-reduced scale (2.5 x 6 cm). Plotting direct shear testing results of a wide variety of the specimens with varying σ_c against the varying normal stress, he was able to develop an unweathered, rough-undulating joint peak strength criterion (Eq. 3).

$$\sigma_c/\sigma_n \geq 100 ; \quad \tau = \sigma_n \tan 70^\circ$$

Eq. 3

$$100 > \sigma_c/\sigma_n \geq 1.0 ; \quad \tau = \sigma_n \tan \left[20 \log_{10} \left(\frac{\sigma_c}{\sigma_n} \right) + 30^\circ \right]$$

Where:

σ_c = unconfined compression strength of the rock

σ_n = normal stress

τ = peak shear strength

30° represents the basic friction angle, φ_b gathered from the model specimen shear tests

Using the criteria in Eq. 3, Barton developed a chart showing Normal Stress versus Shear Stress envelopes (unshown) and could be used for obtaining a rapid estimate of shear strength for σ_c between 10 and 2000 kg/cm². Dotted lines were provided in the chart to represent uncertainty of that specific curve's practical relevance.

Table 2-2 displays the classes and descriptions of unweathered rock joints and their respective shear strength criterion. At the time of publication, the value of 20 in Class A was justified while the value of 10 and 5 in Class B and C was purely empirical; selected by Barton as preliminary efforts to understand non-planar joints. He denoted the values of 20, 10 and 5 as being the values of the Joint Roughness Coefficient, JRC.

Table 2-2: Predictions of classes and descriptions and their corresponding peak shear strength criterion (Barton, 1973b).

<i>Class and Description</i>	<i>Estimate of Shear Strength</i>
A. Rough Undulating – tension joints, rough sheeting, rough bedding.	$\frac{\tau}{\sigma_n} = \tan \left[20 \log_{10} \left(\frac{\sigma_c}{\sigma_n} \right) + 30^\circ \right]$
B. Smooth Undulating – smooth sheeting, non-planar foliation, undulating bedding.	$\frac{\tau}{\sigma_n} = \tan \left[10 \log_{10} \left(\frac{\sigma_c}{\sigma_n} \right) + 30^\circ \right]$
C. Smooth Nearly Planar – planar shear joints, planar foliation, planar bedding.	$\frac{\tau}{\sigma_n} = \tan \left[5 \log_{10} \left(\frac{\sigma_c}{\sigma_n} \right) + 30^\circ \right]$

The σ_c parameter which is used to represent unweathered joint conditions could next be modified by Barton to a value denoted as being the Effective Joint Wall Compressive Strength, JCS. This value is the compressive strength value of the joint wall in its present condition i.e., for unweathered conditions $\sigma_c = JCS$ while for weathered

conditions the value of JCS would be used in the place of σ_c . A formula was developed (Eq. 4) to allow the JRC parameter to be found on unweathered joints but can be modified to a weathered joint condition with the replacement of JCS for σ_c .

$$JRC = \frac{\tan^{-1}\left(\frac{\tau}{\sigma_n}\right) - \varphi_b}{\log_{10}\left(\frac{\sigma_c}{\sigma_n}\right)} \quad \text{Eq. 4}$$

Barton found that laboratory testing on dry joints provided significantly higher shear strength results than joints in saturated in situ conditions. He found that the general reduction of shear strength for saturated non-planar joints is related to moisture and the adverse effects that moisture has on the tensile strength of brittle materials. The compressive strength is in turn affected and controls the shear strength of the non-planar joint. It could be concluded that for saturated joints, the peak shear strength can be obtained with Eq. 5.

$$\frac{\tau}{\sigma_n'} = \tan \left[(JRC) \log_{10} \left(\frac{JCS}{\sigma_n'} \right) + \varphi_b \right] \quad \text{Eq. 5}$$

Where:

σ_n' = effective normal stress

JCS = effective joint wall compressive strength (saturated)

JRC = joint roughness coefficient (Eq. 4)

φ_b = basic friction angle (wet, residual, drained)

Barton and Choubey four years later (1977) modified the peak shear strength formula (Eq. 5) by replacing the basic friction angle, φ_b within the formula to the residual friction angle, φ_r for the general case of unweathered and weathered joints. The modified equation is known as the Peak Shear Strength Criterion and is defined as follows:

$$\tau = \sigma_n \tan \left[JRC \log_{10} \left(\frac{JCS}{\sigma_n} \right) + \varphi_r \right] \quad \text{Eq. 6}$$

They conducted many Residual Tilt tests. For these tests, many rock jointed specimens were sawn, washed, air-dried and then the flat sawn surfaced pairs were mated. The pairs were then tilted until sliding occurred. The tilt angle for sliding to just

begin was taken to be the basic friction angle, φ_b . The authors developed a relationship involving this parameter together with the Schmidt rebound test to find the residual friction angle, φ_r . Eq. 7 shown below considers mineralogical differences, can be used regardless of the degree of weathering, and produces φ_r values that are relevant to saturated conditions.

$$\varphi_r = (\varphi_b - 20^\circ) + 20 \left(\frac{r}{R} \right) \quad \text{Eq. 7}$$

Where:

R = Schmidt rebound number on dry, unweathered sawn surfaces

r = Schmidt rebound number on wet joint surfaces

φ_b = Basic friction angle from dry, unweathered sawn specimens

Additionally, they took 136 joint specimens, profiled each joint (most were profiled in three spots), sheared them and with the obtained parameters, back-calculated JRC values for each. Groups were formed consisting of increment ranges of JRC and a representative joint profile for each, selected as being the most typical in that group. These groups and typical joint profile associated with each were compiled in the chart shown in Figure 2-2.

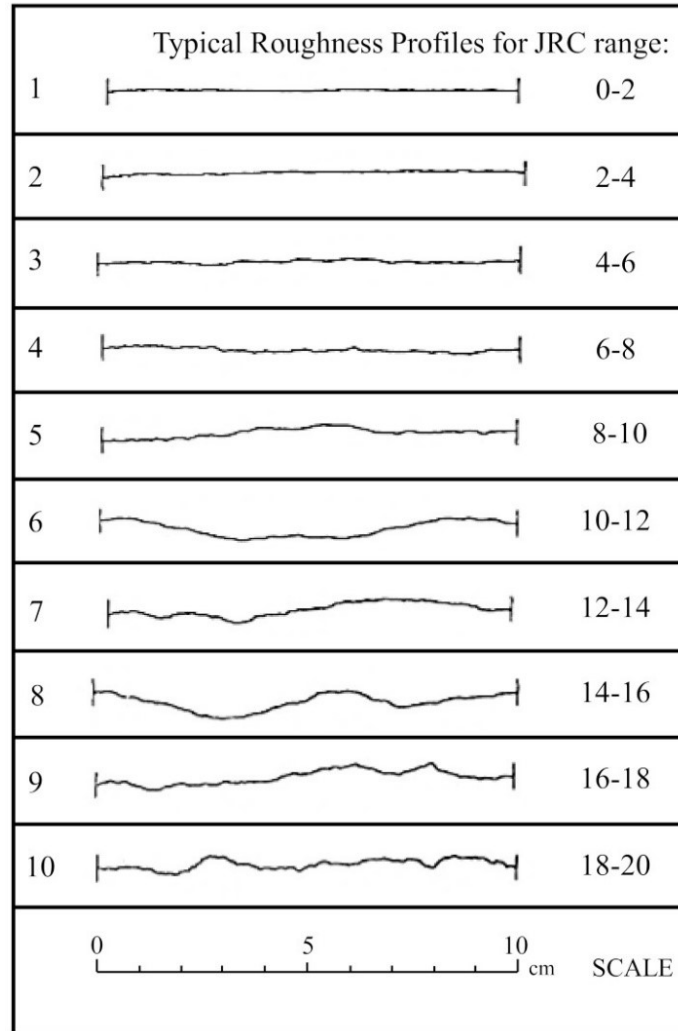


Figure 2-2: Roughness profiles showing the typical range of JRC values (reproduced from Barton and Choubey, 1977)

Moreover, they defined a relationship to estimate JRC values from tilt tests (Eq. 8). The tests need to be performed only on dry joints and three tilt tests need to be conducted on each joint; the mean will be the estimated JRC value. Joint specimens tested in this way can be reused several times without any reduction in strength because of the very low stress level.

$$JRC = \frac{\alpha - \varphi_r}{\log_{10} \left(\frac{JCS}{\sigma_{n0}} \right)} \quad \text{Eq. 8}$$

Where:

$$\sigma_{n0} = \gamma h \cos^2 \alpha \quad \text{Eq. 9}$$

$$\alpha = \arctan\left(\frac{\tau_0}{\sigma_{n0}}\right) \quad \text{Eq. 10}$$

σ_{n0} = the effective normal stress generated by the gravitational force acting on the upper half of the block

α = the angle at which sliding occurs

γ = rock density (kN/m³)

h = thickness of the top half of the block (m)

τ_0 = shear stress when sliding occurs

JCS = Joint Wall Compressive Strength measured on dry joints using the Schmidt hammer

Eq. 9 automatically limits the application range of the tilt test to smooth enough surfaces to be tested without succumbing to overturning failure rather than sliding. Barton and Choubey found that a JRC value of 8 could be attained from their laboratory scale tilt test. For rougher joints, they mention “push” or “pull” tests could be carried out, a method which involves pushing or pulling the top block parallel to the joint plane. Further to this, direct shear tests could be used to test the higher end of the range.

2.2 ROCK WALL MATERIAL RESEARCH USING CONVENTIONAL METHODS

As explained in Section 2.1.2, several parameters have been identified to influence the shear strength prediction of a rock joint. Of these parameters, the JCS parameter, has not seen extensive development quantitatively over the last several decades, unlike JRC (revisit Eq. 4 and Eq. 8) for example. When considering Barton and Choubey’s Peak Shear Strength Criterion (Eq. 6), the overall shear strength prediction can vary significantly depending on the value of JCS selected. Figure 2-3 was prepared to demonstrate the variation of the failure envelope plot for rock joints with JRC values of 10 and 20 (moderately rough and rough) with a φ_r value of 25°, for JCS values of 10, 50 and 100 percent of a selected σ_c value of 50 MPa. It can be seen that the overall prediction of the shear strength of a joint is highly dependent on the selection of the JCS parameter. It is thus imperative to be able to determine a reliable JCS value that represents actual field conditions.

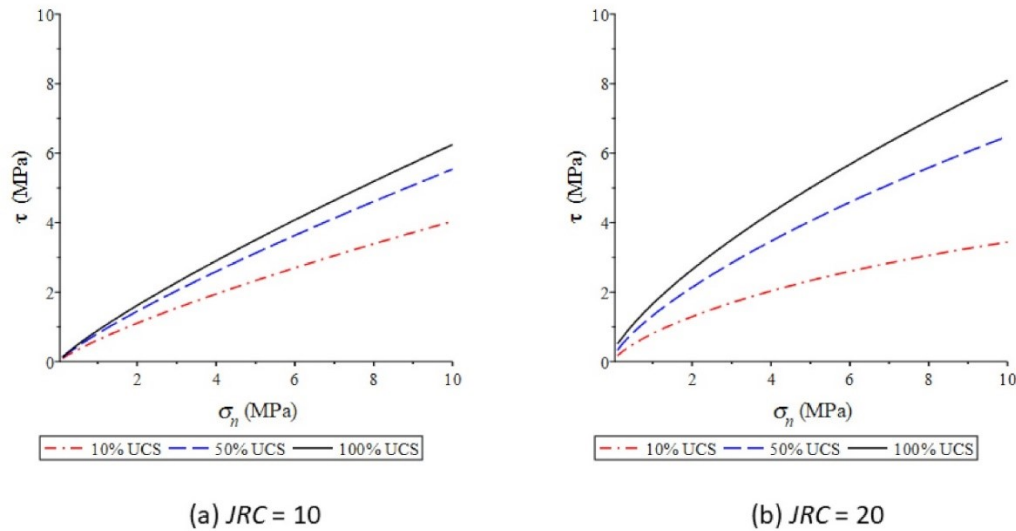


Figure 2-3: Non-linear shear strength envelope based on a range of JCS values as a percentage of σ_c ($\sigma_c = 50 \text{ MPa}$, $\varphi_r = 25^\circ$).

The means of obtaining a reliable JCS value are almost non-existent and are highly dependent on many factors such as the device used, rock strength, impact quantity and methodology to name only just a few of many. There currently is so much subjectivity in the obtained results in the field or the laboratory that it is not uncommon for consultants to simply take a low percentage of σ_c as a seemingly safe JCS value when conducting rock mass stability calculations. Despite the current lack of confidence in the currently proposed methodologies to find JCS amongst practitioners, there has been some attempts to develop a quantification methodology for this parameter. The sections that follow show a brief evolutionary timeline of some quantification attempts to obtain the JCS parameter using conventional methods as well as attempts to quantify the amount of weathering present on a rock surface.

2.2.1 METHODS USED TO FIND JCS

A paper was written by Deere and Miller in 1966 on the physical properties of intact rock rather than on the specific topic of rock discontinuities; however, a certain chart has played a major role in determining the JCS value for rock joints. These authors determined that varying combinations of rock unit weights and Schmidt hardness values could be used to find an approximated uniaxial compressive strength of rock. This is demonstrated in what is known as the ‘Deere and Miller’s Rock Strength Chart’ and is

seen in Figure 2-4. To use this chart, one would obtain a Schmidt hardness value using a Schmidt L-hammer oriented vertically downward. This value, together with the dry unit weight of the rock, can be used to arrive at an approximated σ_c value if performed on intact rock or a JCS if performed on a weathered surface (Hoek, 2007). On the left of the chart there exists a curved line which represents a statistical dispersion, showing the possible strength deviation from the values obtained on the device to that of the correct strength value.

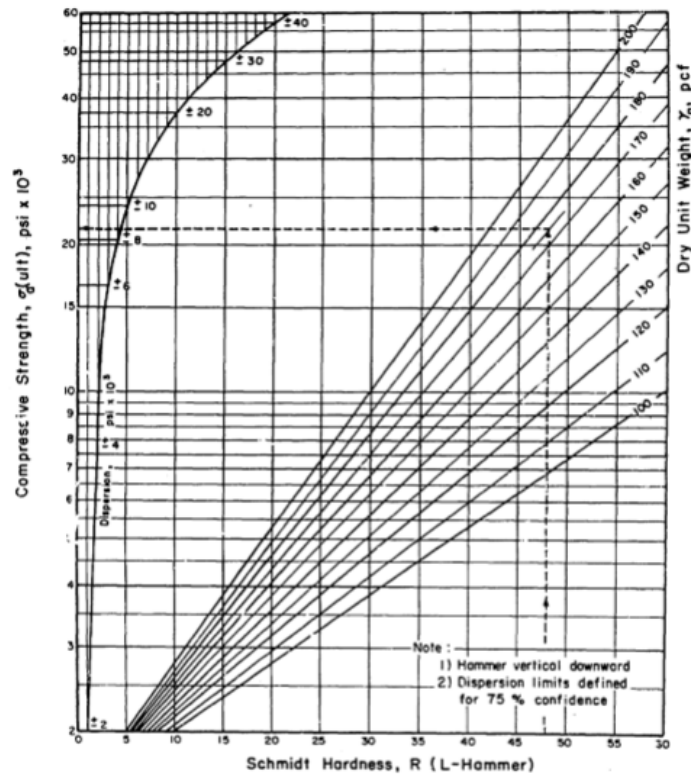


Figure 2-4: Rock strength chart based on Schmidt hardness (Deere and Miller, 1966).

The example shown in Figure 2-4 is showing a Dworshak gneiss with an approximate compressive strength value of 21,500 psi, with an estimated value of strength in the range of $\pm 8,500$ psi. They note that the actual measured strength was 23,500 psi. Their findings predict the presence of greater deviations as the strength of rock increases, as can be seen in the chart.

In 1973, Barton (Barton, 1973b) determined a ratio while examining two rock slope failures. The σ_c was obtained for the rock type present in both slope failures for the

intact, unweathered rock; the JCS values were obtained from back-analysis of the exhibited strength at failure. This ratio, obtained from the results is as follows:

$$\frac{JCS}{\sigma_c} = \frac{1}{4} \quad \text{Eq. 11}$$

Barton found this ratio to be appropriate for approximating a safe and realistic lower-bound shear strength estimate when no direct measurements are available.

In 1977, Barton and Choubey (Barton and Choubey, 1977) discuss the subject of rock joint weathering. Specifically, they expand upon the topic of density change in the joint wall material and the effects that this density change may have on the Schmidt hammer readings to determine JCS. They attempted to saw off thin slices of rock joint wall material on some of their samples, determine the density of that slice, and then compare this to the density of the rock more than 3 to 4 mm into the intact rock from the sliced location. Their particular rock specimens were not overly weathered, and as a result they found a low-density variation of not more than 2%. They prepared a table (Table 2-3) of what they describe as being ‘crude guidelines’, seen below.

Table 2-3: Estimated reductions in density for various degrees of relative alteration (Barton and Choubey, 1977).

Relative alteration (σ_c/JCS)	% change in density ($\Delta\gamma$)
1 – 2	0%
2 – 3	–5%
3 – 4	–10%
4 – 10	–20%

The density reduction percentages seen in Table 2-3 were proposed by the authors to be used to reduce the unweathered rock density value; this reduced value would then be used in Deere and Millers’ Rock Strength chart (Figure 2-4) to obtain a value for JCS.

The first set of guidelines which allows for the selection of the JCS parameter was published as ‘suggested methods’ by the International Society of Rock Mechanics, ISRM in 1978 (ISRM, 1978). A very popular table linking qualitative field descriptions to quantitative uniaxial compressive strength values was developed and is seen in Table 2-4. This was defined as the ‘scratch and geological hammer test’ chart and was an important link between geology and engineering.

Table 2-4: Manual index test criteria (ISRM, 1978).

Grade	Description	Field identification	Approx. range of uniaxial compressive strength (MPa)
S1	Very soft clay	Easily penetrated several inches by fist	< 0.025
S2	Soft clay	Easily penetrated several inches by thumb	0.025 – 0.05
S3	Firm clay	Can be penetrated several inches by thumb with moderate effort	0.05 – 0.10
S4	Stiff clay	Readily indented by thumb but penetrated only with great effort	0.10 – 0.25
S5	Very stiff clay	Readily indented by thumbnail	0.25 – 0.50
S6	Hard clay	Indented with difficulty by thumbnail	> 0.50
<hr style="border-top: 1px dashed black;"/>			
R0	Extremely weak rock	Indented by thumbnail	0.25 – 1.0
R1	Very weak rock	Crumbles under firm blows with point of geological hammer, can be peeled by a pocket knife	1.0 – 5.0
R2	Weak rock	Can be peeled by a pocket knife with difficulty, shallow indentations made by firm blow with point of geological hammer	5.0 – 25
R3	Medium strong rock	Cannot be scraped or peeled with a pocket knife, specimen can be fractured with single firm blow of geological hammer	25 – 50
R4	Strong rock	Specimen requires more than one blow of geological hammer to fracture it	50 – 100
R5	Very strong rock	Specimen requires many blows of geological hammer to fracture it	100 – 250
R6	Extremely strong rock	Specimen can only be chipped with geological hammer	> 250

Note: Grades S1 to S6 apply to cohesive soils, for example clays, silty clays, and combinations of silts and clays with sand, generally slow draining. Discontinuity wall strength will generally be characterized by grades R0-R6 (rock) while S1-S6 (clay) will generally apply to filled discontinuities. Some rounding of strength values has been made when converting to S.I units.

A reproduction of Deere and Miller’s Rock Strength Chart (Figure 2-4) was prepared by Barton (ISRM, 1978) to include metric units. An improvement to this chart was that a Schmidt hammer orientation conversion table was provided where the user could enter the table via the x-axis with a corrected hardness value representative of the hammer orientation used to get that hardness value. Evert Hoek (Hoek, 2007) reproduced this metric chart with five, vertically stacked corrected hardness axes creating efficiency for the user and eliminating the conversion table. The JCS value is said (ISRM, 1978 and Hoek, 2007) to be obtainable with a Schmidt L-hammer with any hammer orientation using any version of this chart on a weathered rock surface. The JCS value obtained in this way, is recommended by Barton (ISRM, 1978) to be used in his Peak Shear Strength Criterion (Eq. 6) and his empirical JRC equation (Eq. 8).

2.2.2 QUANTIFICATION OF WEATHERING

It is mentioned in ISRM, 1978 that an essential part of the rock wall strength description is recording the state of weathering observed on the specific rock mass and on the surface of each discontinuity. A qualitative to quantitative designation system (Table 2-5) was produced to allow the user to grade the weathering present on a rock mass.

Table 2-5: Suggested methods for the quantitative description of discontinuities (ISRM, 1978).

Term	Description	Grade
Fresh	No visible sign of rock material weathering: perhaps slight discolouration on major discontinuity surfaces.	I
Slightly weathered	Discolouration indicates weathering of rock material and discontinuity surfaces. All the rock material may be discoloured by weathering and may be somewhat weaker externally than in its fresh condition.	II
Moderately weathered	Less than half of the rock material is decomposed and/or disintegrated to a soil. Fresh or discoloured rock is present either as a continuous framework or as corestones.	III
Highly weathered	More than half of the rock material is decomposed and/or disintegrated to a soil. Fresh or discoloured rock is present either as a discontinuous framework or as corestones.	IV
Completely weathered	All rock material is decomposed and/or disintegrated to soil. The original mass structure is still largely intact.	V
Residual Soil	All rock material is converted to soil. The mass structure and material fabric are destroyed. There is a large change in volume, but the soil has not been significantly transported.	VI

Likewise, a table describing the rock material of the walls of discontinuities, either individual or in sets was also produced (Table 2-6).

Table 2-6: Weathering grade of rock material (ISRM, 1978).

Term	Description
Fresh	No visible sign of weathering of the rock material.
Discoloured	The colour of the original fresh rock material is changed. The degree of change from the original colour should be indicated. If the colour change is confined to particular mineral constituents this should be mentioned.
Decomposed	The rock is weathered to the condition of a soil in which the original material fabric is still intact, but some or all of the mineral grains are decomposed.
Disintegrated	The rock is weathered to the condition of a soil in which the original fabric is still intact. The rock is friable, but the mineral grains are not decomposed.

The stages of weathering described above may be subdivided using qualifying terms. For example “slightly discoloured”, “moderately discoloured”, “highly discoloured”.

2.3 THE VIABILITY OF THE LEEB DEVICE ON ROCK

At the time, the current methodologies suggested to be used to predict a strength value on a rock surface not only was subjective, but it also had many limitations. In order for the strength value to be better understood, a device capable of reducing the amount of subjectivity and limitations was required.

It can be seen that the original version of the Deere and Miller’s Rock Strength Chart (Figure 2-4) or newer versions (ISRM, 1978 or Hoek, 2007) can be used with a Schmidt L-hammer to find JCS if the unit weight of the rock is known. This method does, however, have its limitations. The method to obtaining the most representative hardness value (ISRM, 1978) is to take groups of 10 hardness readings, discounting the lowest five and averaging the highest five. It is suggested that several groups should be performed on each surface of interest, impacting a new part of the surface each time. From an efficiency standpoint, a lot of impacts are required to be performed with only half attributing to the result when conditions are ideal. When they are not ideal, further results are to be discarded if a ‘drummy’ sound is heard, indicating that the surface is not fixed in place and has moved upon impact. Thus, the use of this device poses challenges in loose rock masses where discontinuities are at shallow depth from the surface. Further,

tests cannot be performed on rock weaker than 15 – 20 MPa with the Schmidt L-hammer; it is recommended to use scratch and geological hammer index tests (Table 2-4) in this case.

Two other authors (Aoki and Matsukura, 2007) examined the effectiveness of the Schmidt hammer in comparison to other hardness testers with the main instrument up for comparison being the Equotip hardness device (Equotip) also known as the Leeb hardness device. A comparison of the compressive strength range for each tester included in the study was provided by the authors (Figure 2-5). It can be seen from the figure that the L-type Schmidt hammer, the Needle-type penetrometer and the Cone penetrometer all have significant compressive strength range limitations in comparison to the Equotip. To understand what a material surface that would produce a hardness value towards the lowest end of the tolerance range, the authors explain that the Equotip can be tested on the surfaces of fruits.

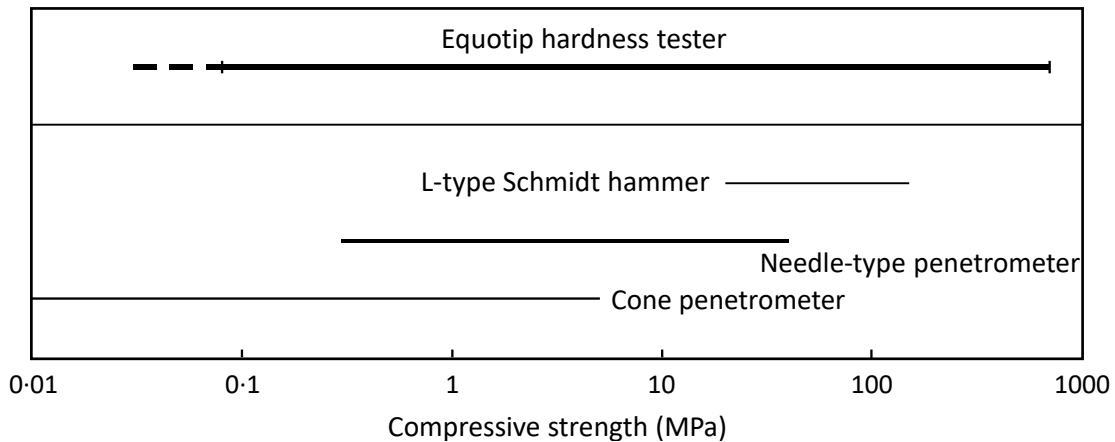


Figure 2-5: Measurement ranges of cone penetrometer (model YH62, Yamanaka, Tokyo), needle-type penetrometer (model SH-70, Maruto, Tokyo), Schmidt hammer, and the Equotip hardness tester (Modified after Aoki and Matsukura, 2007).

These authors tested the Schmidt hammer and the Equotip on weathered surfaces using two impact techniques. The first technique described by the authors as the Single Impact Method consisted of 10 impacts distributed randomly across a rock surface. The second technique described by the authors as the Repeated Impact Method, is the employment of 20 repeated impacts for the Equotip and 10 repeated impacts for the Schmidt hammer; the testing of each device conducted on a single point. The mean of the

10 impacts of the former method produced a value denoted R_s for the Schmidt hammer and L_s for the Equotip. The mean of the highest three impacts of the latter method produced the values denoted as R_{max} for the Schmidt hammer and L_{max} for the Equotip. Due to the variation in the quantity and magnitude of weathering across a rock surface, the Single Impact Method produced values indicative of the strength found at the weathered surface. The densification process occurring from the impact repetition of both devices from the Repeated Impact Method sees a rise in hardness as the rock structure under the impact point collapses and densifies until reaching eventual stabilization of the hardness values. The authors determined that the hardness result obtained from using the Repeated Impact Method on a weathered sandstone surface, produces the same result as this method employed on a freshly cut surface in this rock. This meant that the intact rock hardness could be determined on a weathered surface by employing this method. When plotting R_s versus R_{max} and L_s versus L_{max} , it was found by the authors that the Schmidt hammer data produced a higher correlation than that of the Equotip (Figure 2-6).

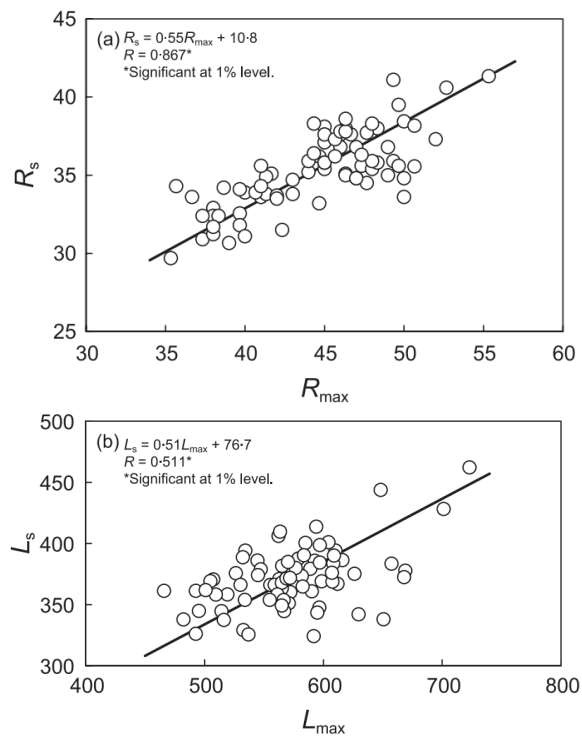


Figure 2-6: Relationship (a) between R_{max} - and R_s -values and (b) between L_{max} - and L_s -values (From Aoki and Matsukura, 2007).

These plots (Figure 2-6) are essentially the hardness found with a single impact on the weathered surface plotted against the intact rock hardness. The authors associate the difference in the correlation strengths to impact energy difference. The higher the correlation between the single impacts and the repeated impacts indicates the lower the attribution of the surface weathering layer on the hardness reading. The higher correlation of the Schmidt is an indicator that the hardness reading obtained on the surface is influenced more by the interior unweathered portion of the rock than the readings of the Equotip. The conclusion that can be drawn from this result is that the Equotip is the better device to be used to find the hardness of a weathered surface.

2.3.1 INTRODUCTION TO THE LEEB DEVICE FOR USE ON ROCK

In 1977, the Equotip, also known as the Leeb device, was developed in Switzerland by Proceq SA (Asef, 1995), the same manufacturer of the Schmidt hammer (Aoki and Matsukuri, 2008). This device has a much lower impact energy than the Schmidt hammer types. It is smaller, lighter and was originally created to be used on metallic materials. A typical use of the device (Leeb, 1979, Proceq, 2007) is on heavy metallic material workpieces that cannot be moved easily to a laboratory hardness testing machine, making it an economical and feasible option for the user. With the press of a release button, the device fires a tungsten carbide impact body with a 3 mm diameter spherical test tip via a loaded spring. A magnet located in the impact body passes through a coil housed in the tube guiding the body. As it passes, an electric voltage on both the impact and rebounding movement is induced and is proportional to the velocity of the respective movement (ASTM A956-02). The quotient of the two velocities multiplied by 1000 produces a unitless, Leeb hardness value by way of the following formula:

$$HL = \frac{VB}{VA} \times 1000 \quad \text{Eq. 12}$$

Where:

HL = Leeb hardness value
 VB = rebound velocity
 VA = impact velocity

The Equotip was originally distributed as a two-unit system consisting of an electronic indicator unit and an impact device (Leeb, 1979). As an upgrade, this device can now be purchased as a one-unit integrated system which operates in the same way. The device used in this research program is of the latter and is a TIME 5100 Portable Digital Hardness Tester produced by Beijing TIME High Technology Ltd. A visualization of this device together with labelled features can be seen in Figure 2-7.

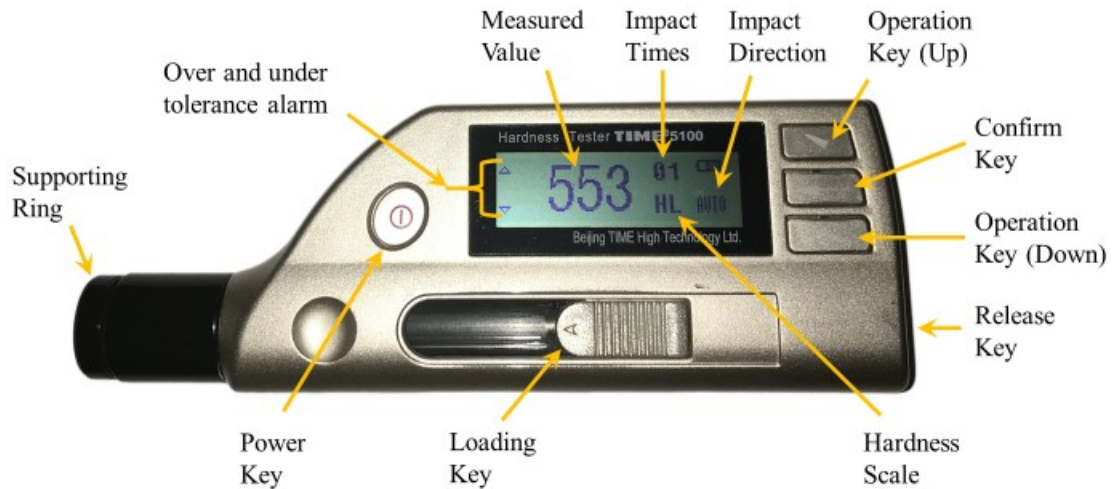


Figure 2-7: TIME 5100 (Leeb) hardness tester used in this research program with labelled features (Modified from TIME Group Inc., n.d.).

In reference to Figure 2-7, the device comes with a standard supporting ring for relatively flat surfaces (as seen); however, a supporting ring set can be purchased that can give the user the ability to test cylindrical and spherical inside and outside surfaces of varying radii. Once the device is powered on, a multitude of options can be selected to set up the device for testing. The first three level of prompts for the device used in this research program can be seen in Figure 2-8. By choosing the ‘Test Set’ folder in the second level of prompts (Figure 2-8), the most important details are set first. The modern Equotip device can be used in any orientation and the readings shown on the display are corrected to account for this, eliminating the need for manual correction by the user. As was mentioned in Section 2.2.1, ISRM, 1978 provides a correction table for the user to use to correct the Schmidt hammer value to that of one determined in the downward direction, to be used in Figure 2-4. While Hoek improved upon this by creating five vertically stacked x-axes with the corrections incorporated into each. Moreover, according to the American standards (ASTM D5873), values obtained by the Schmidt

hammer should only be compared to values obtained by the hammer in that same hammer orientation. The Equotip can clearly be seen to provide efficiency to the user over the Schmidt hammer in this regard. The user can confirm the selected impact direction by looking at the digital display; Figure 2-7 shows an example of the device being set to 'AUTO' indicating that it can be used in any direction.

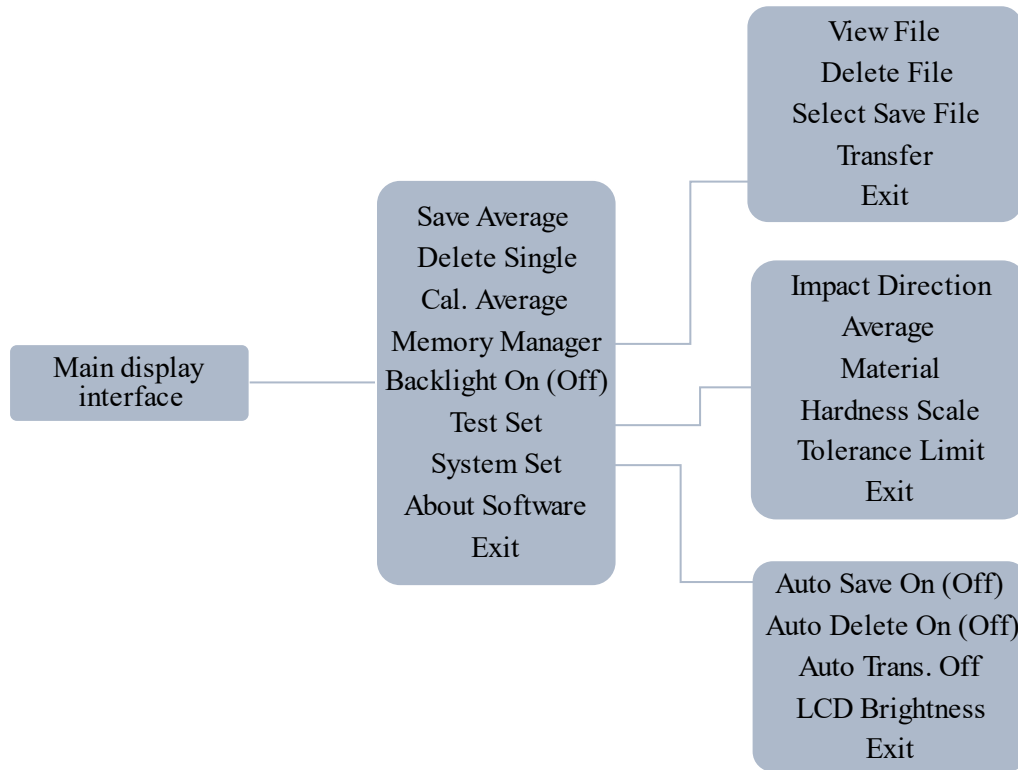


Figure 2-8: First three level of prompts in the Leeb hardness tester (reproduced from TIME Group Inc., n.d.).

The average option, accessible through the 'Test Set' folder is the number of impacts that must be completed before an average value is saved and can be from 1 to 10. In this research program, this value was set to 1 so that each hardness reading would be saved to a file. Doing it in this way, the user can save 30 readings to one file with there being nine total files to choose from. When the number of impacts making up the set 'average' quantity is reached, the averaging of these impacts will be performed and shown on the screen with the text 'AVE' being displayed. Figure 2-7 however shows the current number of impacts as being '01' indicating that the set average quantity has not yet been met and that one impact has been made with the displayed hardness being of that one impact. As an aside, to select the file to save to, the user uses the 'Select Save File'

option in the 'Memory Manager' folder and can select one of nine files. The material type that the device will be tested on, the hardness scale and the tolerance limit must be set to complete the 'Test Set' settings. The user will recognize that the notion of the device originally being made for use on metallic materials is easily believable as the testing ranges in the device are only for variations of steel, iron, alloys, and copper. A Leeb hardness value, HL, understood to be the primary unit of this device and likely the reason for the reference name of the 'Leeb hardness device', is produced on the digital display if the testing range is set to HL. Apart from using HL, hardness test methods that can be selected on the device used in this research program are for Vickers (HV), Brinell (HB), Rockwell (HRC and HRB), and Shore (HS). If any one of these testing methods are selected, then the Leeb hardness value obtained with Eq. 12 is converted to the appropriate value of that hardness test method and the device reveals this converted value on the digital display (Proceq, 2007). It should be mentioned that the material must be selected prior to selecting hardness scale. In this research program, the material selected was "(CAST) Steel" with a hardness scale of HL and tolerance limit from 170 to 960 HL. It should be noted however that surfaces harder than 890 should not be tested with a type D device (Proceq, 2007, ASTM A956). According to Proceq, these surfaces include hard metals and ceramics and testing on these surfaces will damage the impact body tip. In this research program, several specimens had some to many readings slightly exceeding an HL of 890; this observation is an important one, and further examination into whether a maximum limit of rock hardness should be incorporated into future operation standards. As will be discussed later in this thesis, it was found that an HL of 170 can be obtained on a material at the upper end of the R0 category seen in Table 2-4. Figure 2-7 shows the hardness scale of HL on the digital display. In the case where the material is softer or harder than a material able to produce hardness results within the tolerance range selected, the appropriate arrow on the digital display (Figure 2-7) will become bold indicating if it is over or under the selected limit. When the user is done with obtaining data, the 'Transfer' option in the 'Memory Manager' folder is run, while being connected to a computer with a USB cord. This transfers all data saved in the files on the device to the connected computer using software that can be purchased with the device. All files are then deleted off the device when satisfied the data is saved on the computer using the

‘Delete File’ option in the ‘Memory Manager’ folder. If at any time the user would like to review the data, or perhaps count the number of impacts still remaining on a certain surface, the user can enter any file using the ‘View File’ option in the ‘Memory Manager’ folder. Another point worth mentioning, adding to the topic of convenience for this device, is that this device has a backlight feature that lights up the digital display allowing the user to work in dark places and is simply switched on or off. Finally, this device powers off after a certain amount of time, reducing battery usage and the work can be commenced easily immediately after powering it back on.

The work of the authors discussed in the next section (Section 2.3.2) were performed with both the two-unit and the one-unit hardness devices in field of rock mechanics over the past two decades. The terms ‘Equotip’ and ‘Leeb hardness tester’ have been used in this section and throughout the remainder of this thesis and should be regarded by the reader as having the same meaning. Of these devices, some of the more common devices tested in rock mechanics literature are the type C and type D with the impact energies of 3 and 11 mJ. The impact energies of these devices are much lower than the Schmidt hammer with energies of 735 mJ for the L-hammer and 2207 mJ for the N-hammer (Desarnaud et al., 2019). Although seemingly uncommon in rock mechanics literature, type D can also be produced without a spherical ball as the test tip as will be seen in the work of Asef in 1995. In this research program, the device used is the type D with a spherical ball at the impact body tip with an impact energy of 11 mJ (displayed in Figure 2-7). In the next section, unless noted to not have a ball, the description of the work produced by any device should be regarded as being with a spherical ball.

Section 2.3.2 discusses the use of the Equotip hardness tester tested on rock. Although extensive, this section includes literature deemed to be the most purposeful for the work done in this research program. It should be noted that there has been a wealth of authors that produced findings that were evolutionary in their own right that were not included; only the work of those that provide a clear background connection to the scope of this research program were discussed.

2.3.2 EVOLUTIONAL TIMELINE OF THE LEEB DEVICE IN ROCK ENGINEERING

Authors from Delft University in the Netherlands were the first to introduce the use of the Leeb device in the field of rock mechanics beginning in 1992 (Asef, 1995). Of the first, Hack, Hingira and Verwaal in 1993 (Hack et al., 1993) published a paper which explored the quality of the rock wall in a joint with the Equotip hardness device. They wanted to establish a methodology to be able to estimate the strength of a rock discontinuity wall for application in discontinuity strength calculations. At the time of this paper, as was mentioned earlier, there had not been any real progress in the development of a methodology using a certain tool to arrive at a suitable JCS value for all rock types. The authors took blocks of sandstone, limestone and granite and prepared cubes with approximately 20 cm sides which featured a natural discontinuity wall at the top of the block. Beginning with a slight removal of asperities at the discontinuity surfaces in the area of testing, the authors tested a type D Equotip at several locations and took the average of these readings to be the hardness value for that surface. Following this, they ground into the rock, stopping at approximately 1 mm intervals and performed hardness testing. This process was repeated until the authors entered fresh rock; this determination could be made by the retrieval of consistent average hardness values with depth. Using this methodology, the weathered discontinuity wall thickness could be determined as well as what they believed to be the influence of the backing material on the hardness readings seen on the Equotip. The authors assumed that an approximate uniform strength exists in the weathered wall rock material which overlies the stronger, unweathered backing rock. They describe the hardness reading of the Equotip as being a value reflecting the strength of the volume of rock influenced by the impact. With their assumption, this meant that the influence of the underlying backing material on the rebound value could be detected if the impact values began to increase from a seemingly repeatable value as they proceeded with depth into the rock. A maximum influence zone was able to be found in their findings as being the depth associated with the first hardness value rise and the maximum hardness value found in the fresh rock. They found that for the Equotip hardness device, the maximum influence zone was 5 mm. Figure 2-9 shows

average hardness, L_D plotted against distance from original surface, d_s results found on one sandstone and one limestone specimen.

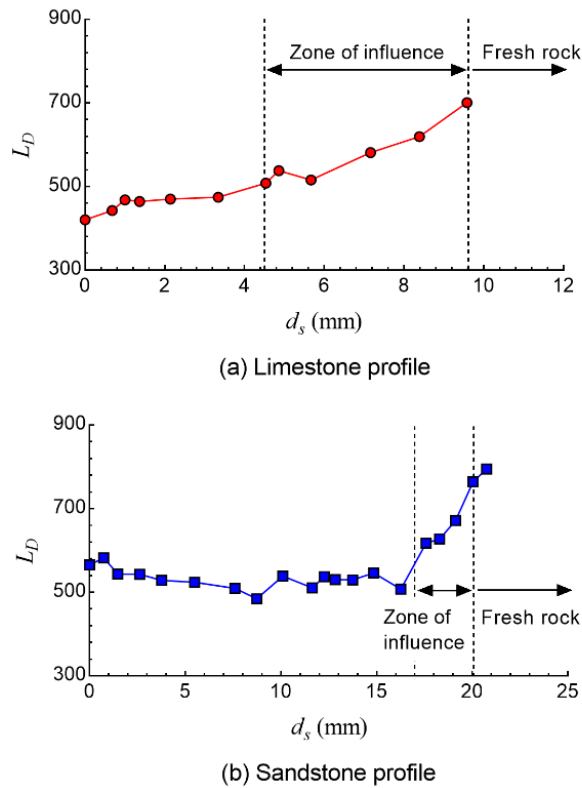


Figure 2-9: Hardness values on weathered sandstone and limestone walls ground down progressively to fresh rock (Modified from Hack et al., 1993).

In addition to the influence zone, these authors found that the hardness values depend on the present surface roughness and on rock strength rather than on the elastic parameters and density. Strength was considered a large influencer in the hardness value as they noticed an apparent damage on the rock surface after impact while elasticity and density were ruled as being less influential as they were unable to correlate the hardness value to any rock's Young's Modulus or to any rock's unit weight. The authors felt that the crushing of surface material and asperities on a rock's surface influenced the rebound results more than the rock's elasticity. They felt that more crushing of asperities occurred on rougher surfaces as opposed to minimally rough surfaces which resulted in more loss of rebound energy.

They also performed UCS testing and found that a correlation could be found for each rock type; each different from the correlations of the other two rock types.

Additionally, they found that a σ_c versus L_D relation produced by Verwaal and his colleague Mulder also from Delft University (Verwaal and Mulder, 1993) also fit their results when all of their $\sigma_c - L_D$ data was considered. For the first time in the literature, a JCS value was able to be predicted using the Equotip hardness tester. Using Verwaal and Mulder's relation, the UCS value associated with L_D found on the discontinuity wall surface was taken to be the JCS. Likewise, the fresh rock average hardness using this relation could be used to predict the UCS value of the rock.

Verwaal and Mulder (1993) were also working with the Equotip at the same time as Hack et al., and according to Asef (1995), were the first ones to begin using this tester on rock; despite publishing after Hack et al. Their work included the preparation of cylindrical cores mostly of limestone but also of sandstone, granite, building stone and man-made gypsum (Verwaal and Mulder, 1993). These specimens were mostly 60 mm long with a 30 mm diameter or 80 mm long with a 40 mm diameter; however, some cores 100 mm long with a diameter of 50 mm were also prepared of weak rock types. These authors found (Figure 2-10) a σ_c to L_D correlation where L_D consisted of the average of 10 impacts, five per each loading surface.

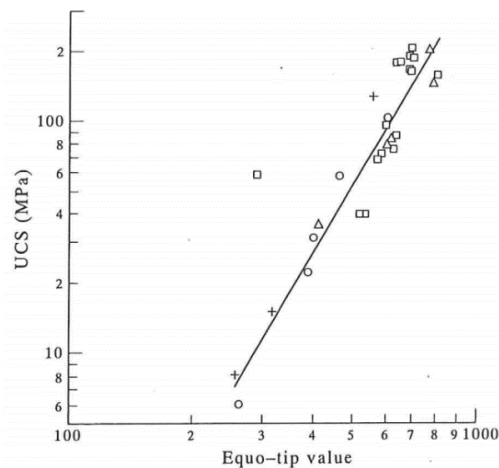


Figure 2-10: Unconfined Compressive Strength against Equotip values: + artificial; o clastic limestone; □ crystalline; and Δ sandstone. (Verwaal and Mulder, 1993).

Surface roughness was also considered by the testing of three different limestones with four different prepared surfaces. These surfaces were a) prepared with a small-grinding stone with a hand-held drilling machine; b) sawn; c) sawn then surface

lapped; and, d) sawn then lapped then polished. Treatment a) was performed on a large block surface described as being 'rough'. Treatments b) through d) were on 60 mm diameter rock cores cut perpendicular to their axes. From their findings it could be concluded that no major differences were seen in the hardness results between the treatments.

The influence of specimen size was also tested using three differing limestone types of varying sizes. Cylindrical core specimens were prepared to 150 mm length with diameters of 30, 60 and 100 mm and were tested with the Equotip device radially as well as axially. Similarly, specimens were prepared to a length of 25, 50 and 150 mm with a 60 mm diameter and tested with the Equotip device axially. It was concluded that the 30 mm diameter cores and cores with 25 mm length produced lower hardness values than those produced from cores of 60 and 100 mm diameter and cores with a length greater than 50 mm.

Under the supervision of Verwaal and Hack at the Delft University of Technology, a Master of Science thesis in Engineering Geology was prepared by Asef in 1995 (Asef, 1995). Asef's work was predominately on the use of three different Equotip probes provided by Proceq (manufacturer) on rock samples in the field and on prepared cylinders from these same samples collected in the Falset area in the Catalonia province in Spain. The field work to obtain the field data and collection of rock to be used in the lab was conducted in two-year stints: in the year 1994 and 1995. The program in 1994 was modified for the return in 1995 which was tailored to capture additional complimentary data to that found in the previous year. Briefly, the preparation of the specimens including the geometrical dimensions and equipment used to produce these specimens was the same in each year while the specifics of specimen quantity, impact quantity, hardness tester type and surface treatment in the field were modified in 1995. Asef found in 1994 that surface roughness even on smooth surfaces greatly affected the obtained hardness readings. To combat this issue, a battery-operated, hand-held polishing machine was incorporated into the program in 1995 for the testing on natural surfaces. Additionally, rock tested in 1994 had a large variety of strength with large gaps in the data with respect to rock strength. In 1995, this strength gap was filled with data strategically collected on rock that would fill this gap.

With the intention of discovering reasonable correlations between L_D and σ_c , Asef in both years of his research trialed many data manipulation combinations with the collected data. It was his goal to find the technique that produced the best correlation with the least amount of standard error. Many different data manipulation combinations were tried for finding the most representative L_D value of a surface using set impact quantities for test methods involving randomly distributed impacts and for repeated impacts on a single location. For each data manipulation combination tried, matrices of correlation were performed between each L_D value and σ_c . With Linear, Multiplicative, and Exponential correlation types, the correlation coefficient as well as the standard error of estimation were calculated for the matrices tried.

Asef determined that the best correlation between L_D and σ_c was found when using a probe type “C with ball” or “D with ball” Leeb device using randomly distributed impacts. He concluded that when testing in the field, the surface must be treated to a smooth finish with a polisher and the representative L_D value must be found using the collection combination that he denotes as M.Avg15. He also concluded that when testing was conducted on prepared lab specimens with the ends being lapped in a polishing machine, that the collection combination that he denotes as M.Avg10 produces the most representative L_D value. These denotations are broken down to mean 15 (field) and 10 (lab) impacts on the surface are collected. The highest and lowest values are discarded from the data, and the remaining 13 (field) and 8 (lab) are averaged. Asef found that a Multiplicative correlation type of the form: $Y = Bx^4$ or $\ln Y = a(\ln X) + \ln b$ best fits hardness data found on rock in comparison to the Linear and Exponential correlation types. He also concluded that if density of the rock is found, the correlation between L_D and σ_c will be further strengthened and the standard error will decrease with its inclusion. The plot of his best fitting correlation was $L_D \times 1000 \times \text{Density}$ plotted against $\sigma_c \times \text{Density}$.

As per the conclusions of the predecessor work by Verwaal and Mulder in 1993, Asef further explored the effects of size on the hardness readings and expanded this scope to include a wide variety of strength ranges of rock. He prepared lap-ended, 4 cm diameter cores, 9 cm long gypsum (weak rock), sandstone (moderately strong), limestone (strong), and granite (very strong). A round of randomly distributed hardness testing with

probe types ‘D with ball’ and ‘C with ball’ on the ends of these cylinder lengths were then conducted while the specimens were secured to the anvil. A transverse cut was made in from both ends followed by surface-lapping to make a cylinder of 5.8 cm length and the same hardness testing procedure was conducted. The same process was conducted on cylinders of 4.3 mm and 2.3 mm length. Analyzing the data for each cylinder using M.Avg10 and the Multiplicative correlation type, it was found that the hardness value slightly decreased for both probe types. It was found that the strongest rock type had the least change in values and the variation increased as the rock type weakened indicating that scale effects are more prominent in weaker rocks. However, when comparing the total change in hardness from thinnest to thickest between each rock type, no comparable differences could be seen indicating that each rock type tested experiences scale effects unique to that rock type only. It was recommended that a lab specimen should have a diameter of 40 mm or larger with a length of at least 6 cm and regardless of setting, that a minimum impact spacing of at least 3 mm was suggested to be maintained. He also found that a field test on a polished surface of those same rock types produced higher readings than those found in the lab even on the largest specimen and concluded that lab derived prediction equation cannot be used for field readings without a correction factor and that the same is also true from field to lab.

In addition to their work discussed in Section 2.3, Aoki and Matsukura (2007) developed a successful methodology to determine the strength change at the surface of weathered sandstone to its unweathered portion using the type D Equotip. They established two impact techniques to be used with the Equotip which, when used in combination can discover this difference. The first technique described by the authors as the Single Impact Method consisted of 10 impacts distributed randomly across a rock surface. The second technique described by the authors as the Repeated Impact Method is the employment of 20 repeated impacts on a single point on a rock surface. The mean of the 10 impacts of the former method produced a value denoted as L_s , while the mean of the highest three impacts of the latter method produced a value denoted as L_{max} . To repeat two sentences from Section 2.3 verbatim: due to the variation in the quantity and magnitude of weathering across a rock surface, the Single Impact Method produced a value indicative of the strength found at the weathered surface. The densification process

occurring from the impact repetition of the Equotip from the Repeated Impact Method sees a rise in hardness as the rock structure beneath the ball collapses and densifies until reaching eventual stabilization of the hardness values. The authors found that the mean of the highest three hardness values found when this method was conducted on a weathered surface or on a sawn surface of this sandstone, produced near exact values to each other. These findings allowed the authors to conclude that the Repeated Impact Method produces an unweathered hardness value indicative of the rock's intact strength. This means that regardless of prepared surface, the intact hardness can be found. The authors establish what they denote as being the 'k-value' which is a number produced from L_s/L_{max} . When the L_s value has been found on a sawn surface (further denoted as L_{intact}) of the rock in question, the found k-value can be used for hardness tests in-situ to estimate L_{intact} of the rock at that particular location by multiplying this k-value by the obtained L_{max} found on the weathered surface. At this same location in-situ, the L_s on the weathered surface (further denoted as $L_{surface}$) is found. The reduction of single impact hardness found on the weathered surface as opposed to that predicted to exist on the intact portion of the rock at that location was denoted by the authors as δ and can be represented by $L_{surface}/L_{intact}$. This δ value when multiplied by the known UCS value of the rock mass, produces the strength existing at the weathered surface i.e., the JCS value of the rock.

In 2008, Aoki and Matsukura combined the Equotip probe type D and porosity data collected by Verwaal and Mulder in 1993 with their own laboratory data found on nine rock types collected in Japan and Indonesia. They find what they denote as being the 'UCS' of cylinders prepared to 25 mm diameter, 50 mm long, dried for 24 hours at 100°C. It should be mentioned that this testing does not conform to the requirements of ISRM 1977 or ASTM D7012 for a proper UCS value. To avoid confusion, single quotations ('UCS') were added to all future reference of this value. For hardness testing with an Equotip probe type D, they also prepared 50x50x70 mm prisms. With the 70 mm face resting on a table and securely clamped, hardness testing was performed using the Single Impact Method and Repeated Impact Method introduced in their 2007 paper. The former method obtained the L_s consisting of the average of 10 impacts and the latter obtained the L_{max} consisting of the average of the highest three impact values of 20 total

impacts. A k-value introduced in their 2007 paper was also found for each rock type consisting of L_S/L_{max} . They also found porosity using Eq. 13.

$$n = (\rho_{true} - \rho_{bulk})/\rho_{true} \times 100 (\%) \quad \text{Eq. 13}$$

Where:

n = porosity of the specimen

ρ_{true} = the true density of the specimen

ρ_{bulk} = the bulk density of the specimen

The true density of specimens was found in accordance with the Japanese Industrial Standards (JIS) A1202 using powder specimens while the bulk density of specimen was found with a calculation that includes volume and dry weight.

They examined the k-values obtained on their nine specimens with ‘UCS’ (Figure 2-11) and found a linear relation existed with an $R^2 = 0.68$. It could be concluded that for lower ‘UCS’, a greater difference exists between L_{max} and L_S .

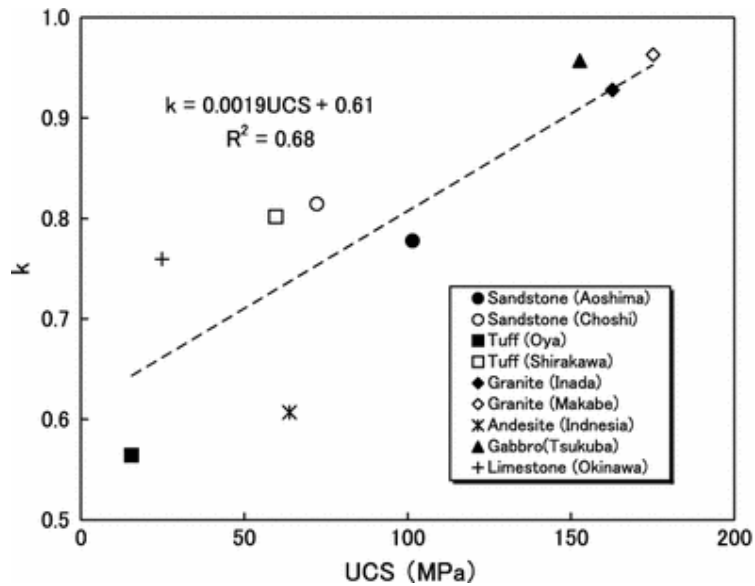


Figure 2-11: 'UCS' (MPa) plotted against k-value (Aoki and Matsukura, 2008).

It is obvious that a single impact produces a hardness value reflecting a lower strength in comparison to the hardness value obtained from 20 impacts which reflects a material of stronger strength due to the occurrence of surface hardening beneath the indenter. They describe the hardened surface impact location to be a micro compression

hollow and indicate that its critical depth depends on the UCS of the material being tested.

The results of the Single Impact Method conducted by the authors compiled with Verwaal and Mulder’s 1993 results were plotted against ‘UCS’ (Figure 2-12).

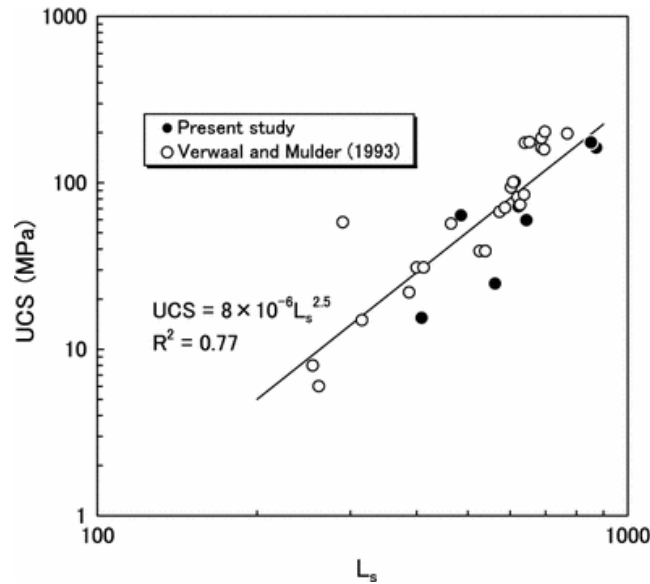


Figure 2-12: ‘UCS’ (MPa) plotted against L_s (Aoki and Matsukura, 2008).

A conclusion drawn by the authors was that a higher ‘UCS’ produces a higher L_s . A trend with an $R^2 = 0.77$ captured the data and can be described by Eq. 14.

$$'UCS' = 8 \times 10^{-6} L_s^{2.5} \quad \text{Eq. 14}$$

For the rebound-value ranges of $L_s < 400$, $400 < L_s < 600$, and $L_s > 600$, the authors next plotted the ‘UCS’ against porosity (Figure 2-13). It was observed that ‘UCS’ is dependent of porosity as well as L_s .

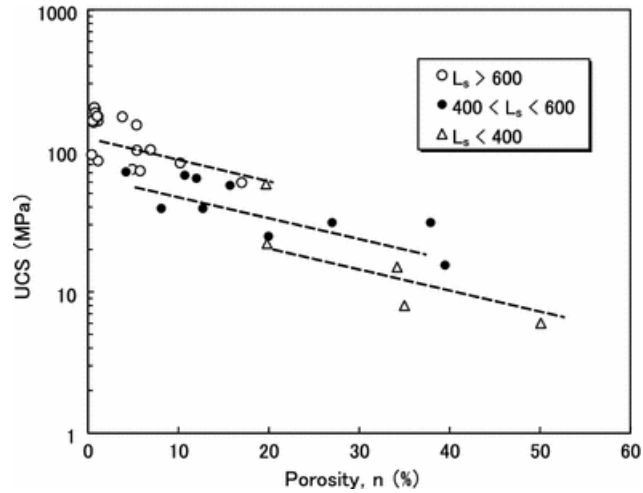


Figure 2-13: 'UCS' (MPa) plotted against porosity (%) for three rebound-value ranges (Aoki and Matsukura, 2008).

An analysis was conducted by the authors using a multiple regression model to find the relation between rebound-value ranges. The founded equation of best-fit can be seen in Eq. 15.

$$'UCS' = 0.079e^{-0.039n}L_s^{1.1} \quad \text{Eq. 15}$$

To determine if a higher degree of accuracy could be obtained in finding 'UCS' with L_s together with porosity rather than just with L_s alone, the calculated 'UCS' found with Eq. 15, was plotted against the measured 'UCS' (Figure 2-14).

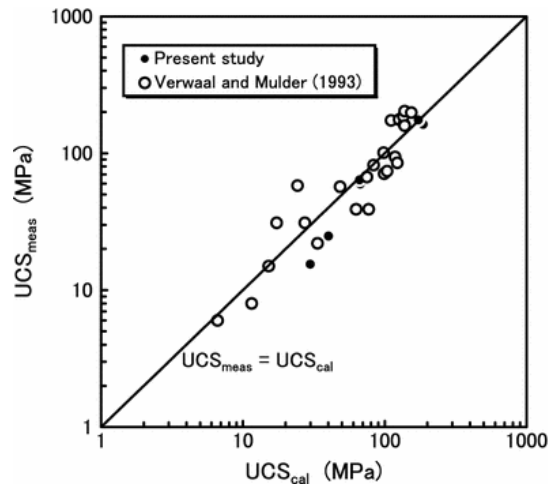


Figure 2-14: Measured 'UCS' (MPa) against Calculated 'UCS' (MPa) found with Eq. 15 (Aoki and Matsukuri, 2008).

With the R^2 coefficient being 0.88 (Figure 2-14), less scatter can be seen in comparison to the ‘UCS’ to L_s plot ($R^2 = 0.77$) shown in Figure 2-12. It could be concluded that the inclusion of porosity into the equation (Eq. 15) increases the level of accuracy in determining ‘UCS’.

Researchers from Dalhousie University (Corkum et al. 2018) further expanded upon the known knowledge base about the application of the Leeb hardness device in rock mechanics. An objective of these authors was to establish simplified methodologies that would be easy for the end user to make reasonable field predictions of the σ_c of the rock. They focused their attention on sample size, scale effects and compiling a large database containing like data obtained from the work of their predecessors for which they could produce a L_D to σ_c correlation.

It is understandable that the more randomly distributed impacts performed on a rock surface with the Leeb hardness device will increase the accuracy of the result. However, there is a point in which the amount of accuracy gain is perhaps not worth the level of effort. These authors were looking to discover the number of impacts that would be practical for the user, that would produce a meaningful result. The first of two avenues they chose to explore in making this determination involved statistical theory applied to the results of 100 randomly located hardness tests on sandstone, schist, and granite rock specimens. With a 95% degree of confidence (standard normal distribution), three Margin of error (ME) calculations were performed on randomly selected sample sizes of 10, 20 and 30 impacts within the population. With the ME calculation being the difference between the sample mean and the population mean, the authors could see the amount of gain that could be achieved by increasing in 10 impact increments to the practical maximum of 30 impacts. It can be seen in Table 2-7 that for all rock types, ME is at its highest for the smallest sample size of 10 impacts and is greatly improved at a sample size of 20. After 20 impacts, an improvement can be seen, but it is only slight.

Table 2-7: Statistical summary based on 100 impacts per rock type (Corkum et al., 2018).

Statistic	Sandstone	Schist-V	Granite
Maximum reading	598	867	938
Minimum reading	479	584	750
Median	552	762	880
Mean	552	759	879
Standard deviation	21	56.5	43
Confidence interval (95%)	± 4	± 9	± 8
Margin of error ($n_L = 10$)	13	35	27
Margin of error ($n_L = 20$)	9	25	19
Margin of error ($n_L = 30$)	8	20	15

The second avenue they chose to explore involved the same data as the previous: 100 impacts on the same three rock types. They performed 10, as the authors describe it, ‘realizations’ which were 10 plots of the average values of randomly generated individual subsets (n_L), ranging in size from 1 to 100. In addition, the mean, and the upper and lower bounds of the 90% confidence intervals for the obtained data for each of the individual rock types were added to the plots. The aforementioned plots and the reduction of the difference between the arithmetic mean and the population mean as sample averages become more refined can be observed in the below illustration (Figure 2-15).

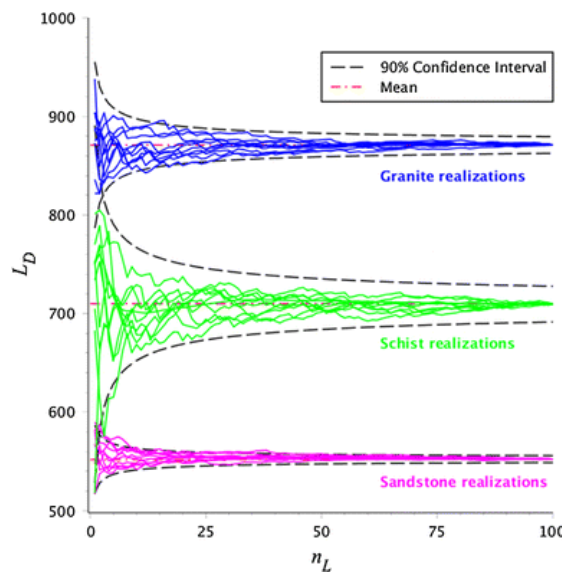


Figure 2-15: Accuracy gain associated with increased number of impacts (Corkum et al., 2018).

From both avenues pursued, the authors were able to quantify a suitable sample size to produce, as they describe to be a “valid” test. They were able to conclude that minimum gains are seen beyond a sample size of 20 and more specifically, that the convergence of L_D is appropriate for a sample between 10 and 20 impacts. It was felt by the authors that the user can decide on which number of impacts best applies for the given situation they are in; however, a suitable balance between accuracy and testing effort was suggested to be a 12-impact trimmed mean; referred to by the authors as the ‘TM12’. The TM12 approach was prescribed as being for the typical case and accounts for outliers by the removal of the highest and lowest reading of a total 12 impacts; the remaining sample size of 10 is then averaged to produce a representative hardness value. If the user is dealing with a project requiring increased sensitivity, the authors suggested that a TM20 approach may be used, where the representative hardness value is the average of a sample size of 18 impacts. It was also suggested that the impacts from the Leeb device be within an area of 25-50 mm diameter as such size can be said to represent a specific location while preventing densification.

Several of the authors mentioned in this section discussed scale effects in their publications and the consensus is that a recognizable effect can be seen in the hardness readings if the specimen is too small. Corkum et al., explored scale effects using prepared blocks and cylinders of differing lengths in a sandstone, quarried in Nova Scotia, coined by the authors as being ‘Wallace Sandstone’. The authors intentionally selected this rock type due to the uniform nature of the rock. It was felt by the authors that hardness values received on this rock type could be better understood than the readings found on rock types of a characteristically complex nature. Four cubic blocks in total were prepared with side dimensions ranging from 25.4 to 203.2 mm, while eight 54 mm diameter (NX size) cylinders were cut to lengths ranging from 25.4 to 203.2 mm. The results they found (Figure 2-16) show that an approximate consistency in L_D (obtained from TM12) was seen when a block’s volume exceeded 90 cm³ or when a cylindrical core’s length exceeds 0.4 times it’s diameter. It could then be suggested by the authors that specimens in exceedance of this criterion for blocks or cores would produce representative hardness values of that rock. Moreover, anything less would be nonrepresentative and reflect the sole influence of its limited size rather than that of the rock.

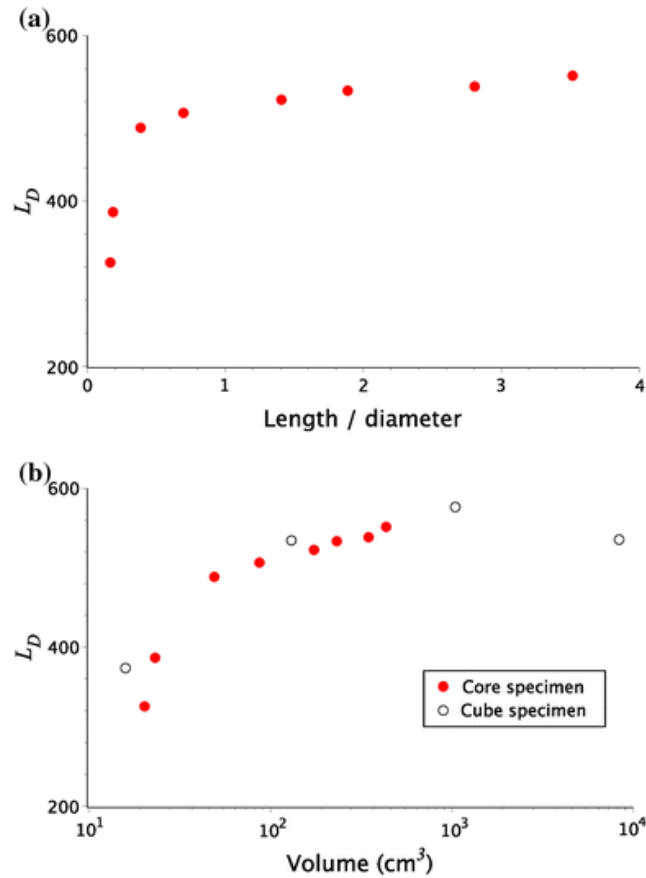


Figure 2-16: Specimen size effects on L_D found with TM12 approach (Corkum et al., 2018).

As a final component of their research, the authors compiled many of the L_D to σ_c databases available in the literature together with additional testing data that they completed as part of their research program. This large database includes 311 data points on rock covering a large strength range giving the authors the opportunity to produce a more robust predictive correlation than ever before. In total, there were 58 igneous, 40 metamorphic, and 213 sedimentary (45 being sandstone) data points included in this database. It was determined that a nonlinear power function (Eq. 16) with the fitting parameters (α and β) displayed in Table 2-8 best represented the data and was provided in the following form:

$$\sigma_c = \alpha L_D^\beta \times 10^{-6} \text{ in MPa} \quad \text{Eq. 16}$$

This equation together with the appropriate fitted parameters in Table 2-8 can be used to determine the σ_c of rock specimens with a correlation specific to its independent rock type category or with a correlation fitted to all of the data within the database.

Table 2-8: Standard error, coefficient of determination and fitting parameters for power function (Corkum et al., 2018).

Data set	R^2	S	Equation coefficients	
			α	β
All rock types	0.70	40.3	15.7	2.42
Sandstone	0.75	29.3	0.9	2.84
Sedimentary rocks*	0.71	33.1	0.1	3.18
Metamorphic rocks	0.79	29.1	0.3	2.98
Igneous rocks	0.65	45.3	3	2.64

*Including sandstone

The entire L_D versus σ_c database and the five correlation curves are presented in Figure 2-17. It can be noticed in Figure 2-17 that the ISRM R grades (Table 2-4, Section 2.2.1) were incorporated into the plot. Similarly, in tabular form (Table 2-9), the associated L_D per ISRM R grade and σ_c was provided for the data included in the database.

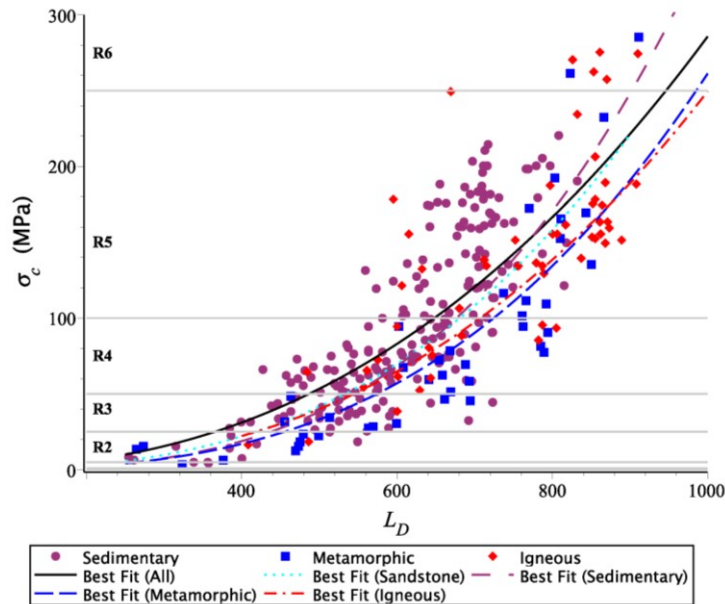


Figure 2-17: Entire database plotted by rock type category with correlation curves corresponding to Eq. 16 with Table 2-8 coefficients (Corkum et al., 2018).

The weakest correlation of all rock type categories is that for igneous rock while the highest was for metamorphic rock. The authors believe that it is the vast spread of individual grain characteristics present in an igneous rock that likely is the cause for it producing the weakest correlation. In general, it was found that the variable L_D is responsible for approximately 20-30% of the relation between σ_c and L_D based on R^2 . With a similar objective, the authors examined the variability in σ_c amongst specimens of the same rock unit. The results of five UCS testing programs from the literature, each program focusing on a specific rock unit, with strength ranging from 48 to 221 MPa, were reviewed statistically. It was found that across the five testing programs, the coefficient of variation range was from 13 to 30% indicating that the σ_c parameter has a range of inherent variability as well and should also be given consideration during evaluation of the effectiveness of a σ_c and L_D correlation. In the high range of σ_c in the compiled database, increased scatter could be seen in L_D while in the low range of σ_c , there is limited data. It was therefore suggested by the authors that an L_D range between 200 and 900 should be regarded as the practical limit of applicability.

Table 2-9: ISRM R Grades and corresponding ranges of σ_c and L_D predicted from correlation curves from Eq. 16 and Table 2-8 (Corkum et al., 2018).

Grade	σ_c (MPa)	L_D range by rock type				
		All types	Sandstone	Sedimentary	Metamorphic	Igneous
R0	0.25-1	Insufficient data in this range				
R1	1-5	Insufficient data in this range				
R2	5-25	255-437	237-418	264-437	265-455	227-418
R3	25-50	437-550	418-533	437-544	455-574	418-544
R4	50-100	550-693	533-681	544-676	574-724	544-707
R5	100-250	693-941	681-940	676-902	724-985	707-1000
R6	>250	Insufficient data in this range				

Note: Insufficient data in R0, R1 and probably R6 (poor fit in this range)

In 2019, Desarnaud et al. explored the use of the Equotip type C and D probes through a heritage science/ geomorphology lens. They strategically gathered four

different types of sandstone representing as they describe a ‘cross-section of sandstone types’ that are used in worldly built heritage. All four types of sandstone largely consist of quartz grains and amongst them, have differing amounts of clay and porosity. Table 2-10 shows the parameters found on each sandstone, displayed in short-form of their actual names: Stanton Moor (SM), Ohio (OH), Locharbriggs (LB), and Prague (PS).

Table 2-10: Summary information on the four sandstone types (modified from Desarnaud et al., 2019).

Rock Type	UCS* (MPa)	HLD (mean and SD**) (MPa)	HLC (mean and SD) (MPa)	Porosity (%)	Bulk Density (kg/m ³)	Clay (%)
SM	60 ± 9	601 ± 51	697 ± 59	12.9	2323	< 2
OH	36 ± 2	436 ± 52	492 ± 66	20	2084	3.5
LB	26 ± 4	456 ± 40	485 ± 86	23.4	2070	3.75
PS	17 ±	327 ± 49	364 ± 75	28.9	1878	8

*The designated UCS does not conform to the requirements of ISRM 1977 or ASTM D7012. The average of a minimum of six 25x25x50 mm prisms tested in uniaxial compression make up this value. To avoid confusion, single quotations (‘UCS’) were added to all future reference of this value.

**SD stands for standard deviation.

They revisited with the intention to improve, several areas of research previously visited in this section including differences between the type C versus D Equotip probes, scale effects, hardness to ‘UCS’ correlations and quantity of impacts. In addition, they examined the effects of moisture content, roughness, and open porosity on hardness readings. They used two impact methodologies, the first denoted as SIM, standing for the Single Impact Method consisting of 45 impacts on randomly selected points. The second method was denoted as RIM, standing for the Repeat Impact Method and follows Aoki and Matsukura’s technique introduced in 2007 with 20 impacts made on a single point and the highest three values averaged. This second method was repeated 3 times on each surface.

Echoing the 2018 work of Corkum et al., (revisit Figure 2-15) they performed ‘realizations’ to a maximum sample size of 45 impacts on each rock type. When evaluating, the authors determined that the 90% confidence lines stabilized for both

devices on all sandstone types at a sample size of approximately 20. It was concluded that 20 impacts are required for a robust test measurement on sandstone.

They examined scale effects with the SIM method on blocks varying in volume from 14 to 200 cm³ at thicknesses ranging from 5 to 53 mm. At 11 sizes total for each sandstone type, three replicates were made (33 blocks total) and tested. The compiled results for the three blocks of each thickness are illustrated in Figure 2-18. For the vast majority of cases, the probe type C produced higher readings than the probe type D while the probe type D seen less scatter in the data. The reason for the higher readings with the probe type C was explained by the authors to be the result of the device having a lower impact energy; less impact energy leads to higher energy restitution but less energy dissipation due to plastic deformation. An aside could be drawn about the importance of the probe type being specified with any presentation of hardness data.

The authors found that specimens do not need to be clamped at a volume greater than 18 mm thick (45 cm³) as the results are unaffected regardless. Specimens less than 13 mm thick were found to require tight clamping as strong vibrations occur. Of the two devices, it was found that the type C probe was unable to obtain reliable results on the 5 mm thick Prague (PS) sandstone and for the other three types, only about 1/3 of the readings were successful. It was concluded by the authors that reliable data was obtained on blocks thicker than 13 mm.

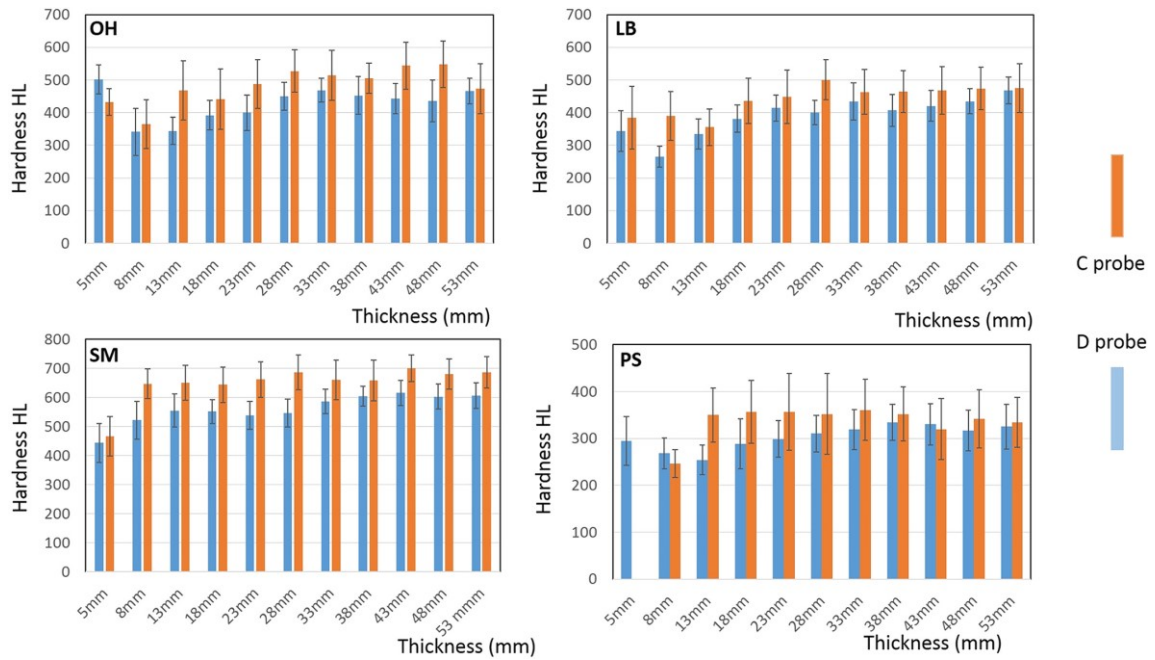


Figure 2-18: Hardness for different thicknesses with both C and D probes (Desarnaud et al., 2019).

Figure 2-19 is an illustration of the probe type D results plotted against volume. The sandstone types tested in this figure were stored at a relative humidity, RH of $48 \pm 2\%$ with a temperature maintained at $20 \pm 2^\circ\text{C}$. According to the authors, Figure 2-18 and Figure 2-19 show that representative hardness is obtained on a sandstone specimen at a volume greater than 60 cm^3 and at a thickness greater than 13 mm.

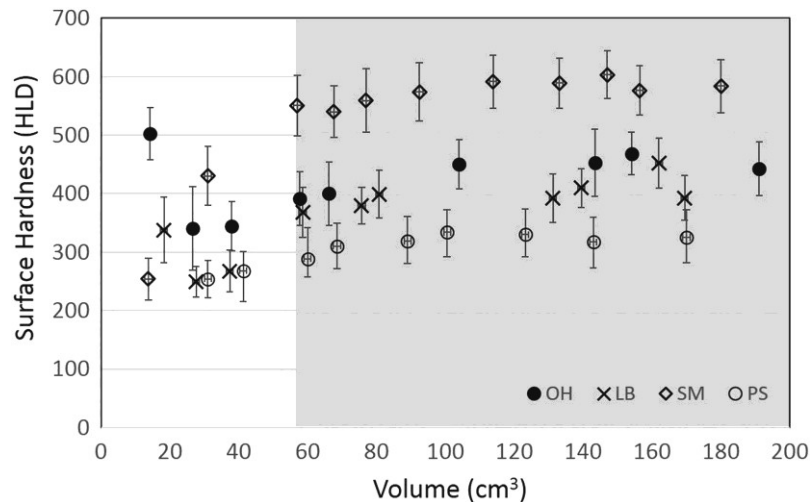


Figure 2-19: Hardness versus volume – specimens stored at $48 \pm 2\%$ RH and $20 \pm 2^\circ\text{C}$ (Desarnaud et al., 2019).

To examine moisture content, nine 50x50x50mm blocks were stored/ prepared in three different ways: three blocks were submerged for 24 hours in water under vacuum, three blocks were stored for two months at an RH of $48 \pm 2\%$, and three blocks were dried for 24 hours at 60°C and cooled down in a desiccator at room temperature ($20 \pm 2^\circ\text{C}$) maintained at an RH of 0%. In the aforementioned order, these blocks were described as being ‘saturated’, ‘medium wet’, and ‘dry’. Using the gravimetric method, moisture contents were calculated. The result of both probes using SIM and RIM on specimens of each moisture condition is illustrated in Figure 2-20. It can be observed from the data that both devices produce similar trends. They analyzed the results of the type D probe and felt they were able to link the results from dry to medium, to pore size. Out of all sandstone types, the LB and SM had pore sizes less than $0.1 \mu\text{m}$ causing the highest uptake of water ($20 \pm 2\%$), while the OH and PS had larger pore sizes and had the lowest uptake of water ($0.03 \pm 0.01\%$ weight increase). As a result, a higher decrease in hardness could be seen in the LB and SM specimens while the OH and PS specimens seen less of a drop in hardness (less than 5% drop).

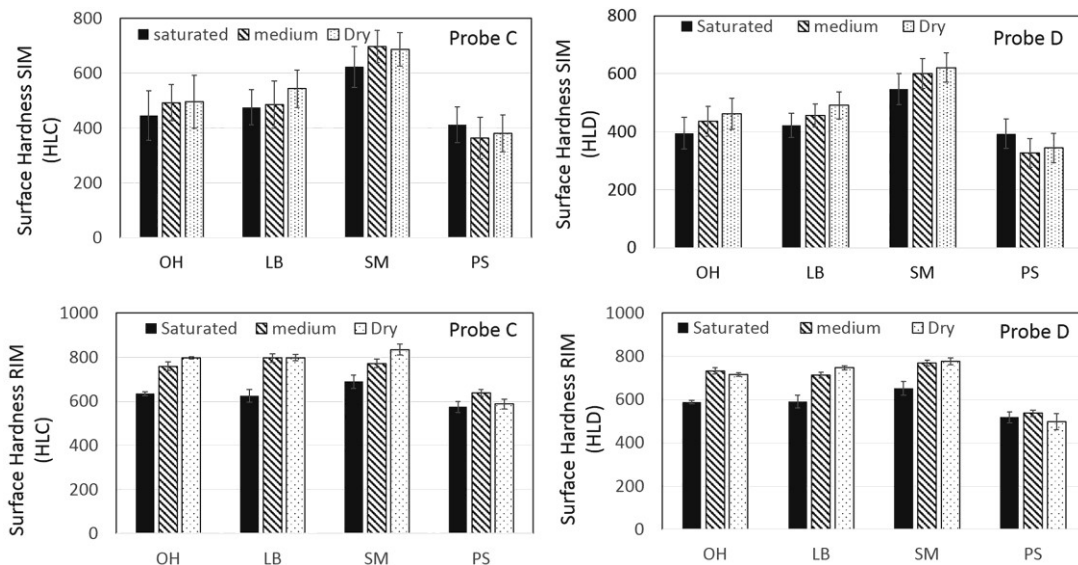


Figure 2-20: Hardness of the four sandstone types at different moisture conditions (Desarnaud et al., 2019).

From dry to saturated, uptake of water from OH, LB, SM, and PS was $10.2 \pm 0.2\%$, $12.2 \pm 0.2\%$, $5 \pm 0.1\%$, and $15.5 \pm 0.2\%$. Of all sandstone types, the PS experienced a hardness increase ($10 \pm 2\%$) for both devices. The occurrence of this is thought to be the result of its high clay content with surface voids being filled with incompressible water. The other three sandstone types seen a decrease in hardness. For OH, LB, and SM, hardness reduced by 17%, 16%, and 13% for the type D probe and 11%, 14%, and 10% for the type C probe. For RIM from dry to saturated, the hardness reduced 20-26% for all sandstone types except for PS. It was concluded that the moisture does influence the hardness readings and that measurements should be performed on dry blocks if possible so that all rock being tested have the same moisture conditions.

To examine roughness, four additional sandstones types were retrieved from Germany and USA. For all eight sandstone types, 10 blocks were prepared to 50x50x50 mm and surfaces were treated with sandpaper ranging in grit from 19 to 715 μm . Using a Keyence VHX6000 3D microscope, roughness measurements were made on each surface prior to testing. On each block, three zones with an area of $1 \times 10^6 \mu\text{m}^2$ were randomly selected and the 3D surface texture parameters of Sz (maximum distance from the deepest point to the highest) and Sa (arithmetic surface roughness) were extracted. Using the type D probe and SIM, the Sz for each prepared surface of each sandstone type was plotted against hardness (Figure 2-21). It was found that hardness readings were unaffected by roughness ranging from 100 to 800 μm . It should be noted that the Leeb hardness manual for device use on metals states that the maximum workpiece roughness should be $\leq 1.6 \mu\text{m}$. The authors result not only verifies Verwaal and Mulder's 1993 conclusion of roughness between differing surface treatment options showed no hardness difference, but for the first time on rock, a roughness within a quantifiable range far rougher than 1.6 μm can be said to not affect hardness readings.

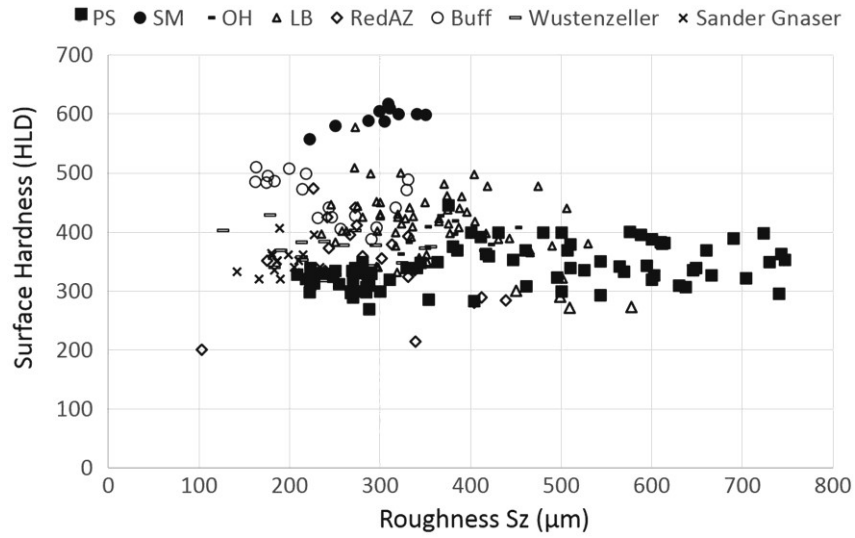


Figure 2-21: Hardness against surface roughness (S_z) found with type D probe (Desarnaud et al., 2019).

As these authors are primarily focused on built heritage, they wanted to investigate the suitability of each probe type on rock surfaces that could be more vulnerable in nature, such as on rock art panels. As the sandstone types involved in their research is used in said built heritage, they wanted to know how much damage would be inflicted on the rock surface after 1, 5, 10, and 20 strikes of each probe. While using the 50x50x50mm cubes of the original four sandstone types used in the roughness determination exercise, strikes were performed in three random locations and analyzed under the microscope in $1 \times 10^6 \mu m^2$ areas surrounding the impact location. Eq. 17 was developed by the authors to quantify surface deformation. A negative surface deformation, $\Delta L/L$ is an indicator of a slight flattening of the surface due to the crushing of asperities, while a positive value indicates an increase in roughness reflecting a newfound deformation.

$$\Delta L/L = -(S_{z0} - S_z)/S_{z0} \quad \text{Eq. 17}$$

Where:

S_z (μm) = largest peak height value summed with largest pit depth value in defined area

S_{z0} (μm) = roughness at impact location prior to impact

S_{zx} (μm) = roughness at impact location after x Equotip impacts

The surface deformation seen on the four sandstones following each successive set of impacts were plotted against hardness found with SIM and RIM and are displayed in Figure 2-22(a)(b). In addition, depth of indentation plotted against ‘UCS’ is displayed in Figure 2-22(c).

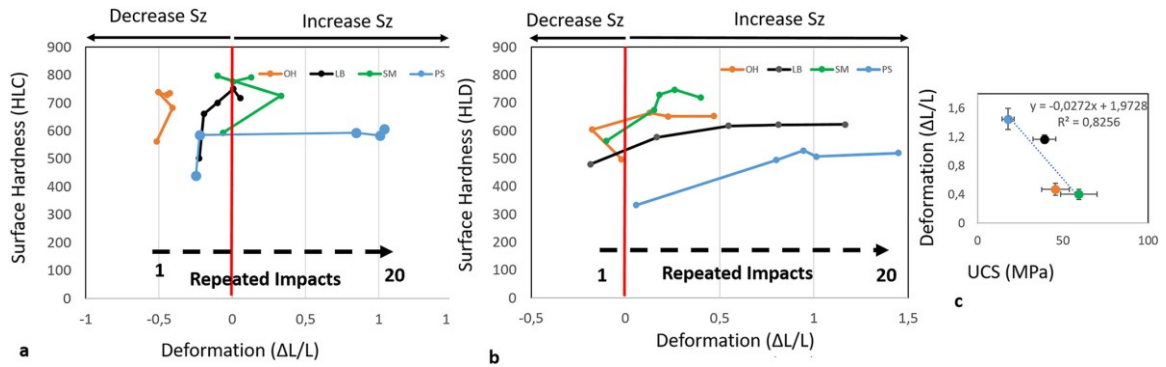


Figure 2-22: Hardness and deformation after 1, 5, 10, 15, and 20 repeated impacts with the probe type C (a) and type D (b) on OH, LB, SM, and PS. (c) Deformation (depth of indentation) against ‘UCS’ (Desarnaud et al., 2019).

With reference to Figure 2-22(a)(b), any plotted points left of the red vertical line represent asperity flattening while any point plotted to the right is a representation of indentation. For probe type D, a single impact on all sandstone types except PS resulted in a slight flattening and for all cases, after initial indentation into the surface, the indentation depth increased with increasement of impact set. For probe type C, all sandstone types seen minor flattening at the outset, with PS being the only sandstone type seeing considerable deformation. Figure 2-23 shows the surface topography of the SM and PS sandstone types after 1, 10, and 20 repeated impacts of the type D probe.

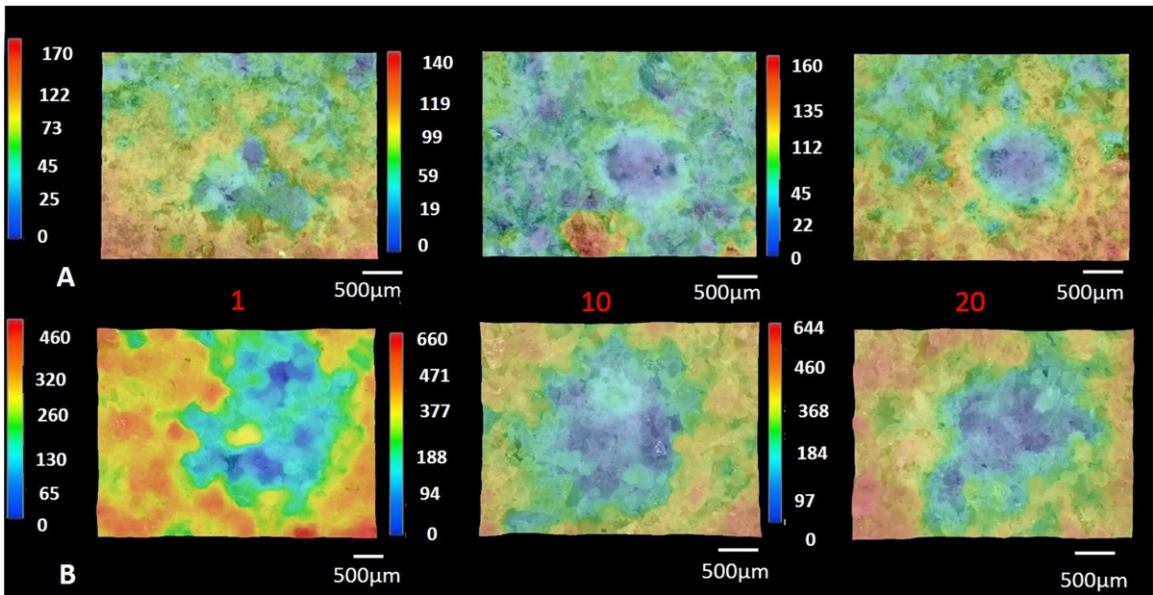


Figure 2-23: 3D microscope representations of 1, 10, and 20 probe type D impacts for (A) SM and (B) PS. The vertical scale bars show the variation in heights in μm (Desarnaud et al., 2019).

Likewise, Figure 2-24 shows the same sandstone types and number of repeated impacts but completed with the type C probe.

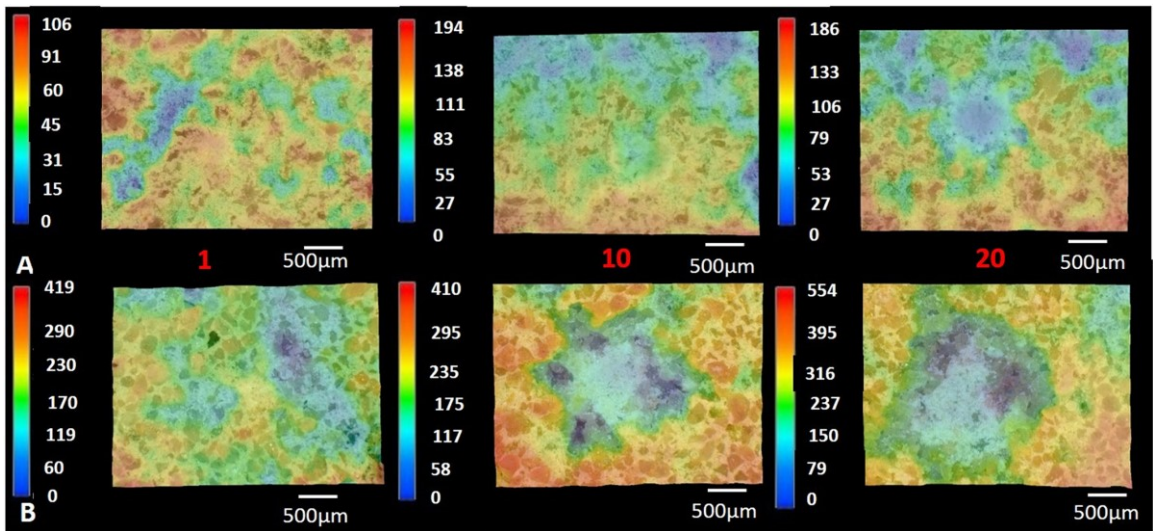


Figure 2-24: 3D microscope representations of 1, 10, and 20 probe type C impacts for (A) SM and (B) PS. The vertical scale bars show the variation in heights in μm (Desarnaud et al., 2019).

The main conclusions from this exercise were that the probe type C is a better device to be used on great-valued heritage sandstone as little damage is observable; however, the authors point out that deformation needs to occur in the surface by the

impact body in order to get a valid hardness result. Their reasoning dates to Hertz in 1882 who said a permanent mark is required at the contact area center to be able to get an absolute hardness value of that material (Hertz 1882 cited in Fischer Cripps 2005). Although unsaid, it is understood that these authors are suggesting the use of the type C probe if a slight deformation can occur on the surface, otherwise the type D should be used. Figure 2-22(c) showcases further novel work by the authors demonstrating a strong correlation between rock strength and amount of deformation. In this plot, a strong correlation ($R^2 = 0.8256$) exists between ‘UCS’ and surface deformation on the four sandstone types tested using the probe type D and RIM with the full 20 impacts. The data from both Figure 2-22b and Figure 2-22c have been digitized and are displayed in Table 2-11 for the probe type D.

Table 2-11: Digitized data from Figure 2-22b and Figure 2-22c for type D probe (after Desarnaud et al., 2019).

Sandstone	‘UCS’ (MPa)	$\Delta L/L$	HLD
SM	60	0.4	720
OH	46	0.5	654
LB	39	1.2	621
PS	18	1.5	520

As a final area of investigation, the relation between ‘UCS’ and hardness was examined with incorporation of the intrinsic rock properties of density and porosity. For each of the eight sandstone types, ten 25x25x50 mm prisms were uniaxially compressed in a 5885H Instron. According to the authors, the result of any individual test was discarded if the test value differed from the average by more than 30 %. The ‘UCS’ value for that specific sandstone type was the average of at least six test results. Following the guidance of the Swedish Standard SS-EN 1936:2006 (European Committee for Standardization, 2006) on natural stone test methods pertaining to density and porosity, the bulk density was obtained using Eq. 18. Each specimen was oven-dried to constant mass at 60°C (m_d), then air within the pores were eliminated in a desiccator under vacuum for 24 hours. Water was then introduced into the vessel and the specimen remained under vacuum for 24 hours. The specimens were next weighed in water (m_h)

and then in air (m_s). With the density of water taken to be 1000 (kg/m^3) by the authors, the bulk density was found.

$$\rho_b = \frac{m_d}{m_s - m_h} \times \rho_{rh} \quad \text{Eq. 18}$$

Where:

ρ_b (kg/m^3) = bulk (apparent) density

ρ_{rh} (kg/m^3) = density of water

m_d (g) = mass of dry specimen

m_s (g) = mass of saturated specimen

m_h (g) = mass of specimen immersed in water

Hardness was found using SIM and RIM with both probe types and a relation was found against ‘UCS’; however, they found that when hardness was multiplied by the bulk density of the rock, the correlation improved (Figure 2-25).

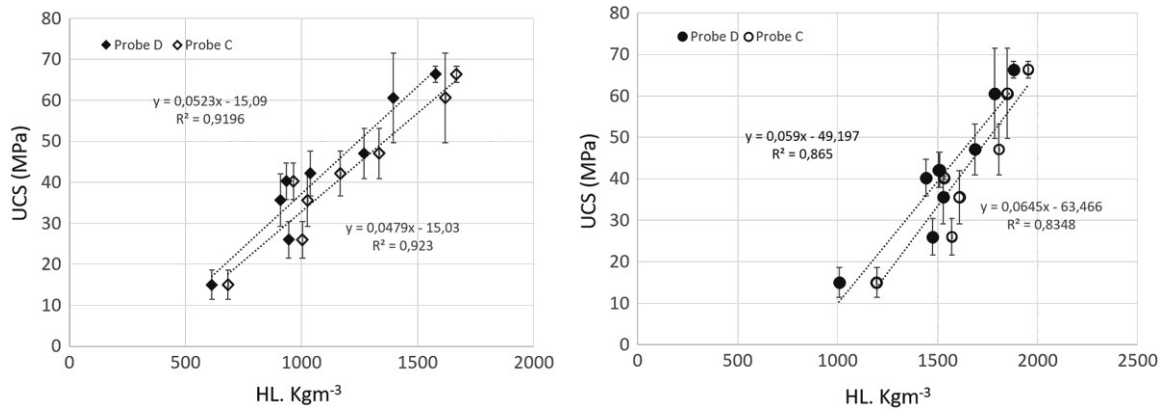


Figure 2-25: ‘UCS’ (MPa) versus hardness x density for probe type D and type C on all eight sandstone types. Results of SIM are shown in the left illustration while results of RIM are shown in the right (Desarnaud et al., 2019).

Although a different methodology was used to find the Unconfined Compressive Strength, the same two conclusions drawn by Asef in 1995 could be drawn by these authors: 1) the randomly located impacts of the SIM produce the stronger correlation than the single location RIM; and, 2) the probe type C when used in SIM produces the highest overall correlation. It should be noted that these authors and Asef found these two conclusions to be true regardless of if density was multiplied with a single parameter

(Desarnaud et al. and Asef) or with both (Asef). A noteworthy difference between the findings of Desarnaud et al. and most of the other successor authors' work is the strong correlation found with a linear relationship. The authors attribute this to being the result of tests performed on the same rock type (sedimentary) with a narrow 'UCS' range of within 10 and 70 MPa for 8 sandstone types.

The guidelines of the Swedish Standard SS-EN 1936:2006 (European Committee for Standardization, 2006) were also followed to find open porosity (Eq. 19).

$$\rho_o = \frac{m_s - m_d}{m_s - m_h} \times 100 \quad \text{Eq. 19}$$

Where:

ρ_o (%) = Open porosity of the specimen

The results of probe type C and D for SIM and RIM are presented in Figure 2-26. It can be observed that hardness reduces with porosity increase.

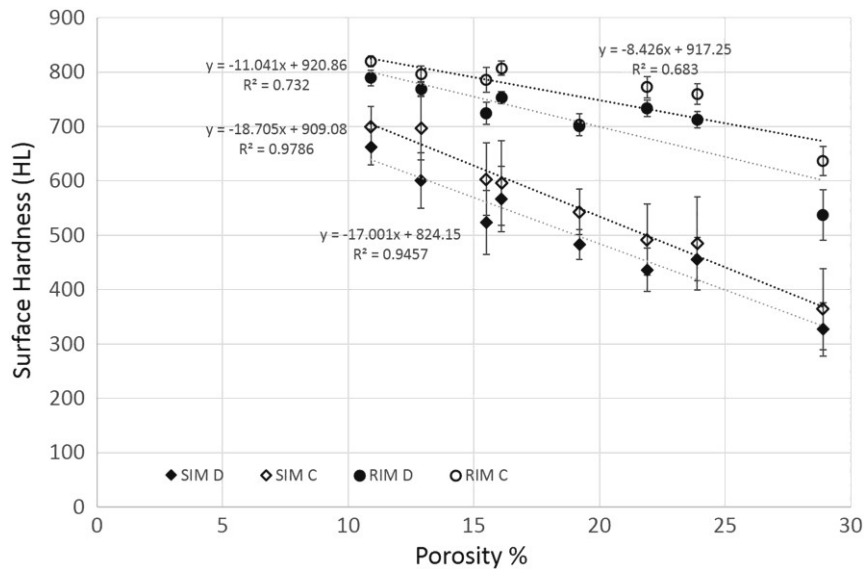


Figure 2-26: Hardness on all 8 sandstone types of varying porosities using SIM and RIM and both probes (Desarnaud et al., 2019).

The sets of data plotted in Figure 2-26 were also best captured with a linear trend line with the strongest correlation being for SIM in comparison to RIM, with the highest correlation being for the type C probe used in the SIM. A conclusion made by the authors is that surface hardness testing does have the ability to determine the degree of rock

weathering present. This is because reduced hardness results found on a surface is partially the result of increased porosity due the deterioration of the surface and near-surface rock material. The increased presence of cracks, blistering, scaling and disintegration seen in the weathered profile of a rock means that there is a greater quantity of voids present than there would be in the intact rock which means an increase in porosity and lower hardness values.

3 RESEARCH METHODOLOGY

Perhaps the best way to find the true extent of weathering is to follow the method used by Hack et al. in 1993 (Section 2.3.2): grind the rock down beginning at the weathered surface and perform hardness testing at each depth interval until a consistent hardness value is found with depth. By performing this method, the hardness gradient and the data scatter found on each tested surface provides valuable insight into determining a realistic L_D value that represents the natural surface. This value substituted into an appropriate L_D to σ_c equation will predict a JCS value for the surface of each rock type. But of paramount importance to understand the validity of the results obtained on the device is to determine the influence zone for the Leeb device and the effects of surface roughness on the results. As a goal of this study is to determine a methodology to predict JCS values, the influence zone for the Leeb device, the weathered depth, the hardness gradient, the amount of scatter on each surface and the roughness effects must be understood.

Inherent variability exists in hardness and strength values found on rock. This is mainly because of the inherent variability of the characteristics of the rock itself. A laboratory derived correlation equation on prepared intact rock specimens is believed by the author to be the best way to reduce this inherent variability as long as the specimens are all prepared the same and to a size unaffected by size effects. A field derived correlation equation on weathered rock, such as that proposed by Asef, is believed by the author to include far more inherent variability and was therefore not pursued. In this study, the correlation equation (Eq. 16) and corresponding ‘All rock types’ constants (Table 2-8) of Corkum et al. 2018 has been used in this research to try and achieve this objective.

A laboratory derived unweathered, intact rock L_D to σ_c correlation equation is an equation that was derived from hardness value that were uninfluenced by any underlying material of differing properties or by surface roughness. An L_D value used with this equation will produce accurate results as long as the L_D value was obtained on surface material that produces hardness results that are uninfluenced by any underlying material or by surface roughness. Therefore, the goal in this study was to determine how thick of weathered material would be required to produce an uninfluenced, representative L_D

value that can be used in Eq. 16. The answer to this is dependent on the influence zone (determined in this study) once roughness influences are removed from the L_D value selected to represent the natural surface. The idea is that a thickness too thin (less than the determined influence zone thickness) would require a correction to truly produce a valid result. If the thickness is greater than the thickness of the determined influence zone, then the L_D value is considered valid. For the case of a weathered profile being too thin it should be considered as producing 'influenced' values rather than being truly invalid. This value is considered by the author as being much more accurate than what can be found with another device such as the Schmidt hammer or a value selected based on a guess. The level of 'influence' is dependent on how thin the weathered thickness actually is. By viewing this L_D value as being 'influenced', the engineer can choose at their discretion how best to work with that value and will likely be based on the specifics of the project and/or their experience. A correction factor once found is envisaged to be in the form of an equation with respect to weathered thickness and is outside the scope of this study.

The author is of the understanding that the validity of any hardness reading found on a natural surface, regardless of any correlation equation used, has to do with three pieces of information: 1) the volume or thickness of material influencing the hardness value; 2) the actual amount of volume or thickness of rock that is present above the intact rock; and, 3) the effects of the present roughness. The second and the third points are dependent on each rock tested, while the first point (influence zone) is considered in this research program as being constant amongst any rock type. Unlike Hack et al. in 1993 (Section 2.3.2) who assumed that the material in the weathered profile is of the same strength and that any increase in readings upon nearing the intact material is an indicator of the sole influence of the underlying material. The author believes that a gradation in hardness with depth in a weathered profile exists. Therefore, to satisfy the first point, in this research program the zone influencing the hardness readings is found using materials that do not vary in hardness with depth so that the influence of the underlying material can be understood. The influence zone, said to be independent of the influences of any underlying rock type in this research program, was found using artificial material and Wallace sandstone. As well, this same influence zone experiment was conducted on

natural rock composed of two rock types in contact with each other. The procedure to make these specimens and to test them are explained in detail in this chapter. The second point is satisfied when the depth of weathering is determined on the rock in question. The third point is determined by evaluation of the standard deviation of the data making up L_D found on the natural surface in comparison to the data making up L_D found on surfaces without surface roughness. Whether the readings seen on the display of the hardness device is showing a true reading of surface hardness or not can be understood with the information of all three of these points. Contained in this chapter is a detailed discussion of the activities that were conducted in this study to find these pieces of information. This chapter discusses how each task in the study was done and the rationale behind each.

3.1 LABORATORY WORK

The main component of this research program involved laboratory work and thus an extensive set of guidelines to be followed while working in the laboratory was developed. The details in this section were established in the early beginnings of this research program as a way to ensure that the author could productively prepare and test all specimens in a thoroughly thought-out manner. This methodology would ensure uniformity amongst the specimens with respect to how they were prepared and to how they were tested, all the while providing confidence to the author that important steps were not being missed while work was being performed. In addition, having a set of guidelines that were methodically established allowed the author to work out whether the operations would be successful and if they could be conducted in a safe and practical way.

It should be mentioned that two terms are predominantly mentioned for the remainder of this thesis document: ‘primary’ and ‘secondary’ materials. These two terms were coined as such to describe a component of each rock specimen used in the research. For all intents and purposes, the primary portion of the rock specimen refers to the lower, or underlying (intact) material while the term secondary is used to describe the upper, or overlying joint surface material. As will be recognizable in the forthcoming sections, secondary material can be the same rock type as the primary material but with a change

in properties, or it can be a completely different material, be it artificial or natural rock. In addition, the denotation of SS refers to specimens, artificial or natural where the ‘secondary material is softer’ than the primary material. Likewise, SH is used to describe specimens where the ‘secondary material is harder’ than the primary material. WA is used to describe ‘weathered and/or altered’ specimens and UM is used to describe ‘uniform material’ specimens where the secondary and the primary material have similar hardness. In the laboratory, three categories of specimens (Figure 3-1) were created and are listed as follows in the assigned category names: 1) artificial material and rock, 2) natural rock transition, and 3) naturally weathered rock. These specimens, how they were prepared and how they were tested are described in this section beginning with the first category of specimens and finalizing with the second and third being described together.

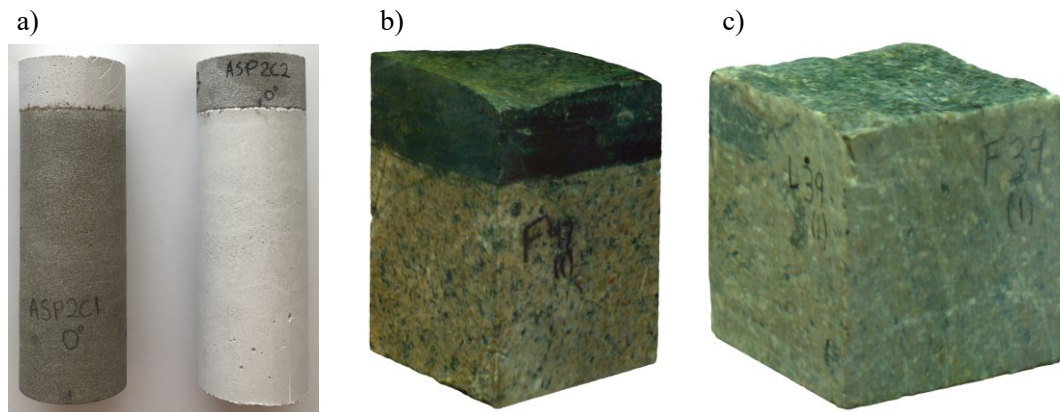


Figure 3-1: Three categories of specimens created in the laboratory: a) artificial composite material (plaster and rock), b) natural rock with a clear primary and secondary material interface, and c) naturally weathered rock (gradient).

3.1.1 ARTIFICIAL MATERIAL AND ROCK

Composite specimens of artificial material and sandstone quarried in Wallace Nova Scotia, hereinafter referred to as Wallace Sandstone, were prepared. As displayed in Figure 3-1a, two configurations were made. The left sample in the figure shows an example of the first configuration: Wallace Sandstone as the primary component with a single artificial material secondary layer of differing thicknesses on each specimen. The right sample in the figure shows an example of the second configuration: artificial

material as the primary component with a single secondary layer consisting of varying thicknesses of Wallace Sandstone on each specimen.

Natural rock is inherently comprised of heterogeneities including, but not limited to the individual grain size, dimensions, orientations, types, stiffnesses as well as the stiffness of the boundaries connecting the grains. In a three-dimensional sense, the number of varying conditions present in any rock is infinitely large. A rock type that truly has a homogeneous and isotropic set of conditions is non-existent; however, if one wanted to find a somewhat close rock type to these conditions for research purposes, a sandstone can be used. Wallace Sandstone was selected in this research program for this reason as well as it can conveniently be obtained in Nova Scotia where this research work was conducted.

Four Plaster of Paris mix designs were selected for the artificial material used in this research. Both the Wallace Sandstone and the Plaster of Paris mixes were considered as being homogenous and isotropic. The hardness of the cured artificial material and the Wallace Sandstone were found and UCS tests were conducted solely on the artificial material to determine an approximate strength for each of the four mixes. It is important to note that from the authors experience, the artificial material properties vary slightly depending on many factors such as: water temperature, atmospheric exposure of the mix (amount of surface exposed to the atmosphere i.e., mixing bowl size), the state of curing present in the mix at the time of the pour, the temperature in the room on the day of the pour and curing conditions such as the level of humidity, air circulation, etc. Moreover, testing conditions can present a significant factor in the results; for example, in UCS testing, the loading rate and the time to failure can cause differences in results. All attempts can be made to make specimens to be identical, however some inherent variability exists regardless of the level of effort in making them. With this being recognized at the outset, and since the Plaster of Paris product cures quickly, a plan was established to focus on pouring two sets of composite specimens with the same mix. Hereinafter referred to as a 'set', these two composite specimens have the same secondary layer thickness, one of artificial material and one of sandstone. As an example of this, both specimens shown in Figure 3-1a were poured at the same time and is what is being referred to as a 'set'. Each set was poured with a single mix of artificial material

and all sets with that mix design were poured in the same day. Testing results found on the artificial material of the one specimen in the set will directly be linked to the other in the set as the characteristics of the mix is the exact same. In this fashion, absolute uniformity across all specimens in this research component is not necessary, instead the results of each set can be viewed independently. With the properties remaining the same, the variation in the hardness results found on differing thicknesses of the material when overlying the alternate material could be explored. Any difference would be an indication of the primary material influence. This difference would be seen as follows: an increase in hardness would be seen for SS specimens and a decrease in hardness would be seen for SH specimens. The objective in testing these specimens was to determine how the thickness of the secondary material affects the hardness test results. It was the goal in this research program to find the thickness range that is affected by the underlying material and the thickness in which hardness results were no longer affected. By preparing and testing specimens with the secondary layer being both harder and softer than the primary material, the true influence of the underlying primary material was anticipated to be discernable in the results.

In rock mechanics literature, correlations between L_D and σ_c for soft rock is scarce but the importance of knowing this information is of great necessity. With this limitation of data, difficulties currently exist with finding a L_D to σ_c correlation equation that is also suitable for soft rock. This is applicable obviously for intact, soft rock, but in regard to rock discontinuity research, this is specifically problematic for weathered surface data if the surfacing material is very weak. As the overall stability of the rock mass relies on the strength of the rock wall material in the discontinuities, the knowledge of soft rock properties is therefore of an apparent need. Figure 2-17, Section 2.3.2 produced by Corkum et al., 2018 is a plot combining nearly all the L_D to σ_c data in the literature prior to 2018 and shows the rock grades produced by ISRM, 1978 seen in Table 2-4, Section 2.2.1. It can be observed from this figure that a scarcity of data exists for rock of lower strengths, especially for the rock grades of R0, R1 and R2: strength ranges easily obtainable with artificial materials. It therefore seemed fitting to create the four artificial material mix designs to produce artificial rock that would represent rock in the three weakest ISRM designated categories of R0, R1, and R2. Largely inspired by the

evolutionary rock discontinuity work of Patton (Section 2.1.2) in 1966, two mix designs were established replicating his Plaster of Paris to sand and water ratios that were seen in Table 2-1. Patton used quartz sand as a strength reducer while the author used a fine-graded, all-purpose sand as a substitute for quartz sand. The other two mix designs were of Plaster of Paris and water as per the manufacturer’s instructions (listed on the bag), and Plaster of Paris and water with Diatomaceous Earth as a strength increaser. The breakdown of the mix designs by mass used in this research can be seen in Table 3-1.

Table 3-1: Artificial mix designs to produce the rock categories of R0, R1, and R2 described in Table 2-4 which shows a table reproduced from the ISRM Suggested Methods (1978).

Mix Classification	Plaster of Paris	Water	Sand	Diatomaceous Earth
3:2	2	0.85	3	-
3:1	1	1.48	3	-
Just Plaster	1	0.5	-	-
Dia Earth	1	0.45	-	0.014

How the curing times for each artificial mix was found, how the composite specimens were made, and how they were tested is presented in the forthcoming sections.

3.1.1.1 STEADY STATE CURING BEHAVIOUR SPECIMENS

The amount of time required for an artificial material mix to reach a state of negligible strength increase with time, can be determined by performing UCS tests on several specimens of that mix, cured to different ages. After a certain curing age, the σ_c value stabilizes and has reached a ‘steady state’. By curing all specimens in this research component to a point of steady state would mean that all hardness readings found on each specimen reflect that of the true strength of the mix. If testing prior to the point of steady state, these hardness results would reflect that of a weaker strength and would differ from the results found on the same specimen if it was cured longer. As the whole objective of this research component was to test a material of a uniform nature, it was imperative that the author was sure that the strength would remain unchanging for each mix during the time of testing. As was mentioned in Section 3.1.1, four artificial material mix designs were used in this research program; all of which used Plaster of Paris, with three exhibiting a strength reducing or increasing filler material. Of these four, two mix designs

were selected to determine the steady state curing behaviour of a Plaster of Paris mix; the results of which were assumed to be characteristic of all four mixes. From Table 3-1, the 3:2 and 3:1 mix designs were selected to undergo the ‘steady state curing age’ evaluation. Cylinders conforming to the recommendations of ISRM, 1978 for UCS testing were made to the dimensions of 135mm × 54mm (length × diameter). To do this, a stainless-steel cylindrical mold hereinafter termed ‘dual specimen cast’ was created to a length allowing for two specimens to be poured with the same mix. The dual specimen cast was fastened together with two hose clamps. The longitudinal interfaces where the casts come together were continuously taped with clear tape and smoothed to ensure no groves or bubbles were present in the tape. Next the inside of the dual specimen cast was coated with canola oil. These mix designs require cold water, between 4.4 and 10°C as specified on the Plaster of Paris packaging. With a quantity appropriate to make two specimens, water was added, the mix was thoroughly mixed, and a timer was set to record the amount of time it would take for the mixes to harden enough to pour, stirring on occasion. As these were relatively wet mixes, this ranged from 8 to 14 minutes to reach a state suitable to pour. The three objects used to successfully complete the pour of two specimens is shown in Figure 3-2 and will be explained as follows.



Figure 3-2: Objects used to create artificial material UCS specimens. From left to right: stainless steel dual specimen cast, cured artificial material specimen, and a thin sandstone disk.

The mixing process was the first step: two mixes were prepared with the first one receiving water and mixing approximately 10 minutes before the second mix received

water and mixing. Standing upright on a vibratory table, the upper specimen was poured first with a hardened UCS-sized artificial material specimen overtopped by an oiled thin disk of sandstone occupying the bottom of the dual specimen cast. The upper specimen was poured in three layers, even in thickness and rodded thoroughly with a steel rod per layer. When reaching the top, the top was screed flat with a metal drywall scraper. When the second mix was nearing a state satisfactory for pouring, the dual specimen cast was flipped over and the hardened UCS-sized artificial material specimen that was occupying the lower part of the cast was removed. The second mix was used to pour the second specimen following the same procedure as was conducted on the first pour. After curing for no less than one hour, the dual specimen cast was opened (Figure 3-3) and the specimens were extracted and set to cure in an enclosed tent-like unit with a Relative Humidity, RH maintained at $45\% \pm 5\%$. For both mixes, 6 specimens were tested ranging in age from 3 to 27 days, and the curing behaviour and the time to reach the point of steady state was identified.



Figure 3-3: Two artificial specimens made to ISRM, 1978 standards for UCS testing.

3.1.1.2 ARTIFICIAL COMPOSITE SPECIMENS

As was alluded to in Section 3.1.1, one set consisting of two specimens was created at a time. In total, 80 artificial composite specimens were created, 20 per mix design (Table 3-1), 40 being SS specimens and 40 being SH specimens. This amounted to 20 individual artificial material pours completed in the same day over four total days. Sandstone cylindrical specimens with a 50 mm diameter were prepared to a length of approximately 125mm to be used in the production of the SS specimens. Similarly, for each mix design, there were 10 sandstone disks of varying thicknesses ranging from approximately 2 to 30 mm and were used in the production of the SH specimens. The following three sections discuss the procedures followed to produce these 80 specimens.

QUANTITY AND LENGTH OF MOLDS

Acrylonitrile-Butadiene-Styrene (ABS) pipe with an inside diameter of 50 mm was used as a mold to produce artificial composite specimens of both composite types. Using a table saw, the ABS pipe was cut transversely to the exact length of the anticipated composite specimen to be prepared within it, then each length was cut longitudinally along one side of the pipe. Jigs were created out of wooden pieces to safely make each cut. Sandpaper of 120 grit was lightly used to remove the burrs present along the cuts. Eight composite specimens were to be poured to the same length, two per mix design, and four mix designs total. To pour the two specimens in a set with the same artificial material mix, two molds were created for each anticipated length of specimen. In total, 20 ABS pipe molds were created to 10 different lengths. The lengths of the molds ranged in length from 127 to 155 mm to produce artificial composite specimens with secondary material thicknesses between 2 and 30 mm. The sandstone cylinders and disks were measured with a digital caliper at marked out locations of 0, 90, 180, and 270° from the assigned front and were recorded. On the molds, the digital caliper was used to measure the lengths of the molds at marked locations of 0, 90, 180 and 270° from the assigned front. By lining up the assigned fronts of the molds with that of the cylinders and disks, the exact thickness of the primary and secondary artificial material were easily found.

MOLD PREPARATION

For all molds, sandstone cylinders were inserted into the molds, and the molds were taped around their circumference in a fashion which would ensure the perfect interior dimension could be maintained within the mold during each pour. The sandstone cylindrical specimens would next be removed and the longitudinal cut on the inside of each mold was taped with a wide, continuous strip of clear tape. Next canola oil was lightly coated on the interior of the molds. Close attention was paid in this step to ensure that the canola oil coating was thin enough to prevent downward running onto the sandstone surfaces during the pours. For the ease of the pouring operation, all 20 molds to be poured were prepared in this way prior to beginning any pours.

COMPOSITE SPECIMEN FORMATION

The sandstone cylinders and disks prior to being used in the formation of these composite specimens, were confirmed by the author as being free of any oil residue produced during the cutting process. This was considered as being paramount to ensuring a fixed connection could be achieved between the artificial material and the sandstone. In all cases, the sandstone components of the composite specimens were placed in the molds to exist at the bottom at the time of the artificial material pour. The methodology behind this was to incorporate gravity into the pour of artificial material for it to uniformly adhere to the sandstone. From experience of the author, air voids could potentially exist along the interface of the sandstone and artificial material if the sandstone is added from the top. However, due to gravity, the flow present in the artificial material due to the weight of the overlying, added artificial material, vibration from the vibratory table, and rodding during placement, all air voids were expected to be eliminated along this interface. To do this, the sandstone components with the selected interfacing surfaces locating upwards, were placed standing upright on a small, flat, and moveable surface i.e., 20 x 10 x 0.5 cm piece of plywood. The reason for the moveable surface was for easy relocation onto a vibratory table at the time of artificial material pour. The molds for each composite specimen were placed over top of the sandstone components and the assigned fronts marked on the sandstone and the molds were aligned (Section 3.1.1.2). The next objective was to establish an expected mass of the artificial material to be present in each composite specimen set. This mass was predicted from the mass of the artificial specimens made for the purposes of finding the steady state curing age (Section 3.1.1.1) based on volume comparison and the retrieved mass found at the time of testing. Next, the quantities of the components of the mix design were found and the mixing process could begin. All 20 specimens for each mix classification (Table 3-1) were poured one set at a time, with 10 individually prepared mixes for each mix classification. Between each artificial material pours, the remnants of the artificial material in the mixing bowls needed to be removed and the bowls left in a clean state for the new mix design components to be added for the next pour. Additionally, for each mix, cold water between 4 and 10° was obtained at the time of mixing and the set-up time of the mix to get it to a state where it could be poured was recorded. As the time varied between mixes,

even of the same mix classification, the author used his judgement from his own experience of when to make the pour. Careful attention was paid to ensure that each mix at the time of pour was not too wet as well as not too hard. In all cases, the vibratory table was initially set on low and was increased when the full pour was completed and maintained until the mixture was seemingly too hard to gain any benefit using vibration. The amount of mix added slightly exceeded the top of each mold and the mixes were vibrated until all air bubbles appeared to have been expelled from the top of the specimen. Next, using a metal drywall compound spreader, the top of each specimen was screed level with the top of the mold. Close attention was paid in each case, especially when sand was present in the mixes, to ensure the top of the specimen was smooth and visually exempt from ambiguities. As was the case for the achievement of a uniform strength described in Section 3.1.1.1, the achievement of a uniform roughness was of great importance to ensure that the effects of roughness could be exempt from the obtained hardness findings. Again, complete homogeneity was the goal so that the findings with the Leeb hardness device could be completely attributed to the thickness of the secondary material.

MOLD EXTRACTION AND CURING

As a full day was typical to complete the pour of a single mix classification (Table 3-1), the specimens were left to cure in the enclosed tent-like unit maintained at $45\pm 5\%$ RH overnight. The next morning, each composite specimen was carefully extracted from the mold. This began by removing the traversing exterior tape on the exterior of the mold then applying a slight twist to a flat-head screwdriver inserted into the longitudinal saw cut of the mold in a few different locations which ‘popped’ the mold from the hardening composite specimen. When the mold ‘popped’, a 5 mm wedge-like object was placed inside the longitudinal cut in the mold to prop the mold open and the mold was then lifted upwards off the specimen. Each specimen, while still on the movable wooden piece of plywood, was placed back in the enclosed unit in a safe location to be left for the duration of the curing period. A $45\pm 5\%$ RH was maintained inside of the enclosed unit for this entire duration.

3.1.1.3 TESTING – ARTIFICIAL MATERIAL STRENGTH

For the purposes of understanding the steady state curing behaviour, the six specimens cured for each mix as discussed in Section 3.1.1.1 were at the ages of 3, 11, 13, 18, 22, and 27 days for the 3:2 mix and 5, 10, 15, 19, 20, and 24 days for the 3:1 mix at the time of UCS testing. The σ_c , the cure behaviour, and the steady-state range across the respective age range for each mix classification was determined. The σ_c value for these two mixes while in the steady state range were taken to be the peak strengths of these two mixes. For the other two mix classifications (Table 3-1), four UCS tests were conducted on the Plaster of Paris specimens mixed with Diatomaceous Earth, hereinafter referred to as ‘Dia Earth’ specimens and one UCS test was completed on the specimens hereafter abbreviated as ‘Just Plaster’. The latter specimens consist of Plaster of Paris and water only. Both the Dia Earth and the Just Plaster specimens were prepared to 125 × 50 mm (length × diameter). It should be noted that no UCS testing was conducted on rock as part of this research program including on the Sandstone used in this research component.

3.1.1.4 HARDNESS TESTING

No Leeb hardness testing was conducted on the steady state curing age specimens described in Section 3.1.1.1 for several reasons. The main reason was that the specimens prepared for that exercise were of the two weakest mixes out of the four (Table 3-1) and even when cured to their steady state was borderline too weak for the Leeb device. Another reason was due to the concern of damage from the impacts to the specimen; namely, the loading surface and the near surface depth. Risking the condition of the specimens to not even get a reading within the tolerance range on the device (Section 2.3.1) was deemed to be not worth it. It is however recommended by the author that this is done on an artificial material mixture that is strong enough to withstand the impacts of the Leeb device without damaging them. A final reason was because extensive collection of hardness data was to occur on the bottom of the SH specimens on the artificial material that is of valid UCS size (as per ASTM, D7012). As this data is pertinent to the main objective of this research component, hardness testing on the ‘steady state curing age’ specimens was not pursued.

Two methodologies were employed in testing the artificial composite specimens. Both methodologies used the TM20 approach and impact diameter range between 25 to 50 mm of Corkum et al., 2018 (Section 2.3.2). The first methodology involved testing on the tops and on the bottoms of the artificial composite specimens (80 total specimens) in their hardened, unaltered state. A reason for this had to do with an initial uncertainty by the author that the interface between the two materials would be capable of undergoing any form of alteration to the secondary material, be it by grinding or by sanding with sandpaper. Another reason had to do with the findings of Hack et al., 1993 (Section 2.3.2) which suggested an influential zone of 5 mm exists. It was initially believed by the author that the influential zone would be noticeable in the hardness findings without any modification of the secondary material thickness based on this finding of 5 mm. The second methodology, which developed after testing and analysis of the first methodology was to ‘thin’ the secondary material layers in a fashion similar to the work performed on the research component involving natural rock, to be discussed in Section 3.1.2.4. That is, by removing material to incremental depths and performing hardness testing until the underlying material is reached. On the SS specimens, this was done using sandpaper.

Sandpaper placed gritty-side up on a table with the secondary material facing downward, the artificial material layer was reduced by sanding with the specimen approximately perpendicular to the table. At each incremental depth reached, verification that a uniform thickness was achieved was confirmed with measurements taken by the digital caliper at 0, 90, 180, and 270° from the assigned front. Hardness measurements were not conducted on a surface unless the thicknesses of secondary material at all four locations were reasonably equal. In reference to Table 3-1, three Dia Earth and three Just Plaster specimens were tested upon using this approach. On the SH specimens, this was done in accordance with the methodology to be discussed in Section 3.1.2.4. Briefly, these specimens were aligned in the v-notch block of the grinding machine with the secondary to primary material interface parallel to the plane of horizontal travel of the grinding wheel. The grinding machine was set at a light grinding depth per pass (feed rate) and the sandstone secondary material was reduced. At the depth of each surface, the surface was dried with paper towel, measurements were taken, nomenclature

was added to include specimen information and surface number, photos were taken and then hardness measurements (TM20) were conducted. In reference to Table 3-1, three Dia Earth specimens were tested upon using this approach. For both specimen types, final hardness measurements were collected on the primary material surface (SS) or slightly within the primary material (SH).

It is iterated for clarity purposes, that the first methodology was employed on specimens with a secondary material that was unaltered by some form of thinning process. It was predicted initially that an increase (SS) or decrease (SH) would be seen in the hardness readings when the underlying material was in close proximity of the testing surface. The idea was that the artificial material hardness of that independent mix would be known based on tests performed on the full-sized UCS specimen in the set (SH). The increased hardness anticipated on the SS specimen in the set would have been obvious. The second methodology was employed when the thinnest secondary material thickness (~2 mm) for both SS and SH specimens tested in the first methodology were too thick to experience any notable influence of the underlying material on the hardness readings. The influence of the underlying material was detectable during the employment of the second methodology.

3.1.2 NATURAL ROCK OF DIFFERING ROCK PROPERTIES

In this category, there are two rock specimen groups: 1) specimens with an abrupt rock type transition i.e., two differing rock types are in contact and hosted in the same specimen, and 2) specimens with a naturally weathered surface (i.e., graded hardness). The transitions of rock types present in the specimens of Group 1 could be from in-filled joints, metamorphic transitions, or from sedimentary bedding to list a few examples. Group 2 specimens, although the same rock, the properties differ in the weathered profile in comparison to the unweathered rock and is therefore viewed for the purposes of this study in a similar fashion to the Group 1 specimens consisting of two different rock types separated at the transition from unweathered to weathered rock. The transition line between the two rock types in Group 1 and between the unweathered and weathered rock in Group 2 is hereafter referred to as ‘rock type transition line’ or ‘transition line’ for clarity purposes. Viewing these specimens with the same mind-frame as the artificial

specimens in Section 3.1.1.2, the rock above the transition line in both groups is hereinafter referred to as the ‘secondary material’ while the rock below is hereinafter referred to as the ‘primary material’. For clarity, the contents of this section were prepared to describe the work done on both groups of specimens in this category and is thus described as if they were the same. Unless otherwise specifically stated, the remainder of this section should be interpreted to mean that the work described is pertinent to both groups of specimens.

Natural rock in the form of boulders (samples) were prepared as cylinders and as blocks (specimens). In both cases, the specimens are prepared with a predominant primary component and an overlying secondary component. The work covered in this component of the research can be considered as a parallel to the artificial composite work described in Section 3.1.1; the difference being natural rock is present for both the secondary and primary components of a specimen and it was formed naturally. As was the case in Section 3.1.1, the strength and the hardness of the primary and of the secondary material are different. The work on the specimens in this category provide information on the influences of the underlying material when the rock type is different (Group 1) and when it is the same but has different properties caused by weathering (Group 2). In this section, the methodology used to be successful in completing this research objective is discussed including the planning and collection of rock in Nova Scotia, the preparation of specimens, and testing.

3.1.2.1 COLLECTION OF NATURAL ROCK SAMPLES

The third edition of the Nova Scotia Geological Highway Map was purchased at the outset of the collection process. This unique map relates the geological systems in Nova Scotia, Canada to the highway system in the province. With this map, one can identify where a specific geologic feature is exposed and accessible from a highway, be it in a rock cut along the highway, in a river, on a beach or along a coastline. This map also provides a description of what can be found at the identified location, discusses details the user would benefit from such as the distance from the road, the difficulty of the terrain in which the user would need to traverse to enter the location and information such as low tide access only. Additionally, hazards information is identified in some

locations as well as collection restrictions or regions where permits need to be acquired prior to collection. The procedure used to find suitable rock samples is described as follows:

PLANNING

The author studied the Geological Highway Map and planned one- or two-day trips to visit certain areas on the map to collect a wide variety of samples hosting unique geological features. The goal was to collect a large variety of weak to strong rock types featuring weathering/ alteration or a transition to another rock type. The characteristics and features described to be present in each rock mass would be assessed and the author would make a decision as to whether a sample obtained from this location would be a compliment to the research program or not. When several locations within close proximity of each other could be identified to have rock with characteristics and features deemed suitable to the research program, then a trip would be planned. Each trip was planned to consider cost and travel efficiency, the capacity of the authors vehicle to carry samples, tide times (if applicable), weather, restrictions, and locations of gas stations. In addition to thinking of having enough food and water, the thought of having no cell phone reception, vehicular problems such as a flat tire or hazards related to working alone were all considered.

COLLECTION

The author was successful in collecting a variety of different rock types featuring different geological attributes. It was found, however, that some locations on the Geological Highway map were not accessible; for example, a trail was no longer present or no samples could be obtained from the rock mass due to inaccessibility or no loose rock hosting the desired feature was present to take. Further, some landforms were at great distance from the nearest location accessible by road. A major limitation in this regard had to do with the authors personal carrying capacity. The author would typically hike into landform locations with a duffle bag and pick and choose the best samples that could be carried. In selecting a sample to take, apart from the obvious fact that a sample needed to be a size that could be carried back to the authors vehicle, the author followed

some rules-of-thumb: 1) a sample needed to have the ability to produce a block solely in the primary material, to the dimensions of the smallest possible size of 90 mm² as determined by Corkum et al., 2018; 2) a sample needed to have the ability to produce specimens that could have a weathered or altered surface at the top that was flat across the specimens; 3) a sample collected to host a rock type change, needed to have a contact line that was reasonably flat across the specimen and below this contact line, the smallest possible sized block (90 mm²) needed to be able to be extracted solely in the primary material; 4) the rock type and its features had to be unique to the collection (the same rock type with the same geological feature could be found in a multitude of places) and needed to offer something new to the study's findings; 5) a rock needed to be able to survive the transportation process and the specimen preparation process i.e., if the geological attributes of specific interest would not survive the cutting process, as an example, regardless of how great it seemed, it was deemed not worth it for that to be the potential outcome; and, 6) in the case of their being a limited carrying capacity and an unlikely return, samples which provided the most benefit to the study were taken and the ones that provided the least were left behind. All specimens collected were transferred back to Room 4 of the G building at Dalhousie University and the assigned sample numbers, the locations, descriptions of the anticipated geology and other information of note were added to an interactive map (Figure 3-4). Approximately 70 samples were taken from 24 locations in Nova Scotia and Prince Edward Island.

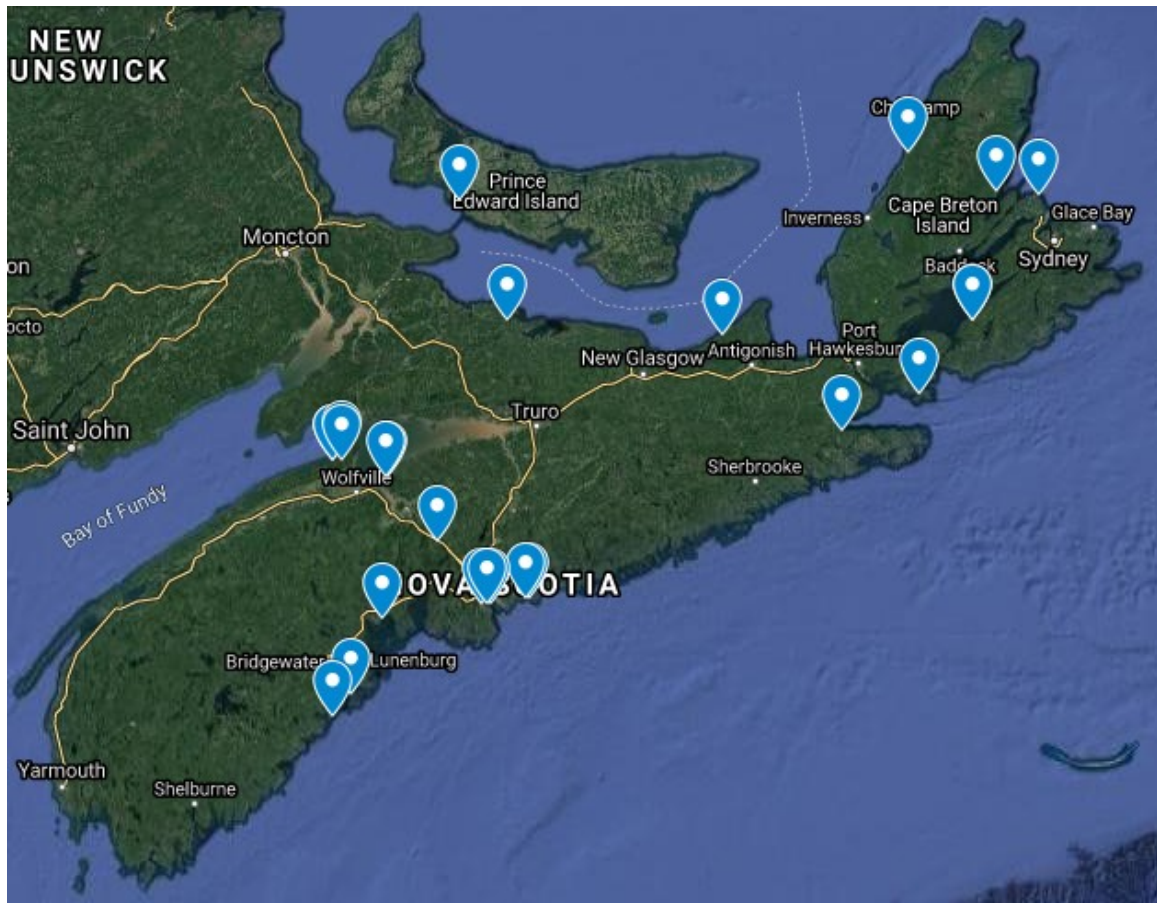


Figure 3-4: Interactive sample collection map (Google, 2021).

CLASSIFICATION

Once the sample had arrived at the laboratory of Room 4 in Dalhousie University’s G-building, sample numbers were assigned, and scaled photos were taken. All samples, regardless of actual use in the research program, were placed for photos on a clean piece of white Bristol board. Two sets of labels were created with the wording: “Front”, “Back”, “Top”, “Bottom”, “Left Side”, and “Right Side”. Further, three sets of numbers from 0 to 9 were created. Both the labels and the numbers were reused as required for the photography of each sample. A metric geological scale obtained from Dalhousie University’s bookstore, produced to supply the Earth Sciences department, was obtained for the photos. Six photos were taken for each rock sample with reference to the assigned front, to be of its front, back, top, bottom, left side, and right side. Moreover, all samples were shimmed with different objects to capture the true face of the

specified orientation and the top of each oriented face was positioned to be horizontal in the photo. Attention was paid to ensure no shims were visible in the photos. In each photo, the specimen number, the scale bar and the orientation label were included together with the sample. In all cases, prior to reorienting a sample for the next photo, review of the photo would take place to ensure the labeling, the scale bar and the sample were clear and of good quality. The original photos were filed, but as a final measure, the photos were rotated, cropped and saved to a 600 pixel per inch resolution in height and width in the image manipulation software GIMP 2.10.8. Figure 3-5 illustrates the classification photograph in the finalized form for Sample 1, showing the front orientation as assigned, together with a 10 cm long scale bar.

As a final step to the characterisation process, the author confirmed the geology with Dr. Richard Cox, an instructor in the department of Earth Sciences at Dalhousie University for most of the rock samples used to conduct testing in this study.



Figure 3-5: Photo showing the assigned front of Sample 1 together with a 10 cm scale bar.

3.1.2.2 SPECIMEN PREPARATION - BLOCKS

Room 4 in Dalhousie University's G building is termed amongst the author's research group as the 'Sample Preparation Lab'. As this term depicts, in this laboratory, rock specimens are prepared. This laboratory is host to two primary pieces of equipment that were essential in producing block specimens required for this research program: 1) an enclosed rock cutter, and 2) a rock grinder. The contents of this section contain procedures required to successfully use these pieces of equipment to produce block specimens from the collected rock samples. These specimens were prepared for Leeb hardness device testing and so the minimum volume recommendation by Corkum et al. 2018 of 90 cm³ was followed; this is a 4.5 cm cube.

SIZE, QUANTITY AND LOCATION

Each sample, also referred to as 'boulder', was thoroughly reviewed prior to the marking of cut lines to ensure the boulder would be utilized fully. No matter how many blocks were to be removed from a boulder, the primary rock component of the proposed specimen needed to meet or exceed the 90 cm³ volume requirement. The first step was to determine the dimensions of the primary rock component given what was available to take from the boulder. Focusing on the 'proposed' surface of the secondary rock component, the number of blocks were determined and their respective dimensions. Two cases (hereinafter referred to as "Category" or "categories") exist amongst the boulders collected and can be visualized in Figure 3-6. For boulders to be included in the first category, the secondary rock portion of the boulder locates in such a way that equally sized blocks can only be removed from one side of the secondary rock. To fall into the second category, at least one block can be removed from either side of the secondary rock present in the boulder. Specimens produced from the second category have a saw cut surface in the secondary material while those produced from the first category are produced with the original surface.



Figure 3-6: Example of boulders with two different procedures for block extraction: a) Category 1: blocks can only be taken from one side of the secondary rock; b) Category 2: blocks can be taken from both sides of the secondary rock.

To determine the number of specimens that can be extracted from a boulder that falls into Category 1, templates were made of paper for individual block surface areas (Figure 3-7) and for configurations of four which account for the 2 mm width of the cutting wheel.

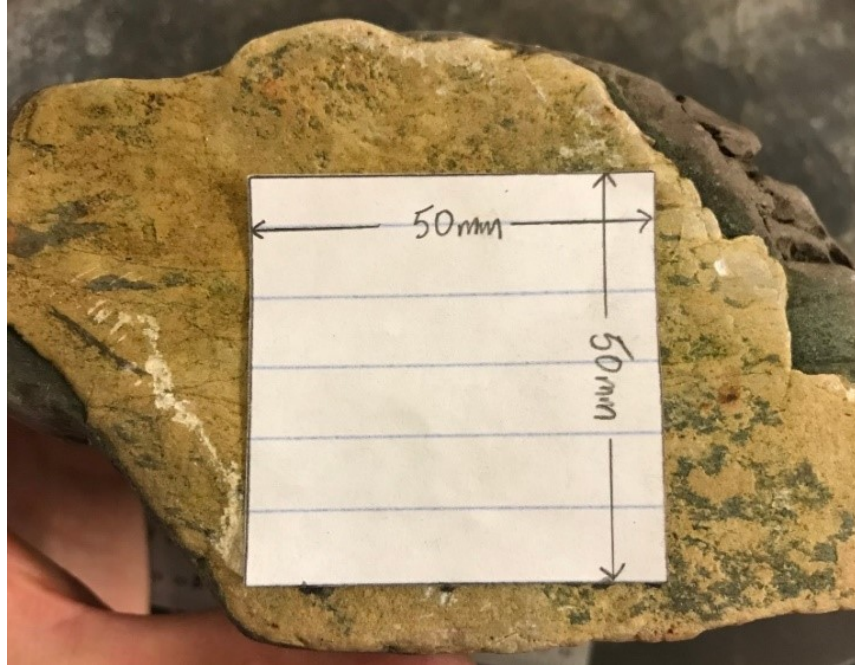


Figure 3-7: Paper template showing the dimensions of the surface of a cube with 50 mm side length positioned on the secondary rock surface of a boulder.

For boulders falling into Category 2, the surface of the secondary rock cannot be accessed without prior cutting. The first step in this case was to determine if at least one cube, larger than 90 cm^3 could be obtained in the primary rock from at least one side. As most of these boulders were relatively small, the one side of the secondary material could typically be determined to not be able to produce a specimen and could therefore be disregarded. However, when the boulder was seemingly large enough to produce specimens from each side, this determination could be verified by scaling the photos of the boulder. If at least one block could be extracted, then the specimen size findings were next confirmed by visual inspection and by measurements made on the boulder. The boulder was carefully assessed to confirm measurements and to ensure unaccounted for abnormalities did not exist.

MARKINGS AND FIRST CUT LINES

After determining the proposed cube dimensions, the first cut line marked out for Category 1 boulders was the bottom cut of the proposed specimens i.e., a cut line parallel to the secondary to primary rock transition line at the determined cube dimension depth measured from this transition line. For ease and simplicity during the cutting process,

three lines were to be marked out on the Category 2 boulders when blocks were to be removed from both sides of the secondary material, and two lines when blocks were to be taken from only one side¹. In the former case, the three cut lines would be for both bottom cuts and a centreline cut to be made in the secondary rock. While for the latter, the cut lines would be for the bottom cut and the centerline cut to be made in the secondary material. These lines (hereinafter referred to as “first cut lines”) and all future cut lines could be measured and marked out in several ways depending on the boulder. For whatever method that was used, the cut line was marked at a vertical or horizontal distance rather than the distance measured along the present surface. A small vice was used to fix the smaller boulders in a set orientation for ease of marking. In terms of drawing lines to connect measured markings, three methods were used as a means to draw along depending on the present surface: a) a standard ruler was used if the surface of the rock was flat; b) a string pulled taut around the boulder if the surface was convexly curved, or c) a flexible object with a straight-edge that can be manipulated to take on the shape of the surface when the rock exhibits concavity or undulations. For boulders with large undulations, marks were closely placed and were connected without a straight edge.

GUIDE MARKS AND PLACEMENT IN VISE

Once the first cut lines were completely drawn, a final measurement was taken around the specimen to ensure each line was accurate. In instances where the final dimension of the proposed block met one side of the line, an arrow was drawn on that side of the line indicating that the blade should be set to cut to that particular side of the cut line in that location; Figure 3-8 shows an example of this on a random cut line.

¹ Due to the tremendous amount of work that is required to line up any boulder in the vise in its original state, making two or three cuts, one after the other while fastened in the correct orientation not only saved time, it can also ensure all cuts are completely parallel to each other. To do this, the boulder is fastened in such a way so that all cuts could be completed without moving the boulder in the vise. The cutting machine has a function where the boulder can be moved inward toward the cutting blade and this function is used to make the two or three cuts. Set up in this way, the first cut completed is the bottom cut line farthest away from the fastened mass of the boulder, followed by the cut made in the secondary material. If three cuts are to be made, the second bottom cut line is the final cut.



Figure 3-8: Cut line displaying arrow indicating the final dimension of the cut-off piece is to be taken to edge of the line indicated with a black arrow. Photo shows a boulder fastened in the cutting machine vise with the cut line aligned with the cutting wheel and the guide marks aligned with the edges of the upright vise components.

For ease of setting up the boulder in the vise of the cutting machine, measurements were taken by the author from the edge of cutting wheel to the edges of the upright components of the vise closest to the cutting wheel, at a typical location during the cutting operation. As the cutting machine allows for the vise to move closer or farther away for the cutting wheel, these measurements can be retaken according to the desired boulder and vise setup. In any case, these measurements (hereinafter referred to as “guide marks”) were marked out on each boulder at a distance from the first cut line (or any line being cut) at that particular distance inwards towards the end of the boulder to be secured in the vise. When fastening the boulder in the vise, the edges of the upright components of the vise were lined up to these guide marks. This method not only sped up the process of lining up a boulder, it also provided surety that the three-dimensional plane needing to

be cut could be done adequately. From the authors experience, if the three-dimensional plane is not cut to that exact intended plane, it is very unlikely that the correct plane can be achieved by cutting again. Once the cut is made, realignment of the boulder to a position where the cutting wheel is crudely parallel to the cut surface will cause for the wheel to reorient itself to follow the plane of the previous cut. To complete this cut to a different three-dimensional orientation, more depth of the rock needs to be cut to keep the cutting wheel in the rock rather than ‘gliding’ along the incorrectly oriented cut plane. It was thus considered paramount to not rush the fastening process in the vise. Further, it was found that the end of the vice closer to the back of the cutting machine, upon fastening of a boulder, sits twice the distance from the cutting wheel than the end nearest the front. Thus, for the typical case, guide marks were placed at 11 mm at the back and 5.5 mm at the front. There were four guide marks total for each first cut line, two on the top at the immediate ends and two on the front and back face of the boulder marked at the immediate bottom or in a location near the bottom that can be seen while looking down from the top. Figure 3-8 shows the placement of guide marks on the top of the boulder at the immediate front and back, used to line up the boulder in the vise.

PROPER ALIGNMENT AND CUTTING

The boulder was placed into the vise and the four guide marks for the line intended to be cut would be aligned with the edges of the upright components of the vise. Shims consisting of wood or rock were selected and placed beneath the boulder or between the boulder and the upright components of the vise to meet the required orientation. The vise was tightened in this position. A large carpenter’s ruler (L-shaped measuring device) was next placed firmly against the cutting wheel in a way that does not move the cutting wheel. In this fashion, the carpenter’s ruler could be extended out and rested on the top of the boulder to ensure the cutting wheel will cut along the marked line during operation. For the bottom side of the boulder, the long end of carpenter’s ruler, inserted from the front, could be held firmly to the cutting wheel and the short end could be used at the front of the boulder to ensure the bottom front would be cut as per the cut line. Close attention was paid at this point to ensure the cutting wheel would be cutting on the correct side of the marked line. If the boulder needed to be moved slightly inward towards the

cutting wheel or outward, the crank wheel which moves the vise toward or away from the cutting wheel was used. At this step, the cutting process could be commenced for all first cut lines.

FINAL CUTS

Upon completion of the cut of the first cut lines, all components of the boulder were rinsed under hot tap water to remove the oily residue produced from the saw and then dried with paper towel. At this stage, all freshly cut portions hosting proposed specimens were set on a workbench with the freshly cut primary rock surfaces down with their respective secondary rock component upwards. The next step was to accurately determine the locations of the proposed specimens. These were situated to optimize what was available within the boulder with one selected size for all specimens removed. For both categories of boulders, the paper templates introduced in Section 3.1.2.2 were used to aid in this determination. Selecting the locations of specimens for both categories of boulders are discussed below.

1) *Category 1 Boulders*: For instances where only one block could be removed from a boulder, this block was created as big as possible. When dealing with multiple blocks, the location of these blocks needed to be selected. As the objective to gain Leeb hardness data was to uniformly grind down the secondary material layer, uniformity of that layer was important for the hardness results to be reflective of that specific thickness. Thus, the amount of secondary material present on the top of each proposed block needed to be considered before delving into the final cutting process. This was not an issue with naturally weathered specimens, but it was for rock type transition specimens when the secondary material across the boulder was of varying thickness. Thus, the locations of specimens were selected to gain the most uniform thickness of secondary material while retrieving the maximum number of blocks. For instance, if a sample were large enough to just extract four blocks of the minimum cube size, but to do this would mean that the secondary material on one of the outer extents of all four blocks would have a thin layer of secondary material after extraction, a more viable option should be considered. If four blocks were produced and the thickness of secondary material was ground down to the point of uniform thickness, then there would be four specimens created with a very thin

secondary material layer present. However, extracting two or three blocks, would produce one or two less specimens, but the secondary material on each could be thicker. This is an example of how the boulder would be best utilized to allow for the collection of better data during hardness testing.

2) *Category 2 Boulders*: It has been established that at least two specimens would be removed from the remnants of the boulder in this category. As the cut made through the secondary rock was through the centre of this rock type, all proposed specimens at this stage would have approximately the same thickness of secondary rock overlying the primary rock portion of the specimen. Having several specimens with secondary material being of the same thickness allowed for a full comparison of the collected data on each. However, in the event where one or more specimens from these boulders had to have a reduced secondary material layer so that more blocks could be produced, these were still extracted.

FIRST DIRECTION OF VERTICAL CUTS

Next, a direction was selected to start making cuts vertical to the bottom cut. Following the guidance set out earlier in this section, these vertical cuts could be made. In this direction, the outermost cut line with respect to the boulder's extent was marked first together with the four guide marks. This line's orientation and location was marked following the edge of the proposed first specimen. As was the case for all cut lines made in this direction as well as from this point forward, one line was drawn and then cut rather than all lines being drawn and then cuts made; this ensured greater accuracy. This first cut was made. After removing the oily residue with hot tap water and drying with paper towel, the next cut line in this direction was drawn parallel to the first, at the width of the proposed specimen. This cut was then made. This process was completed until all cuts were made in this direction. Figure 3-9 below shows the first vertical cut in a Category 1

boulder made perpendicular to the bottom cut line made following the guidance set forth earlier in this section².



Figure 3-9: First vertical cut made perpendicular to the primary rock specimen bottom and secondary to primary rock contact line.

SECOND DIRECTION OF VERTICAL CUTS

The cut portions derived from these cuts (hereinafter denoted in the remainder of this section as “slice” or “slices”), hosting a bottom cut and two side cuts, could now be marked out to complete the final two sides of each specimen. Taking the selected specimen size paper template, exact specimen locations were determined. Methods mentioned earlier in this section were followed for making these determinations. Briefly,

² With the bottom cut made parallel to the secondary to primary material transition line, true perpendicular cuts could be made in any direction in the cutting machine as the cutting wheel is perpendicular to the levelled vice bottom; this statement is true if the boulder is fastened in the vise with the bottom cut resting on the vice bottom. In this way, preparation time to orient the boulder in the vise is greatly reduced as shims no longer are required underneath the boulder.

beginning with one slice, the leftmost cut line and guide marks were drawn. Next, the specimen was fastened into the cutting machine and cut. During cutting, the leftmost cut lines and guide marks were drawn on the other slices (if any) and would be placed in the queue to be cut. Working from left to right across the slices, cut lines, guide marks, and the associated cuts were made until all specimens were extracted.

SECONDARY MATERIAL CUT

At this stage, the primary rock portion of each specimen was complete in the shape of a cube. In most cases, no further cutting was required as the surface of the secondary material was moderately flat and could receive hardness testing as it was. However, in some cases, a final step was required where the secondary material required a cut. The reason for this could be because the variation in thickness of secondary material was large across the specimen or that there was excessive roughness on the surface. In these situations, the secondary rock was cut just beneath the lowest undulation to maximize the amount of secondary material. Two methods were used to mark out the cut lines within the secondary rock to ensure precision cutting: a) a fine-tipped scribe marking along a metal straight-edge if the material was relatively soft, or b) a fine-tipped permanent marker marking along any straight-edge. These lines and associated guide marks were marked at the appropriate distances from the ‘line of best fit’ of the transition line between the two rock types. Close attention was paid to ensure cutting was completed as intended. Specimens after cutting were rinsed under hot tap water, dried with paper towel, and stored.

3.1.2.3 SPECIMEN PREPARATION – CYLINDRICAL CORES

Rock cores were obtained by the author using a rock drill on specimens where the length of the primary rock could be that required to complete a proper UCS test as per ASTM D7012-14^{e1} standard after all data was obtained on the secondary rock portion of the specimen. As per this standard, the desirable length to width ratio is between 2.0:1 and 2.5:1. For a 54 mm diameter rock core, the required length is between 108 and 135 mm to conduct this test. It should be noted at the outset that UCS testing was considered outside of the scope of this research program and so no rock cylindrical cores

were tested. However, hardness values were obtained, and the cylinders were left in storage for future UCS testing under the scope of another research program if so desired. The following procedures were followed to create these specimens.

FIRST CUT LINES

Great attempts were made to ensure that cores were extracted from a location where no fractures were present within the specimen in both the secondary and primary rock. If it were determined by the author that the primary rock length could be extracted to a length long enough for UCS testing, a first cut line was planned at a length slightly longer than the proposed specimen in the planned direction of coring. The method used to successfully cut a first cut line for boulders planned for block extraction (Section 3.1.2.2) was employed on these boulders³. In instances where it was deemed beneficial to make a cut parallel to the secondary to primary rock transition line in the secondary material as well prior to coring, this was done in accordance with methods discussed in Section 3.1.2.2. Briefly, this includes two first cut lines, a bottom of specimen line and a line made in the secondary rock. If it was possible to secure the boulder in the vise of the cutting machine at the desired orientation so that both cuts could be made without moving the boulder in the vise, then this was done. Otherwise, these two cuts would need to be performed with different vice setups.

CORING OPERATION

The next step was aligning and fastening the boulder on the drilling platform. To be able to do this, each boulder was assessed, and a proper method was incorporated to not only ensure it was fastened down, but that it would not move during the coring process. For smaller boulders a small vise was used to fasten the boulder upright in the correct orientation. The vise itself was fastened to the platform with two clamps (Figure 3-10). Beneath the boulder on the vise, a thin piece of plywood was placed to catch the drill bit

³ As the platform on the drill is level in all directions, placing this cut surface down on the platform ensures that the coring operation occurs perpendicular to the secondary to primary rock transition line. In addition, this flat surface allows for greater stability during the coring process as it is easier to secure the boulder to the platform.

rather than allowing the bit to hit the vise. Depending on the size and shape of a boulder, wooden pieces could be set up between the sides of the boulder and the jaws of the vise to allow for more surface area on the exterior of the boulder to be included in the fastening.

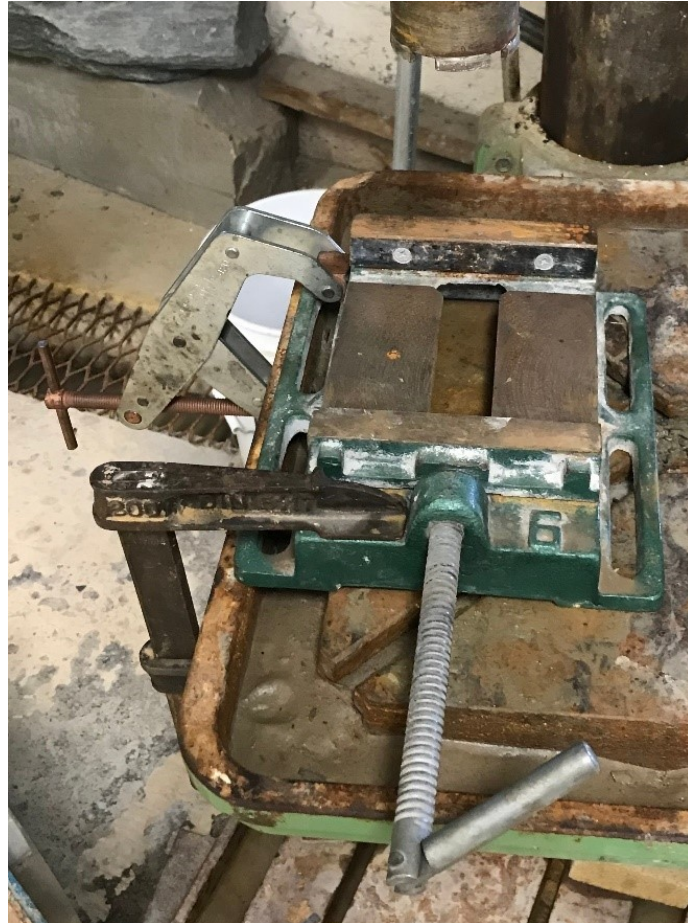


Figure 3-10: Photo of vise secured to drill platform with two clamps.

Finally, a ratchet strap was used as a final measure to fasten the boulder and vise setup to the platform. During all stages of the setup of the boulder in the vise, close attention was paid that the secondary to primary rock transition line of the boulder was level in all directions and that the intended location of the borehole was aligned with the drill's core barrel. When boulders too large for the vise were drilled, the freshly cut surface made along the first cut line would be placed down on plywood pieces that sit directly on top of the drill platform and were secured with one or two ratchet straps to the drill platform.

After each core was completed, the boulder was moved to the next location for a core and secured in this same fashion.

FINAL CUTS

Being of a 54 mm diameter core, the primary rock was cut to a length between 108 and 135 mm in the cutting machine with the preference being 135 mm, if achievable. If a cut was deemed by the author to be required in the secondary material because of an excessively rough surface, it would be made to the maximum thickness possible i.e., to just under the deepest undulation on a Category 1 boulder. Section 3.1.2.2 was followed to complete these cuts using the most applicable method mentioned as it relates to each cylindrical core specimen in question. The primary rock portion of all specimens extracted from a single boulder were cut to the same length.

3.1.2.4 TESTING

Up until this point, all specimens for this component of the research were prepared. The overall concept of the work to be performed on these specimens includes hardness testing on the secondary material surface, followed by grinding to a selected depth, then hardness testing on this new surface. This process commences until the newest surface is well into the primary material and the hardness values obtained from surface to surface see a consistency amongst the results. The procedure that follows is applicable to both blocks and cylindrical cores. The setup of the Leeb device used in this research program and used to conduct the work described in this section, was mentioned in Section 2.3.1. It should be briefly mentioned that rock specimens are heterogeneous and anisotropic with conditions that are much less controlled than that of artificial material which is far closer to being homogeneous and isotropic. Therefore, it should be understood that an increased number of obscurities is to be expected in the hardness data found on natural rock surface than what would be found on artificial material.

PRIMARY MATERIAL HARDNESS

A crucial component of the research was understanding when the secondary material was surpassed (fully removed) in the grinding process. This not only gave the ability to

locate the secondary to primary rock transition line, but it also was an indication of when the readings were of unweathered primary rock. Two methodologies were employed to determine a representative hardness for the primary material using the TM20 approach per tested surface proposed by Corkum et al., 2018, as seen in Section 2.3.2. The first method involved gathering hardness values (TM20) using the Leeb device on the sides and bottom of the primary material for each specimen and averaging the TM20 values. The second method involved grinding the primary material bottom of the specimen in the same manner as that performed on the surface of the secondary material, then gathering readings (TM20) on the bottom surface. For the first method, if the secondary material was thick enough, this methodology was performed on the secondary material as an attempt to understand the representative hardness of this material. Also, for this method the appropriate supporting ring for a curved exterior surface impact replaced the standard supporting ring on the Leeb tester to perform testing on the cylindrical surfaces of cores.

The selected representative value was important as it was a target value to achieve with the tester indicating that the fresh primary rock was reached. A discrepancy with using the first method was that the prepared surfaces on the sides and bottom of the block were prepared differently than the top grinded surface. The topic of surface treatment and the associative hardness results will be discussed in Section 4.5. For the case of the first method, this was abandoned as the believed-to-be representative value was always too high to be achieved regardless of grinding depth; however, the second method was able to be achieved with little difficulty for most cases. As the second method replicates the surface treatment present on the top of the block during the obtention of hardness readings, this is believed to be the reason for its validity. While the first method was performed on cut surfaces that were in a dry state.

THE GRINDING PROCESS

Each specimen was fastened in the v-notch block on the grinding machine after the specimen was adequately aligned. As an extra measure of preciseness, efforts were made to ensure that the secondary to primary transition line (not the top surface) was exactly parallel to the travel plane of the grinding wheel. This provided surety that the

thickness of the secondary material at each grinding increment was uniform across the specimen.

For rock type transition specimens, on each side of a block or continuously around the exterior of a core, thin but sturdy cardboard of equal length was taped to the specimen with their bottom following the exact orientation of the rock type transition line. The top of the cardboard pieces represented the plane that the grinding wheel needed to be travelling with respect to the specimen. But, since the grinder travels horizontally at each height, the specimen would require an adjusted alignment in the v-notch block with shims. For ease of the alignment process, which is especially useful when aligning more than one specimen at the same time, the top of the v-notch block could be marked out on the specimen. By using shims, adjustments to the specimen were made until this marked line matched the top of the v-notch block and then the block or cylinder was fastened in the v-notch block as such. To do this, the specimens were flipped upside-down on a level workbench with the tops of the cardboard stock resting flat on the workbench surface. Using a ruler that produces a true 90° vertical measurement from the bench surface, a selected measurement could be marked out on the specimen to represent the proposed top location of the v-notch block. This measurement is made around the specimen and a continuous line connecting these marks was made. This specimen was now placed in the v-notch block and wooden shims were added, however slight they may be, to ensure that the continuous line was even with the top of the v-notch block and then the specimen was fastened in that alignment. Once in alignment, the cardboard pieces were removed. Figure 3-11 illustrates the usefulness of this method in ensuring accuracy. In the photo three specimens were prepared and fastened in the way described. At this stage, hardness readings (TM20) were obtained on the top natural surface for all specimens unless the roughness was so prominent that representative hardness values were unable to be obtained.



Figure 3-11: Three rock type transition block specimens aligned in the v-notch block on the grinder. On all specimens, the Leeb strikes can be seen on the visible face (method 1, Section 3.1.2.4) as well as the marked line aligned with the top of the v-notch block.

Following hardness testing (if possible), the grinding operation occurred next. With the specimens secured in the grinder, the first step was to perform grinding to the minimum depth required to reach a uniform plane across the specimen. The purpose of this grinding phase was to take the surface currently present in the secondary material and grind it to the true plane required to reach a uniform secondary material thickness. This new plane produced in the secondary material was considered by the author to be the ‘second surface’ or ‘Top 2’ as seen in the Appendices. At this stage and after each stage of grinding, all components of the hydraulic system of the grinding machine were shut off stopping the automatic-driven force of the grinder but maintains the digital grinding depth on the display. On the second surface, the display showing depth was reset for the only time during the grinding process. By maintaining a cumulative depth of grind on the digital display, the author was able to stop the grind at a pre-determined depth. At the top surface and at any grinding surface, the specimen was manually wheeled to the far left on the grinding table and was dried thoroughly on all surfaces with paper towel. A digital

caliper was used to measure the total height of the specimen. As this device was sensitive to the cooling fluid, which is predominantly water, close attention was paid to ensure that all cooling fluid was removed from the block prior to measurement. Additionally, on the top surface and on all subsequent surfaces following grinding, assigned nomenclature was added. The digital caliper was used to confirm the height of the specimen and a photo was taken of the digital measurement whilst the nomenclature denoting the specimen, block and surface number were captured within the photo.

DATA RETRIEVAL PROCESS

All hardness testing was conducted using the TM20 approach proposed by Corkum et al., 2018, as was mentioned in Section 2.3.2. Using this approach, twenty impacts were completed on a single surface, the lowest and highest readings were discarded, and the remaining 18 values were averaged. Beginning with the natural surface, while in the v-notch grinding block, the TM20 approach was conducted within a 25 to 50 mm diameter impact zone. Following this, the specimen was wheeled to the right and positioned beneath the grinding wheel and the hydraulic functions of the grinding machine were powered on and the grinding operation commenced. The aforementioned process of stopping the grinder, moving and drying the specimens, applying markings to the current surface, measuring with a caliper, taking a photo, performing hardness testing and then recommencing the grinding operation is repeated until the final grinding surface is reached. As this final surface location was approximated at the beginning, an evaluation could be made at this approximate depth if further grinding was required or not based on the hardness values. Hardness values were relatively consistent with the representative primary rock hardness found with the second method of Section 3.1.2.4 if the fresh primary rock was reached. In making this determination, two or three surface depths were typically prepared and tested to confirm this in the primary rock. Additionally, a graphical plot updated per surface would be examined by the author to ensure that a hardness consistency was achieved, and that this hardness value was close to that of the representative primary hardness value. If this was the case, nothing further would occur with that specimen. The data retrieval process was no longer continued once the fresh primary rock was determined to be reached.

SPECIMENS FOR UCS TESTING

If UCS testing were to be conducted on a cylindrical specimen, the remaining primary material after the secondary material is removed would be modified if it needed to be, to meet the ASTM D7012-14^{e1} standards for UCS testing. As was identified in Section 3.1.2.4, no UCS testing was conducted on any of the prepared rock cylindrical cores in this research program; however, these have been left to be done by future students if it is deemed necessary.

4 RESULTS

The results of the work conducted in this study described in Chapter 3 are presented in this chapter together with the respective discussion for each study topic. The current ISRM suggested method produced in 1978 describes the procedure to predict the JCS value of a rock joint (Section 2.2.1). In these suggested methods, apart from the subjective scratch and geological hammer test chart (Table 2-4, Section 2.2.1), a JCS value is found with the L-type Schmidt hammer in combination with the Rock Strength Chart originated by Deere and Miller (Figure 2-4). It has been identified by Aoki and Matsukura in 2007 (Section 2.3) that the Leeb hardness device is a more suitable option than the Schmidt hammer in determining properties of the wall rock material of a rock joint. As was the case for Barton in the 1970s with the Schmidt hammer, a great deal of effort is required to get the knowledge base of the Leeb hardness device to a status eligible for a standard or suggested method of ISRM to be written for its use. Many authors have recognized the devices potential (Section 2.3.2) and have been developing a quantifiable knowledge base for this device. The findings of this research program also contribute to this evolving knowledge base and have expanded into areas yet to be discovered by any other author.

In this chapter, the influence zone results are discussed first on the artificial material specimens. With this understanding, the natural rock transition specimens for SS, SH, and UM specimens are discussed and further validate the result of the artificial material specimens. Next, the hardness gradation results of the weathered rock specimens are discussed. The influence zone findings are evaluated using a simplified numerical modelling exercise. The hardness result found on surfaces treated differently in dry and wet states are discussed. An evaluation of results of JRC evaluations and the prediction of JCS for the test specimens is presented.

4.1 ARTIFICIAL MATERIAL SPECIMENS

As was discussed in Section 3.1.1, artificial material specimens were created for the obtention of information on 1) steady state curing behaviour, and 2) the influence of the underlying material on the hardness readings. The age to reach a steady state in a Plaster of Paris mix is discussed first followed by the results found on SS and SH specimens.

4.1.1 STEADY STATE CURING AGE

The two artificial material mix designs inspired by Patton in 1966 (Section 2.1.2) classified in Table 3-1 as being the 3:1 and 3:2 mixes were used for the steady state curing age exercise. Six specimens were tested for both mixes and ranged in age from 3 to 27 days. The need for this step was discussed in Section 3.1.1.4 and was required for the first methodology of artificial material testing where each single set was poured independently of all other sets. By curing to an age that ensures a steady state, all sets for a mix design could be best understood as each material in each set exhibited its maximum strength. The results of the 3:1 mix are shown in Figure 4-1.

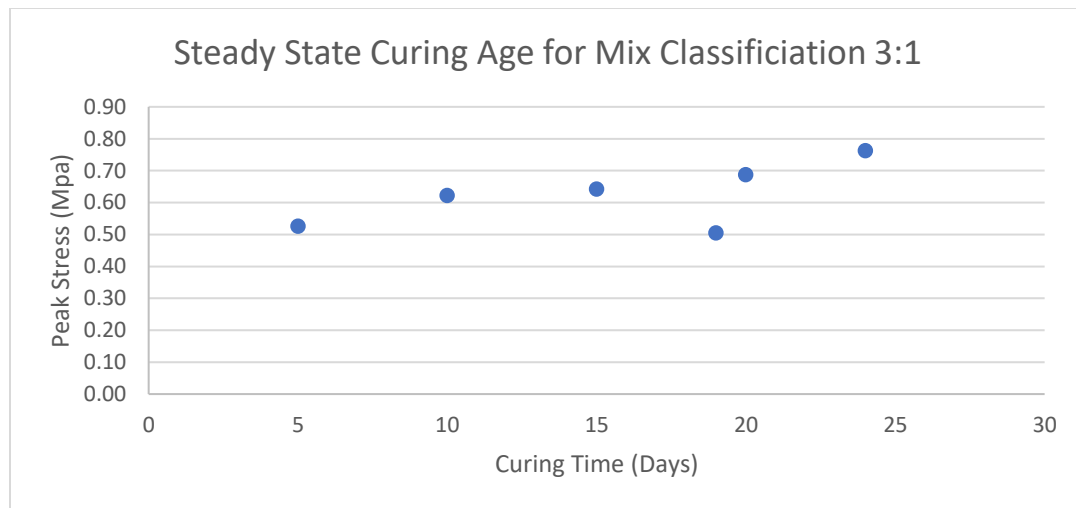


Figure 4-1: Steady state curing behaviour of the 3:1 mix.

The result of the 3:1 mix appear to have some variation in strength for the three oldest specimens making it difficult to determine a point of steady state. As was mentioned in Section 3.1.1, regardless of the level of effort used to make the specimens, an inherent variability exists in these specimens and that several factors can be the cause for the drastic differences in the found properties during testing. As each specimen cured for this exercise was poured independently of the other specimens, it is believed that the behaviour of the oldest three for the 3:1 mix is the result of inherent variability, characteristic of each cured specimen. Further, it is believed by the author that this exercise could be conducted again in the exact same way and the results in the range of steady state would still vary. By testing a second Plaster of Paris mix, the curing

behaviour results of both mixes could be compared and the results of the 3:1 mix could be better understood. The results of the 3:2 mix are shown in Figure 4-2.

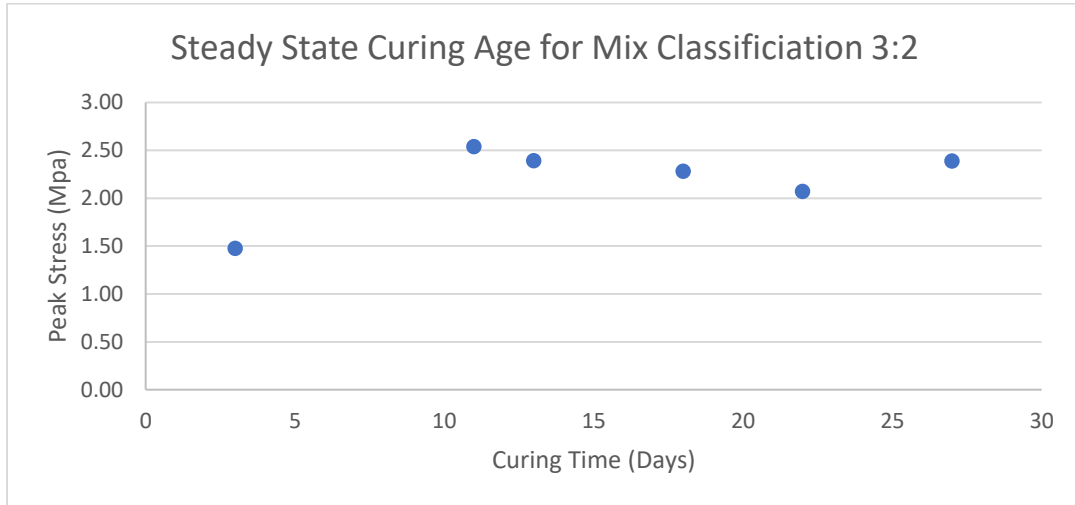


Figure 4-2: Steady state curing behaviour of the 3:2 mix.

The results found with the specimens made of the 3:2 mix show that after 11 days, the mix is in a point of steady state with inherent variability within the specimens being the reason for the subtle variance in the plot. By comparing the results of the first mix seen in Figure 4-1 with that of the second mix in Figure 4-2, it can be seen that comparable steadying behaviour seems to occur at the 10th and 11th day. Thus, a steady state was assumed to be reached after 11 days in a Plaster of Paris mix and was taken to be the case for all mix designs used in this research program (Table 3-1). However, as an extra precaution, all testing done using the first methodology, explained in Section 3.1.1.4, was performed after 14 days for additional assurance that the steady state would be reached.

4.1.2 SS SPECIMENS

This section describes the results found on the artificial SS specimens using the first methodology introduced in Section 3.1.1.4 then finalizes with the results found using the second methodology. As was stated in Section 3.1.1.4, the first methodology was originally believed by the author to be the only methodology needed to achieve sufficient results. The reason for this was because Hack et al. in 1993 determined that a maximum

influence zone of 5 mm (Section 2.3.2) exists on rock. Thus, it was anticipated that the specimens with secondary material thicknesses thinner than 5 mm would produce results showing a clear influence of the underlying material. Additionally, the author was unsure if a reduction of the secondary material layer thickness for both SS and SH specimens by way of sanding or grinding could be done without disturbance of the rigid connection between the materials. It was for this reason that a methodology not involving this said reduction was examined first. The target objective of creating equal secondary material thicknesses for the specimens in each set was achieved with ± 1 mm accuracy.

At a curing age of 14 days, the collected hardness data of the artificial, primary material of the SH specimen in each set was collected. This L_D value derived from the TM20 approach and denoted as $L_{D(primary)}$, was taken to represent the true hardness of the artificial material in the set as it was independent of any underlying material. Testing was next conducted on the artificial, secondary material of the SS specimen in each set using the TM20 approach and the L_D value was denoted as $L_{D(secondary)}$. Amongst specimens, a trending difference between $L_{D(secondary)}$ and $L_{D(primary)}$ was considered as being the result of an influence of the underlying material. The results of the first methodology with the mix classifications of 3 to 2, Just Plaster and Dia Earth listed in Table 3-1 are shown in Figure 4-3. It should be mentioned that the 3 to 1 mix classification was unable to produce any hardness readings as all readings fell outside of the tolerance limit range of the hardness device (Section 2.3.1). Appendix A shows the $L_{D(secondary)} - L_{D(primary)}$ versus secondary material thickness data collected in this exercise.

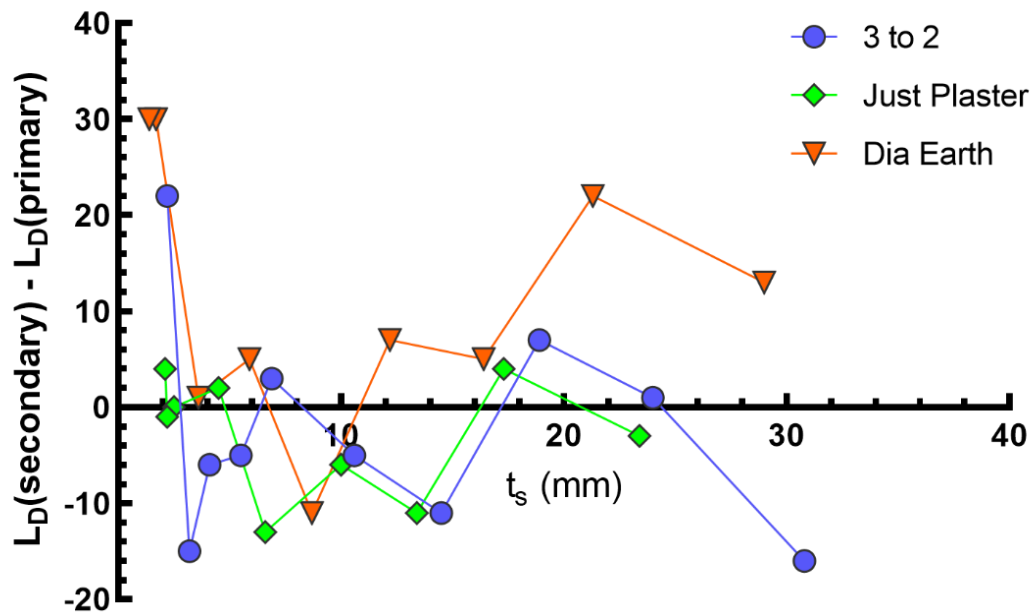


Figure 4-3: TM20 hardness versus secondary material thickness found on the artificial SS specimens using the first testing methodology (specimens with no secondary material thickness reduction) identified in Section 3.1.1.4.

The results did not show a trending increase of hardness as was expected to have been seen at and below a thickness of 5 mm. After the curing process it had been seen that the specimens with the two thinnest secondary material thicknesses of the Dia Earth mixture were thinner than the specimens with the thinnest secondary material thicknesses for the other two mix designs. The two thinnest artificial material thicknesses of the Dia Earth specimens were 1.4 and 1.7 mm while the thinnest artificial material layers of the specimens of the other two mix designs were 2.1 mm for Just Plaster and 2.2 mm for 3 to 2. This definite discrepancy in the production of these specimens from the intended plan of having the same artificial material thicknesses in each set, across all mix designs, actually exposed results that encouraged the development of the second methodology introduced in Section 3.1.1.4. Out of all three mix designs, these two Dia Earth specimens produced trending results across the two specimens. The other two suggested an increase in hardness on the specimens of the thinnest secondary layer but could not confirm if this was due to the inherent variability characteristic of the mix itself. This inherent variability is believed by the author to be the cause for the results of the thicker artificial material layers which resulted in hardness differences fluctuating above and

below the zero-hardness difference axis (Figure 4-3). However, by comparing the results of the three mix designs, a general trend of this fluctuation seems to be seen. The main objective of finding the influence zone was considered to not have been achieved in this exercise. The development of the second methodology introduced in Section 3.1.1.4 occurred next and was conducted on three specimens of each of the two strongest mix designs: Just Plaster ($\sigma_c \approx 5$ MPa) and Dia Earth ($\sigma_c \approx 10$ MPa).

It should be noted that Figure 4-3 shows a hardness difference plot showing the difference in hardness between the artificial material in the SH specimens and the SS specimens in each set. As each set was poured individually, a plot such as this allowed for all specimens to be compared as an integrated system rather than individually. The specimens tested using the second methodology however, were compared individually and so a plot showing the secondary material hardness of the tested specimens was all that was required. Figure 4-4 shows the hardness versus depth results for the six specimens. The naming convention used to describe the artificial material composite specimens tested under the second methodology can be seen in the legend. The first two letters, 'SP' stand for 'Specimen', this is followed by a number which is the specimen number. Finally, the two ending letters denote the mix design: JP for Just Plaster and DE for Dia Earth. The methodology used on natural rock described in Section 3.1.2.4 was followed for this process but using a process involving sandpaper as mentioned in Section 3.1.1.4.

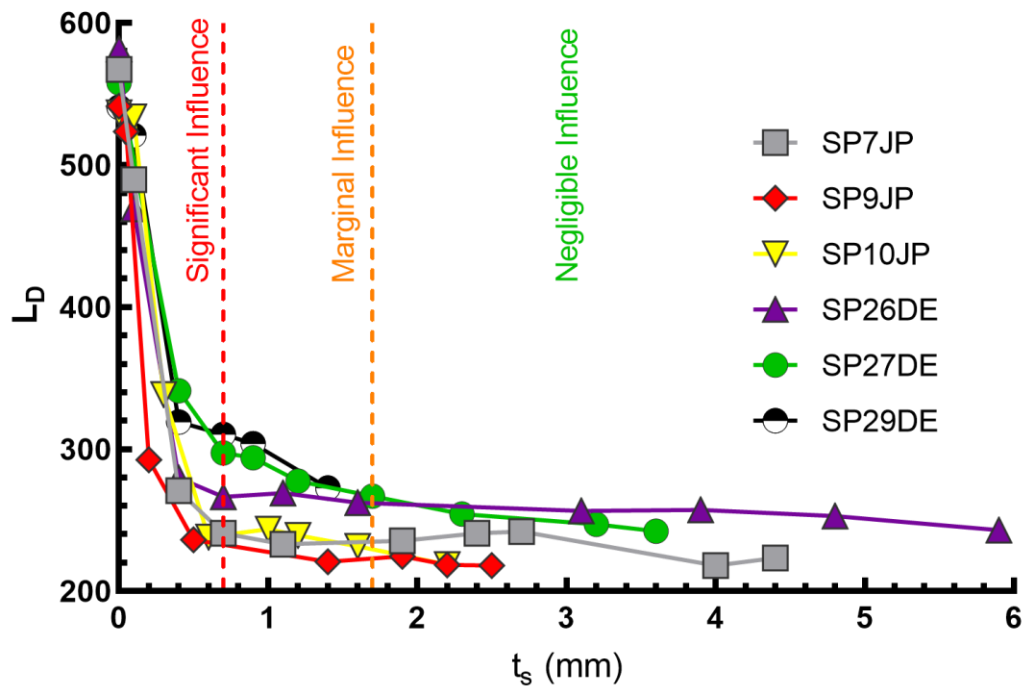


Figure 4-4: TM20 hardness versus secondary material thickness found on the artificial SS specimens using the second testing methodology (specimens with secondary material thickness reduction) identified in Section 3.1.1.4.

It can be observed in Figure 4-4 that all six specimens produced similar results and that an ‘influence zone’ was captured. From the results it can be observed that the hardness readings are marginally influenced by the underlying material near a thickness of 1.7 mm down to about 0.7 mm. However, from 0.7 mm down to the surface of the underlying material (0 thickness), a significant influence can be seen. From Figure 4-3, it is apparent that a slight rise in hardness exists beginning at approximately 2.1 mm in the Just Plaster mix and 2.2 mm in the 3 to 2 mix. The characteristic inherent variability in the mix designs could have been the cause for these results; however, as large variability about the zero-hardness difference axis was seen to exist between adjacent specimens with thicker secondary material layers. Additionally, an adjacent data point could not confirm the increasing trend. The results of the six specimens in Figure 4-4 compare nicely amongst all specimens in the plot. From the results of Figure 4-3 and Figure 4-4, a number suitable for use in practice of 2 mm was selected to describe the ‘influence zone’ for rock with native conditions representative of an SS specimen. Therefore, hardness testing on secondary material that is softer than the underlying material, such as on a

weathered surface, if the secondary material is thicker than 2 mm, the reading will be unaffected by the hardness of the underlying, primary material. Similarly, if the thickness of the secondary material is thinner than 2 mm to the underlying, primary material, then the hardness results will be affected by the hardness of the underlying, primary material. In the context of a weathered rock joint, this means that a weathered profile thickness greater than 2 mm can produce hardness results that can be correlated to a JCS value using a laboratory derived, intact rock correlation equation such as that of Corkum et al., 2018 (Section 2.3.2). Conversely, any weathered profile thicknesses less than 2 mm will not be of the true hardness of the rock wall material but will be harder and will be representative of a combination of the hardness at the surface and of the underlying, unweathered intact rock. For the latter case, a hardness correction factor would need to be established to be able to be used in a laboratory derived, intact rock correlation equation: to be examined as part of a future study. Appendix A and Appendix B shows the Leeb hardness versus secondary material thickness data collected in this exercise for both methods conducted.

4.1.3 SH SPECIMENS

In the same fashion as Section 4.1.2, the first methodology introduced in Section 3.1.1.4 for the artificial SH specimens will be discussed first followed by a discussion of the results found on the specimens using the second methodology. It should be iterated that testing using the first methodology was deployed on both the SS specimens (Section 4.1.2) and the SH specimens prior to commencing with the second methodology. The artificial SH specimens were made with an artificial material together with thinly cut sandstone cylinders hereafter referred to as ‘disks’ of varying thickness with a limitation on the thinnest disk being approximately 2 mm thick. The odd sandstone disk could be cut slightly thinner than this, but it was seldom the case as the sandstone disk would break or crumble in the cutting machine during the cutting process. For these specimens, grinding was originally considered to be too harsh so it was the initial hope of the author that the objective of locating the ‘influence zone’ could be reached at a secondary material thickness of greater than 2 mm. The results of the testing using the first methodology on the artificial SH specimens are shown in Figure 4-5.

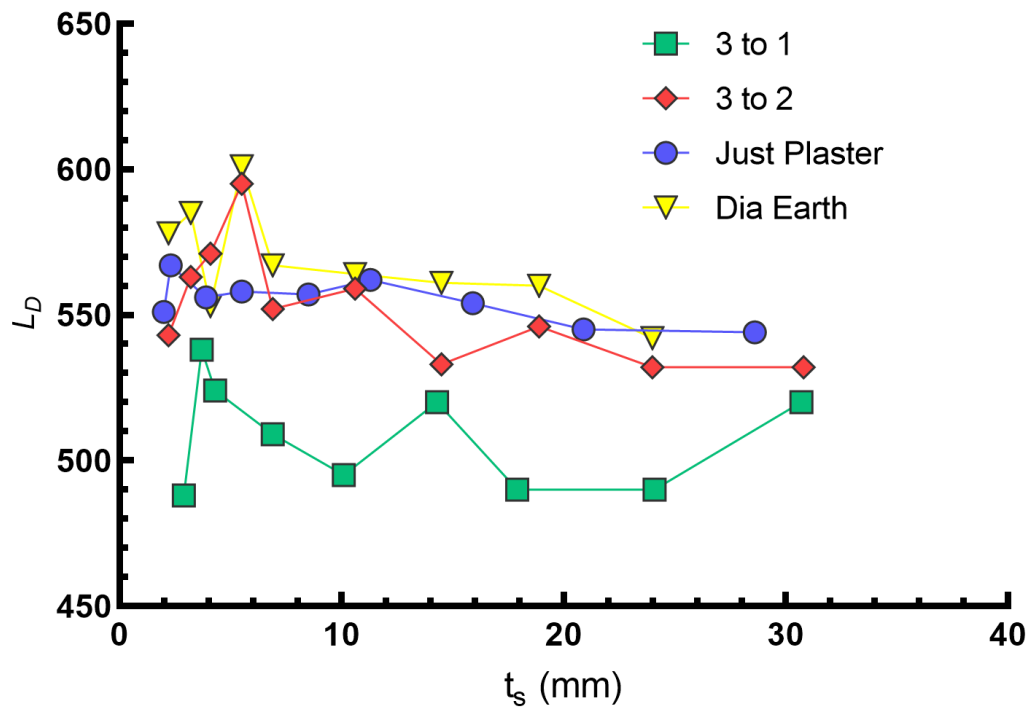


Figure 4-5: TM20 hardness versus secondary material thickness found on the artificial SH specimens using the first testing methodology (specimens with no secondary material thickness reduction) identified in Section 3.1.1.4.

It can be observed in Figure 4-5 that a definitive ‘influence zone’ was not discovered in the findings using the first methodology. However, there seems to be an influence in the results based on the strength of the underlying material. It can be observed that hardness readings increase with underlying, primary material strength increase. It seems odd that the 3:1 mix produced such low results in comparison to the other three mixes; the exact reason for this is uncertain. The author has suspicions that it has to do with the incredibly low hardness of the artificial material present in the specimens. The artificial material when tested on its own was unable to produce a hardness reading due to it being too soft for the lower tolerance limit of the device. This is a study finding on its own: an ISRM classified R0 (Table 2-4) material, in this case having a $\sigma_c \sim 0.7$ MPa (Figure 4-1), falls outside of the lower tolerance limit of the Leeb device. Perhaps the strength of the material was too low to adequately support the sandstone during impact. The Leeb device manual (Proceq, 2007) mentions that lighter and smaller samples can flex or yield under impact producing hardness values of

excessively large variation and that are too small. It is purported by the author that regardless of being securely fastened and having a seemingly rigid connection, the underlying material was unable to provide sufficient support to the sandstone disks ultimately causing globally low L_D values. To further explain using an extreme example of this that is likely to produce findings even lower than the 3 to 1 results in Figure 4-5 would be if the same sandstone disks were placed on loose sand and then tested with the Leeb device.

As will be seen in Section 4.5, a cut sandstone surface in a dry state when impacted 100 times with the Leeb device while being of a full-sized UCS specimen adequately secured, produced an average hardness value of 569. It can be observed in Figure 4-5 that apart from a couple of spikes in hardness for the 3 to 2 and Dia Earth specimens beginning around 6 mm to their thinnest secondary material layers, that no L_D results met the average hardness value of 569. As can be seen in Figure 4-5, the global L_D values of all mixes increase as the strength of the mixes increase. The fact that this occurred and that the average hardness value was unobtainable for the global case of each mix design apart from a couple of hardness spikes, perhaps is an indicator that none of these materials truly provided full support to the overlying sandstone disks. If they did have sufficient support, the average hardness value of 569 would have been the approximate value of L_D on all thicknesses of sandstone disks. A conclusion to this exercise is that if full support is not provided to the overlying secondary material, then the hardness values will be lower than the average hardness value of the secondary material. The results of the natural rock transition SH specimens as will be discussed in Section 4.2.2 show approximate uniformity in the hardness results in the harder secondary material and are believed to show results indicative to that of a fully supportive underlying material.

In the cases of the three strongest mixes, 3 to 2, Just Plaster, and Dia Earth, the specimens hosting the thickest secondary, sandstone layer produced the lowest L_D values of each mix. Conversely, for specimens of these mix designs, as the sandstone layer thins, the L_D values increase to within close to or exceed the average sandstone hardness value of $L_D = 569$ then immediately drop to a much lesser L_D hardness value. This behaviour is believed by the author to be related to an influence indicative of the two composite

materials when tested in combination. Another observation is the final decrease in L_D values in the thinnest sandstone layer. As this behaviour occurred in all mix designs, it seemed that the obvious next step would be to employ the second methodology introduced in Section 3.1.1.4.

For the strongest mix design Dia Earth, three specimens with the thinnest secondary material layers were ground down and tested in accordance with the procedure outlined in Section 3.1.2.4. The results of the tests on the three specimens are shown in Figure 4-6.

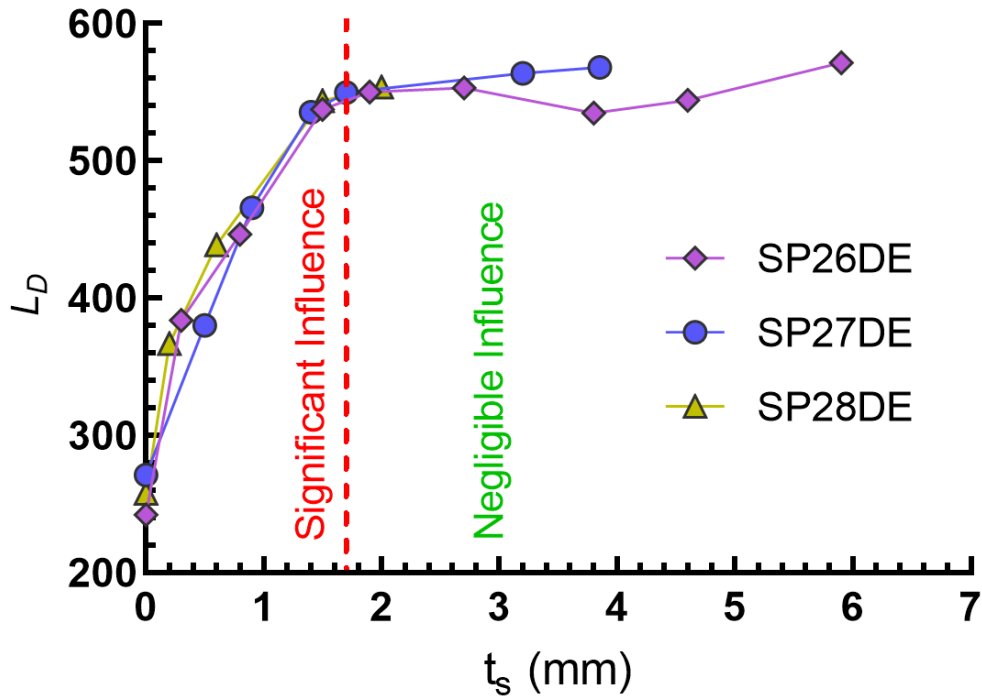


Figure 4-6: TM20 hardness versus secondary material thickness found on the artificial SH specimens using the second testing methodology (specimens with secondary material thickness reduction) identified in Section 3.1.1.4.

The findings presented in Figure 4-6 display results of close similitude but of an opposite nature to those seen in Figure 4-4. It can be observed that a zone of significant influence is present between 1.75 mm and that of the interface between materials at 0. In Figure 4-5, a minor fluctuation of hardness findings can be seen until at least 5 mm thickness and is considered by the author as being indicative of either the characteristic

inherent variability of each mix or due to an influence indicative of composite material testing when in close contact to each other. It should be reiterated here that it is only at these maximum hardness spikes that the average hardness value found on a UCS-sized specimen of sandstone is closely achieved or surpassed, so the increase in strength in this area is not greatly exceeding that of the actual scale-unaffected rock itself. The reason for this is unknown; however, a fluctuation in hardness occurred for all mix designs with sandstone thicker than 1.75 mm but, all materials are of very low strength; a question of whether this would occur on native rock can be raised. In Figure 4-6, SP26DE shows some hardness fluctuation with depth to 5 mm, while SP27DE shows some trending variation even though it is of the same mix design as SP26DE. Although slight, it is the opinion of the author that this findings difference indicates that the underlying material does not influence the readings of the secondary material thicknesses greater than 1.75 mm. It was thus concluded that secondary material thickness greater than 1.75 mm experience negligible influence of the underlying material. By comparing the results of the artificial SS specimens (Figure 4-4) and the SH specimens (Figure 4-6), an influential zone 1.75 mm thick is apparent in both cases. It can be further concluded that a practical thickness value of 2 mm holds true to explain the ‘influence zone’ for both SS and SH specimens and ultimately, for the Leeb device. Appendix A and Appendix B show the Leeb hardness versus secondary material thickness data collected in this exercise for both methods conducted.

4.2 NATURAL ROCK TRANSITION SPECIMENS

Thirteen natural rock transition specimens were prepared in this research program and fall into the categories of SS, SH and UM. As a recap from its introduction in Chapter 3, the category of UM is a rock transition specimen where the secondary and primary material are of different material but are of similar hardness. It was defined in this research program by the author that a specimen falling into this category is one that meets the following criteria: the mean of all L_D values found on all smooth surfaces of the secondary material (hereinafter referred to as $MeanL_D$), is within $\pm 5\%$ of the L_D value found on the primary material. It should be noted that the $MeanL_D$ value is exempt of surfaces that are naturally rough as the results found on these surfaces are not

indicative of the actual hardness of that material as was discussed by Asef (Section 2.3.2). Instead of excluding all natural surface L_D values from the $MeanL_D$ calculation, the author evaluated the data scatter found on these surfaces by reviewing the box and whisker plots. If the natural surface experienced a much larger standard deviation than that seen in the remainder of the results found in that secondary material, then it was exempt from the calculation. Conversely, if the standard deviation was similar, then it was included in the calculation of $MeanL_D$.

In the forthcoming sections, hardness versus depth box and whisker plots are shown with the $MeanL_D$ line as a green horizontal line. The box and whisker plot identified with a red star shows the first L_D value used in the calculation for $MeanL_D$ and is an identification of the first surface to produce, what is considered as being legitimate hardness results. The L_D value for this surface is hereafter denoted as L_{DS} . The $MeanL_D$ line ends at the contact location between the rock types, shown with a black vertical line. To the right of this contact line, a red horizontal line represents the mean hardness of the primary material found on the bottom of each specimen and is denoted hereafter as L_{DP} . The blue dashed line connects the TM20 values of all surfaces tested for each specimen. The parameters of L_{DS} and L_{DP} can be used to predict the strength change between the surface and intact portion of a rock and will be described in further detail in Section 4.6.2. It should be noted that the red L_{DP} line represents the hardness of the bottom of the block. This data was collected as a form of check to see if the plateaued hardness readings found on the top surfaces of the block are of a similar agreement to the bottom surface. If they were in close agreement, then the testing of the block was considered finished. If they were not, then an evaluation of the data was found and methods were tried to reduce this difference. Methods tried included, further grinding of the top surface if it was anticipated that the fresh rock was not yet reached, further collection of hardness data on the bottom surface, or further grinding of the bottom surface and hardness testing. It was not uncommon for one or all of these methods having to be employed for a single block.

Appendix C and Appendix D show the hardness versus depth data found on every natural rock specimen tested in the study. All data collected that was considered as being exempt by the author and the reason for the exemption is listed in the table on the final

page of the Appendix. The 'Exemption Number' corresponds to the column in the appropriate table which has been exempt. If the bottom of the primary material was different than the top of the primary material, the general consensus made by the author was that this was the result of a grain structure heterogeneity. This could usually be commandeered by removal by grinding of that surface followed by retesting. For this mentioned case, the data collected on the surface considered to be subject to this heterogeneity, this increased or reduced collective hardness data was exempt from analysis once the author made this realization after further testing. In the tabular data of Appendix D, the exemption of this data is listed in the respective columns and reference the table on the final page of the Appendix. For each specimen, an image of the 3D scan is also shown (Appendix C) and information on where the rock sample was collected from and the geology of both rock types making up each specimen is identified. Each specimen tested is identified in the form of 'Specimen A Block B' where A is the original number assigned to the rock sample collected and B is the assigned number given to the extracted block from that sample that is undergoing testing.

An objective of this study was to see if the influence zone results found on the artificial material specimens could also be observed on natural rock transition specimens. Unlike the artificial material specimens, the natural rock specimens represented real geological conditions including but not limited to, having a much stronger secondary material layer, anisotropic and heterogeneous conditions, and an undulating contact line. The expectations in conducting this exercise was not necessarily to find the exact same results seen in the artificial material composite specimens, but to see if the results noticeably differ or are for the most part similar. For example, both artificial composite specimen combinations determined an influence zone depth to be within 2 mm of the surface. It was an objective of this exercise to see if an influence zone larger than 2 mm could be observed in natural rock. If it was not observed to be larger than 2 mm, than the findings were considered to successfully match that of the artificial material results. The level of detail found on the artificial material composite specimens were not anticipated to be retrieved on these natural rock specimens less than 2 mm depth to the transition line.

4.2.1 SS SPECIMENS

Six natural rock SS specimens were prepared and tested in this study. Two blocks were tested from Sample 37 while four blocks were tested from Sample 47. The results from one of each of these specimens is displayed in Figure 4-7. The remaining four specimens can be viewed in Appendix C and will be discussed in this section. In addition, the hardness versus grinding depth data for all of these specimens can be viewed in Appendix D.

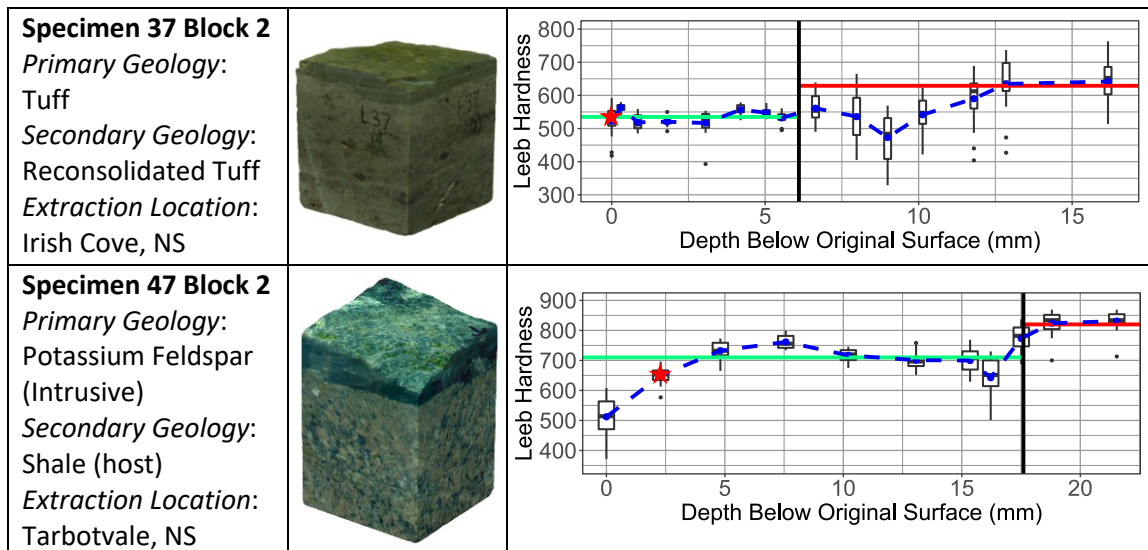


Figure 4-7: Geology classification, extraction location, image, and hardness results for two of the six natural rock transition SS specimens.

The $MeanL_D$ value was calculated using the first surface L_D value for both Specimen 37 Block 1 and 2. The natural surface for both blocks were smooth enough to produce representative hardness values of that material, shown in the box and whiskers plots. Both specimens showed an increase in hardness from one rock type to the other; however, this hardness change did not occur immediately once into the primary rock. It seems that a similar mean hardness value could be found on either side of the rock type transition line; however, once into the primary rock, the variability in the data increased, the rock became softer, then it became harder. With the secondary material being that of reconsolidated tuff material, it is believed by the author that the secondary material may have been consolidated back to a material of similar hardness to its original rock. The primary tuff material was filled with voids and this explains the variation in the data once

into the primary material. The reconsolidated secondary tuff material did not have any voids in it which is the reason for the reduced variability in the hardness data found. This explains why no increasing hardness gradient can be seen near the rock type transition as both materials are of the same hardness. A weathering profile existed at the top of the primary material. The overlying mass together with the fine, weathered rock debris which would have occupied the natural/ weather-induced voids of the primary material, is the reason for the harder results at the surface, which decreased with depth. The Leeb device captured the minimum hardness in the weathered material once through the primary rock occupied by weathered debris. Then the hardness began to increase until the unweathered, primary material was reached. Both blocks extracted from Sample 37 produced interesting results but the similar hardness seen on both sides of the rock type transition line was a scenario that differed from the scenario that was seen in the artificial SS specimens. It is for this reason that these specimens were considered to not provide information that can be used to better understand the artificial material results.

The first surface was exempt from the calculations of $MeanL_D$ for all blocks extracted from Specimen 47 as the scatter shown in the data found on the first surface is different than that predominately seen in the remaining hardness data found in that material. The excess scatter, or increased standard deviation, is considered to be an indication of the effects of roughness rather than of that of the material. As will be shown in Section 4.6.1, roughness effects found by a comparison of the standard deviation between the first surface and mean of the subsequent surfaces in the secondary material, is an effective way to understand whether the results found on the surface were affected by roughness. For all blocks of Sample 47, an increase in hardness from one rock type to the other can be seen. For these specimens, an increasing hardness gradient appears to have been captured. This confirms the results of the artificial material SS specimens to be true in that the underlying, harder material can be seen to influence the hardness readings found on the Leeb device in close proximity to the primary material. For all four specimens, a dip in hardness can be seen immediately above the primary material. With the shale material being the host rock, the interfacing surface in the shale could have been weathered prior to the intrusion of the plutonic rock or it was weakened during the intrusion. Regardless of the cause, the Leeb device was able to successfully detect this

softer material just before the influence of the underlying primary material began to be detectable by the Leeb. The results of the blocks extracted from Sample 47 show that an influence zone does exist even in natural rock. The exact start of the influence zone was not able to be captured; however, the influence zone detected in the natural SS specimens does not appear to be larger than that detected in the artificial material SS specimens. This proves that the results found on the artificial material SS specimens holds valid for natural rock.

4.2.2 SH SPECIMENS

Two natural rock specimens were tested in the SH category and are both extracted from Sample 1. Figure 4-8 below shows the results of one of the two specimens. The other specimen can be seen in Appendix C and will be discussed in this section. In addition, the hardness versus grinding depth data for both of these specimens can be viewed in Appendix D.

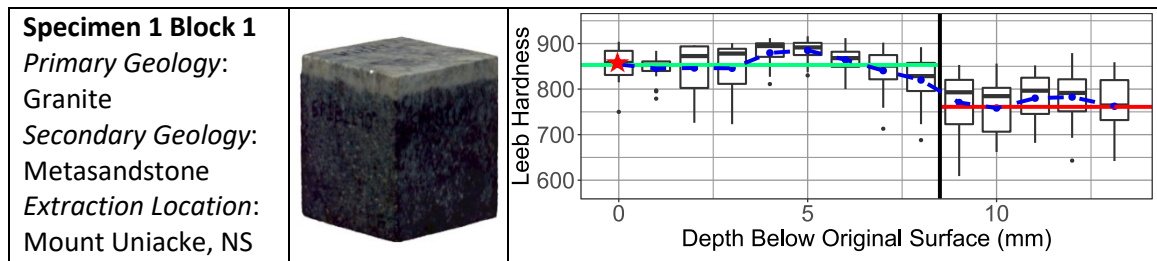


Figure 4-8: Geology classification, extraction location, image, and hardness results for one of two natural rock transition SH specimens.

The first surface L_D value was used to calculate the $MeanL_D$ for both specimens. The first surfaces for both were saw cut to create a uniform secondary material layer as the natural surface significantly varied in thickness prior to cutting. The final surface in the secondary material was 0.5 and 0.6 mm (Block 1 and 2) from the approximate interface location and decreasing hardness values can be observed to have been found on both of these nearest surfaces. Based on the results in the artificial material SH specimens (Section 4.1.3), it is believed by the author that this subtle decrease in hardness seen on both specimens can be attributed to the influence zone. These findings also show that an influence zone larger than 2 mm does not appear to exist concluding that the results found on the artificial material SH specimens hold valid in natural rock.

4.2.3 UM SPECIMENS

Five natural rock transition specimens were deemed as UM as their secondary material hardness fell within 5 percent of their primary material hardness. Figure 4-9 shows the results of three of the five specimens. The other two specimens can be seen in Appendix C and will be discussed in this section. In addition, the hardness versus grinding depth data for all of these specimens can be viewed in Appendix D.

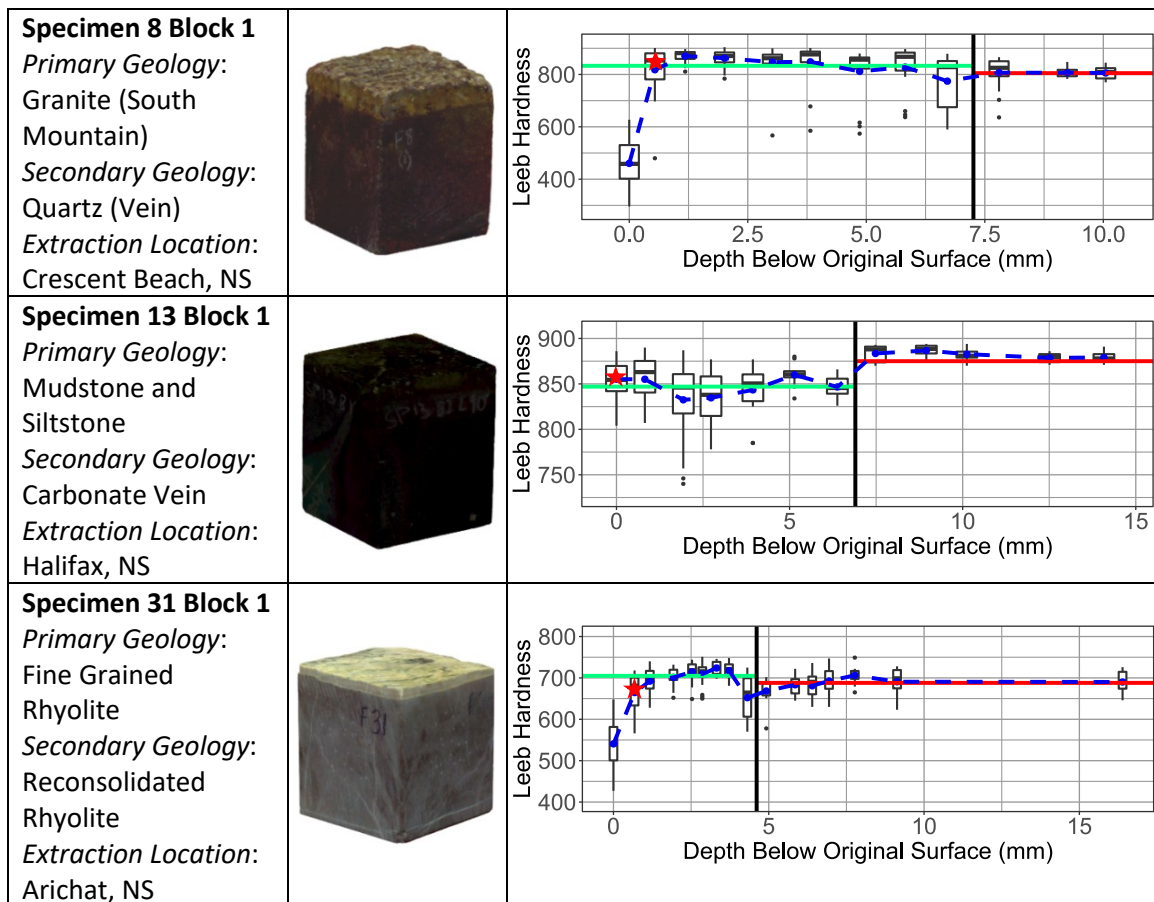


Figure 4-9: Geology classification, extraction location, image, and hardness results for three of five natural rock transition UM specimens.

The three blocks extracted from Sample 8 had a rough, quartz crystalline surface that was difficult to test with the Leeb device. The natural surface was tested on the first block but was abandoned as the roughness was too great to gather reasonable data. As a result, the first tested surface for all three of these blocks was a surface after several passes of the grinder. This was to remove the sharp peaks of the crystalline structure so that the device would be able to successfully impact a flat enough surface to produce a

reading. There were however many troughs still on these first surfaces, and in the case of Block 3, the first three surfaces proved difficult to gather data on a flat, void-free surface. The first surface shown in the plots for the blocks of Sample 8 show the results on the first ground surface and for all three blocks, the data found on this surface was exempt from the calculation of $MeanL_D$. The results of all three specimens show relatively stable hardness in the secondary material with a slight softening seen above the primary material. The reason for this reduced hardness could have been the result of the heating and cooling process at the time of the intrusion of the quartz vein into the host rock which altered the rock properties of the quartz near the wall of the host rock. It seems that a slight increase can be seen in the mean value once into the primary material but no recognizable increasing hardness gradient can be seen for any. No recognizable gradient can be seen likely because of the similar hardness between the secondary material and the primary material. This is not to say that one did not exist. It is believed by the author that individual data points could show the influence of the primary material but overall, the data does not consistently show an increase as say, the blocks of Sample 47.

It should be mentioned that it is understandable that capturing the influence of the primary material in the results found on the secondary material is not a straight-forward task when dealing with natural rock specimens. The significant secondary material influence zone, measured at 0.7 mm thick above the primary material, measured with confidence on the artificial material specimens seen in Section 4.1.2, is seldom even attainable on natural rock transition specimens. Being able to perform testing with this level of accuracy using a large grinding machine on natural rock containing geological heterogeneity, specifically an undulating contact line, was a difficult task. In order to capture this level of accuracy consistently, it is envisaged that careful planning, the use of precise equipment, and close monitoring would be required to potentially be able to capture data within this range of measurement with suitable accuracy. It should be further noted that the location of the rock type transition line is only approximate as the natural undulation of the contact line was cause to some secondary material being present during testing while in other areas it had been fully removed. The greatest success in accurately locating a contact line and of being sure of the remaining thickness in the secondary material to that contact line was dependent on the smoothness of the primary material at

the interface. This is why the influence zone could be easily captured in the artificial material specimens as the primary material was flat at the interface in three dimensions. However, all attempts were tried by the author to get within a close proximity to the rock type transition line.

For specimens Specimen 13 Block 1, the first surface was a saw cut surface as it was a Category 2 specimen as per the definition in Section 3.1.2.2, and illustrated in Figure 3-6. In the secondary material, a larger standard deviation could be seen for the first five surfaces while a lesser standard deviation could be seen for the surfaces nearing the primary material. This apparent property change is believed by the author to be the result of an occurred phenomenon at the time of geological formation. An increasing hardness gradient was not captured for this specimen. Instead, an abrupt transition of overall hardness was seen. Although the influence zone limit was not captured on this specimen, an influence zone thickness in exceedance to that seen on the artificial material composite specimens (Section 4.1.2) was not observed.

The natural, first surface of Specimen 31 Block 1 was discarded for the calculation of $MeanL_D$. This block had similar traits as the blocks from Sample 37 discussed in Section 4.2.1; that is, a secondary material layer comprised of consolidated, weathered host rock material. In a similar fashion to the results of the blocks from Sample 37, the hardness of the secondary material immediately above the transition line reduced to a mean hardness value comparable to that of the material immediately below the transition line. The large variation in hardness values found on this surface is likely due to the natural undulation seen on the top surface of the primary material where the slight remnants of the secondary material was still present while some areas of the primary material was slightly exposed. As was the case of the blocks of Sample 37, an increasing hardness gradient can be seen in the primary material. This hardness increase shows indicative results to that of a typical weathered surface as will be seen in Section 4.3. The fine-grained Rhyolite primary material and the reconsolidated weathered debris produced results of comparable standard deviation. As this specimen had a secondary material overlying a weathered primary material, the influence zone results of the artificial material composite specimens (Section 4.2.2) could not be compared to this.

The majority of the blocks discussed in this section produced comparable mean hardness results on both sides of the rock type transition line which did not allow for an examination of whether an influence zone was even present. The only block that showed a recognizable hardness change across the rock type transition line was Specimen 13 Block 1; however, the influence zone in the secondary material was not captured. A conclusion that can be drawn on the results of the testing done on the natural rock UM specimens is that an influence zone larger than 2 mm was not seen to exist further proving the results found on the artificial material specimens to be valid.

4.3 WEATHERED/ ALTERED ROCK SPECIMENS

In this section, the results of the natural rock specimens featuring a weathered surface are displayed and discussed. For all cases, the Leeb hardness device was successful at capturing a reduced hardness value at the weathered surface in comparison to that seen in the fresh rock. Like the natural rock transition specimens, a $MeanL_D$ value was calculated and this line was plotted showing the mean hardness of the secondary material (weathered profile). For all specimens, the first surface was not discarded from this calculation regardless of roughness. Section 4.6.1 discusses different suggested ways to interpret the data found in the secondary material to arrive at a reasonable prediction of hardness found at the natural surface.

Fourteen weathered natural rock specimens were prepared and tested in this study. Figure 4-10 shows the results of four of these specimens selected for illustrative purposes, chosen to represent the majority of cases. The results of the remainder of these specimens can be viewed in Appendix C and will be discussed in this section. In addition, the hardness versus grinding depth data for all of these specimens can be viewed in Appendix D.

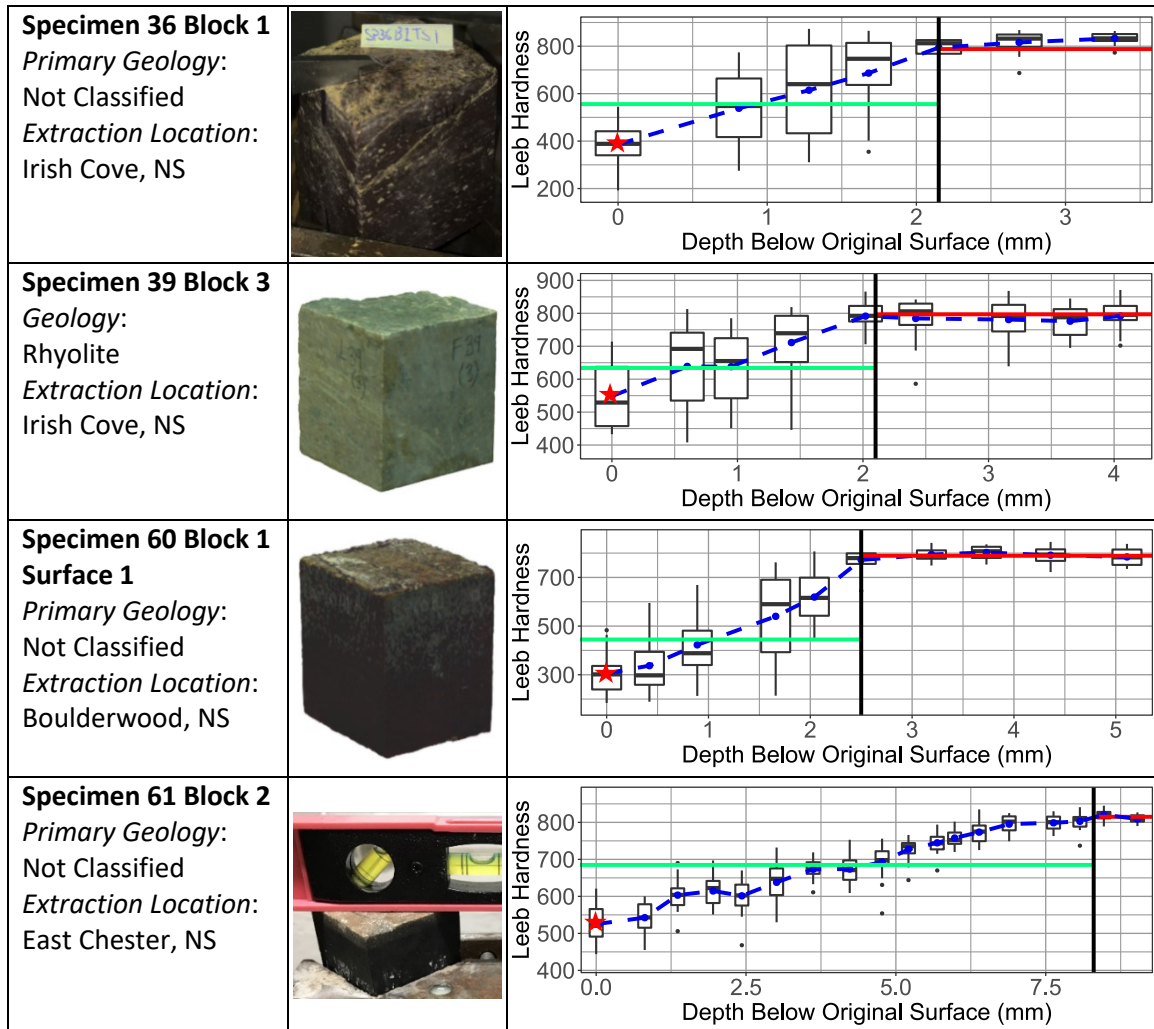


Figure 4-10: Geology classification, extraction location, image, and hardness results for four of the 14 weathered natural rock specimens.

Similar trending results as was given by Hack et al. in 1993 (Section 2.3.2) were seen with all fourteen specimens tested in this study: the lowest L_D value was found on the natural surface (except for one specimen where it was found on the first ground surface), the L_D values on the subsequent surfaces increased with depth until the L_D values plateaued, becoming relatively consistent with depth once into the fresh rock. In all cases except for Specimen 53 Block 3 and Specimen 62 Block 1, an increasing hardness gradient with depth was captured in between the natural surface and the fresh rock. Section 4.6.2 discusses recommended strategies for determining a reasonable L_D value to be used to predict the JCS value of the rock. The findings on these specimens not only show the change in hardness with depth, they also show the depth of weathering.

The blocks of Sample 53 showed the shallowest weathering depth while the blocks of Sample 61 showed the deepest.

A conclusion that can be drawn from the findings from the specimens tested and described in this section is that the Leeb device adequately was able to capture a hardness change with depth throughout the weathered profile of a naturally weathered rock surface. Unlike the rock type transition specimens, the secondary material does not have a consistent hardness throughout that allows for the influence zone to be recognized by a dramatic hardness change within close proximity to the underlying primary material. Although, an influence zone can be realized in the hardness data for thicknesses of material of similar properties thinner than 1.7 mm thick (Figure 4-4) that overlies a harder underlying material. Therefore, each L_D value found in the weathered profile is not of the true hardness of that material but that of an increased hardness influenced by the underlying, harder material. Additionally, the L_D value found at the natural surface, if used to correlate to a JCS value, will be higher than its true, uninfluenced L_D value resulting in a higher, more conservative JCS value. Future research could be to come up with a correction value to predict the true surface L_D value irrespective of the influences of the underlying material. In this way, the evaluator would be able to predict a more-refined JCS value. The usage of the word ‘more-refined’ was deliberate as there could be other factors that could result in JCS values that are not exactly ‘true’ such as the inherent variability characteristic of the rock itself or the correlation equation not being completely accurate. A way to better understand the difference between the Leeb-derived JCS value and perhaps a ‘more-true’ JCS value used on weathered surfaces could be to perform direct shear tests. The difference between the back-calculated JCS value from the direct shear test and that of the Leeb-derived JCS value could show the overall difference in the accuracy between the two methods. Inside this difference would exist the influence zone effect on the result inherent in the Leeb-derived JCS value.

4.4 NUMERICAL MODELING

The two-dimensional finite element code RS2 by RocScience was used in this research program during the laboratory lockout period at Dalhousie University during the COVID-19 pandemic. Apart from providing a task that could be conducted from home,

the goal was to develop a model that gives insight into the resulting depth of stress distribution into a rock shortly after an impact with the Leeb device. Using properties of intact Wallace sandstone used in the artificial material specimens (Section 3.1.1), an axisymmetric model was created. The rock in the model was 10 mm thick and was 54 mm (NX size) in diameter, drawn from its centerline to its far right. Half of a tungsten carbide ball, hereinafter referred to as 'ball', of the Leeb hardness device was modelled from its vertical centerline to its far right in the shape of a quarter dodecagon, for simplicity. The radius of this ball was 1.5 mm and the flat contact diameter of the ball, separated from the sandstone by a stage boundary, was 750 μm long; 375 μm in the axisymmetric model. A free boundary condition was set to exist on the top surface of the sandstone and on the sides of the quarter dodecagon ball, a roller condition was set on the axisymmetric axis for the ball and sandstone and the bottom and right side were pinned. A graded mesh with 6-noded triangular elements was used with increased mesh discretization and density in the sandstone beneath the ball.

The impact energy of the device, irrespective of any material it impacts, is known to be 11 mJ (TIME Group Inc., n.d). As the force is not known, an approach was conducted whereby the ball which consists of a much stiffer material than the sandstone, is displaced downward into the much softer sandstone in factored increments. As will be discussed in detail shortly, a certain combination of stress together with an associated ball displacement will produce this 11 mJ impact energy. Therefore, a uniform, maximum displacement boundary of 102 μm was added to the horizontal cross-section of the ball and was incrementally factored over a number of stages. This maximum displacement value was taken from Desarnaud et al., 2019 (Section 2.3.2) and was found after 20 repeated impacts on a Stanton Moor sandstone specimen; a sandstone of similar characteristics to the Wallace Sandstone. The idea was that at a displacement value equivalent to a certain fraction of the maximum displacement value would equal the impact energy of the device. The stress depth below the ball at this determined vertical displacement quantity would be the approximated influence zone depth predicted using finite element methods. A view of the model is displayed in Figure 4-11.

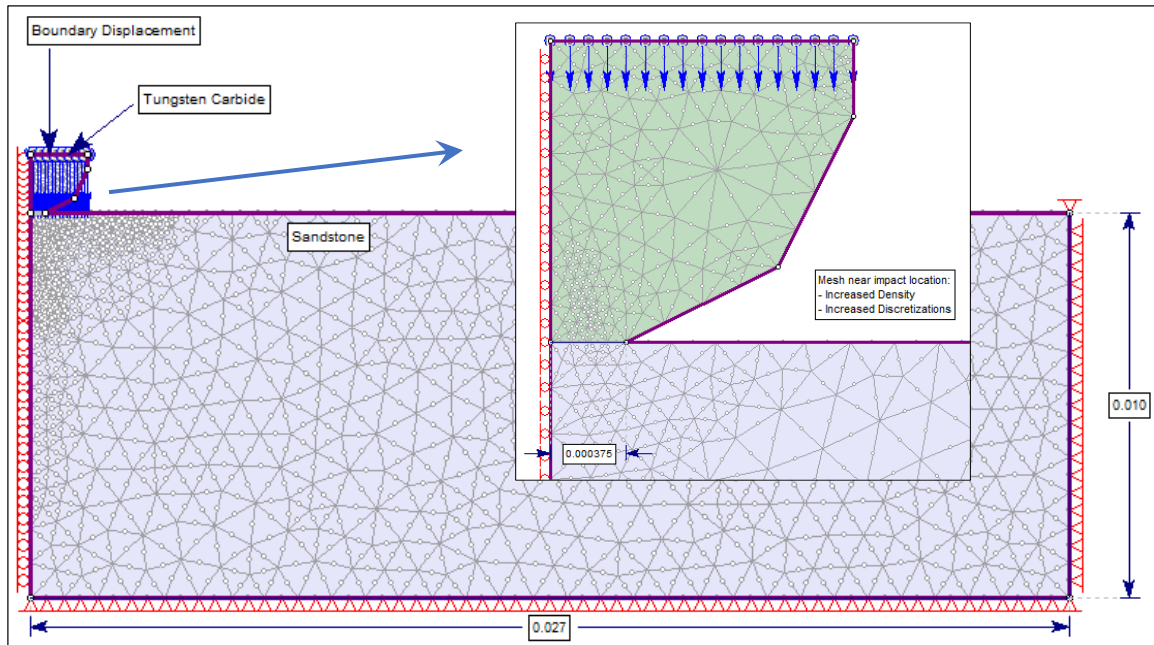


Figure 4-11: Axisymmetric model of a tungsten carbide (Leeb) ball on the surface of a sandstone produced using RS2 by Rocscience.

It should be recognized that the model has a simplified, fixed contact between the ball and the sandstone which disagrees with the dynamic process that would occur during actual use. There is also no slippage that can occur between the ball and the rock which is also unrepresentative of what would occur during actual use. Despite these limitations, the model was assumed to be sufficient to provide insight for the purposes of this research program. In the model, the ball was taken to be isotropic and elastic. The Poisson's ratio and the Young's Modulus were set to 0.18 and 707000 MPa (Ungar et al., 1999) with a unit weight of 0.155 MN/m^3 (Kurlov and Gusev, 2013). For the Wallace sandstone, the Poisson's ratio and Young's Modulus were taken to be 0.22 and 17,500 MPa (Ghasemi and Corkum, 2020). Additionally, a σ_c and unit weight of 90 MPa and 0.0255 MN/m^3 (Wallace Quarries Ltd, n.d.) were used. For both materials, an initial element loading of 'none' was selected indicating that no body forces (gravity) or field stresses were considered by the author to be applicable. For a σ_c of 90 MPa, a GSI value of 100, a Young Modulus of 17,500 MPa, and an m_i value for a sandstone being 17 (Hoek, 2007), the Mohr-Coulomb equivalent parameters were found using equations provided by Hoek. The input parameters of peak tensile strength, peak friction angle and peak cohesion were found to be 5.3 MPa, 48° , and 16.4 MPa and confirmed

with RocData, a software produced by Rocscience. Both elastic and plastic constitutive models were run with the residual strength parameters equaling that of the peak strength parameters for the latter model.

To properly assess the depth of stress seen below the Leeb ball into the sandstone, some calibration work needed to be completed to ensure that the returned results were representative of an actual impact by the Leeb device. As was previously mentioned, the Leeb device delivers 11 mJ of energy to an impacted surface (TIME Group Inc., n.d). Regardless of material, this impact energy is delivered by this device. Thus, as each rock tested upon has different properties, the stress depths into the rock below the ball on impact will be different for each. This is also true for the amount of vertical displacement that would occur into the material from the ball. With the following three equations, the model was considered calibrated to actual conditions if the right side of Eq. 20 equaled to the left side.

$$e_i = F \times \delta_v \quad \text{Eq. 20}$$

With:

$$F = \sigma_v \times A \quad \text{Eq. 21}$$

And:

$$A = \pi r^2 \quad \text{Eq. 22}$$

Where:

e_i (N-mm) = Impact energy of the ball

F (N) = Impacting force of the ball

δ_v (μm) = Vertical displacement of the ball

σ_v (N/mm^2) = Average vertical stress across the centreline of the ball

A (mm^2) = Cross-sectional area of the ball

r (mm) = Radius of the ball

With a displacement boundary condition in the y-direction only, applied across the horizontal centreline of the ball to a maximum displacement of 102 μm , 11 stage factors from 0 to 1.0 of equal increments of 0.1, beginning with 0, were simulated in the model. Each stage applies a δ_v value equal to the factor of that stage multiplied by the maximum displacement value to the centreline of the ball. By computing the model, the σ_v was

determined and was used to find F for each stage. With the notion that a certain combination of F and δ_v will equal an 11 mJ energy, the stage factor taken to the thousandths decimal place was found. By evaluation of the two nearest stage factors to the target impact energy of 11 mJ, nine stage factors were added to the hundredth decimal place between the nearest stage factors in equal increments. This process was again completed to the thousandths decimal place between the nearest stage factors and the nearest stage factor to produce an impact energy of 11 mJ was taken to be the calibrated stage that is representative of actual conditions. The stress depth into the sandstone produced from the computation of this stage, was taken to be the influence zone for the Leeb device on an intact piece of Wallace Sandstone. Using this iterative process, it was found that a displacement factor of 0.281 when applied to the maximum displacement value of 102 μm , produced an impact energy of 11 mJ. Figure 4-12 shows the vertical stress (Sigma YY) results for the displacement factors of 0.1, 0.21, 0.281, 0.6, and 1.0. Not surprisingly, it can be seen that the vertical stresses for all displacement factors are the highest at the surface and reduce with depth. The red plot showing a displacement factor of 0.281, represents the results of the Leeb device.

Elastic: Sigma YY with Depth

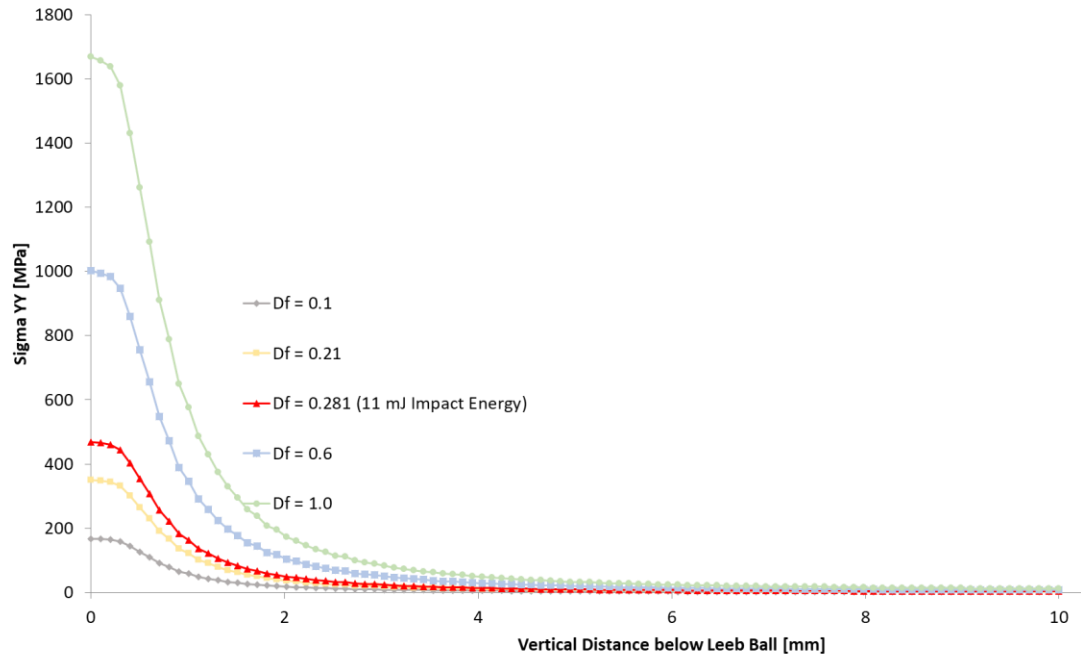


Figure 4-12: Influence zone depth into sandstone beneath the impact location of the Leeb device using the finite element code RS2.

The influence zone shown in this plot appears to be relatively consistent with the results found on the artificial material composite specimen results seen in Section 4.1.2 and Section 4.1.3. It is believed by the author that the identified zone of ‘negligible influence’ illustrated in Figure 4-4 and Figure 4-6 on the artificial composite specimens to be between approximately 1.7 and 1.8 mm is in agreement with the stress distribution from the model results. Likewise, the zones of ‘marginal and significant influence’ from 0 and 1.7, or 1.8 mm depth also appears to be believable from this plot. It also appears true that an approximate influence zone depth value of 2 mm would be a suitable conclusion to describe the influence zone depth.

It should be noted again that this model does not represent actual conditions, but a greatly simplified illustrative example. The results were not considered to be an exact match to real conditions; instead, they chiefly serve as an aid to better understand and to more or less confirm the accuracy of, the findings on the artificial composite specimens. The fact that the modelled results are in such close agreement to the results found on actual materials, is a testament to the success of the influence zone findings for this device.

4.5 SURFACE TREATMENT EVALUATION

As described in Section 2.3.2, Verwaal and Mulder in 1993 found that surfaces prepared that were sawn, sawn then lapped, and sawn then lapped and polished did not see a noticeable difference in Leeb hardness readings. Desarnaud et al., 2019 examined different surface treatments found by using sandpaper and found the same result; however, they found that moisture content did influence the hardness readings. As was mentioned in Section 3.1.2.4, it was determined in this study that cut surfaces were observed to produce different hardness readings than those found on freshly ground surfaces. During the testing on natural rock specimens, it was recognized that hardness values obtained on surfaces prepared with the grinder seemingly produced lower values than those found on the same rock with surfaces prepared with a saw. The intact hardness of the primary material was originally planned to be taken as the hardness value obtained on the bottom of the specimen on the saw cut primary material surface. It was assumed that a comparable moisture content would be seen on the bottom of the specimen as it would on the top as the specimen was drenched in cooling fluid during grinding. The ground surface and the cut surface were assumed to produce similar values. Prior to completing the grinding/hardness testing procedure on a single specimen, the primary material hardness found on the specimen bottom was compared to the results found on the top of this material and a determination could be made as to whether the intact primary material had been reached or not. Hack et al., 1993 (Section 2.3.2) described the values to stabilize when into the unweathered primary material. Thus, during testing in this research program, unweathered primary rock was considered to be reached when the findings on each surface would stabilize. It therefore seemed logical that the hardness values found on the saw cut bottom of the specimen would closely match the stabilized values found at the top of the specimen in this material. From the outset, the stabilized hardness values on the top were found to be lower than the hardness findings found on the saw cut bottom surfaces. Advancing the grinding operation further was tried initially, but the value found on the bottom could not be achieved on the top.

As a trial, the bottom of the primary material was ground and tested in a similar condition to that seen on the top i.e., ground, then dried with paper towel and tested immediately afterwards. It was found that the stabilized values seen at the top of the

specimen closely matched the findings found on the bottom. Upon this discovery, it seemed necessary to conduct testing on saw cut and ground specimens of different moisture contents.

An experiment was carried out in which 100 single impact readings were taken on the surface of cylindrical Wallace sandstone specimens that were a) freshly cut, b) cut and air-dried for an extended amount of time, c) freshly ground and, d) ground and air-dried for an extended amount of time. The fresh surface tests were dried with paper towel and the testing was immediately commenced while the air-dried specimens were dried with paper towel and then left to air-dry in the laboratory. The saw cut, air-dried specimen was dried for an unrecorded amount of time in excess of a month, while the ground, air-dried specimen was tested after three days. As a simple form of delineation between them, the former was described to have a moisture condition of dry, while the latter was described to have a moisture condition of moist-dry. It should be noted that the moisture content was not measured in this experiment; the soul intent of this experiment was to see if a change in hardness could be detected. The intent of these findings was originally planned to better understand the clear discrepancy found in the results between the top and the bottom of the primary material during testing. The idea was that if it was found that the bottom needed to be prepared like the top (i.e, ground, dried with paper towel, then tested), then the testing methodology would be changed to reflect this, as was the case. The specimen diameter was 50 mm and the starting length of the specimen was approximately 125 mm, equating to 2.5 times the diameter. This length to diameter ratio matches the higher end of the ASTM D7012 standard for rock specimens prepared for UCS testing. The testing occurring in this exercise stayed within the acceptable length to diameter range of 2:1 and 2.5:1 as outlined in the ASTM D7012 standard so as to avoid any size effects. Additionally, the Wallace sandstone was used due to its relatively homogenous and isotropic nature with the intention of reducing the number of factors that might influence the hardness readings.

The results found on each surface are displayed as individual box and whisker plots, seen in Figure 4-13. The ‘Cut Dry’ surface was tested first and was taken on a specimen that had been in the laboratory for an unrecorded amount of time. This specimen surface was then saw cut a couple of millimeters down from the top surface,

dried with paper towel, then tested to produce the results of ‘Cut Wet’. The specimen was next ground down a couple of millimeters and the surface was dried with paper towel and tested to produce the results of ‘Grind Wet’. The specimen was next ground down a couple of millimeters, dried with paper towel, left to air-dry, and tested after 3 days to produce the results of ‘Grind Moist-Dry’.

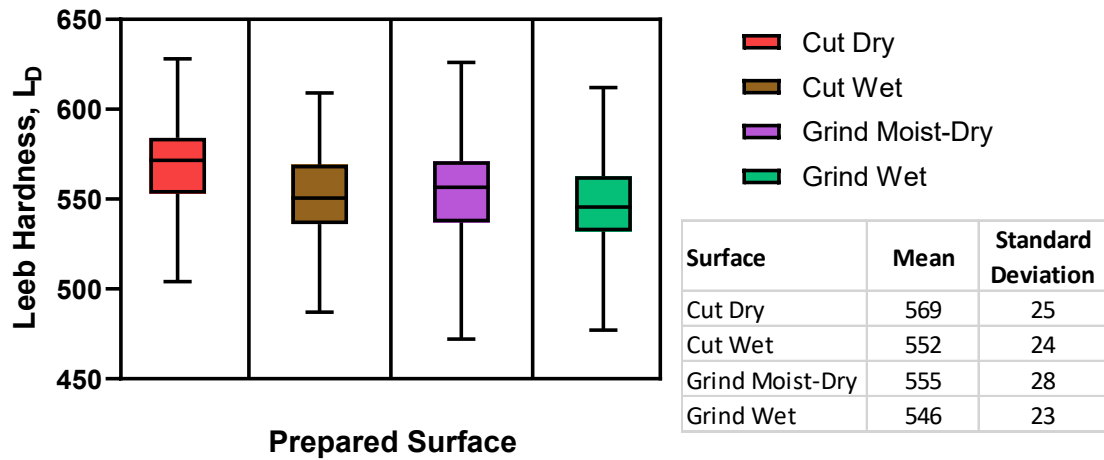


Figure 4-13: Surface treatment evaluation on Wallace Sandstone cylinder surfaces saw cut and ground.

The best example of moisture content change was found between the ‘Cut Dry’ and ‘Cut Wet’ surfaces which seen a similar standard deviation and a decrease of mean hardness of 17. The ‘Grind Moist-Dry’ surface seen the highest standard deviation while the ‘Grind Wet’ surface seen the lowest. It is believed that the moist-dry condition is the cause for the larger data scatter found on the ‘Grind Moist-Dry’ surface as it is likely that different moisture conditions were present across the surface. Some voids for example could have still been filled with water while others could have been free of water. The mean hardness between the ground surfaces was 9. The data found in this exercise suggests that moisture content affects the hardness testing results.

From the hardness/ grinding testing process on natural rock specimens, it was seen repeatedly that a drenched cut surface on the bottom of the primary material when dried with paper towel produced much higher values than the top ground surface of the primary material. The difference was in exceedance than what can be seen in the results in Figure 4-3 between that found on a ‘Cut Wet’ and a ‘Cut Dry’ surface. The author believes that the reasons for this relates to the time of a surface to uptake water. A dried cut surface for

example is dealing with surface tension forces alone when wetted while a treated surface deals with surface tension forces as well as a certain pressure from the grinding wheel or cutting disk that applies force to the water to enter the voids. Moreover, when water is in the voids of the surface, more of a vacuum effect should exist to draw more water in. For the case of a dry surface which has no water in the voids initially, the uptake of water would take longer than if water was currently partially occupying the voids. It is thus believed that a surface that is wetted for the same duration of time as a surface being treated, takes on different moisture conditions than the treated surface. Further, it is believed that each treatment could entrain a different amount of water into the surface. This determination is merely speculative from testing and is not proven. Further research could be conducted to determine if this is in fact true.

In this study, the testing was performed on the natural surfaces of each specimen while they were in a dry state. This means that the results found on all subsequent surfaces were collected on surfaces prepared in a different way, having different moisture conditions. This does not mean that the data collected on the first surface is incorrect, it is just different than the other surfaces and is higher than if it were at the same moisture content as the subsequent surfaces. Therefore, hardness data collection on a natural surface should be considered as being harder than it would be if it was at the same moisture content as that seen on the subsequent ground surfaces. A method suggested in Section 4.6.2, visualized in Figure 4-16 could potentially be used here to adjust the L_D value found for this surface if tested in a dry state when a grinding/ hardness testing approach is used to find the hardness gradient of the rock. The main conclusion of this exercise is that moisture and how the surface was prepared must be considered in performing hardness testing if the found results between surfaces are to be compared.

4.6 JRC AND JCS PREDICTIONS

In Section 2.3.2, it was seen that too rough of a surface influences the hardness readings found on the Leeb device. This finding was also found in this study. In addition to hardness reading impacts, roughness also affects the depth of shear.

In a weathered rock joint, a certain depth into the rock would be sheared off during movement with an adjacent block. If both a smooth joint surface and a rough joint surface

of the same properties were subjected to the same confining conditions and sheared, a smooth surface would allow for the rock blocks to shear to a lesser depth than would be seen on a rougher surface. For a rougher joint, greater dilation would be required for the rock block to move past the other requiring a greater volumetric increase that is unable to occur. For it to successfully shear, the asperities would need to shear off.

The strength of the material at the depth of shear plane or all the material between the surface and the shear plane would resist the shear. Thus, it is envisaged that the L_D value selected to determine JCS should represent either the material at the shear plane or the material between the surface and the shear plane. By understanding the shearing depth, the hardness gradient data (if the material from the surface to the shear plane resists the shear) or the hardness of the material at the shear plane gained from the grinding/ hardness testing procedure, would be ideal to determine this representative L_D value. However, without a knowledge of the shearing depth into the rock for the given scenario in which the joint is being subjected to, this representative L_D value can only be approximated. Without shearing depth information, the L_D value in this study produced on the natural surface was used to represent the weathered material of the block.

The forthcoming sections identify the amount of roughness that was present on the specimens in this study as well as the effects of roughness found in the hardness readings. Suggested methods are described to exclude these roughness influences during the selection process of a representative L_D value for the weathered material. Additionally, the process of determining a JCS value using the representative L_D value is shown via suggested methods of the author.

4.6.1 JRC DETERMINATION

In this research program, a desktop 3D scanner was used to scan the natural surfaces of all specimens tested. The programming language Python was used to work with the scan data from 3D Object files for each surface. Two orthogonal profiles for each surface, one in the x-direction and one in the y-direction, in the center of each surface were created. A package containing these two profiles for 23 surfaces was prepared and was sent to consultancies that work in the specialty of rock mechanics for each to be evaluated against the Barton and Choubey JRC chart (Figure 2-2) seen in Section 2.1.2.

The evaluators were asked to state their names, the firm or institution they work for, their position, and their experience level in terms of a numerical value as follows: 1: no technical background, 2: no experience of JRC estimation, 3: some experience of JRC estimation, 4: very experienced at JRC estimation. This experience level criterion was adopted from Beer et al., 2002 who performed a similar survey. In this package, the specimen number, an image of the specimen, and the x- and y-direction roughness profiles are shown. The scale of each x- and y-direction roughness profile matched the scale of the Barton and Choubey JRC chart included on the final page of the package. Appendix E shows the evaluation survey package that was sent out to each of the 11 participants who took part in the survey.

A graph showing floating bar plots for each specimen is shown in Figure 4-14.

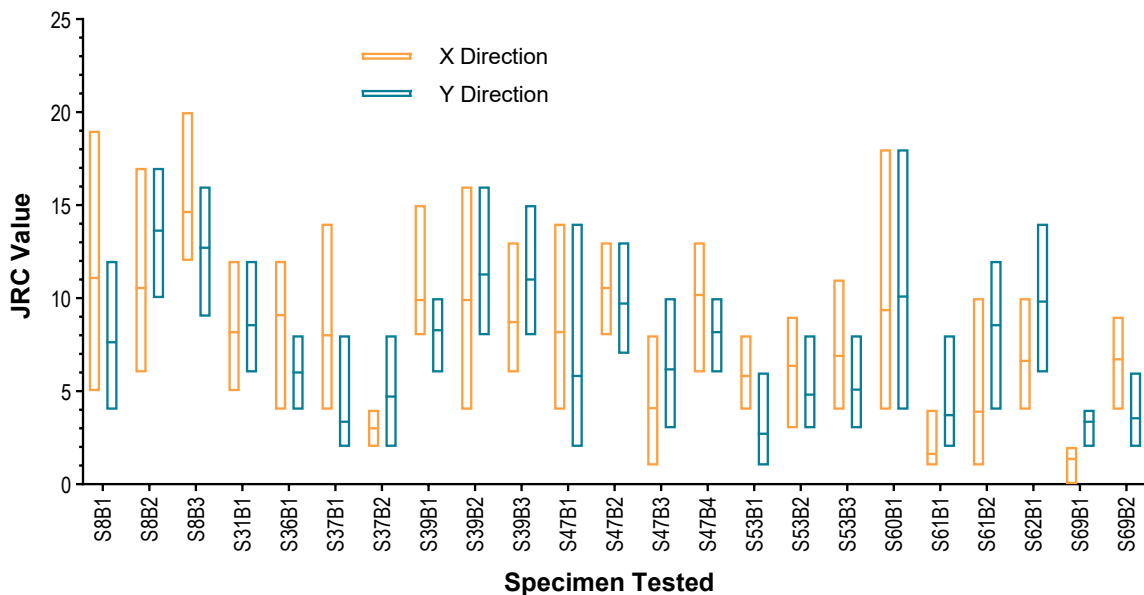


Figure 4-14: JRC evaluation survey results for all of the specimens tested in this study.

In Figure 4-14, the orange plots represent the results of the x-direction profiles for each specimen, while the dark blue plots represent the results of the y-direction profiles. In all cases, the floating bar plots show the length of the bar ranging from the minimum to the maximum value with the mean value represented with a horizontal line within the bar. It should be noted that the x- and y-direction was chosen arbitrarily at the time of making the profiles meaning that these directions do not necessarily match the directions

assigned to the other blocks from that sample. If the average JRC value for each direction of a particular surface is evaluated against the other directions' average JRC value, it is seen that in all cases, the quantity of roughness differs.

Table 4-1 shows the results of the JRC survey. It can be seen that overall, the standard deviation ranges from 1 to 5 but on average is 2. The individual x- and y-direction JRC values determined in this section not only provide an understanding of roughness variation per direction reviewed, they also could potentially provide an important link to our interpretation of roughness effects seen in the hardness data produced with the Leeb device. As was adopted from Corkum et al., 2018 (Section 2.3.2), a testing area of within 50 mm on the top surface of the specimen was used to evaluate L_D for the surface. As the hardness testing was conducted on the surface irrespective of direction, the average JRC value, gathered by averaging the 22 evaluations (11 per direction) made on each surface was used in an attempt to make this link and is displayed in the far-right column of Table 4-1.

It should be mentioned that JRC was originally obtained to help determine a shear depth versus roughness understanding. However, without shear testing data, only assumptions can be made as to how deep the shear plane would be. These collected JRC values for each surface are planned for future research outside of this study with plans to develop a better understanding of the amount of material that should be considered in the determination of JCS. In this study, preliminary efforts were made to try and link the JRC values for each surface to the roughness effects found in the hardness data found on the specimens. From the outset however, this was not a carefully planned objective being conducted and improvements could be made for future study. Specifically, if this task were to be conducted again, an algorithm based JRC method could be used to eliminate subjectivity in the JRC value found. The hardness testing could be conducted in the location specifically within the boundaries of where the JRC value was derived from. A specific rock type could be evaluated such as a sandstone of various roughness such as how Desarnaud et al. did it in 2019 (Section 2.3.2). Basically, far more control can be added to this procedure to see if a legitimate link can be found between roughness effects found in the hardness data and JRC.

Table 4-1: Table showing JRC survey results showing min, max, median, and standard deviation for both the X- and Y-direction profiles. The mean of the combined X- and Y-direction results is shown on the far right.

Spec	X					Y					X & Y
	Min	Max	Mean	Med	St dev	Min	Max	Mean	Med	St dev	Mean
S8B1	5	19	11	9	5	4	12	8	8	2	9
S8B2	6	17	11	10	3	10	17	14	13	2	12
S8B3	12	20	15	15	3	9	16	13	13	2	14
S31B1	5	12	8	8	2	6	12	9	8	2	8
S36B1	4	12	9	9	2	4	8	6	6	1	8
S37B1	4	14	8	8	3	2	8	3	3	2	6
S37B2	2	4	3	3	1	2	8	5	4	2	4
S39B1	8	15	10	10	2	6	10	8	8	1	9
S39B2	4	16	10	10	3	8	16	11	10	3	11
S39B3	6	13	9	8	2	8	15	11	10	2	10
S47B1	4	14	8	8	3	2	14	6	5	3	7
S47B2	8	13	11	11	2	7	13	10	10	2	10
S47B3	1	8	4	4	2	3	10	6	6	2	5
S47B4	6	13	10	10	2	6	10	8	8	1	9
S53B1	4	8	6	6	1	1	6	3	2	1	4
S53B2	3	9	6	7	2	3	8	5	4	1	6
S53B3	4	11	7	8	2	3	8	5	5	1	6
S60B1	4	18	9	9	4	4	18	10	9	4	10
S61B1	1	4	2	1	1	2	8	4	3	2	3
S61B2	1	10	4	4	2	4	12	9	8	2	6
S62B1	4	10	7	6	2	6	14	10	10	3	8
S69B1	0	2	1	1	1	2	4	3	4	1	2
S69B2	4	9	7	8	2	2	6	4	4	2	5

Appendix D shows the hardness versus depth results found on the surfaces of each specimen. Apart from the specimens with saw cut first surfaces, it can be seen that each specimen with a roughness ranking at the higher end, sees a larger variation in hardness data than the subsequent surfaces in that specimen. Table 4-2 shows the standard deviation seen in the hardness data found on the natural surfaces of 15 of the specimens tested in this study together with the average standard deviation found on the subsequent surfaces for each particular specimen. It should be noted that the blocks of Sample 8 is exempt from this evaluation as the surface was so rough that the vast majority of the strikes were outside of the lower tolerance limit of the hardness device

resulting in a null value. The author chose to disregard the rough surface hardness values on these natural surfaces and began recording the hardness values beginning on the saw cut, second surface. The standard deviation on these specimens were still quite high on the first couple of surfaces where hardness was recorded. This was due to the large crystalline structure of the quartz with a large amount of voids being present throughout the entire grinding process in the secondary material, but more so nearest the natural surface. A preliminary, with limited factual proof conclusion drawn by the author is that JRC values matching the ones found on these specimens are at the upper limit of what the Leeb device is capable of being used on. Further to that notion, irrespective of the assigned JRC value, the author can also preliminarily conclude that the greater the steepness of the asperity, the less capable the device is at generating a hardness value. Specimens with asperities of similar height and that are more rounded seem, from the authors experience, to be more capable of producing values than one that has a more pointed asperity. As the hardness reading is dependent on a surface large enough to impact, it is understandable that the tip of a sharp point is less likely to be successfully struck than a rounded point.

With the exemption of the data collected on Specimen 8 Blocks 1 to 3, the remaining 20 specimens were examined. Specifically, the standard deviations found on the natural surface was compared to the average standard deviation found for all remaining surfaces in the secondary material. As a preface to the results, five blocks were deemed nonrepresentative by the author and not included in comparative evaluation. The second surface prepared by grinding on S53B3 and S62B1 were considered to be in the fresh, unweathered primary rock meaning no standard deviation comparison in the secondary material could be made. These two blocks were not considered in the comparative evaluation with the other specimens in the study for this reason. The other three, S36B1, S39B3, and S60B1 had smaller standard deviations on the natural surface: 74, 14, and 53 less than the average standard deviation found on three, three, and four ground surfaces for each respective block in the secondary material. These blocks were deemed by the author as being nonrepresentative and were not involved in the comparative evaluation with the other specimens for reasons described in the forthcoming paragraphs.

The first specimen, S36B1 with depth into the specimen, an increasing gradient in hardness could be seen, but there was a lot of scatter in the data (see Appendix C). Fractures were increasingly abundant with what appeared to be sealed fractures with depth. In the weathered profile, weakened grains as well as hardened grains seemed to be present. A solid impact attributed to the increase in hardness while a softened grain or sealed fracture strike resulted in the lower values. The results found on this specimen were not discarded; however, they were excluded from the comparative results discussed in this section as it is believed by the author to not be a usual case.

The cause for the lower standard deviation on the surface of the second specimen, S39B3 is believed by the author to be due to a variation in the magnitude in weathering seen across the specimen surface. The blocks in Specimen 39 seemed to have a variation in weathering depth and it was noticeable from the saw cut sides. The weathered material was a lighter colour and some locations would have approximately 1 mm of secondary material and immediately adjacent there would be nearly 0 mm of weathering. It is believed that the first surface was tested at random as the undisturbed surface looked equally weathered. But during the grinding process, the lighter-coloured material became present, and the testing process on the subsequent surfaces in the secondary material was conducted solely on the lighter areas as an attempt by the author to capture the hardness of the witnessable, weathered material. This however created a biased sampling strategy that differed from that on the natural surface. It is believed by the author that this was the reason for the standard deviation being lower than the average standard deviation found in the subsequent surfaces in the secondary material. This specimen was chosen to be exempt from the comparative analysis as it is believed to not match the results found on the other specimens tested in this study.

The third specimen, S60B1 had a highly porous weathered profile so impacts within the weathered profile were greatly impacted by their strike location i.e., if a pit was hit, the result was low and if a pit was not hit, the value would be high. This was deemed by the author to not match the conditions seen on the other specimens in this study and was therefore exempt from the comparative analysis.

It should be iterated that the data retrieved on the aforementioned three specimens were not discarded. The data was considered as being legitimate data that could be

obtained in the field; however, they were exempt from the comparative analysis as they were believed to be outliers to the data collected on the remaining, considered by the author to be representative, 15 specimens. In Table 4-2, it should be noted that ‘n’ is the number of surfaces, exempt of the natural surface, in the weathered profile attributing to the standard deviation values that are averaged (Avg SD).

Table 4-2: The difference in standard deviation found in the hardness data received on the natural surface in comparison to the average standard deviation found in the subsequent, secondary material surfaces for that specimen.

Spec	Natural Surface		Subsequent Surfaces		
	JRC	SD	n	Avg SD	Diff
S39B2	11	123	5	77	46
S47B2	10	66	5	26	40
S47B4	9	99	5	26	73
S39B1	9	81	3	54	27
S31B1	8	59	8	27	32
S47B1	7	101	7	27	74
S53B2	6	62	1	37	25
S61B2	6	50	15	35	15
S37B1	6	27	7	23	4
S47B3	5	76	7	25	50
S69B2	5	28	9	12	15
S53B1	4	65	1	32	33
S37B2	4	47	7	19	28
S61B1	3	46	12	39	7
S69B1	2	20	6	20	1

It can be seen in Table 4-2 that for the 15 specimens, a larger standard deviation was seen on the natural surface of the specimen in comparison to the average standard deviation found on the subsequent surfaces. Figure 4-15 shows the standard deviation increase found on the surface versus the JRC value of the specimen.

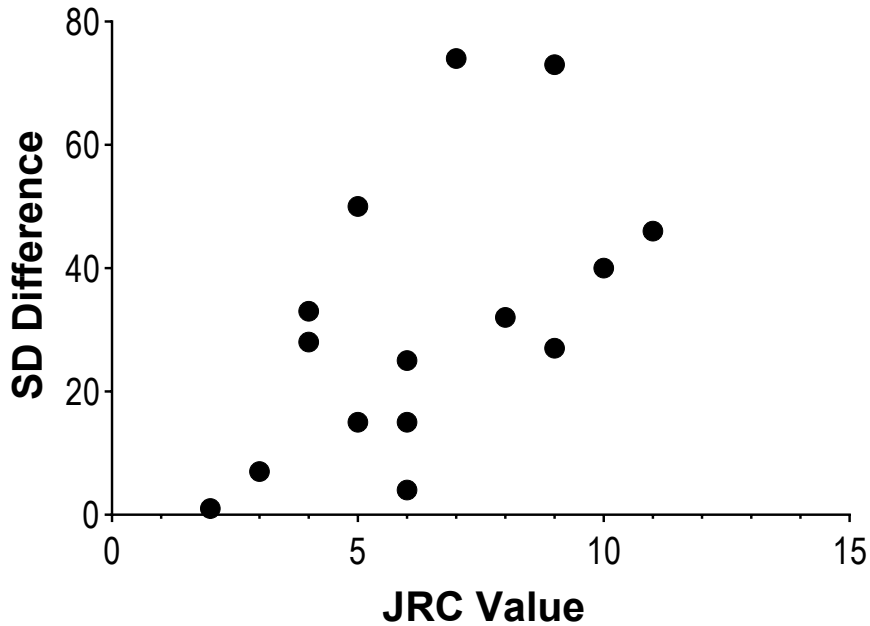


Figure 4-15: JRC value plotted against standard deviation increase.

There does not seem to be a recognizable connection between JRC and standard deviation difference. However, a conclusion that can be drawn from this exercise is that the standard deviation difference found on the surface and subsequent surfaces appears to be a valid way to determine if roughness is currently affecting the collected readings. In the next section, methods are discussed to potentially eliminate the roughness effects in the data found on a natural surface to find a representative hardness value that can be used to predict JCS.

4.6.2 JCS DETERMINATION

From Section 2.3.2, the methodology to predict JCS proposed by Hack et al., 1993 together with the correlation equation (Eq. 16) and equation coefficients for ‘All Rock Types’ (Table 2-8) by Corkum et al. 2018, was used in combination in this study. As introduced in Section 4.2, the L_{DS} value, which is a representation of the hardness of the surface of the secondary component of the rock, and the L_{DP} value, which is a value representing the unweathered primary component of the rock are used as input parameters. The L_{DS} value when submitted into Eq. 16 with the respective correlation coefficients, produces the correlation equivalent JCS value of the rock, denoted as JCS_{LD} . In the same fashion, L_{DP} produces the correlation equivalent σ_c value of the rock,

denoted as σ_{CLD} . The strength change from the surface of any rock type to its intact interior is found by subtracting L_{DS} from L_{DP} .

As was mentioned in Section 4.2 and seen in Section 4.6.1, it was found in this study that the standard deviation is a valuable indicator of the validity of the hardness data received on a natural surface. By examination of the scatter in the data found on the natural surface in comparison to the data found on the subsequent surfaces in the secondary material, the examiner can determine if roughness influenced the data or not. It is important to note that all rock types are different and some data scatter seen can be the result of differing hardness of the variation of grains present in the rock. An attentive user of the device will recognize this at the time of collection and should be able to delineate at least in part, the difference between the effects of roughness and grain stiffness. If a significant standard deviation is seen on each surface as a result of grain heterogeneity and this matches that found on the first surface, then the first surface can be deemed representative of the rock. However, if there is a larger standard deviation at the natural surface in comparison to the other surfaces in the secondary material, then the user can be certain that roughness is influencing the data. It is therefore left to the sole discretion of the user to determine the surface to take as being L_{DS} i.e., the natural surface, or a polished surface. If the user decides to use the first surface to be the nonrepresentative L_{DS} value highly influenced by roughness, this will mean that the predicted JCS value determined by Eq. 16 will be lower than what its actual prediction would be. This could be considered as a benefit to the user or as being too conservative of a prediction and should therefore be chosen at the discretion of the user.

As was seen in Section 4.2, the value of L_{DS} in this research program was determined after hardness data was found using an iterative grinding/ hardness testing procedure according to Section 3.1.2.4. The hardness data found on the natural surface was evaluated against the rest of the hardness data found in the secondary material. If significant scatter in the data could be observed in the data found on the first surface in comparison to the other L_D values, then the next surface tested with the roughness removed, was considered to be the L_{DS} value. For the rock type transition specimens, the determination of L_{DS} could also be reviewed against the $MeanL_D$ value as the secondary material transitioned to the primary material. For the weathered rock specimens, the

secondary material sees an increasing hardness gradient to the primary material. Thus, the $MeanL_D$ cannot really aid in the determination of L_{DS} .

In the case of significant roughness on a weathered surface, the trend of the weathered gradient should be examined and a suitable L_{DS} value should be selected. It should be kept in mind however that if too much roughness is removed then the L_{DS} value selected could be higher than what is representative at the surface which could result in an underestimation of JCS. In this study, two methods were considered in determining a suitable L_{DS} value when the first surface was relatively rough:

Option A) the hardness readings found on the natural surface greater than the lowest single value out of the 18 valid hardness readings found on the second surface are averaged; Option B) the value at $x = 0$ of a linear trendline created through the L_D values of the surfaces in the secondary material. These two options are two examples of what could be tried to determine a reasonable L_{DS} value although further study is suggested to find the best methodology for this selection.

Figure 4-16 shows the grinding/ hardness results for Specimen 39 Block 1. The surface L_D values are broken into three colour schemes described as follows, displayed from right to left on the plot: yellow – fresh rock, blue – weather gradient, and pink – natural surface value, described in the legend as the ‘discarded value’. The standard deviation, SD value for the hardness readings found on the natural surface was 81. The L_D value for this natural surface is noticeably lower than a value that would follow the trend of those surface L_D values in the weather gradient. The standard deviation values for the three succeeding surfaces are 55, 57, and 51, averaging 54. The practitioner evaluating the data can conclude that the natural surface value is perhaps not appropriate to take as the representative L_{DS} value as roughness has influenced the readings. The result of Option A, which eliminated all but 8 values out of the original 18 values found on this surface, produced a hardness value of 638 and is shown in green. A simple linear regression analysis was conducted, and the linear, best-fit line is shown. The result of Option B, produced a hardness value of 642. The practitioner may find that an L_{DS} value obtained by using Option A, B or another method may achieve a more realistic value of L_{DS} opposed to the value found on the first, natural surface.

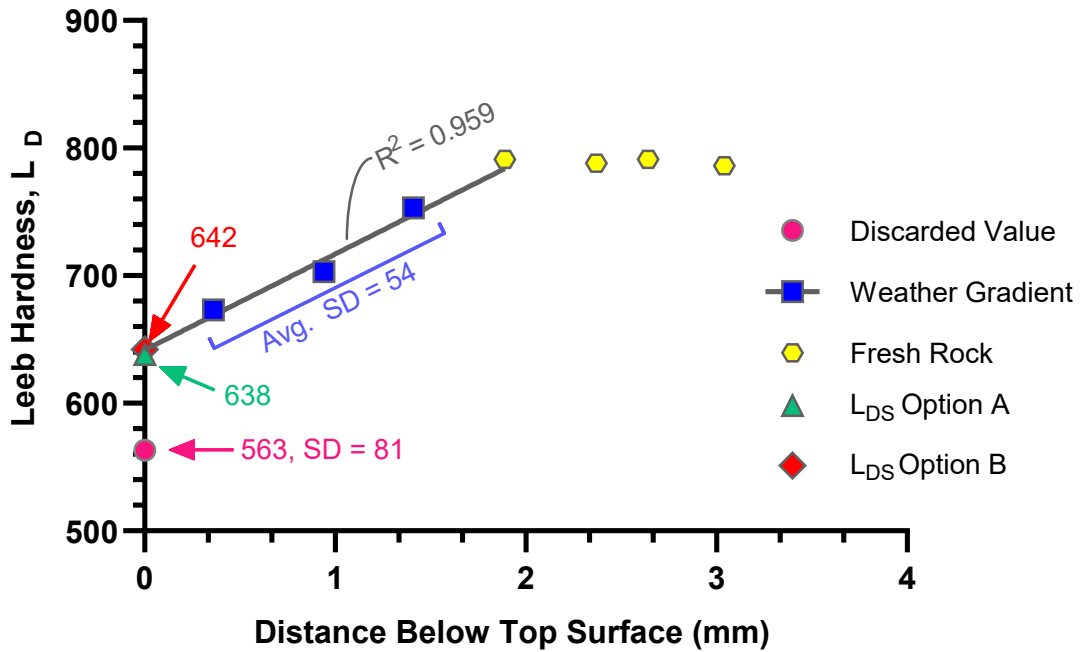


Figure 4-16: Simple linear regression of the representative L_D values in the weathered gradient. The value found on the natural surface was influenced by roughness and resulted in a larger standard deviation and lower TM_{20} value. A more representative L_{DS} value could be 642 rather than 563. Data was produced on Specimen 39 Block 1: The Box and Whisker plot and data can be seen in Appendix C and D.

The L_{DS} value once obtained, can be submitted into Eq. 16 together with the equation coefficients for ‘All Rock Types’ listed in Table 2-8: the obtained value is $JCSL_D$.

Likewise, the average primary material value L_{DP} produces the σ_{CLD} value. The $JCSL_D$ value predicts the compressive strength at the rock discontinuity surface, the σ_{CLD} value predicts the compressive strength of the unweathered intact rock, and the difference between σ_{CLD} and $JCSL_D$ is the predicted strength change across the secondary material.

The practitioner may also wish to find what the author describes to be the ‘strength gradient’ by finding the respective strength values produced from the L_D values found on each surface across the weather gradient. An example of a predicted strength gradient, including the $JCSL_D$ and σ_{CLD} values, can be seen in Figure 4-17 found on Specimen 61 Block 1. The box and whisker plots for the TM_{20} hardness results are shown in the upper plot while the correlated strength box and whisker plots are shown in the lower plot.

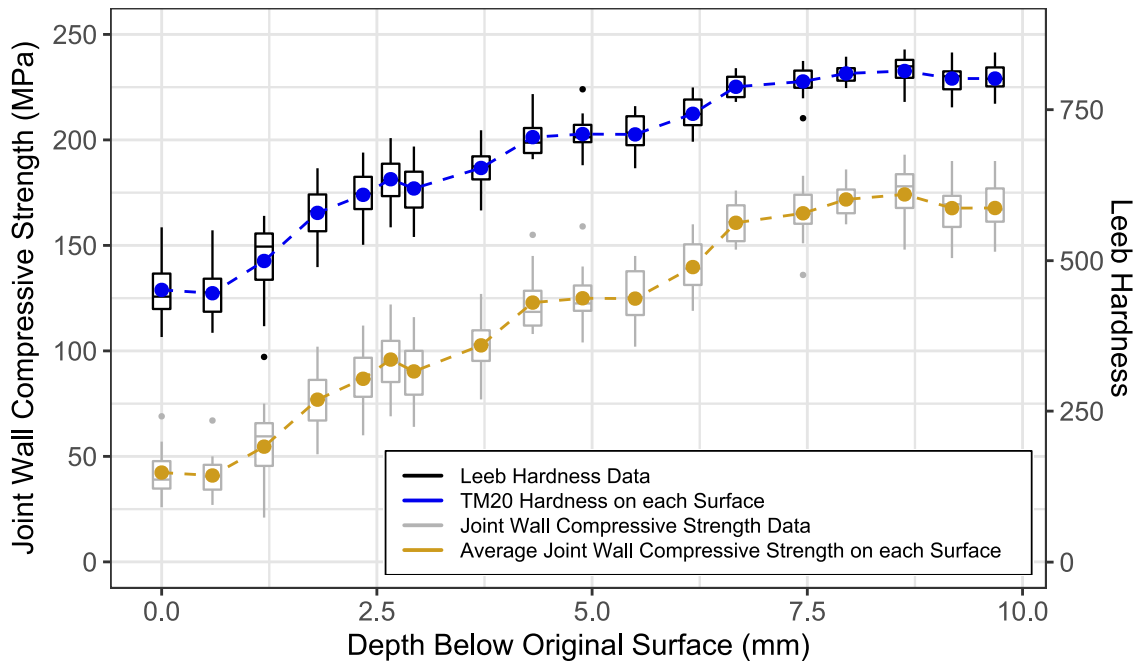


Figure 4-17: A dual axis chart showing box and whisker plots for the TM20 data found on each surface of Specimen 61 Block 1. The L_D results, displayed via the right axis is the upper plot while the $JCSL_D$ results, displayed via the left axis is the lower plot.

If the practitioner were to evaluate the data seen in Figure 4-17, they are likely to determine that the surface roughness influences are marginal. Whether this is true or not in this case does not really matter as the second surface produced an average strength value lesser by 2 MPa and is likely to be chosen as the $JCSL_D$ as it is the lowest value. However, depending on the level of sensitivity that is required for the project, the practitioner may feel more comfortable taking the single, lowest correlated strength value to be $JCSL_D$. The lowest single value found on the natural surface was 26 MPa. Thus, it is reiterated that the selection of JCS using the methodologies defined in this section, to be used in Barton and Choubey's Peak Shear Strength Criterion (Eq. 6) is left to the discussion of the practitioner whom will make their selection based on their judgement and targeted objectives.

For the example shown in Figure 4-17, Specimen 61 was the most weathered specimen of all specimens tested in this study. The original sample was found at low tide in the ocean; the rock had split along a discontinuity and the thick weathering profile was recognizable from a distance. A perhaps consequential or in fact significant discovery was found with the results found on Specimen 61 Block 1 that match Barton's findings in

1973. For this block, the first surface $JCSL_D$ value was 42 MPa, and the σ_{cLD} value was 168 MPa. The same findings were found in this study as Nick Barton's lower-bound JCS value determination introduced in Section 2.2.1, Eq. 11. These findings can be defined as:

$$\frac{JCSL_D}{\sigma_{cLD}} = \frac{1}{4} \quad \text{Eq. 23}$$

On this specific specimen, the lowest and highest, single strength findings were 21 and 193 MPa, on surface 3 and 16. The relation between $JCSL_D$ and σ_{cLD} using the maximum and minimum values is approximately 1/10. Specimen 61 Block 1 produced an L_D value on the natural surface slightly higher than the L_D value found on the second surface. The result of this could be due to the surface being tested in a dry state which was shown in Section 4.5 to produce higher hardness values than in a wet state as would be the case for the second surface, tested following grinding. This is not to say that the natural surface value is incorrect, it merely suggests that it was obtained in a different way than the other surfaces and if anything, matches the testing that would occur in the field. For this reason the first value, although larger than that found on the second surface, was selected in the correlation with JCS.

5 CONCLUSION

Rock samples were collected in Nova Scotia and Prince Edward Island in Canada and were cut into blocks larger than 90 cm³ as per the recommendations of Corkum et al., 2018. These blocks hosted a rock type transition consisting of two different material in contact or were of a single rock type and had a naturally weathered surface. In all cases, the material locating at the top, be it of a different rock type or a weathered profile, this material was considered to be the secondary material of the block. The lower rock type or the unweathered rock was considered as the primary material of the block. In a similar fashion to the natural rock type transition specimens, artificial material composite specimens were created using Plaster of Paris and sandstone. Hardness testing was conducted on the first surface and on surfaces at incremental depths. On the natural rock specimens, this was continued until the secondary material was completely removed and a recognizable consistency was obtained in the hardness values per surface in the primary material. For the artificial material composite specimens, this was commenced until the secondary material was completely removed.

The artificial material specimens determined that a zone of influence exists on a relatively homogeneous and isotropic material at a thickness of less than 1.7 mm, rounded to 2 mm to better accommodate a practical value for field use. This zone of influence value was true for both SS and SH artificial material specimens. The natural rock type transition specimens proved this result to be accurate as testing on secondary material with a thickness greater than 2 mm showed no influence of the underlying primary material in the hardness readings. Preliminary numerical modelling was conducted and the findings concluded that an influence zone depth detectable by the Leeb device at 2 mm was consistent with static stress distribution influences.

The results found on the weathered natural rock specimens revealed that within the weathered profile of a rock, a clear increase in hardness with distance from the weathered front exists. At or near the surface of the weathered rock face has the softest material and an increase in hardness is seen until the weathered profile is completely removed. The Leeb device successfully captures this hardness increase. Due to the degradation process of the rock, it is understandable that the strength and hardness would increase with depth into the rock. From the influence zone findings in this study, the strength or hardness

gradient present in a weathered profile would be subject to influences from the underlying material. However, the influence zone findings found in this study was on materials with a significant hardness difference (~225 HL to ~570 HL) that hosted an abrupt transition rather than a gradient. At this time, the magnitude of the influence on the hardness readings from underlying material of a gradual strength increase, as is the case in a weathered profile, is unknown. It may be marginal, which would mean a weathered profile in exceedance of 1.7 mm depth could produce hardness results which would be considered as being relatively uninfluenced. Regardless of the influence of the material in the weathered profile, it seems that with a weathered profile thickness in exceedance of 1.7 mm, the unweathered, intact rock will not be detectable in the readings found on that surface. In this study it was determined that weathered profile thicknesses less than 1.7 mm will be influenced by the unweathered, intact rock. At this time, a method to find the representative L_D value to be used to predict JCS for this case, has not been determined. The influence on a surface overlying material featuring an indefinite gradual strength increase was outside the scope of this study but this would provide valuable insight into the occurring data influences seen on any natural weathered surface. Additionally, it is understood that more material than just the natural surface is involved in resisting the shearing action on a rock joint. Thus, the selection of a representative L_D value to be used to predict JCS is open to interpretation and should be selected with consideration of the conditions of the rock joint being analyzed. Selection of the lowest L_D value found on all surfaces when performing the grinding/ hardness testing approach used in this study, may be an appropriate level of conservativeness for all weathered joints but this choice should ultimately be decided upon by the evaluator. In all scenarios, close attention needs to be paid that roughness effects (if any) are not inherent in the hardness data before any choice on the selection of L_D should be made. Whichever L_D value is selected to represent the material comprising the joint wall, the equation produced by Corkum et al., 2018 (Eq. 16) can be used to predict the JCS value with the appropriate fitting parameters (Table 2-8).

It was determined that for nearly all specimens tested in this study that roughness effects were detectable on the first surface by evaluation of the standard deviation found in the data for that surface. In nearly all cases, the natural surface produced data with

standard deviations larger than the average standard deviation value found on the subsequent surfaces in the secondary material for that block highlighting the influence of roughness on the result.

In terms of shear strength, the JCS value is undoubtedly linked with JRC as a deeper shearing depth would be seen for rougher surfaces in comparison to what would be expected on smoother surfaces. As part of a further study, JRC values were determined for all of the specimens prepared in this research program by 11 consultants who work in the field of rock mechanics using Barton and Choubey's JRC chart published in 1977. As the depth of shear is dependent on conditions subjected on that particular joint, the author had no ability to link the shear depth associated with JRC to the JCS value. However, preliminary efforts were tried to link the average JRC value per specimen to the roughness effects uncovered in the hardness data found on the specimen. No definitive link could be seen between JRC and roughness effects found in the hardness data. It should be mentioned however that if an improved method that focuses on reducing the level of subjectivity was attempted, this link may be able to be made.

In addition to the influence of the underlying material and roughness, a third impedance to the end hardness result is in regard to how the surface was prepared. It was found in this study that ground surfaces and sawn surfaces immediately after being prepared produced different hardness values. A belief of the author, although unproven, is that different amounts of moisture are entrained into the surface of the rock with each method. It is suggested by the author that specimen surfaces be prepared in the same way to prevent differences in the collected data where possible and that corrections be applied to the collected data if required to the surfaces that are natural or prepared differently.

REFERENCES

- Aoki, H. and Matsukura, Y. (2007) 'A new technique for non-destructive field measurement of rock-surface strength: an application of the Equotip hardness tester to weathering studies', *Earth Surface Processes and Landform*, 32, p1759-1769.
- Aoki, H. and Matsukura, Y. (2008) 'Estimating the unconfined compressive strength of intact rocks from Equotip hardness', *Bulletin of Engineering Geology and the Environment*, 67, p23-29.
- Asef, M.R. (1995) 'Equotip as an index test for rock strength properties', Master of Science thesis, International Institute for Aerospace Survey and Earth Sciences, Delft.
- ASTM International. (2014) *Standard test methods for compressive strength and elastic moduli of intact rock core specimens under varying states of stress and temperatures*. D7012-14e1. West Conshohocken, PA: Author.
- ASTM International. (2014) *Standard test method for determination of rock hardness by rebound hammer method*. D5873-14. West Conshohocken, PA: Author.
- ASTM International. (2017) *Standard test method for Leeb hardness testing of steel products*. A956/A956M-17a. West Conshohocken, PA: Author.
- Barton, N. (1973a) 'A review of the shear strength of filled discontinuities in rock', *Fjellsprengningsteknikk, Bergmekanikk, geoteknikk*, p19.1-19.38.
- Barton, N. (1973b) 'Review of a new shear strength criterion for rock joints', *Engineering Geology*, 7, p287-332.
- Barton, N. (1976) 'Rock Mechanics Review: The shear strength of rock and rock joints', *International Journal of Rock Mechanics and Mineral Science & Geomechanics Abstracts*, 13, p255-279.
- Barton, N. and Choubey, V. (1977) 'The shear strength of rock joints in theory and practice', *Rock Mechanics Felsmechanik Mecanique des Roches*, 10, p1-54.
- Beer, A.J., Stead, D., and Coggan, J.S. (2002) 'Technical note: estimation of the joint roughness coefficient (JRC) by visual comparison', *Rock Mechanics and Rock Engineering*, 35(1), p65-74.
- Corkum, A.G., Asiri, Y., El Naggari, H., and Kinakin, D. (2018) 'The Leeb hardness test for rock: an updated methodology and UCS correlation', *Rock Mechanics and Rock Engineering*, 51, p665-675.
- Deere, D.U. and Miller, R.P. (1966) 'Engineering classification and index properties for intact rock', Technical Report No. AFWL-TR-65-116, University of Illinois, Urbana.

Desarnaud, J., Kiriyaama, K., Bicer Simsir, B., Wilhelm, K., and Viles, H. (2019) 'A laboratory study of Equotip surface hardness measurements on a range of sandstones: What influences the values and what do they mean?', *Earth Surface Processes and Landforms*, 44(7), p1419-1429.

European Committee for Standardization. (2006) Natural stone test methods: determination of real density and apparent density, and of total and open porosity. Swedish Standard SS-EN 1936:2006. 2nd edn. Stockholm: Author.

Fischer-Cripps, A.C. (2007) Introduction to contact mechanics. 2nd edn. New York: Springer, pxxi.

Ghasemi, M. and Corkum, A.G. (2020) 'A three hinge buckling laboratory test', *Rock Mechanics and Rock Engineering*, 53, p.4077-4090.

Google. (2021) 'Trial round rock locations', Interactive Online Map. Available at: https://www.google.com/maps/d/edit?mid=1YiFiAsq_GFIqyeqRFRyq3T1Pt7NGkVfx&ll=45.29329922712871%2C-62.403664449999994&z=7. (Accessed: June 7, 2021).

Hack, H.R.G.K., Hingira, J., and Verwaal, W. (1993) 'Technical note: determination of discontinuity wall strength by Equotip and ball rebound tests', *International Journal of Rock Mechanics and Mineral Science & Geomechanics Abstracts*, 30(2), p151-155.

Hoek, E. (2007) Practical rock engineering [Online]. Available at: <https://www.rocscience.com/assets/resources/learning/hoek/Practical-Rock-Engineering-Full-Text.pdf> (Accessed: 12 March 2019).

ISRM. (1978) 'International society for rock mechanics commission on standardization of laboratory and field tests: suggested methods for the quantitative description of discontinuities in rock masses', *International Journal of Rock Mechanics and Mineral Science & Geomechanics Abstracts*, 15, p319-368.

Kurlov, A. and Gusev, A. (2013) *Tungsten carbides: structure, properties and application in hardmetals*. Vol. 184. Switzerland: Springer International Publishing.

Leeb, D. (1979) 'Dynamic hardness testing of metallic materials', *NDT International*, 12(6), p274-278.

Müller, L. (1964) 'The rock slide in the Vajont valley', *Felsmechanik und Ingenieurgeologie*, 2(3/4), p148-212.

Müller, L. (1979) 'Dedication, Chapter 1 - Josef Stini: contributions to engineering geology and slope movement investigations' in Voight, B. (ed.) *Rockslides and Avalanches*, 2. 14B. Amsterdam: Elsevier Scientific Publishing Company, p95-109.

Proceq SA. (2007) 'equotip^{R3} Swiss portable hardness tester': Operating instructions. 1st edn. Schwerzenback, Switzerland: Author.

Patton, F.D. (1966) 'Multiple modes of shear failure in rock', *1st ISRM Congress 1966*, Lisbon, Portugal, September 1966, p509-513.

Terzaghi, K. (1946) 'Rock defects and loads on tunnel supports', *Rock Tunneling with Steel Supports*, p16-99.

TIME Group Inc. (n.d.) 'Integrated hardness tester TH170': Instruction manual. Retrieved from <https://www.bamr.co.za/instruction-manual/th170-integrated-portable-hardness-tester-instruction-manual.pdf>.

Ungar, T. and Borbely, A. (1999) 'Particle-size, size distribution and dislocations in nanocrystalline tungsten-carbide', *NanoStructured Materials*. 11(1), p.103-113.

Verwaal, W. and Mulder, A. (1993) 'Technical note: estimating rock strength with the Equotip hardness tester', *International Journal of Rock Mechanics and Mining Sciences & Geomechanics Abstracts*, 30(6), p659-662.

Wallace Quarries Ltd. (n.d.), Wallace quarries – test data [Online]. Available at: <http://www.wallacequarries.com/test-data.html> (Accessed: June 10, 2020).

APPENDIX A – ARTIFICIAL MATERIAL SPECIMEN DATA PART 1

SH	SP1 to SP9 (Mix Design: 3 to 1)								
Specimen No.	1	2	3	4	5	6	7	8	9
Sec Mat Thick (mm): Sandstone	30.7	24.1	17.9	14.3	10.1	6.9	4.3	3.7	2.9
Prim Mat Thick (mm): Artificial	125.3	125.4	125.2	125	124.8	124.8	125	123.5	123.2
Hardness Readings	539	440	506	523	440	419	484	485	441
	526	474	435	518	460	467	496	491	450
	536	445	476	505	464	461	518	548	468
	484	445	504	501	502	485	507	536	493
	564	474	529	540	457	522	527	557	502
	491	505	462	540	486	510	492	534	485
	493	553	512	525	490	541	533	568	491
	537	474	494	528	458	550	504	542	482
	517	477	460	504	468	465	513	523	481
	475	502	440	546	497	501	530	536	484
	548	505	455	522	537	555	545	494	500
	541	441	508	509	524	517	511	542	510
	530	460	465	491	506	590	553	551	483
	513	507	537	484	520	536	563	561	511
	488	546	524	550	541	471	542	556	486
	501	493	538	515	563	529	517	538	494
	535	599	513	533	501	522	541	594	475
544	553	471	511	503	484	544	564	472	
505	484	495	538	491	528	523	507	520	
534	489	474	505	501	523	529	528	512	
Highest	564	599	538	550	563	590	563	594	520
Lowest	475	440	435	484	440	419	484	485	441
L _D (TM20)	520	490	490	520	495	509	524	538	488
Std Dev	21	35	28	16	26	30	18	22	16
JCS	59	51	51	59	52	56	60	64	50

SH	SP1 to SP10 (Mix Design: 3 to 2)									
Specimen No.	1	2	3	4	5	6	7	8	9	10
Sec Mat Thick (mm): Sandstone	30.8	24	18.9	14.5	10.6	6.9	5.5	4.1	3.2	2.2
Prim Mat Thick (mm): Artificial Mat	125.2	125.5	124.2	124.8	124.3	124.9	123.8	123.1	122.9	122.9
Hardness Readings	526	533	568	500	588	527	551	582	578	547
	520	529	457	515	550	560	597	579	551	526
	529	473	560	498	558	515	592	574	563	536
	547	558	596	570	519	508	592	614	554	532
	506	500	574	534	534	548	594	540	594	537
	529	537	482	504	524	561	610	553	524	549
	534	532	522	581	585	581	587	558	572	536
	512	532	578	535	562	543	623	552	563	533
	539	540	554	582	571	523	583	582	564	553
	570	538	542	525	577	519	609	564	534	545
	486	540	542	596	532	563	641	552	543	548
	512	550	538	558	624	585	589	585	563	546
	520	527	534	499	532	567	566	582	566	541
	587	536	551	434	595	538	556	561	557	525
	575	543	544	520	593	589	630	577	588	542
	523	516	552	504	582	604	588	604	556	560
	546	538	564	550	585	538	585	594	561	548
517	533	565	571	487	563	619	550	570	575	
535	509	548	517	521	570	613	556	643	563	
537	542	510	531	561	550	577	572	549	537	
Highest	587	558	596	596	624	604	641	614	643	575
Lowest	486	473	457	434	487	508	551	540	524	525
L _D (TM20)	532	532	546	533	559	552	595	571	563	543
Std Dev	19	12	24	29	27	23	19	16	15	10
JCS	62	62	66	62	70	68	81	74	71	65

SH	SP2 to SP10 (Mix Design: Just Plaster)									
Specimen No.	2	3	4	5	6	7	8	9	10	
Sec Mat Thick (mm): Sandstone	24	18.9	14.5	10.6	6.9	5.5	4.1	3.2	2.2	
Prim Mat Thick (mm): Artificial Mat	125.5	124.2	124.8	124.3	124.9	123.8	123.1	122.9	122.9	
Hardness Readings	507	539	526	602	549	581	538	590	532	
	527	514	528	524	537	591	536	595	582	
	514	620	513	607	594	593	581	552	555	
	503	597	552	538	569	601	523	593	571	
	513	572	573	556	529	587	545	582	595	
	550	587	552	576	590	611	565	581	619	
	574	572	599	597	603	620	546	580	566	
	574	576	565	582	545	599	531	519	578	
	519	604	511	550	531	584	559	565	552	
	557	567	562	580	605	591	510	606	613	
	567	560	560	544	532	617	564	607	545	
	563	565	588	568	574	635	533	606	563	
	535	515	564	551	586	574	574	577	572	
	501	569	597	569	511	591	584	564	608	
	571	552	537	570	617	587	552	581	576	
	577	546	629	548	576	616	582	575	555	
	573	503	589	584	568	615	541	603	574	
	566	569	585	573	546	588	536	617	607	
501	576	548	543	549	645	562	574	580		
538	507	565	499	618	605	580	601	638		
Highest	577	620	629	607	618	645	584	617	638	
Lowest	501	503	511	499	511	574	510	519	532	
L _D (TM20)	542	560	561	564	567	601	553	585	578	
Std Dev	27	27	25	21	28	15	19	16	22	
JCS	65	70	71	71	72	83	68	78	76	

SH	SP21 to SP29 (Mix Design: Dia Earth)								
Specimen No.	21	22	23	24	25	26	27	28	29
Sec Mat Thick (mm): Sandstone	28.6	20.9	15.9	11.3	8.5	5.5	3.9	2.3	2
Prim Mat Thick (mm): Artificial	127.4	128.5	127.2	128	126.4	126.3	125.4	124.9	124.1
Hardness Readings	534	525	558	573	596	522	557	516	564
	493	521	603	585	561	550	555	550	538
	537	518	546	554	580	534	592	543	530
	538	593	566	576	559	522	554	559	546
	532	552	576	572	551	536	519	567	541
	537	605	530	574	546	583	543	574	504
	506	550	543	537	541	572	568	576	531
	531	590	548	542	525	555	552	566	572
	571	541	523	555	586	535	586	600	606
	611	548	572	577	532	558	558	595	571
	558	515	559	566	547	600	555	623	576
	570	527	552	548	550	545	553	531	540
	576	512	555	561	542	581	555	572	515
	557	526	537	499	559	574	587	563	570
	570	528	547	586	567	564	539	553	575
	501	562	536	540	559	557	576	550	551
	504	563	574	540	527	541	546	574	569
	542	565	564	558	575	541	543	594	546
559	565	525	588	568	594	516	585	530	
563	440	578	571	578	622	562	555	548	
Highest	611	605	603	588	596	622	592	623	606
Lowest	493	440	523	499	525	522	516	516	504
L _D (TM20)	544	545	554	562	557	558	556	567	551
Std Dev	24	25	16	16	17	22	16	19	19
JCS	65	66	68	71	69	70	69	72	67

Artificial Material Hardness		SP1 to SP10 (Mix Design: 3 to 2) - Hardness Difference																			
Specimen No.	1		2		3		4		5		6		7		8		9		10		
Category No.	1	2	1	2	1	2	1	2	1	2	1	2	1	2	1	2	1	2	1	2	
Specimen Surface Testing was Conducted on:	Top	Bot	Top	Bot	Top	Bot	Top	Bot	Top	Bot	Top	Bot	Top	Bot	Top	Bot	Top	Bot	Top	Bot	
Artificial Mat Thick (mm):	30.8	125.2	24	125.5	18.9	124.2	14.5	124.8	10.6	124.3	6.9	124.9	5.5	123.8	4.1	123.1	3.2	122.9	2.2	122.9	
Sandstone Thick (mm):	30.8	125.3	24	125.5	18.9	125.7	14.5	125.2	10.6	124.8	6.9	125.1	5.5	125.4	4.1	124.8	3.2	124.5	2.2	125.1	
Hardness Readings	185	194	201	171	170	192	208	202	192	178	195	189	181	186	187	199	195	205	201	187	
	182	220	183	171	236	198	192	199	231	206	186	175	203	201	188	185	196	191	224	192	
	187	224	186	200	214	176	188	193	177	191	190	197	184	186	197	211	194	210	211	197	
	194	172	184	178	202	176	181	221	179	197	181	172	194	203	182	205	187	217	217	192	
	176	203	180	197	197	177	197	212	196	200	186	196	184	191	191	199	178	205	201	205	
	194	238	171	191	190	188	221	207	188	197	191	170	190	230	196	178	198	208	229	198	
	186	199	197	176	183	178	207	214	216	190	180	176	181	195	192	221	193	222	219	208	
	198	205	175	182	220	246	196	209	202	193	209	179	191	202	188	189	189	210	209	200	
	183	194	174	191	185	197	202	218	182	194	202	197	196	207	190	216	199	201	195	179	
	178	216	175	187	191	178	177	178	176	206	195	183	192	207	198	188	222	208	221	184	
	171	180	200	190	202	218	195	191	174	196	176	193	198	194	193	208	201	209	215	198	
	182	206	183	196	177	172	201	205	184	202	173	175	197	198	178	198	182	207	217	174	
	199	199	179	188	231	196	204	212	188	211	177	183	195	207	189	202	210	201	231	193	
	182	199	175	176	185	215	197	192	183	200	172	185	198	195	189	190	192	209	209	192	
	222	217	182	175	226	173	186	206	215	190	205	176	206	195	197	172	183	213	202	198	
	187	196	257	202	196	194	191	213	212	201	194	182	198	192	184	190	185	220	227	186	
	206	212	187	185	178	191	186	225	178	190	177	199	193	181	172	192	180	214	192	192	
	178	185	210	195	193	197	170	190	177	181	199	191	191	185	204	188	223	203	217	179	
	184	191	180	212	178	193	204	200	181	270	199	218	183	194	177	176	193	213	222	197	
	192	221	224	181	194	181	189	208	248	195	192	199	180	192	207	205	187	206	207	184	
Highest	222	238	257	213	236	246	221	225	248	270	209	218	206	220	207	221	232	222	237	208	
Lowest	171	177	171	171	170	173	170	178	174	178	172	170	180	181	173	172	178	191	193	174	
L ₀ (TM20)	187	203	188	187	197	190	195	205	192	197	189	186	192	196	190	196	194	209	214	192	
L ₀ (sec) - LD (prim)		-16		1		7		-11		-5		3		-5		-6		-15		22	
Std Dev	8	13	14	9	16	13	9	9	16	7	10	9	7	7	7	11	10	5	10	7	
JCS	5	6	5	5	6	5	5	6	5	6	5	5	5	6	5	6	5	6	7	5	

Artificial Material Hardness		SP2 to SP10 (Mix Design: Just Plaster) - Hardness Difference																	
Specimen No.	2		3		4		5		6		7		8		9		10		
Category No.	1	2	1	2	1	2	1	2	1	2	1	2	1	2	1	2	1	2	
Specimen Surface Testing was Conducted on:	Top	Bot	Top	Bot	Top	Bot	Top	Bot	Top	Bot	Top	Bot	Top	Bot	Top	Bot	Top	Bot	
Artificial Mat Thick (mm):	23.4	125.5	17.3	124.2	13.4	124.8	10	124.3	6.6	124.9	4.4	123.8	2.1	123.1	2.5	122.9	2.2	122.9	
Sandstone Thick (mm):	125.5	24	125.7	18.9	125.2	14.5	124.8	10.6	125.1	6.9	125.4	5.5	124.8	4.1	124.5	3.2	125.1	2.2	
Hardness Readings	228	241	193	220	192	222	231	227	203	240	231	226	210	212	220	199	223	221	
	232	228	213	222	222	215	223	217	213	238	225	207	213	210	232	208	236	226	
	234	218	238	222	203	214	214	230	218	233	228	224	222	217	227	224	225	231	
	231	238	236	227	204	219	218	216	200	223	216	216	220	215	208	228	217	228	
	240	224	202	232	186	214	207	212	246	246	205	209	215	230	212	240	237	219	
	220	214	211	209	203	216	207	211	218	235	232	219	233	223	205	233	222	220	
	225	229	247	218	207	222	211	217	220	220	221	228	224	219	199	211	221	212	
	218	230	221	224	198	219	210	228	214	238	189	198	227	207	214	221	214	205	
	220	234	242	228	206	213	205	217	225	207	230	215	228	214	225	211	210	204	
	229	238	237	211	204	219	213	230	217	226	231	238	219	217	227	211	209	221	
	234	219	221	220	208	200	207	202	225	235	228	214	229	214	230	216	233	223	
	224	228	216	220	199	208	207	223	219	240	217	219	217	216	223	219	219	224	
	230	234	229	206	202	219	200	219	230	251	227	232	225	222	217	204	212	221	
	213	220	215	208	216	224	219	212	247	226	220	230	213	225	218	229	226	227	
	234	234	230	210	208	206	213	213	221	236	199	231	221	224	202	221	216	221	
	222	228	232	222	203	204	224	202	212	242	235	215	222	211	218	207	215	216	
	217	227	228	221	203	216	215	217	233	226	226	218	231	214	221	230	202	224	
	228	227	211	221	206	218	203	218	228	239	231	228	232	221	219	214	210	209	
	223	232	215	224	201	217	206	216	230	238	229	218	216	219	212	221	217	225	
	229	239	216	218	203	209	200	215	228	248	225	233	204	228	226	217	211	213	
Highest	240	241	247	232	222	224	231	230	247	251	235	238	233	230	232	240	237	231	
Lowest	213	214	193	206	186	200	200	202	200	207	189	198	204	207	199	199	202	204	
L ₀ (TM20)	227	229	223	219	204	215	211	217	222	235	223	221	221	218	218	218	219	220	
L ₀ (sec) - LD (prim)		-3		4		-11		-6		-13		2		4		0		-1	
Std Dev	6	6	11	6	5	5	7	7	10	8	9	8	7	5	8	9	8	6	
JCS	8	8	8	7	6	7	7	7	8	9	8	7	7	7	7	7	7	7	

Artificial Material Hardness		SP21 to SP29 (Mix Design: Dia Earth) - Hardness Difference																	
Specimen No.	21		22		23		24		25		26		27		28		29		
Category No.	1	2	1	2	1	2	1	2	1	2	1	2	1	2	1	2	1	2	
Specimen Surface Testing was Conducted on:	Top	Bot	Top	Bot	Top	Bot	Top	Bot	Top	Bot	Top	Bot	Top	Bot	Top	Bot	Top	Bot	
Artificial Mat Thick (mm):	199	199	179	188	231	224	204	212	188	226	177	230	195	207	189	229	210	227	
Sandstone Thick (mm):	230	234	229	206	202	219	200	219	230	251	227	232	225	222	217	204	212	221	
Hardness Readings	228	243	253	242	235	239	239	238	235	241	237	233	241	248	259	235	263	239	
	242	210	249	232	250	230	252	235	230	239	225	252	243	239	266	244	251	242	
	249	226	256	219	249	240	243	233	241	253	235	252	249	239	271	239	270	240	
	230	209	255	231	238	245	247	235	236	237	233	235	246	243	268	232	254	242	
	255	206	246	248	252	240	251	242	235	240	234	238	238	241	250	238	258	247	
	238	222	261	230	241	242	235	231	227	248	253	238	245	248	274	237	260	236	
	235	222	241	227	243	244	238	233	236	249	247	239	244	242	272	236	276	242	
	224	204	263	239	253	241	244	223	231	238	253	231	243	238	257	237	265	252	
	230	210	259	227	248	241	253	235	219	237	245	239	243	246	286	231	264	240	
	227	207	252	246	237	228	238	242	226	239	250	231	241	238	272	245	275	245	
	236	215	253	232	243	235	239	240	230	245	239	239	242	241	254	239	269	240	
	235	239	267	238	249	236	239	242	224	242	244	231	237	248	277	221	276	246	
	226	232	254	231	254	240	241	238	235	237	241	246	242	234	269	245	277	244	
	235	225	228	223	235	249	252	233	228	232	238	241	234	241	263	249	279	244	
	205	203	248	227	247	238	239	230	232	246	244	238	241	223	280	241	294	247	
	228	205	261	223	231	234	239	224	235	239	255	244	242	238	278	242	291	242	
	223	219	238	229	250	245	243	240	226	237	247	223	240	243	263	237	275	241	
	221	240	251	239	241	242	229	234	235	250	244	236	249	243	264	232	281	245	
	223	210	278	218	244	248	240	235	224	235	242	231	246	236	249	238	293	246	
	230	228	259	229	248	238	226	233	226	243	245	244	234	244	283	226	281	238	
Highest	255	243	278	248	254	249	253	242	241	253	255	252	249	248	286	249	294	252	
Lowest	205	203	228	218	231	228	226	223	219	232	225	222	234	223	249	221	251	236	
L ₀ (TM20)	231	218	254	231	245	240	242	235	231	241	243	238	242	241	268	237	273	243	
L ₀ (sec) - LD (prim)		13		22		5		7		-11		5		1		30		30	
Std Dev	7	12	8	7	6	4	6	5	4	5	6	6	4	4	9	5	11	3	
JCS	8	7	10	8	9	9	9	9	8	9	9	9	9	9	12	9	12	9	

APPENDIX B – ARTIFICIAL MATERIAL SPECIMEN DATA PART 2

SS	Artificial Composite Specimen 7 Category 1 (Just Plaster)									
Grind Depth (mm)	0	0.5	1.8	2.1	2.6	3.4	3.8	4.1	4.4	4.5
Sec Mat Thick (mm)	4.5	4	2.7	2.4	1.9	1.1	0.7	0.4	0.1	0
Surface	Orig	Top 1	Top 2	Top 3	Top 4	Top 5	Top 6	Top 7	Top 8	Top 9
Hardness Readings	231	228	240	237	230	227	254	258	485	586
	225	228	249	258	234	227	252	305	524	555
	228	217	278	221	211	230	240	316	499	581
	216	220	230	248	233	234	241	312	461	524
	205	224	218	249	243	227	243	296	485	542
	232	214	269	247	226	212	237	278	480	589
	221	226	242	228	239	228	235	254	483	579
	189	209	251	235	292	238	217	250	477	539
	230	195	237	241	304	250	263	232	504	548
	231	221	245	236	218	256	253	261	497	578
	228	219	245	234	219	276	236	261	494	588
	217	221	241	234	228	234	247	250	477	542
	227	217	235	256	227	229	238	257	448	611
	220	232	239	232	238	234	241	292	500	565
	199	216	182	244	228	235	229	288	508	561
	235	234	242	250	238	212	241	274	533	572
	226	196	250	253	243	232	182	255	495	592
	231	211	230	255	232	231	227	269	503	552
	229	198	248	223	231	227	250	270	483	573
	225	225	245	232	240	241	251	241	460	569
Highest	235	234	278	258	304	276	263	316	533	611
Lowest	189	195	182	221	211	212	182	232	448	524
L _D (TM20)	223	218	242	241	236	233	241	271	490	567
Std Dev	9	10	11	10	16	10	10	21	16	18
JCS	8	7	9	9	9	8	9	12	51	72

SS	Artificial Composite Specimen 9 Category 1 (Just Plaster)							
Grind Depth (mm)	0	0.3	0.6	1.1	2.0	2.3	2.45	2.5
Sec Mat Thick (mm)	2.5	2.2	1.9	1.4	0.5	0.2	0.05	0
Surface	Orig	Top 1	Top 2	Top 3	Top 4	Top 5	Top 6	Top 7
Hardness Readings	220	211	215	212	262	314	555	548
	232	222	224	220	254	308	533	567
	227	226	228	205	243	317	537	518
	208	246	234	207	245	301	491	582
	212	226	230	219	235	287	498	544
	205	231	213	209	225	282	497	555
	199	172	197	224	206	295	549	518
	214	210	222	211	238	284	417	510
	225	225	217	221	256	274	579	519
	227	220	218	234	232	290	576	577
	230	201	216	236	235	296	564	549
	223	210	233	232	232	279	532	547
	217	226	230	224	232	260	499	551
	218	216	240	209	229	293	527	531
	202	211	229	211	256	287	473	574
	218	229	231	230	236	281	527	506
	221	221	220	227	224	281	536	520
	219	223	226	215	237	339	460	530
212	221	232	238	210	281	494	533	
226	202	223	230	232	315	574	553	
Highest	232	246	240	238	262	339	579	582
Lowest	199	172	197	205	206	260	417	506
L _D (TM20)	218	218	225	221	236	293	523	541
Std Dev	8	9	7	10	12	13	34	20
JCS	7	7	8	7	9	15	60	65

SS	Artificial Composite Specimen 10 Category 1 (Just Plaster)							
Grind Depth (mm)	0	0.6	1	1.2	1.6	1.9	2.1	2.2
Sec Mat Thick (mm)	2.2	1.6	1.2	1	0.6	0.3	0.1	0
Surface	Orig	Top 1	Top 2	Top 3	Top 4	Top 5	Top 6	Top 7
Hardness Readings	223	230	232	253	240	314	520	565
	236	236	244	244	238	313	538	506
	225	231	236	250	233	351	537	542
	217	238	237	243	242	340	488	540
	237	219	247	242	236	343	522	557
	222	217	242	241	256	346	532	507
	221	224	238	237	241	345	568	534
	214	229	240	250	235	291	535	497
	210	222	222	246	232	341	501	566
	209	233	243	253	249	381	571	570
	233	219	240	236	236	307	491	510
	219	238	237	246	238	362	519	504
	212	246	232	239	239	333	549	501
	226	236	238	239	237	373	554	532
	216	230	243	244	240	373	555	540
	215	228	245	245	238	302	547	571
	202	241	252	231	241	309	508	506
	210	235	235	239	230	367	561	585
217	239	246	251	235	381	555	562	
211	239	233	239	234	290	520	549	
Highest	237	246	252	253	256	381	571	585
Lowest	202	217	222	231	230	290	488	497
L _D (TM20)	219	232	239	244	238	338	534	537
Std Dev	8	7	5	5	4	27	22	25
JCS	7	8	9	9	9	21	63	63

SS	Artificial Composite Specimen 26 Category 1 (Dia. Earth)									
Grind Depth (mm)	0	1.1	2.0	2.8	4.3	4.8	5.2	5.5	5.8	5.9
Sec Mat Thick (mm)	5.9	4.8	3.9	3.1	1.6	1.1	0.7	0.4	0.1	0
Surface	Orig	Top 1	Top 2	Top 3	Top 4	Top 5	Top 6	Top 7	Top 8	Top 9
Hardness Readings	237	261	262	252	269	263	264	277	404	567
	225	256	250	260	257	275	256	257	452	581
	235	258	240	260	268	281	272	273	531	554
	233	251	276	263	259	267	281	299	409	590
	234	253	257	268	257	269	281	302	428	551
	253	259	254	251	266	257	275	274	475	548
	247	246	269	266	257	272	270	270	507	573
	253	244	279	271	262	283	259	270	515	584
	245	246	264	260	254	288	252	274	483	613
	250	240	239	253	260	258	252	291	453	612
	239	241	249	222	266	258	273	306	501	525
	244	264	245	240	261	268	275	275	415	574
	241	261	272	268	268	260	254	283	476	564
	238	256	250	262	253	271	264	276	512	606
	244	250	254	251	269	271	275	278	464	586
	255	266	280	258	261	260	272	253	421	544
	247	248	238	258	262	272	260	287	451	613
	244	251	261	255	262	273	250	293	529	602
242	251	256	233	267	279	265	259	422	607	
245	255	254	257	264	260	274	297	532	618	
Highest	255	266	280	271	269	288	281	306	532	618
Lowest	225	240	238	222	253	257	250	253	404	525
L _D (TM20)	243	253	257	256	262	269	266	280	469	582
Std Dev	6	6	12	9	4	8	9	13	40	24
JCS	9	10	11	11	11	12	12	13	46	77

SS	Artificial Composite Specimen 27 Category 1 (Dia. Earth)								
Grind Depth (mm)	0	0.4	1.3	1.9	2.4	2.7	2.9	3.2	3.6
Sec Mat Thick (mm)	3.6	3.2	2.3	1.7	1.2	0.9	0.7	0.4	0
Surface	Orig	Top 1	Top 2	Top 3	Top 4	Top 5	Top 6	Top 7	Top 8
Hardness Readings	241	246	261	286	304	308	293	317	560
	243	244	257	291	302	304	291	312	572
	249	252	256	277	276	286	305	338	527
	246	236	258	270	272	282	301	316	558
	238	243	250	264	266	285	289	310	584
	245	252	235	254	249	292	280	343	581
	244	252	251	264	261	259	283	398	572
	243	249	254	249	276	292	295	408	559
	243	246	241	262	277	300	307	349	562
	241	244	258	265	280	312	306	325	559
	242	239	258	272	280	296	298	313	524
	237	250	244	271	279	308	295	330	596
	242	249	265	290	280	303	297	342	547
	234	246	254	277	276	305	300	376	532
	241	247	253	265	269	285	291	338	540
	242	252	254	260	278	265	294	348	583
	240	246	263	261	285	277	296	309	544
	249	250	240	250	285	292	311	315	540
246	246	259	242	284	303	300	362	543	
234	245	268	265	270	306	321	443	580	
Highest	249	252	268	291	304	312	321	443	596
Lowest	234	236	235	242	249	259	280	309	524
L _D (TM20)	242	247	254	267	278	294	297	341	558
Std Dev	4	3	7	11	9	12	7	29	18
JCS	9	10	10	12	13	15	15	21	70

SS	Artificial Composite Specimen 29 Category 1 (Dia. Earth)					
Grind Depth (mm)	0	0.5	0.7	1.0	1.3	1.4
Sec Mat Thick (mm)	1.4	0.9	0.7	0.4	0.1	0
Surface	Orig	Top 1	Top 2	Top 3	Top 4	Top 5
Hardness Readings	263	282	307	313	476	574
	251	294	302	320	543	520
	270	303	314	334	485	528
	254	301	313	316	502	444
	258	309	301	319	544	539
	260	306	307	317	521	530
	276	303	316	327	523	579
	265	304	322	317	553	547
	264	295	326	307	532	534
	275	221	300	318	503	543
	269	301	322	310	506	546
	276	313	309	318	519	536
	277	321	302	308	492	537
	279	298	307	322	516	526
	294	302	309	317	520	566
	291	314	254	315	539	556
	275	320	319	318	541	506
	281	314	315	326	524	515
	293	305	309	332	526	582
	281	304	313	330	540	550
Highest	294	321	326	334	553	582
Lowest	251	221	254	307	476	444
L _D (TM20)	273	304	310	319	521	541
Std Dev	11	9	7	6	18	20
JCS	12	16	17	18	59	65

SH	Artificial Composite Specimen 26 Category 2 (Dia. Earth)								
Grind Depth (mm)	0	1.3	2.1	3.2	4.0	4.4	5.1	5.6	5.9
Sec Mat Thick (mm)	5.9	4.6	3.8	2.7	1.9	1.5	0.8	0.3	0
Surface	Top 1	Top 2	Top 3	Top 4	Top 5	Top 6	Top 7	Top 8	Top 9
Hardness Readings	542	522	483	562	521	558	469	404	253
	554	537	552	557	539	548	477	416	246
	599	550	573	539	594	528	456	425	251
	573	587	530	533	548	542	433	367	235
	589	543	527	525	563	516	406	330	239
	535	523	520	577	583	545	407	366	227
	568	570	502	559	523	546	424	406	230
	543	539	560	595	571	509	387	377	239
	600	494	522	592	575	531	452	375	232
	584	534	488	524	551	532	501	370	253
	567	527	536	525	534	547	460	402	245
	569	569	569	562	503	493	493	424	247
	572	558	553	554	510	567	445	364	245
	607	550	560	561	553	532	436	395	242
	572	575	508	563	542	507	446	396	232
	568	514	559	551	610	558	455	367	248
	549	542	559	536	537	567	503	379	258
588	585	517	564	548	567	409	327	247	
583	542	576	541	522	520	459	421	233	
569	516	492	557	588	524	408	347	240	
Highest	535	494	483	524	503	493	387	327	227
Lowest	607	587	576	595	610	567	503	425	258
L _D (TM20)	572	544	535	553	550	538	446	384	242
Std Dev	17	21	27	18	25	18	29	26	7
JCS	74	66	63	68	67	64	41	28	9


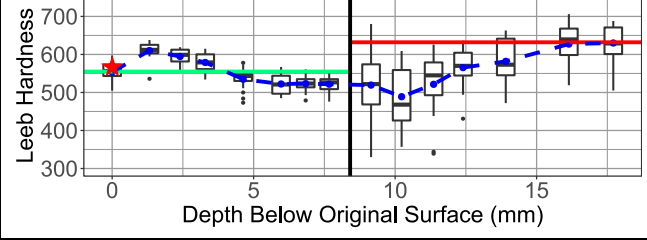

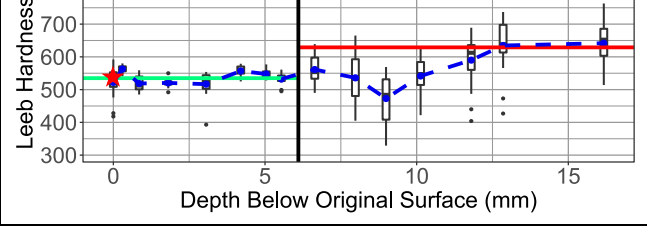

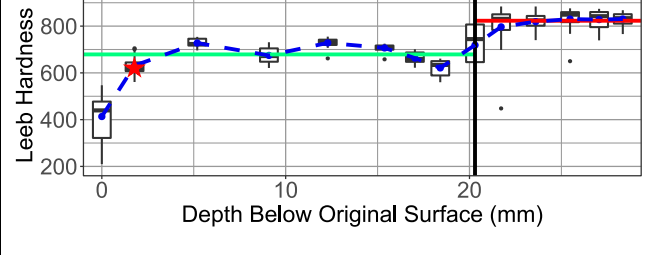

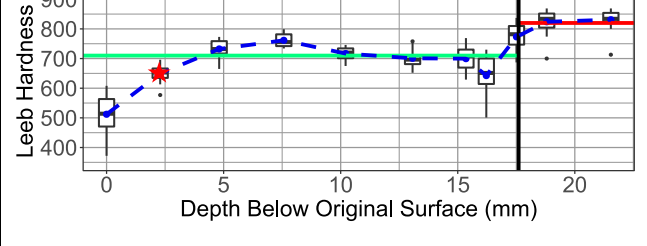

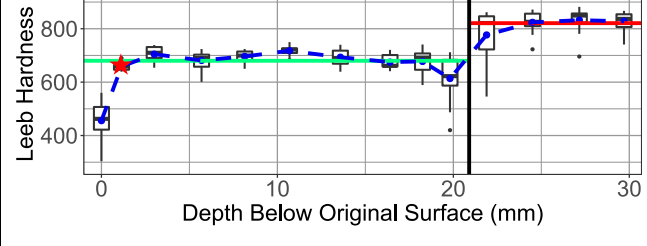
SH	Artificial Composite Specimen 27 Category 2 (Dia. Earth)						
Grind Depth (mm)	0	0.7	2.2	2.5	3.0	3.4	3.9
Sec Mat Thick (mm)	3.85	3.2	1.7	1.4	0.9	0.5	0
Surface	Top 1	Top 2	Top 3	Top 4	Top 5	Top 6	Top 7
Hardness Readings	571	569	583	581	467	437	275
	534	575	495	530	477	436	279
	601	547	546	551	448	404	270
	592	573	540	491	491	370	266
	510	520	554	501	478	399	260
	531	549	599	549	467	411	265
	570	549	562	562	467	373	263
	562	601	550	529	498	362	268
	558	523	587	537	432	363	277
	573	554	508	529	417	393	274
	566	587	564	542	448	361	268
	561	558	504	529	465	329	268
	588	549	531	542	455	388	273
	639	605	509	556	494	382	274
	570	538	599	519	457	369	282
	552	620	571	518	472	366	250
	577	583	565	559	478	356	265
565	591	550	503	520	359	348	
580	552	510	523	454	393	278	
578	543	564	561	439	358	277	
Highest	510	520	495	491	417	329	250
Lowest	639	620	599	581	520	437	348
L _D (TM20)	568	564	550	536	466	380	271
Std Dev	18	23	28	19	18	22	6
JCS	73	71	67	63	45	28	12

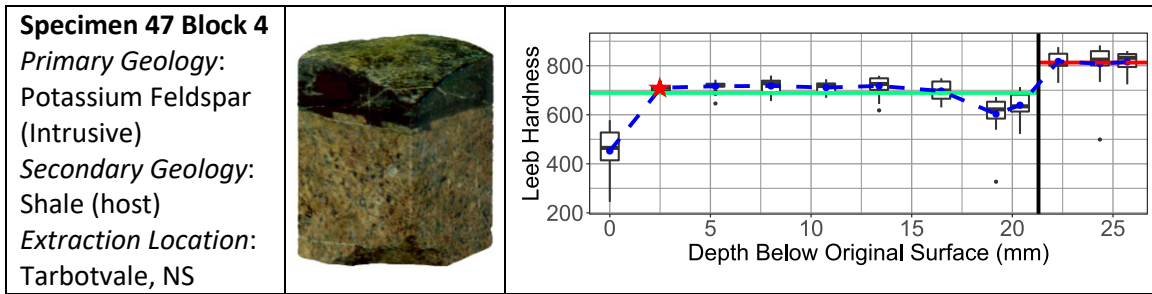
SH	Artificial Composite Specimen 28 Category 2 (Dia. Earth)					
Grind Depth (mm)	0	0.2	0.7	1.6	2.0	2.2
Sec Mat Thick (mm)	2.2	2	1.5	0.6	0.2	0
Surface	Top 1	Top 2	Top 3	Top 4	Top 5	Top 6
Hardness Readings	574	566	497	471	355	268
	518	576	541	451	413	271
	528	518	552	416	415	231
	553	579	582	382	356	250
	502	526	493	512	331	248
	521	596	510	508	378	251
	558	523	541	499	366	259
	531	552	544	433	363	262
	523	551	557	380	331	258
	563	532	544	434	349	262
	487	559	557	408	398	270
	562	545	573	383	351	252
	512	589	573	497	383	266
	515	554	579	532	376	272
	499	500	591	396	309	233
	510	603	567	379	383	262
	556	571	530	395	416	259
	540	565	501	460	356	263
486	507	483	443	312	257	
518	559	549	429	387	251	
Highest	486	500	483	379	309	231
Lowest	574	603	591	532	416	272
L ₀ (TM20)	528	554	544	439	367	258
Std Dev	23	25	28	45	28	9
JCS	61	68	65	39	25	11

Exemption No.	Explanation
AS28C2 - Top 1	Surface was artificially wetted by the cooling fluid used in the grinding machine and dried with paper towel. This was done to avoid testing on a dry surface. The lowered result is believed by the author to be because of this artificial wetting as the surfaces were not prepared in the same manner i.e., wet grinding followed by drying with paper towel. By viewing the combined tab, one can see that the data up until this value are consistent with the results from the other specimens. Thus this top surface was discarded. The top surfaces of the other specimens could be discarded as well.

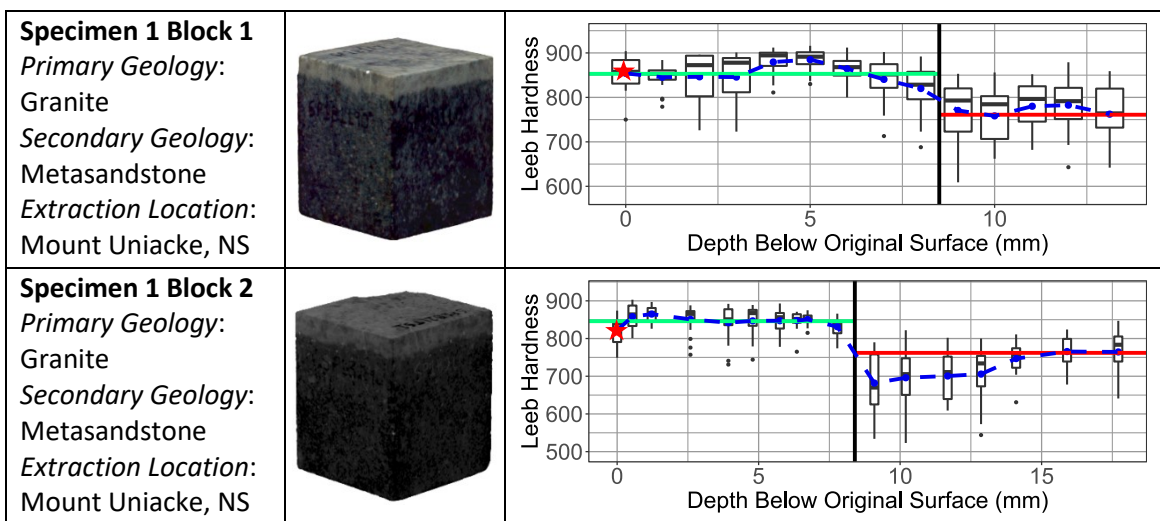
APPENDIX C - HARDNESS VS DEPTH: NATURAL ROCK DATA PART 1

Secondary Material is Softer than Primary Material, SS ($P_H > S_H$)


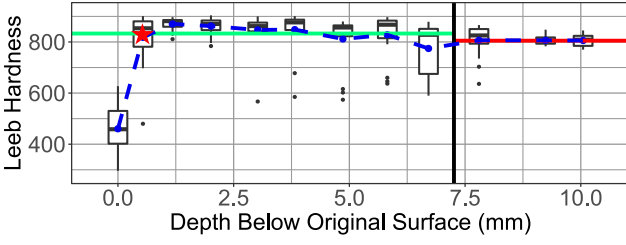

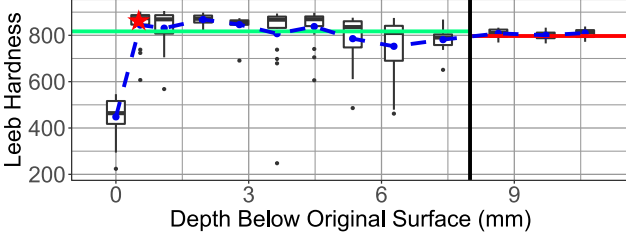

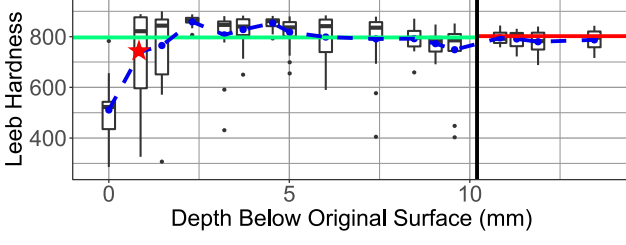

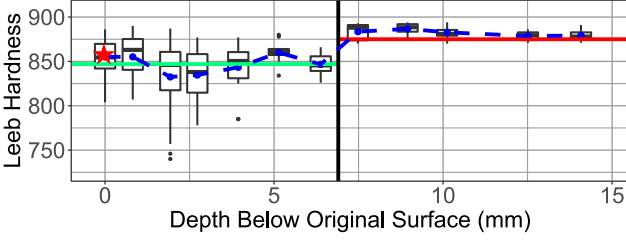

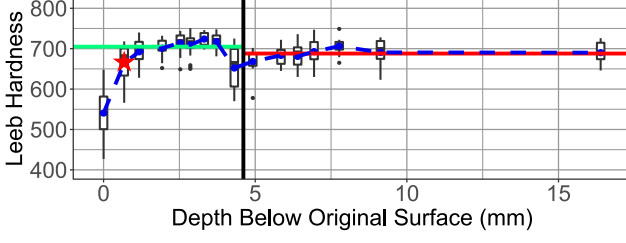
<p>Specimen 37 Block 1 <i>Primary Geology:</i> Tuff <i>Secondary Geology:</i> Reconsolidated Tuff <i>Extraction Location:</i> Irish Cove, NS</p>		
<p>Specimen 37 Block 2 <i>Primary Geology:</i> Tuff <i>Secondary Geology:</i> Reconsolidated Tuff <i>Extraction Location:</i> Irish Cove, NS</p>		
<p>Specimen 47 Block 1 <i>Primary Geology:</i> Potassium Feldspar (Intrusive) <i>Secondary Geology:</i> Shale (host) <i>Extraction Location:</i> Tarbotvale, NS</p>		
<p>Specimen 47 Block 2 <i>Primary Geology:</i> Potassium Feldspar (Intrusive) <i>Secondary Geology:</i> Shale (host) <i>Extraction Location:</i> Tarbotvale, NS</p>		
<p>Specimen 47 Block 3 <i>Primary Geology:</i> Potassium Feldspar (Intrusive) <i>Secondary Geology:</i> Shale (host) <i>Extraction Location:</i> Tarbotvale, NS</p>		




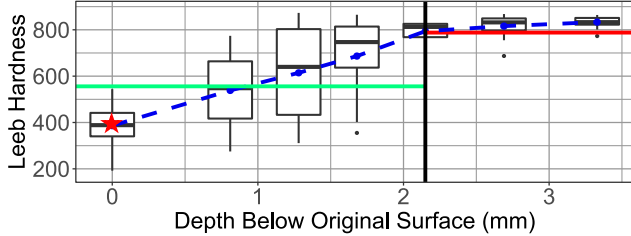

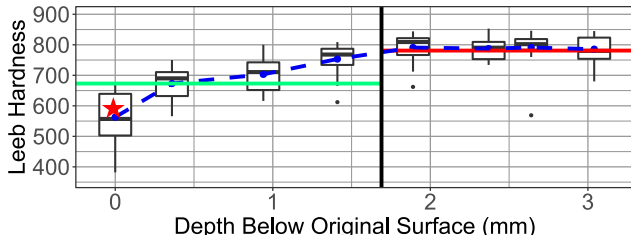

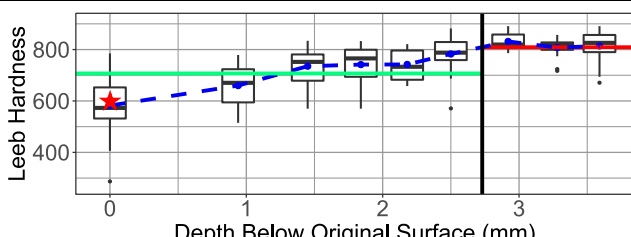

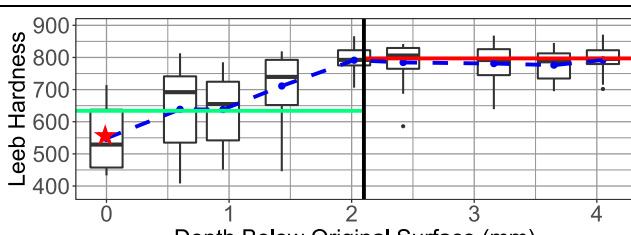

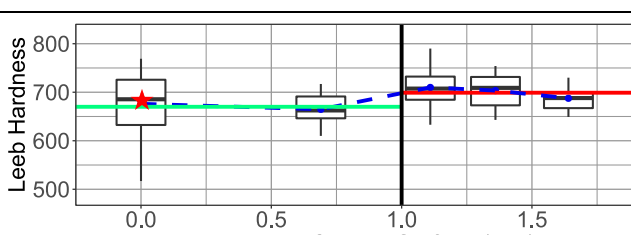

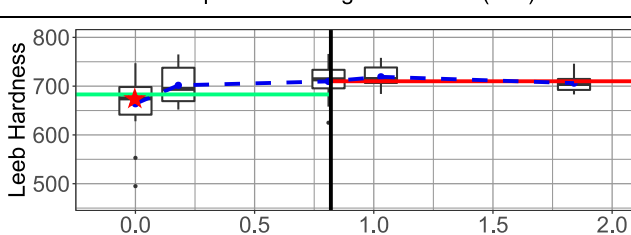
Secondary Material is Harder than Primary Material, $S_H < P_H$


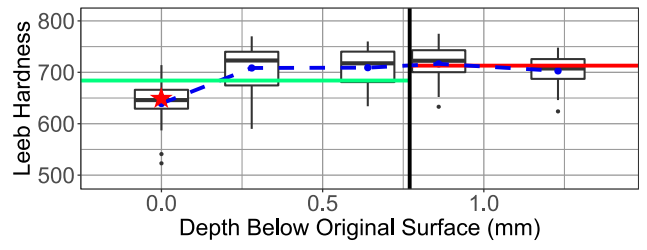

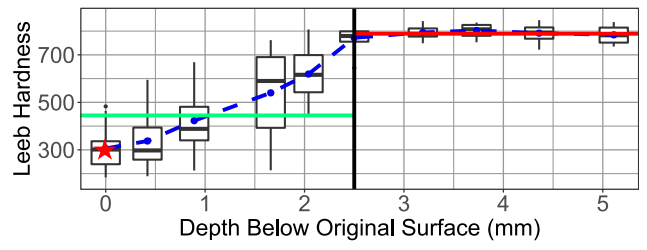

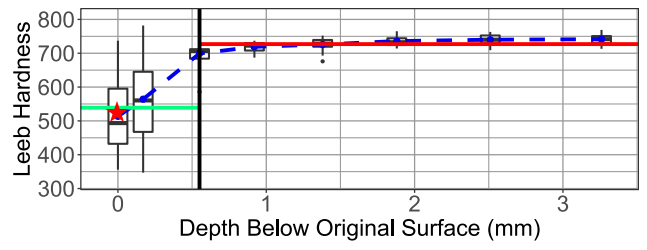

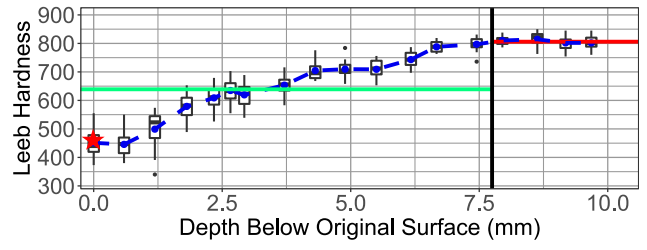

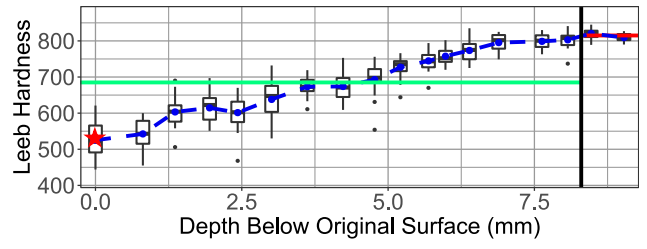
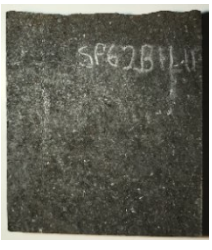
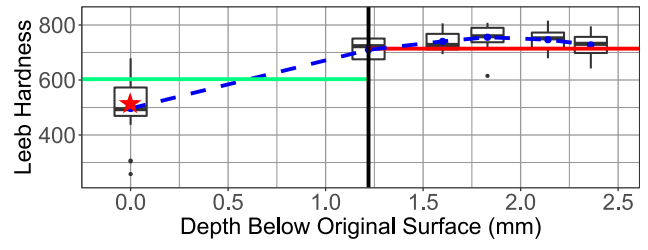


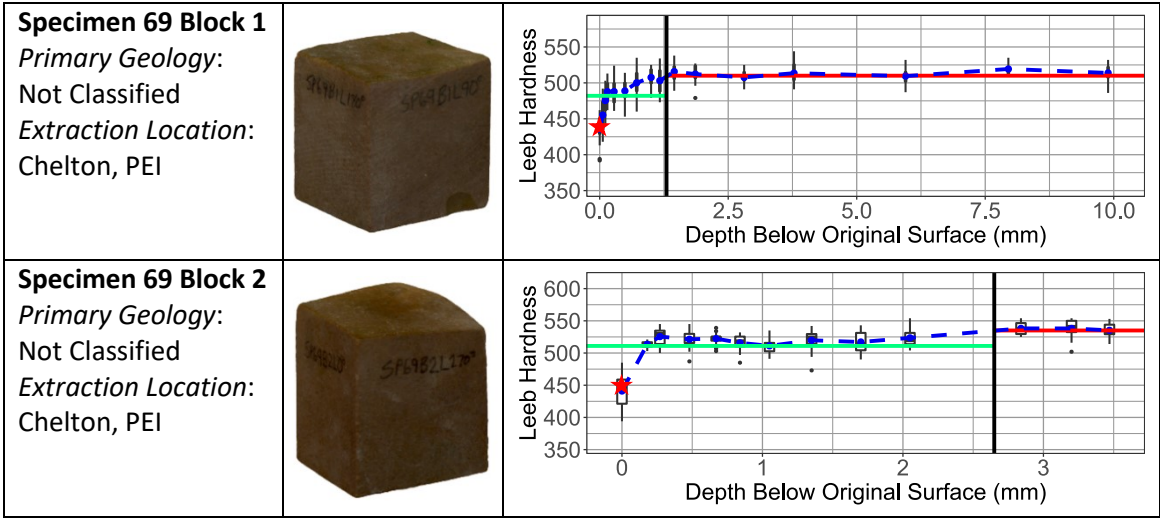
Uniform Hardness Material, UM ($P_H \cong S_H$)

<p>Specimen 8 Block 1 <i>Primary Geology:</i> Granite (South Mountain) <i>Secondary Geology:</i> Quartz (Vein) <i>Extraction Location:</i> Crescent Beach, NS</p>		
<p>Specimen 8 Block 2 <i>Primary Geology:</i> Granite (South Mountain) <i>Secondary Geology:</i> Quartz (Vein) <i>Extraction Location:</i> Crescent Beach, NS</p>		
<p>Specimen 8 Block 3 <i>Primary Geology:</i> Granite (South Mountain) <i>Secondary Geology:</i> Quartz (Vein) <i>Extraction Location:</i> Crescent Beach, NS</p>		
<p>Specimen 13 Block 1 <i>Primary Geology:</i> Mudstone and Siltstone <i>Secondary Geology:</i> Carbonate Vein <i>Extraction Location:</i> Halifax, NS</p>		
<p>Specimen 31 Block 1 <i>Primary Geology:</i> Fine Grained Rhyolite <i>Secondary Geology:</i> Reconsolidated Rhyolite <i>Extraction Location:</i> Arichat, NS</p>		

Weathered or Altered Surface, WA – a class of SS ($P_H > S_H$)

<p>Specimen 36 Block 1 <i>Primary Geology:</i> Not Classified <i>Extraction Location:</i> Irish Cove, NS</p>		
<p>Specimen 39 Block 1 <i>Geology:</i> Rhyolite <i>Extraction Location:</i> Irish Cove, NS</p>		
<p>Specimen 39 Block 2 <i>Geology:</i> Rhyolite <i>Extraction Location:</i> Irish Cove, NS</p>		
<p>Specimen 39 Block 3 <i>Geology:</i> Rhyolite <i>Extraction Location:</i> Irish Cove, NS</p>		
<p>Specimen 53 Block 1 <i>Primary Geology:</i> Basalt <i>Extraction Location:</i> Baxters Harbour, NS</p>		
<p>Specimen 53 Block 2 <i>Primary Geology:</i> Basalt <i>Extraction Location:</i> Baxters Harbour, NS</p>		

<p>Specimen 53 Block 3 <i>Primary Geology:</i> Basalt <i>Extraction Location:</i> Baxters Harbour, NS</p>		
<p>Specimen 60 Block 1 Surface 1 <i>Primary Geology:</i> Not Classified <i>Extraction Location:</i> Boulderwood, NS</p>		
<p>Specimen 60 Block 1 Surface 2 <i>Primary Geology:</i> Not Classified <i>Extraction Location:</i> Boulderwood, NS</p>		
<p>Specimen 61 Block 1 <i>Primary Geology:</i> Not Classified <i>Extraction Location:</i> East Chester, NS</p>		
<p>Specimen 61 Block 2 <i>Primary Geology:</i> Not Classified <i>Extraction Location:</i> East Chester, NS</p>		
<p>Specimen 62 Block 1 <i>Primary Geology:</i> Not Classified <i>Extraction Location:</i> East Chester, NS</p>		



APPENDIX D - HARDNESS VS DEPTH: NATURAL ROCK DATA PART 2

SS	Specimen 37 Block 1 (1st surface was natural)															
Grind Depth (mm)	0.00	1.32	2.40	3.29	4.63	5.97	6.84	7.67	9.15	10.23	11.36	12.40	13.91	16.14	17.71	0.10
Surface	Top 1	Top 2	Top 3	Top 4	Top 5	Top 6	Top 7	Top 8	Top 9	Top 10	Top 11	Top 12	Top 13	Top 14	Top 15	Bot 1
Hardness Readings	523	536	597	593	543	547	520	508	566	444	626	618	622	607	590	779
	549	616	613	606	544	553	512	542	575	420	438	585	574	519	632	301
	561	606	617	615	534	514	493	531	465	529	586	661	648	653	505	682
	563	620	596	621	441	488	538	527	680	606	495	570	525	711	586	527
	552	608	600	612	574	551	547	492	554	597	496	624	596	695	600	610
	506	631	598	573	546	490	539	504	571	428	339	570	492	629	591	658
	597	638	611	563	532	485	527	476	603	412	473	620	563	546	674	727
	584	603	583	601	473	533	583	411	591	609	552	428	376	650	704	622
	562	627	581	598	581	511	517	563	501	450	517	431	678	686	619	539
	585	604	554	596	578	578	535	545	513	600	344	582	654	693	680	420
	616	609	604	561	552	492	561	511	528	620	328	522	590	706	673	669
	544	628	519	567	544	515	527	516	465	314	548	542	655	644	610	746
	575	603	610	585	500	567	515	557	330	426	552	556	652	673	686	635
	520	368	619	567	530	527	535	532	305	561	542	567	542	635	604	643
	505	598	616	534	549	487	513	526	693	486	655	516	663	489	626	667
	583	651	636	601	531	565	535	541	611	427	616	636	472	648	688	689
	547	629	557	539	555	514	479	527	468	499	492	611	572	597	371	683
543	617	558	560	484	441	408	501	342	553	586	552	555	584	661	688	
424	595	576	549	546	535	504	519	470	357	558	494	563	522	652	445	
569	615	614	457	511	527	520	536	516	395	626	581	535	603	665	723	
Highest	616	651	636	621	581	578	583	563	693	620	655	661	678	711	704	779
Lowest	424	368	519	457	441	441	408	411	305	314	328	428	376	489	371	301
L _D	554	610	595	579	535	522	523	522	519	489	521	565	582	627	630	632
Std Dev	27	22	22	25	28	27	20	20	89	82	84	52	58	57	47	92
JCS	68	86	81	76	63	59	60	59	59	51	59	72	77	92	93	94

SS	Specimen 37 Block 2 (1st surface was natural)																
Grind Depth (mm)	0.00	0.30	0.85	1.81	3.06	4.20	5.04	5.54	6.64	7.98	8.99	10.13	11.80	12.85	16.17	0.10	
Surface	Top 1	Top 2	Top 3	Top 4	Top 5	Top 6	Top 7	Top 8	Top 9	Top 10	Top 11	Top 12	Top 13	Top 14	Top 15	Bot 1	
Hardness Readings	520	559	471	515	545	525	566	532	534	634	436	624	668	639	551	492	
	535	561	493	505	487	574	535	535	490	462	513	585	661	637	664	674	
	570	549	493	520	393	569	546	535	533	405	553	571	620	729	711	654	
	480	566	508	525	551	558	546	522	680	476	547	604	487	629	514	537	
	513	580	506	523	568	561	565	534	545	459	371	563	605	630	656	629	
	307	567	545	504	533	571	528	546	573	583	581	550	638	473	591	532	
	563	562	559	550	514	518	549	548	558	682	485	448	576	655	618	671	
	554	533	543	552	490	557	533	561	637	596	507	518	628	572	763	659	
	507	542	541	517	490	561	535	499	519	509	329	505	601	608	615	602	
	418	578	530	466	536	574	597	487	554	582	462	513	622	688	478	594	
	476	572	517	530	350	527	541	532	525	549	178	422	688	636	691	453	
	550	578	537	529	549	526	539	532	639	615	569	711	404	427	670	556	
	513	589	530	519	541	563	557	495	611	494	565	606	385	701	649	733	
	428	575	501	524	501	558	557	540	553	533	532	619	630	737	798	750	
	538	559	567	525	512	578	537	570	606	534	483	244	709	193	656	724	
	592	568	485	533	549	579	507	554	539	625	480	545	507	741	748	731	
	601	541	548	492	554	540	577	527	498	431	399	582	603	654	600	573	
	539	555	501	522	522	580	549	522	560	665	367	534	555	728	519	569	
	554	568	495	522	507	547	547	544	490	384	384	434	440	566	721	743	
	546	554	504	512	526	555	551	526	629	495	530	526	689	716	613	640	
Highest	601	589	567	552	568	580	597	570	680	682	581	711	709	741	798	750	
Lowest	307	533	471	466	350	518	507	487	490	384	178	244	385	193	478	453	
L _D	522	563	519	520	517	557	548	532	561	536	473	542	590	635	642	629	
Std Dev	47	12	23	13	38	17	13	17	46	75	75	61	82	85	72	76	
JCS	59	71	58	59	58	69	67	62	71	63	47	65	80	95	98	93	

SS	Specimen 47 Block 1 (1st surface was natural)																		
Grind Depth (mm)	0.00	1.78	5.19	9.09	12.29	15.38	17.03	18.41	20.30	21.72	23.60	25.47	27.05	28.34	0.10				
Surface	Top 1	Top 2	Top 3	Top 4	Top 5	Top 6	Top 7	Top 8	Top 9	Top 10	Top 11	Top 12	Top 13	Top 14	Bot 1				
Hardness Readings	516	546	696	623	738	717	694	645	835	845	773	876	798	825	851	825	862	815	860
	333	575	752	711	719	702	676	638	661	862	884	856	844	803	830	804	801	846	832
	210	616	748	712	743	720	649	652	775	815	845	799	854	818	863	850	802	825	850
	199	605	720	646	747	695	652	661	457	761	839	864	841	867	844	833	851	652	829
	547	641	747	691	662	657	644	660	666	854	848	645	880	871	831	788	836	823	866
	604	646	723	733	743	716	670	560	439	698	848	855	739	868	836	851	825	850	832
	459	607	754	596	728	721	647	568	763	745	811	829	862	832	822	843	824	841	849
	401	707	747	621	737	700	705	635	788	849	669	861	849	845	845	840	737	850	855
	405	696	737	659	713	702	648	663	840	853	740	849	773	764	800	829	863	835	855
	292	701	733	678	734	712	667	595	830	890	835	863	873	766	842	809	851	844	843
	460	620	682	682	707	696	672	633	816	448	805	767	795	851	851	836	836	813	757
	451	615	716	731	518	739	652	619	711	884	818	813	822	813	820	794	825	808	851
	317	641	708	663	760	719	617	587	726	821	904	851	784	856	865	690	824	861	839
	278	699	743	695	721	725	691	584	592	781	814	848	874	803	864	857	737	841	822
	318	610	715	630	747	716	693	655	804	851	777	888	868	836	791	865	863	856	851
	547	599	720	708	739	695	701	534	641	841	801	650	855	806	824	804	851	819	825
	458	561	724	645	755	699	638	635	808	791	831	802	783	851	813	808	858	833	
	483	705	720	653	729	658	622	624	820	841	767	848	625	839	819	767	866	799	
	538	613	697	666	729	716	701	652	618	802	832	849	820	855	766	698	843	814	
	428	611	754	730	718	710	623	579	627	251	878	861	870	810	806	723	738	802	
Highest	604	707	754	733	760	739	705	663	840	890	904	888	880	871	NA				
Lowest	199	546	682	596	518	657	617	534	439	251	669	645	625	764	NA				
L ₀	413	631	728	675	728	707	663	621	719	797	819	830	828	830	823				
Std Dev	101	43	18	35	21	16	25	34	105	99	38	53	41	27	26				
JCS	34	94	132	110	133	123	106	90	128	165	176	182	181	182	178				

SS	Specimen 47 Block 2 (1st surface was natural)												
Grind Depth (mm)	0.00	2.29	4.81	7.57	10.21	13.07	15.35	16.22	17.51	18.80	21.54	0.10	
Surface	Top 1	Top 2	Top 3	Top 4	Top 5	Top 6	Top 7	Top 8	Top 9	Top 10	Top 11	Bot 1	
Hardness Readings	510	625	726	737	748	708	633	683	829	857	863	861	829
	372	654	715	745	685	678	623	643	811	794	856	798	826
	398	667	726	740	675	679	704	707	785	869	869	842	829
	557	640	779	788	700	488	634	435	796	840	682	764	828
	589	712	712	767	718	697	710	746	744	821	835	814	811
	527	651	751	782	744	681	762	724	858	826	861	822	857
	512	613	755	750	736	760	629	651	772	802	831	837	859
	357	652	723	803	659	682	684	661	530	852	833	830	865
	494	615	705	797	722	696	769	566	806	831	803	806	806
	608	676	665	781	687	730	636	649	827	700	840	790	798
	460	674	724	735	743	710	666	676	768	859	839	724	
	565	544	760	751	729	721	710	652	720	811	817	791	
	511	696	676	742	694	693	680	609	794	799	848	818	
	463	665	738	760	725	698	725	706	687	774	832	819	
	433	577	773	799	725	758	732	546	837	850	822	810	
	574	665	768	734	705	679	756	710	704	851	833	877	
	559	675	762	742	746	652	795	730	812	877	800	818	
610	663	741	786	717	712	752	630	691	859	872	814		
516	647	504	729	739	688	719	501	779	696	713	831		
571	633	762	771	713	753	693	523	756	837	861	836		
Highest	610	712	779	803	748	760	795	746	858	877	872	NA	
Lowest	357	544	504	729	659	488	623	435	530	696	682	NA	
L _D	512	649	732	762	717	701	700	643	773	824	831	820	
Std Dev	66	29	31	23	22	27	46	69	47	41	35	31	
JCS	57	100	134	148	128	121	120	98	153	179	182	177	

SS	Specimen 47 Block 3 (1st surface was natural)														
Grind Depth (mm)	0.00	1.14	3.00	5.69	8.14	10.69	13.58	16.40	18.25	19.81	21.89	24.50	27.16	29.70	0.10
Surface	Top 1	Top 2	Top 3	Top 4	Top 5	Top 6	Top 7	Top 8	Top 9	Top 10	Top 11	Top 12	Top 13	Top 14	Bot 1
Hardness Readings	582	690	730	676	722	589	678	703	726	748	836	822	790	819	845
	521	657	704	672	731	725	683	721	708	583	808	841	854	855	848
	304	642	738	653	707	719	661	641	696	501	852	855	696	773	854
	505	664	659	686	722	728	693	651	663	278	826	818	882	866	771
	419	639	724	714	716	722	733	661	741	698	849	828	839	867	837
	440	662	689	638	704	750	703	646	569	625	858	829	852	841	771
	507	653	739	696	698	708	715	716	642	640	822	824	863	805	833
	431	660	697	643	711	722	735	659	615	706	573	857	781	844	841
	549	620	724	531	697	734	689	659	706	712	546	874	820	739	852
	524	661	716	695	689	689	663	697	659	676	862	723	640	804	792
	463	642	732	652	679	757	687	642	631	615	818	868	862	855	853
	296	730	665	718	696	727	730	659	678	620	675	807	832	846	790
	560	670	748	676	701	717	692	715	688	599	689	866	848	828	846
	505	645	700	724	662	723	634	682	603	420	821	865	855	870	829
	462	677	656	727	650	702	666	729	706	518	727	777	844	803	867
	433	657	654	720	587	713	740	626	772	487	840	778	858	852	822
	507	679	734	697	719	683	719	661	589	688	403	496	793	741	838
312	651	694	705	680	724	639	706	739	686	721	821	889	811	741	
394	645	732	601	724	744	654	660	697	601	858	780	859	833	738	
366	663	618	696	656	687	754	673	709	670	865	872	851	861	810	
Highest	582	730	748	727	731	757	754	729	772	748	865	874	889	870	867
Lowest	296	620	618	531	587	589	634	626	569	278	403	496	640	739	738
L _b	456	659	705	681	696	718	693	675	678	614	777	824	832	828	821
Std Dev	76	14	30	33	23	18	30	27	46	84	99	40	44	34	34
JCS	43	104	123	113	119	128	118	110	111	88	155	179	183	181	177

SS	Specimen 47 Block 4 (1st surface was natural)												
Grind Depth (mm)	0.00	2.54	5.25	8.01	10.75	13.38	16.47	19.19	20.38	22.28	24.35	25.71	0.10
Surface	Top 1	Top 2	Top 3	Top 4	Top 5	Top 6	Top 7	Top 8	Top 9	Top 10	Top 11	Top 12	Bot 1
Hardness Readings	446	712	717	688	704	709	749	667	685	868	805	765	839
	538	716	725	712	716	644	755	565	728	802	784	816	850
	475	727	743	761	742	758	744	655	628	797	845	832	840
	571	711	718	729	679	748	694	660	630	810	781	840	848
	446	698	723	724	719	762	667	595	638	756	883	833	782
	319	740	725	679	678	759	662	605	674	818	865	860	800
	578	697	711	657	729	684	609	651	637	730	250	848	820
	556	712	715	728	682	749	704	239	522	799	870	847	823
	239	692	731	754	724	618	737	672	691	644	800	858	788
	494	705	685	628	738	731	633	638	487	883	849	724	837
	245	718	696	739	734	588	720	613	632	852	818	810	831
	589	697	646	739	669	721	732	613	696	873	832	797	788
	409	721	620	745	682	752	668	633	623	840	839	794	828
	455	703	727	691	724	743	675	581	610	876	811	728	837
	492	708	742	698	745	711	645	771	713	814	499	842	827
	390	713	749	731	704	752	630	654	699	876	814	857	815
	258	692	736	734	644	699	742	558	600	811	734	860	817
497	689	715	753	712	723	665	539	580	785	863	566	771	
547	723	722	760	719	688	746	327	604	805	863	774	499	
430	739	718	656	753	728	732	631	642	803	889	852	749	
Highest	589	740	749	761	753	762	755	771	728	883	889	860	850
Lowest	239	689	620	628	644	588	609	239	487	644	250	566	499
L _D	453	710	716	718	711	718	697	603	639	818	809	815	813
Std Dev	99	13	23	32	24	39	42	79	48	41	86	43	28
JCS	42	125	127	128	125	128	119	84	97	175	171	174	173

SH	Specimen 1 Block 1 (1st surface was saw-cut)																	
Grind Depth (mm)	0.00	0.99	2.00	3.00	4.00	5.00	6.00	7.00	8.00	9.01	10.00	11.02	12.00	13.12	14.45	15.33	0.10	
Surface	Top 1	Top 2	Top 3	Top 4	Top 5	Top 6	Top 7	Top 8	Top 9	Top 10	Top 11	Top 12	Top 13	Top 14	Top 15	Top 16	Bot 1	
Hardness Readings	881	795	799	877	899	772	800	800	858	648	822	784	714	832	796	700	670	812
	831	858	850	828	811	872	848	818	837	837	799	771	824	650	749	714	807	804
	864	842	893	898	840	904	859	841	798	609	857	737	806	738	806	806	728	674
	870	863	877	887	901	905	832	759	723	720	786	825	775	751	776	522	786	841
	904	797	894	789	869	906	899	852	878	722	817	776	726	774	645	811	775	799
	815	839	868	914	880	888	915	702	688	726	785	834	874	730	830	817	721	824
	733	860	726	723	895	884	912	879	815	818	803	830	641	850	603	804	814	799
	750	858	800	889	895	830	856	862	866	568	684	683	793	705	752	771	831	767
	899	881	895	898	894	861	817	860	755	853	721	784	751	645	777	789	702	793
	816	872	810	895	780	895	882	797	820	818	649	825	846	828	619	768	710	703
	816	848	896	883	896	902	880	859	874	786	835	812	887	822	744	795	808	
	845	859	747	862	827	900	874	851	906	835	662	829	643	567	763	824	688	
	895	696	895	901	908	925	882	904	846	818	723	852	767	772	770	712	839	
	895	884	771	879	902	880	890	902	856	775	702	809	790	813	727	598	609	
	885	861	686	846	912	877	839	886	854	821	856	691	693	875	871	598	866	
	909	848	884	806	891	874	877	884	795	855	802	816	879	859	832	801	679	
	851	844	845	881	928	898	898	893	786	821	687	682	814	642	842	857	769	
	831	779	900	732	901	837	653	832	818	800	784	701	812	756	720	859	835	
	850	828	896	694	834	899	862	713	552	677	663	870	752	806	817	785	611	
	874	884	886	748	876	916	852	841	892	786	720	619	827	748	660	720	777	
Highest	909	884	900	914	928	925	915	904	906	855	857	870	887	875	871	859	NA	
Lowest	733	696	686	694	780	772	653	702	552	568	649	619	641	567	603	522	NA	
L _p	854	845	846	846	880	885	864	841	820	771	758	780	783	762	757	759	761	
Std Dev	40	29	56	60	31	24	30	49	55	71	63	57	62	69	64	73	70	
JCS	195	190	191	190	209	213	201	188	177	152	146	157	158	148	146	147	148	

SH	Specimen 1 Block 2 (1st surface was saw-cut)																			
Grind Depth (mm)	0.00	0.54	1.22	2.59	3.93	4.79	5.75	6.35	6.73	7.78	9.09	10.20	11.68	12.86	14.10	15.90	17.71		0.10	
Surface	Top 1	Top 2	Top 3	Top 4	Top 5	Top 6	Top 7	Top 8	Top 9	Top 10	Top 11	Top 12	Top 13	Top 14	Top 15	Top 16	Top 17	Bot 1		
Hardness Readings	841	873	832	849	741	836	877	765	868	866	800	822	629	578	735	672	765	825	833	753
	830	838	889	857	833	742	802	869	862	860	654	695	652	544	708	764	757	715	733	816
	892	867	843	870	884	880	886	865	849	829	786	623	609	755	811	790	807	721	751	831
	839	828	881	823	813	891	762	848	858	790	726	718	802	502	772	783	604	777	649	780
	847	834	878	865	843	883	859	826	891	836	760	772	424	659	631	806	649	808	583	866
	851	801	869	878	849	841	868	863	850	847	523	622	749	739	793	777	641	581	776	826
	660	902	897	799	855	878	825	831	827	824	665	677	787	730	759	824	733	663	845	613
	749	872	894	877	850	843	856	680	872	807	561	523	794	738	765	815	792	750	774	846
	785	886	889	891	843	744	857	872	834	854	647	673	753	800	791	767	801	663	794	782
	808	893	881	868	880	866	778	852	846	726	534	756	753	759	606	822	827	793	782	629
	841	806	853	859	871	833	898	828	809	840	622	722	634	573	839	754	799	634	723	857
	873	890	838	873	883	793	858	867	843	845	790	488	637	729	775	726	763	845	837	837
	841	860	858	852	896	877	893	871	856	866	752	825	647	717	721	759	832	805	830	712
	825	748	867	776	852	869	852	850	847	790	586	775	832	716	727	730	799	754	792	824
	777	809	814	872	867	779	880	860	875	843	785	643	738	751	759	760	847	520	631	755
	753	903	875	888	714	818	794	845	853	810	705	716	615	802	732	678	662	717	814	784
	846	833	833	755	731	873	867	852	871	826	635	798	743	767	782	734	860	841	786	817
	866	861	826	866	781	870	831	860	815	774	781	594	693	611	763	802	775	818	735	783
	754	888	900	887	889	872	852	841	854	845	610	719	647	787	704	688	843	744	778	841
	874	902	865	757	892	889	816	866	828	839	675	681	729	750	716	822	668	803	762	759
Highest	893	903	900	891	896	891	898	877	891	874	800	825	837	802	839	827	860		NA	
Lowest	660	748	814	755	714	742	762	680	809	726	523	488	434	507	606	677	604		NA	
L _o	822	858	865	851	842	847	847	848	850	832	682	696	701	706	747	766	764		762	
Std Dev	41	34	23	38	48	41	33	25	17	27	82	76	67	78	43	43	67		78	
JCS	178	197	201	193	188	191	191	192	193	183	113	119	121	123	141	150	149		148	

UM	Specimen 8 Block 1 (1st natural surface removed by grinding without hardness data collection)												
Grind Depth (mm)	0.00	0.54	1.18	2.01	3.02	3.82	4.86	5.82	6.71	7.80	9.24	10.05	0.10
Surface	Top 2	Top 3	Top 4	Top 5	Top 6	Top 7	Top 8	Top 9	Top 10	Top 11	Top 12	Top 13	Bot 1
Hardness Readings	296	883	887	870	876	678	864	791	693	800	774	783	775
	549	901	858	885	884	874	602	895	640	791	795	827	777
	407	831	865	869	901	885	836	901	839	825	784	845	827
	407	869	896	880	861	855	854	810	854	777	817	775	705
	577	883	883	893	900	875	865	646	894	851	807	783	800
	594	280	824	904	866	873	863	884	870	844	784	799	736
	405	877	903	784	833	882	871	857	810	800	832	826	838
	627	480	884	841	875	901	870	844	667	735	823	775	839
	538	855	886	881	835	900	882	882	843	825	809	769	852
	496	882	890	486	896	888	616	853	821	849	818	813	816
	507	881	864	896	866	897	818	891	735	853	848	815	533
	475	754	897	829	863	878	844	475	624	853	806	790	837
	340	827	841	862	843	894	808	879	843	827	783	805	831
	265	697	811	913	351	585	331	637	669	860	793	827	808
	354	902	881	885	567	885	859	897	590	826	849	794	831
	442	852	881	869	857	839	874	878	835	521	806	770	812
	491	762	473	871	858	505	857	829	870	636	795	817	846
401	766	882	872	841	909	880	879	574	866	794	818	862	
638	880	883	796	836	836	574	660	859	893	793	840	788	
380	846	854	833	890	844	856	894	879	703	828	889	768	
Highest	638	902	903	913	901	909	882	901	894	883	849	889	862
Lowest	265	280	473	486	351	505	331	475	574	521	774	769	533
L _D	460	818	870	862	847	848	812	828	775	807	806	806	805
Std Dev	94	102	24	33	73	83	101	88	100	61	18	23	40
JCS	44	176	204	200	191	192	172	181	154	170	170	169	169

UM	Specimen 8 Block 2 (1st natural surface removed by grinding without hardness data collection)													
Grind Depth (mm)	0.00	0.55	1.09	1.97	2.79	3.64	4.48	5.35	6.28	7.39	8.64	9.71	10.60	0.10
Surface	Top 2	Top 3	Top 4	Top 5	Top 6	Top 7	Top 8	Top 9	Top 10	Top 11	Top 12	Top 13	Top 14	Bot 1
Hardness Readings	471	871	891	865	865	867	606	611	839	808	804	789	795	825
	535	889	783	855	864	848	854	862	852	737	769	833	767	795
	486	893	885	845	858	679	418	863	819	801	763	765	789	805
	420	882	864	887	869	879	835	462	409	802	833	831	841	806
	457	902	887	880	846	698	741	486	620	769	784	827	812	792
	216	545	830	886	864	900	882	686	876	754	823	787	772	773
	644	844	806	898	855	874	880	853	864	651	782	794	790	683
	422	853	812	873	856	850	858	879	841	868	811	806	792	788
	337	724	871	855	874	881	877	876	462	800	800	781	826	754
	442	890	705	818	845	841	874	870	479	761	825	774	821	790
	494	872	908	855	867	206	803	869	842	757	832	808	821	816
	538	900	891	860	691	738	876	825	721	781	781	743	807	754
	415	903	886	883	854	880	897	786	801	805	809	836	824	762
	538	877	867	784	837	889	884	841	785	790	792	814	829	764
	546	876	887	832	849	883	894	857	655	791	802	811	818	754
	224	607	900	895	866	829	705	830	739	812	832	798	816	794
	417	860	337	870	838	868	892	735	680	869	824	803	791	817
518	738	905	897	874	894	907	851	875	831	830	812	812	757	
294	842	715	899	833	884	858	816	841	609	817	786	838	831	
512	878	568	875	629	248	865	625	832	747	836	791	823	796	
Highest	644	903	908	899	874	900	907	879	876	869	836	836	841	831
Lowest	216	545	337	784	629	206	418	462	409	609	763	743	767	683
L _D	448	844	831	868	846	807	838	786	753	781	808	801	810	786
Std Dev	90	77	89	22	41	154	78	112	127	46	20	19	18	24
JCS	41	190	182	203	191	170	186	159	144	157	171	167	171	159

UM	Specimen 8 Block 3 (1st natural surface removed by grinding without hardness data collection)																		
Grind Depth (mm)	0.00	0.88	1.47	2.31	3.20	3.72	4.54	5.01	6.01	7.40	8.38	8.46	9.05	9.58	10.84	11.30	11.89	13.45	0.10
Surface	Top 2	Top 3	Top 4	Top 5	Top 6	Top 7	Top 8	Top 9	Top 10	Top 11	Top 12	Top 13	Top 14	Top 15	Top 16	Top 17	Top 18	Top 19	Bot 1
Hardness Readings	543	824	868	892	881	837	849	778	590	842	818	777	742	773	778	776	726	795	766
	526	884	900	833	805	792	831	832	842	859	813	786	810	749	796	812	676	755	795
	536	902	894	882	854	798	861	836	752	782	582	835	778	831	775	789	753	759	808
	425	843	877	878	842	865	854	853	841	808	339	815	787	448	828	747	802	716	793
	423	884	800	855	779	883	871	655	875	260	858	766	759	789	774	786	818	807	817
	645	526	867	866	858	868	874	892	735	405	458	644	789	828	776	808	748	691	796
	396	326	198	862	777	831	830	837	850	853	771	818	607	820	872	814	827	825	817
	543	492	853	872	841	831	809	875	818	577	608	753	741	403	768	815	748	849	820
	176	759	844	871	431	835	882	610	876	693	631	822	828	789	800	718	775	836	839
	286	889	843	842	842	650	867	876	856	761	840	823	691	864	818	752	787	837	861
	783	875	648	864	869	843	858	792	897	846	611	798	720	349	753	758	778	723	847
	526	564	635	860	877	796	869	699	639	879	739	856	739	800	791	819	688	747	729
	519	819	906	858	379	869	482	825	839	874	371	871	703	737	792	722	809	761	774
	656	771	307	861	860	877	839	725	636	849	778	746	848	782	844	838	840	843	783
	490	875	880	881	843	862	867	859	262	879	812	794	822	852	817	815	850	758	817
	299	261	571	799	850	872	862	873	863	825	778	760	767	814	758	813	821	797	789
	513	694	661	807	860	713	866	880	869	811	854	659	794	742	812	758	791	803	820
620	537	859	888	591	627	793	843	884	829	676	742	801	741	833	831	741	797	788	
811	877	637	726	867	882	897	846	874	892	751	889	786	781	771	818	833	778	766	
466	886	828	875	900	889	880	836	735	871	868	836	848	796	783	807	755	836	801	
Highest	811	902	906	892	900	889	887	893	887	882	868	889	848	864	878	838	850	849	861
Lowest	176	261	198	736	379	627	483	610	363	269	313	644	607	349	753	718	676	691	729
L ₀	511	740	765	859	807	828	853	818	799	791	682	792	773	749	795	791	780	787	802
Std Dev	122	175	157	24	115	62	24	64	94	122	161	50	43	122	25	32	42	40	23
JCS	56	138	149	198	170	181	195	176	166	162	113	163	153	142	164	162	157	160	167

Exemption No. SP883 - Top12

UM	Specimen 13 Block 1 (1st surface was saw-cut)													
Grind Depth (mm)	0.00	0.82	1.93	2.73	3.94	5.14	6.38	7.48	8.95	10.12	12.51	14.08	0.10	
Surface	Top 1	Top 2	Top 3	Top 4	Top 5	Top 6	Top 7	Top 8	Top 9	Top 10	Top 11	Top 12	Bot 1	
Hardness Readings	888	876	896	834	834	864	866	888	892	884	879	882	870	867
	838	842	847	865	830	884	844	892	897	884	888	891	877	873
	842	870	877	827	825	858	852	888	892	879	886	877	881	879
	856	847	825	842	785	850	826	891	892	873	874	887	880	886
	804	868	884	872	704	828	839	888	878	894	874	871	870	877
	780	896	829	820	846	861	840	876	889	894	879	878	866	879
	867	840	795	794	877	858	852	893	886	894	873	877	866	865
	886	884	746	751	829	858	866	889	893	881	883	891	877	865
	876	842	856	879	861	855	847	892	871	883	882	873	874	873
	872	830	845	806	785	847	841	836	883	870	871	870	880	863
	829	812	856	826	855	863	857	891	889	879	885	885	888	
	867	880	857	778	850	864	840	870	886	886	873	878	884	
	840	807	740	781	838	834	851	873	894	881	875	883	885	
	869	828	757	856	851	860	824	880	894	892	885	878	879	
	886	873	834	864	859	857	835	871	889	893	881	879	880	
	842	794	572	877	874	878	833	892	879	879	881	873	867	
	851	865	862	854	864	880	866	884	878	881	883	874	864	
845	877	873	856	877	863	864	872	874	879	871	873	874		
853	861	887	813	867	865	827	873	885	877	880	887	884		
870	890	815	859	851	864	860	894	888	861	870	878	862		
Highest	888	896	896	879	877	884	866	894	897	894	888	891	NA	
Lowest	780	794	572	751	704	828	824	836	871	861	870	870	NA	
L _D	855	855	833	835	843	860	847	884	887	883	879	879	875	
Std Dev	21	25	46	31	26	10	13	9	6	7	5	6	8	
JCS	196	196	183	184	189	198	191	212	214	211	209	209	207	

UM	Specimen 31 Block 1 (1st surface was natural)																										
Grind Depth (mm)	0.00	0.68	1.17	1.93	2.53	2.86	3.32	3.65	3.72	4.31	4.92	5.85	6.40	6.94	7.77	9.13	16.39	16.39	16.39	16.39	16.39	0.10					
Surface	Top 1	Top 2	Top 3	Top 4	Top 5	Top 6	Top 7	Top 8	Top 9	Top 10	Top 11	Top 12	Top 13	Top 14	Top 15	Top 16	Top 17(1)	Top 17(2)	Top 17(3)	Top 17(4)	Top 17(5)	Bot 1					
Hardness Readings	668	696	706	696	723	712	721	674	642	701	657	676	660	630	706	614	621	661	652	639	693	666	655	634	654	685	
	561	607	698	731	737	719	724	719	699	750	651	730	694	691	697	724	595	712	680	683	726	633	723	662	711	727	
	512	718	721	721	744	727	715	699	748	704	688	722	717	690	722	643	712	641	674	652	718	641	729	716	722	712	
	484	714	700	703	711	721	706	736	721	694	702	658	697	725	718	716	618	704	693	631	718	684	733	726	720	731	
	535	682	718	629	726	707	744	734	729	725	662	694	642	707	749	682	678	680	669	686	686	679	658	744	702	692	717
	297	665	519	652	713	701	740	731	728	668	655	692	701	682	707	623	705	632	664	719	721	610	694	701	703	738	
	516	699	712	701	685	713	698	723	711	689	668	639	632	733	711	651	691	658	616	692	703	621	572	739	668	685	
	635	621	647	698	719	719	744	743	705	620	520	649	704	747	660	728	679	671	683	695	628	714	686	667	707	621	
	551	701	675	732	752	744	715	743	712	664	660	683	748	715	708	674	670	711	658	633	674	644	719	707	706	662	
	471	632	674	723	726	751	739	733	736	607	657	706	622	666	765	698	651	674	686	682	690	660	722	676	683	709	
	584	699	741	716	646	734	682	730	751	606	663	645	710	753	717	677	667	675	697	670	658	692	705	742	666	687	
	497	702	650	727	649	722	777	745	734	593	698	691	630	717	696	709	608	678	679	674	646	726	724	688	648	743	
	648	718	714	676	713	615	698	744	724	550	676	687	666	671	716	685	677	664	690	662	659	700	655	572	725	719	
	583	680	632	712	735	659	708	681	681	570	691	657	708	692	719	703	709	691	684	661	732	632	694	715	748	698	
	604	658	682	700	677	650	733	731	713	575	683	646	667	652	689	700	655	693	711	541	705	711	707	682	706	722	
	530	702	733	664	699	711	746	662	738	713	697	714	687	635	665	721	613	645	681	698	655	675	707	687	684	701	
	473	583	740	695	718	753	738	689	686	665	578	698	736	510	700	720	692	671	717	714	703	681	714	699	644	721	
577	558	719	675	709	740	718	707	722	706	702	719	649	686	679	734	687	715	684	609	683	707	700	682	711	675		
427	638	628	701	742	654	738	732	736	589	664	685	662	725	705	720	703	653	744	682	718	723	733	680	615	628		
544	566	712	735	736	683	706	705	691	651	679	680	696	704	708	660	653	674	682	685	674	691	591	696	599	696		
Highest	669	719	741	735	757	753	777	745	751	750	707	730	748	753	765	734	712	715	744	719	731	NA					
Lowest	297	558	519	629	646	615	692	667	643	550	570	639	627	510	660	614	595	632	616	541	629	NA					
L ₀	541	665	692	701	715	709	724	720	717	652	668	683	681	693	706	691	665	675	682	669	689	688					
Std Dev	59	46	34	23	25	30	17	22	19	52	28	24	31	33	18	31	32	21	16	27	25	39					
JCS	65	106	117	121	127	124	131	129	128	102	108	114	113	117	123	117	107	110	113	108	116	116					

WAS	Specimen 36 Block 1 (1st surface was natural)											
Grind Depth (mm)	0.00	0.81	1.28	1.68	2.15	2.69	3.33	0.10	0.10	0.10	0.10	0.10
Surface	Top 1	Top 2	Top 3	Top 4	Top 5	Top 6	Top 7	Bot 1(1)	Bot 1(2)	Bot 1(3)	Bot 1(4)	Bot 1(5)
Hardness Readings	450	792	619	815	825	847	801	748	824	716	743	771
	389	664	542	639	698	786	824	692	744	675	777	788
	205	550	826	355	766	807	822	789	702	756	668	819
	488	444	661	834	850	861	831	678	725	728	783	823
	442	697	857	439	691	803	881	679	701	691	712	788
	362	336	359	340	823	796	852	716	727	745	758	805
	319	557	223	636	784	757	838	743	732	698	743	764
	336	774	873	777	813	855	720	686	684	727	733	733
	359	408	361	792	775	868	841	776	725	631	715	817
	183	761	800	504	808	868	822	679	703	731	724	763
	556	275	808	828	852	603	860	699	559	752	697	787
	440	690	481	784	863	836	823	672	695	654	753	790
	424	408	716	852	649	844	820	671	658	745	770	813
	532	450	457	865	829	829	773	668	696	656	732	765
	192	268	425	665	812	835	835	755	673	695	752	804
	315	486	876	402	826	804	849	712	784	838	726	766
	388	594	804	717	846	755	855	712	712	708	774	771
	415	387	418	644	736	874	863	569	697	653	787	809
	544	546	311	811	816	850	864	721	706	692	701	778
	353	664	741	873	741	687	826	675	710	742	791	788
Highest	556	792	876	873	863	874	881	789	824	838	791	823
Lowest	183	268	223	340	649	603	720	569	559	631	668	733
L _D	386	538	614	687	794	816	833	730	737	747	765	788
Std Dev	95	149	196	164	50	47	23	33	28	34	28	19
JCS	29	64	88	115	163	175	184	133	137	141	149	161

WAS	Specimen 39 Block 1 (1st surface was natural)												
Grind Depth (mm)	0.00	0.36	0.94	1.41	1.89	2.37	2.64	3.04	0.10				
Surface	Top 1	Top 2	Top 3	Top 4	Top 5	Top 6	Top 7	Top 8	Bot 1				
Hardness Readings	382	522	744	858	662	746	810	676	823	789	867	705	821
	628	746	645	777	818	808	839	836	772	856	796	821	784
	672	631	664	768	840	856	782	870	778	831	856	634	641
	605	635	649	768	844	794	569	845	851	852	787	651	600
	528	566	735	791	761	820	760	739	766	836	814	731	803
	473	629	794	723	844	810	768	822	739	819	771	823	793
	560	760	800	758	806	807	827	805	690	816	820	769	796
	554	661	660	544	816	853	798	680	788	820	830	805	862
	327	587	738	780	808	759	789	746	850	712	832	821	736
	649	697	806	764	823	734	846	777	820	817	749	818	859
	495	703	710	809	818	751	811	780	749	790	796	748	765
	478	713	596	700	810	748	847	766	625	836	774	666	814
	546	589	693	612	632	821	469	812	803	687	845	810	809
	643	732	759	791	712	783	765	824	812	860	793	842	794
	702	695	722	766	731	765	818	824	836	726	749	594	874
	659	695	616	665	787	743	806	749	626	743	815	793	744
	500	685	752	790	783	794	840	750	831	858	813	795	840
	511	683	635	784	835	787	797	776	592	822	863	819	836
600	750	711	726	835	726	797	831	649	655	754	745	733	
651	719	630	788	748	853	819	780	870	653	773	789	875	
Highest	702	760	806	858	844	856	847	870	NA				
Lowest	327	522	596	544	632	726	469	676	NA				
L _D	563	673	703	753	791	788	791	786	781				
Std Dev	81	55	57	51	50	37	61	43	69				
JCS	71	110	122	144	162	160	162	159	157				

WAS	Specimen 39 Block 2 (1st surface was natural)													
Grind Depth (mm)	0.00	0.94	1.45	1.84	2.18	2.50	2.92	3.28	3.59	0.10				
Surface	Top 1	Top 2	Top 3	Top 4	Top 5	Top 6	Top 7	Top 8	Top 9	Bot 1				
Hardness Readings	745	602	735	795	674	830	899	827	761	806	825	862	831	726
	736	592	764	570	821	814	820	817	799	638	858	643	786	769
	658	681	780	809	797	882	861	797	862	618	542	867	862	860
	565	524	772	760	667	877	708	828	671	838	829	865	861	743
	715	752	662	800	705	794	821	847	851	651	879	880	802	871
	814	564	339	700	816	571	891	724	891	846	849	820	815	796
	548	535	833	739	725	766	786	679	825	613	819	823	841	813
	492	515	729	830	658	866	798	825	556	837	800	848	872	887
	491	702	834	513	808	759	851	805	804	720	810	803	813	846
	785	771	658	771	733	759	882	813	845	833	778	851	784	852
	637	706	729	833	831	776	825	717	856	866	805	820	862	861
	527	729	614	589	783	717	819	774	802	831	763	857	711	818
	567	658	781	797	710	894	794	857	857	766	864	855	880	891
	274	779	601	673	806	859	807	822	863	861	860	810	669	815
	287	782	781	821	794	827	875	885	694	871	863	771	655	843
	611	707	570	748	675	470	816	824	787	809	822	801	857	812
	406	742	740	647	674	804	809	813	897	830	851	905	854	827
	546	658	864	692	517	782	816	781	827	839	806	811	783	813
	579	365	820	855	779	719	816	833	868	801	714	845	755	694
	587	660	831	773	733	687	880	833	787	782	823	829	842	864
Highest	814	782	864	855	831	894	899	885	897	NA				
Lowest	274	365	339	513	517	470	708	679	556	NA				
L _D	582	660	735	742	742	783	832	808	814	809				
Std Dev	123	86	82	80	59	77	33	38	59	68				
JCS	77	104	136	139	139	158	183	170	174	171				

WAS	Specimen 39 Block 3 (1st surface was natural)															
Grind Depth (mm)	0.00	0.60	0.95	1.43	2.02	2.42	3.16	3.65	4.05	0.10					0.10	
Surface	Top 1	Top 2	Top 3	Top 4	Top 5	Top 6	Top 7	Top 8	Top 9	Bot 1					Bot 1(1)	
Hardness Readings	668	759	582	816	786	781	892	701	749	875	836	827	845	809	801	
	714	688	519	589	741	812	639	842	875	809	749	876	673	812	797	
	442	293	647	816	728	804	826	764	792	836	821	829	821	789	715	
	537	531	688	676	826	687	852	789	702	848	719	864	819	834	772	
	694	736	624	571	857	514	868	805	715	774	708	786	828	735	855	
	477	813	451	644	866	833	754	809	785	785	808	630	827	741	766	
	368	696	753	788	645	778	792	845	828	854	Exemption No. SP39B3 -Bot 1	836	785	898	813	625
	450	433	542	739	706	742	825	697	806	797	854	851	783	870	775	
	433	522	753	823	789	842	549	739	798	811	844	624	863	844	862	
	529	408	699	707	775	844	813	839	840	844	840	712	833	863	806	
	538	622	529	756	832	841	793	695	821	901	831	803	796	856	814	
	529	784	663	446	733	776	700	835	830	737	833	777	706	799	814	
	641	843	785	794	818	810	853	732	796	727	828	833	880	801	845	
	492	721	542	746	781	586	704	824	778	833	850	870	586	752	808	
	692	585	432	800	824	756	790	814	784	852	790	852	847	805	878	
	512	743	733	711	776	819	786	773	871	804	821	896	665	769	694	
	446	444	797	644	879	761	689	687	795	865	796	807	765	781	783	
	451	547	513	740	811	841	840	789	823	851	813	812	874	846	834	
	715	752	681	819	801	842	742	733	696	783	853	825	857	823	851	
	627	713	779	435	796	808	792	787	743	831	808	746	808	874	745	
Highest	715	843	797	823	870	844	892	847	875	NA					878	
Lowest	368	293	432	435	645	514	549	687	696	NA					625	
L _D	548	639	638	711	791	784	781	776	792	809					797	
Std Dev	98	130	104	101	44	65	64	50	43	59					47	
JCS	67	97	96	125	162	159	157	155	162	171					165	

WAS	Specimen 53 Block 1 (1st surface was natural)									
Grind Depth (mm)	0.00	0.69	1.11	1.36	1.64	0.10				
Surface	Top 1	Top 2	Top 3	Top 4	Top 5	Bot 1				
Hardness Readings	751	703	679	744	668	709	695	675	702	745
	612	643	671	718	647	726	715	612	670	746
	691	610	733	748	726	744	654	643	717	733
	706	671	725	665	730	675	648	703	647	692
	710	701	693	673	675	741	725	696	601	725
	731	615	761	721	680	728	628	744	675	702
	245	662	712	708	710	645	704	805	635	669
	706	681	686	664	661	760	750	673	673	729
	746	653	703	735	695	716	404	698	751	722
	592	644	628	754	695	701	616	701	706	722
	680	653	801	711	699	751	723	722	694	707
	649	717	678	643	699	706	693	688	618	686
	517	660	695	710	659	672	623	730	717	753
	781	663	735	673	730	667	698	708	667	678
	627	683	742	654	649	732	716	729	707	735
	664	702	790	741	689	674	741	680	726	725
	674	578	730	700	687	727	682	713	829	706
	769	694	633	700	739	727	663	725	714	720
613	612	727	771	667	736	668	738	700	714	
731	718	684	635	657	689	699	685	680	696	
Highest	781	718	801	771	739	NA				
Lowest	245	578	628	635	647	NA				
L _D	676	665	710	703	688	699				
Std Dev	65	32	37	35	25	49				
JCS	111	106	125	122	115	120				

WAS	Specimen 53 Block 2 (1st surface was natural)					
Grind Depth (mm)	0.00	0.18	0.81	1.03	1.32	0.10
Surface	Top 1	Top 2	Top 3	Top 4	Top 5	Bot 1
Hardness Readings	495	652	694	743	709	712
	636	658	608	723	734	712
	664	752	709	700	746	725
	669	765	734	708	702	666
	658	698	739	702	684	692
	662	828	680	713	691	699
	700	631	732	777	697	697
	553	690	716	746	684	723
	689	682	625	744	683	726
	707	691	704	717	723	664
	747	700	720	658	728	659
	681	749	700	710	690	753
	747	741	766	714	714	707
	749	728	712	706	707	736
	693	742	767	694	747	701
	419	659	736	758	696	731
	702	682	757	684	701	710
	628	663	658	743	670	752
629	665	666	715	715	724	
691	713	727	724	708	706	
Highest	749	828	767	777	747	753
Lowest	419	631	608	658	670	659
L _D	664	702	710	719	706	710
Std Dev	62	37	36	20	18	22
JCS	106	121	125	129	123	125

WAS	Specimen 53 Block 3 (1st surface was natural)							
Grind Depth (mm)	0.00	0.28	0.64	0.86	1.23	0.10		
Surface	Top 1	Top 2	Top 3	Top 4	Top 5	Bot 1		
Hardness Readings	666	779	736	727	724	736	716	728
	649	753	680	745	737	764	756	751
	628	736	772	757	721	753	729	713
	658	695	634	730	624	713	652	660
	587	734	741	700	687	724	720	633
	698	670	677	772	575	690	731	650
	658	732	709	775	748	738	626	693
	639	590	694	721	734	763	716	707
	600	760	729	655	646	738	685	736
	541	422	726	763	705	727	747	658
	714	658	754	677	694	649	699	
	737	648	688	701	699	730	705	
	633	714	645	737	756	687	706	
	523	740	583	628	677	710	743	
	264	710	760	633	726	708	755	
	640	761	748	652	732	715	695	
	666	740	755	711	710	752	732	
	680	770	738	785	673	745	751	
643	688	684	724	688	758	722		
685	653	665	716	725	679	677		
Highest	737	779	772	785	756	NA		
Lowest	264	422	583	628	575	NA		
L _D	639	708	709	716	703	713		
Std Dev	50	49	39	41	33	35		
JCS	97	124	124	127	122	126		

WAS	Specimen 60 Block 1 Surface 1 (1st surface was natural)									
Grind Depth (mm)	0.00	0.42	0.89	1.66	2.04	2.50	3.19	3.73	4.36	5.11
Surface	Top 1	Top 2	Top 3	Top 4	Top 5	Top 6	Top 7	Top 8	Top 9	Top 10
Hardness Readings	239	591	326	576	752	754	824	794	766	824
	375	213	271	629	809	800	773	756	780	746
	483	486	446	726	699	807	801	734	788	743
	295	258	407	383	712	848	776	784	722	822
	310	289	358	532	547	777	760	826	771	714
	184	364	369	692	566	769	809	806	846	822
	275	293	202	230	663	760	733	827	800	811
	508	209	390	360	699	804	816	753	800	750
	410	189	493	578	519	719	780	826	767	773
	241	595	406	798	217	796	842	841	847	816
	309	705	213	280	807	760	785	826	716	848
	464	323	588	640	448	832	843	767	759	765
	308	185	665	184	467	645	832	829	818	790
	256	482	702	714	699	506	812	809	805	799
	337	230	669	422	597	808	791	833	817	748
	334	404	271	762	528	753	787	791	831	756
	221	303	387	686	541	790	803	778	781	838
	237	302	337	695	556	747	749	826	827	804
	228	280	667	214	635	782	786	779	757	775
	180	261	349	602	710	791	773	836	811	735
Highest	508	705	702	798	809	848	843	841	847	848
Lowest	180	185	202	184	217	506	733	734	716	714
L _D	306	337	423	540	619	772	794	803	791	784
Std Dev	84	125	140	180	103	42	25	28	31	34
JCS	16	21	36	64	90	153	164	168	162	159

WAS	Specimen 60 Block 1 Surface 2 (1st surface was natural)							
Grind Depth (mm)	0.00	0.17	0.55	0.92	1.38	1.88	2.51	3.26
Surface	Top 1	Top 2	Top 3	Top 4	Top 5	Top 6	Top 7	Top 8
Hardness Readings	484	347	696	732	744	742	763	740
	663	475	675	717	726	732	751	750
	429	542	711	726	693	729	709	721
	442	637	749	730	746	714	702	727
	737	618	747	708	719	755	740	739
	598	516	586	711	734	759	761	742
	587	402	728	719	727	719	713	762
	527	720	702	730	723	703	743	751
	356	648	682	706	737	765	737	769
	488	782	738	708	731	717	722	741
	361	316	679	732	707	725	753	722
	499	465	710	731	717	733	737	724
	486	502	690	668	740	766	727	776
	749	743	678	687	742	724	740	748
	378	579	695	739	720	721	722	758
	626	616	736	730	757	737	737	713
	389	416	712	706	656	762	763	704
	336	785	532	737	730	737	740	742
539	710	712	728	752	745	768	738	
653	437	710	707	676	730	761	759	
Highest	749	785	749	739	757	766	768	776
Lowest	336	316	532	668	656	703	702	704
L _D	513	564	699	719	726	736	740	741
Std Dev	112	128	35	14	19	16	17	16
JCS	57	71	120	129	132	136	138	139

WAS		Specimen 61 Block 1 (1st surface was natural)																							
Grind Depth (mm)	0.00	0.59	1.19	1.81	2.34	2.66	2.93	3.71	4.31	4.89	5.50	6.17	6.67	7.45	7.95	8.63	9.18	9.68	0.10	0.75					
Surface	Top 1	Top 2	Top 3	Top 4	Top 5	Top 6	Top 7	Top 8	Top 9	Top 10	Top 11	Top 12	Top 13	Top 14	Top 15	Top 16	Top 17	Top 18	Bot 1	Bot 2					
Hardness Readings	437	409	391	616	605	694	627	702	748	824	716	743	771	786	795	820	805	746	843	807	806	754	777	811	
	515	421	494	601	638	606	579	715	692	744	675	777	788	732	816	809	782	791	802	807	782	796	806	805	782
	441	448	544	564	589	627	689	648	789	702	756	668	819	821	803	824	780	845	765	815	862	764	785	816	
	410	408	534	544	657	659	599	634	678	725	728	783	823	795	812	766	803	761	801	827	830	770	796	845	
	416	482	571	602	607	526	662	745	679	701	691	712	788	822	811	802	810	801	834	804	817	795	799	816	
	498	380	340	489	634	555	677	716	716	727	745	758	805	789	838	832	819	794	860	776	805	831	829	816	
	332	591	431	589	527	586	535	653	743	732	698	743	764	788	800	837	790	760	832	797	831	819	829	792	
	373	487	474	653	526	615	624	632	686	684	727	733	733	824	777	794	845	793	808	813	823	826	842	824	
	430	379	557	659	630	651	771	660	776	725	631	715	817	831	843	806	808	788	838	824	809	794	803	747	
	486	429	574	582	639	609	539	659	679	703	731	724	763	781	798	850	809	832	848	785	826	807	780	792	
	438	475	552	561	556	703	584	636	699	558	752	697	787	780	799	851	754	802	812	794	796	802	834	823	
	452	466	500	648	688	650	552	583	672	695	654	753	790	736	786	833	855	825	833	775	824	787	777	804	
	410	436	527	545	584	611	623	672	671	658	745	770	813	798	813	825	826	804	822	799	795	826	790	820	
	555	446	532	559	599	661	608	667	668	696	656	732	765	797	830	841	781	774	853	797	802	810	841	799	
	479	550	677	535	679	681	633	592	755	673	695	752	804	809	820	806	781	815	859	827	829	781	784	838	
	474	469	466	452	554	581	619	639	712	784	838	726	766	803	795	831	826	806	840	814	788	796	806	842	
	476	385	434	634	674	712	664	673	712	708	774	771	844	836	786	793	836	813	813	764	815	774	794	786	
	599	413	519	612	615	701	639	603	569	697	653	787	809	817	806	763	815	784	878	806	805	809	787	804	
	392	448	330	506	647	597	650	678	721	706	692	701	778	799	794	741	752	822	809	793	804	885	794	790	
	439	470	545	581	497	639	582	543	675	710	742	791	788	769	832	833	806	858	821	810	822	801	833	801	
Highest	599	591	577	659	688	712	771	745	789	824	838	791	823	844	843	851	855	858	878	NA					
Lowest	333	370	330	452	497	526	535	543	569	559	631	668	733	732	777	741	752	746	765	NA					
L _p	451	446	499	579	609	635	619	653	705	710	709	743	788	797	810	814	802	802	829	806					
Std Dev	46	41	65	46	46	43	42	38	33	28	34	28	19	23	16	25	22	24	19	22					
JCS	42	40	53	76	86	95	90	102	122	125	124	139	161	165	172	174	167	167	182	169					

WAS	Specimen 61 Block 2 (1st surface was natural)																		0.10					1.22				
Grind Depth (mm)	0.00	0.81	1.36	1.95	2.43	3.01	3.62	4.23	4.77	5.21	5.69	5.98	6.39	6.89	7.63	8.07	8.47	9.03	0.10					1.22				
Surface	Top 1	Top 2	Top 3	Top 4	Top 5	Top 6	Top 7	Top 8	Top 9	Top 10	Top 11	Top 12	Top 13	Top 14	Top 15	Top 16	Top 17	Top 18	Bot 1					Bot 2				
	521	594	444	646	545	685	667	669	649	716	741	748	813	743	798	810	810	808	843	891	870	815	835	775	879	786	817	829
	466	490	594	641	429	651	661	710	756	745	736	722	787	796	812	807	842	827	831	840	854	851	849	808	839	829	825	823
	547	583	575	639	633	660	701	631	726	741	755	726	748	770	777	779	822	803	798	868	856	784	844	770	848	842	896	802
	522	545	396	505	590	576	679	448	524	747	670	747	779	817	784	799	813	820	799	828	884	849	835	767	842	850	809	813
	553	505	600	630	663	651	667	674	696	752	751	759	772	821	763	809	829	822	822	875	864	861	807	790	869	798	835	835
	571	514	635	551	668	611	704	637	554	486	726	802	776	805	814	787	815	828	881	840	867	849	825	788	837	779	821	825
	505	572	615	648	220	482	633	644	688	740	726	745	736	810	819	737	801	816	832	826	865	824	824	799	804	843	797	808
	540	519	615	618	468	601	719	369	731	369	785	756	793	799	829	815	803	820	800	840	858	853	849	818	841	825	841	786
	570	624	608	697	591	615	661	641	707	766	715	740	753	780	790	790	848	802	830	835	802	808	832	811	792	823	775	828
	461	455	591	646	670	644	690	676	710	716	746	484	835	824	790	784	809	807	827	852	848	856	877	854	831	832	802	783
	429	558	581	595	617	226	659	609	746	644	750	773	822	825	824	819	825	799	845	842	813	819	873	812	771	833	798	844
	463	536	673	585	574	678	636	647	700	733	393	776	733	759	781	807	389	799	819	842	839	787	810	841	780	816	830	826
	516	542	624	627	628	687	333	718	690	738	763	720	795	814	783	841	814	811	834	853	828	848	855	817	780	768	847	825
	581	501	563	575	559	642	681	673	670	708	666	822	302	778	764	813	825	809	820	831	836	849	827	830	772	755	754	797
	444	588	663	206	607	583	712	700	692	740	794	797	778	755	252	820	789	820	822	844	821	862	825	841	816	817	817	816
	582	454	558	581	575	690	693	753	365	717	722	771	725	840	830	788	824	803	820	837	860	856	829	823	807	818	818	837
	488	544	690	579	644	668	667	662	704	725	771	742	774	808	807	811	826	801	821	868	805	851	847	792	786	828	793	818
	201	600	506	607	598	732	611	745	689	678	787	800	767	749	816	834	837	790	828	863	811	851	846	763	810	810	854	869
	501	538	559	557	576	581	679	689	731	766	737	742	737	787	803	686	845	807	827	827	843	857	862	804	814	836	843	828
	621	581	610	642	620	530	596	651	631	718	730	771	823	818	818	823	843	382	857	794	860	822	828	824	833	809	759	800
Highest	639	621	736	705	720	736	733	763	765	769	797	821	871	840	835	870	848	839				NA					NA	
Lowest	201	454	434	505	429	453	596	448	524	596	666	691	703	743	753	686	789	781				NA					NA	
I ₂	525	543	603	615	601	638	673	674	693	727	745	758	774	795	799	803	821	809				839					815	
Std Dev	50	40	45	38	50	51	28	39	47	30	30	26	31	25	21	24	15	10				22					28	
JCS	60	65	84	88	83	96	110	110	118	132	140	146	153	164	166	168	177	171				187					174	

WAS	Specimen 62 Block 1 (1st surface was natural)								
Grind Depth (mm)	0.00	1.22	1.60	1.83	2.14	2.36	0.10		
Surface	Top 1	Top 2	Top 3	Top 4	Top 5	Top 6	Bot 1		
Hardness Readings	640	774	761	737	777	711	607	687	663
	726	643	708	796	762	771	656	740	627
	487	643	731	766	752	745	683	707	708
	501	609	733	825	736	758	728	695	751
	539	730	722	759	825	810	608	690	740
	258	722	806	717	798	729	703	693	751
	437	635	714	803	775	795	708	658	749
	584	707	711	753	765	765	753	814	762
	527	767	806	725	712	691	760	748	607
	468	738	696	794	695	698	669	710	750
	596	802	681	806	779	642	732	782	
	307	771	724	615	679	753	731	768	
	231	724	712	738	742	734	761	572	
	679	672	798	777	816	642	758	732	
	487	612	770	558	760	722	698	683	
	503	772	740	767	646	776	715	740	
	483	685	798	720	710	687	750	628	
	304	725	703	808	751	745	772	677	
	665	702	814	759	730	669	706	781	
	474	755	694	758	698	699	726	820	
Highest	726	802	814	825	825	810	NA		
Lowest	231	609	681	558	646	642	NA		
L _D	497	710	740	755	747	727	713		
Std Dev	118	51	39	46	37	41	54		
JCS	53	125	138	145	141	132	126		

WAS Specimen 69 Block 1 (1st surface was natural)																			
Grind Depth (mm)	0.00	0.06	0.11	0.15	0.28	0.49	0.72	1.00	1.17	1.45	1.86	2.81	3.78	5.95	7.95	9.89	0.00	0.00	3.43
Surface	Top 1	Top 2	Top 3	Top 4	Top 5	Top 6	Top 7	Top 8	Top 9	Top 10	Top 11	Top 12	Top 13	Top 14	Top 15	Top 16	Bot 1 (1)	Bot 1 (2)	Bot 2
Hardness Readings	434	482	482	492	513	473	466	499	515	514	502	525	508	515	522	517	530	525	512
	463	458	462	475	520	453	488	514	511	522	531	519	493	499	535	498	527	532	513
	433	427	513	497	496	494	524	511	473	515	509	515	554	493	511	534	536	552	505
	442	422	493	513	524	523	530	501	521	504	525	515	533	514	513	519	547	519	495
	392	472	487	500	497	500	506	519	518	502	524	512	507	515	512	509	538	546	518
	466	491	439	512	465	500	468	509	497	514	513	505	478	516	531	513	556	546	526
	434	441	458	462	524	506	535	523	507	516	516	502	509	511	526	510	549	534	511
	413	462	474	502	489	459	514	504	507	542	515	505	533	512	520	523	557	524	539
	462	418	479	482	473	489	535	479	534	516	506	492	507	513	517	501	518	518	512
	394	340	477	485	500	483	512	496	542	537	470	491	524	515	512	532	534	533	424
	453	458	497	468	487	428	450	481	509	538	479	528	514	517	504	529	542	527	498
	446	434	445	503	483	499	493	512	487	488	524	517	492	513	521	523	513	535	507
	428	477	472	482	487	497	511	511	492	538	509	507	544	476	527	518	521	537	521
	454	474	463	472	461	456	501	525	519	523	496	506	491	515	517	502	548	525	508
	449	467	503	470	473	500	472	519	502	511	519	521	535	553	521	528	552	532	503
	458	421	485	496	472	479	491	517	482	501	497	480	526	489	541	507	542	518	508
	451	482	455	488	500	514	494	494	527	514	511	503	504	487	522	486	525	527	489
	415	440	492	434	475	505	460	522	473	533	525	508	497	517	514	465	538	529	522
	439	457	490	514	467	494	503	550	481	496	527	504	505	497	511	516	545	552	505
	444	492	443	481	442	497	537	479	466	489	523	491	521	532	516	518	522	495	519
Highest	466	493	513	514	524	523	537	550	542	542	531	539	554	553	541	534	557	552	539
Lowest	363	240	439	434	442	429	450	479	466	488	470	490	479	476	504	465	513	495	474
L _D	436	455	475	488	488	489	500	508	503	516	512	508	514	509	519	514	537	531	510
Std Dev	20	24	18	15	19	18	23	14	18	14	13	10	16	12	7	12	11	10	10
JCS	38	43	47	50	50	51	53	55	54	58	57	55	57	56	59	57	64	62	56

WAS	Specimen 69 Block 2 (1st surface was natural)																
Grind Depth (mm)	0.00	0.18	0.27	0.48	0.67	0.84	1.05	1.35	1.70	2.05	2.84	3.20	3.47	0.00	1.49	3.61	4.26
Surface	Top 1	Top 2	Top 3	Top 4	Top 5	Top 6	Top 7	Top 8	Top 9	Top 10	Top 11	Top 12	Top 13	Bot 1	Bot 2	Bot 3	Bot 4
Hardness Readings	450	510	545	545	511	528	514	539	502	526	533	534	560	546	528	564	528
	458	520	540	539	523	510	505	541	539	518	537	535	541	556	544	557	526
	443	520	536	530	524	505	528	504	526	554	526	554	539	559	563	516	542
	459	518	497	546	534	540	516	527	510	513	554	539	544	542	541	559	540
	402	512	531	522	523	520	507	516	550	519	545	536	531	549	540	559	530
	418	513	524	515	525	518	495	530	537	556	554	551	521	559	542	537	536
	371	514	513	482	512	484	515	514	490	513	524	553	552	556	534	545	544
	394	521	512	520	503	532	520	466	501	521	536	552	544	534	540	553	544
	453	516	514	523	525	485	502	534	521	519	531	529	553	564	554	556	531
	485	522	529	520	525	527	512	514	505	507	537	542	549	553	546	549	541
	399	510	500	522	524	514	491	527	511	504	525	528	530	553	544	544	542
	444	508	530	487	524	518	529	547	499	540	526	555	513	556	560	544	559
	488	516	530	537	539	519	502	515	506	516	554	542	521	553	553	557	502
	451	513	547	523	524	511	535	521	540	485	529	502	529	581	496	529	527
	431	517	543	507	540	497	514	528	517	508	550	547	514	544	548	566	558
	461	508	537	529	518	510	486	473	504	529	553	516	535	531	507	565	523
	474	495	516	512	497	526	497	494	489	539	528	488	520	541	521	566	540
	437	503	531	517	529	526	538	542	543	532	547	544	550	549	555	527	520
	403	508	514	502	507	524	514	510	524	545	539	551	531	569	551	542	535
	476	516	514	535	532	515	505	527	533	521	538	532	530	562	568	552	518
Highest	488	522	547	546	540	540	538	547	550	556	554	555	560	581	568	566	559
Lowest	371	495	497	482	497	484	486	466	489	485	524	488	513	531	496	516	502
L _D	441	514	526	521	522	516	511	520	517	524	538	538	535	553	543	550	535
Std Dev	28	5	13	14	9	12	12	17	16	14	10	14	12	9	14	12	10
JCS	39	57	60	59	59	58	56	59	58	60	64	64	63	68	65	67	63

The table below lists the exemptions that were made at the discretion of the author and the reason why this choice was made. The data collected from the surfaces listed in this table are exempt from the illustrative plots in Appendix C and were not included in the discussion in the thesis document. It should be noted that these exemptions do not mean that the data is considered by the author as being invalid. They are considered by the author as being nonrepresentative of that particular material being evaluated and was made based on a review of collected data found in that same material. An inherent variability exists in testing natural rock and any user of the Leeb device or evaluator of the data needs to choose at their discretion how best to refine-out nonrepresentative data inherent in the collected data. To this end, the author made the following exemptions listed in this table. It is recognized by the author that not all evaluators of the data collected in this study may feel that these exemptions should have been made in the illustrative plots. For those individuals, it is strongly recommended by the author to evaluate the data found on each specimen without these exemptions and draw your own conclusions.

Exemption No.	Explanation
SP8B3 - Top12	The hardness data collected on this surface was very scattered (highest standard deviation) and was of the opinion of the author to not be representative of the secondary material. This determination was made based on the collective findings in the secondary material on all three Sample 8 specimens tested. The author deliberately tested the next surface at a minimal depth from this surface to determine if a trending decrease in hardness data could be seen or if an isolated event occurred on that surface and could therefore be exempt.

SP31B1-Top8	Data is exempt from the plot to reduce clutter in the plot as this data was collected at a thickness 0.07 mm thicker than the next surface. It can be seen that the data collected is of a near match to the data collected on the adjacent surfaces.
SP31B1-Top 17(1-4)	The testing on the final top surface (top 17) produced results that were much lower than the previous surface. This was clearly a characteristic issue of the primary material. In an attempt to reach a similar value to the previous surface, the same surface was tested in rounds of 20 impacts at randomly located points. On the fifth surface, a comparable value was reached. The exact reason for the variation collected on this surface is unknown to the author. It is believed by the author that this surface hosted a larger quantity of mineral grains of reduced strength than the previous surfaces. This data potentially reflects the innate heterogeneity of the natural primary material, specifically that of the individual structural grains.
SP36B1-Bot 1(1-4)	It was determined that the bottom of this specimen exhibited a lower hardness. Five attempts on the same surface was tried at 20 impacts per round to see if a comparable hardness value could be found as on the top of the block. It is clear from the hardness data on the top of the block that the bottom of the block comprises a layer of material of different properties. The data is believed to reflect the innate heterogeneity present in the primary rock. For illustrative purposes, the bottom surface with the highest hardness value (Bot(5)) was plotted.

SP39B3-Bot 1	All 100 impacts on the first bottom surface produced results that were much higher than the hardness that was seen on the top surfaces. This was an indication that perhaps the top surface was not ground down enough to be completely into the fresh primary rock. This being the third block from this sample, it seemed that this was an unlikely case. The bottom was ground down a small increment for the second time and 100 impacts were taken which produced similar results to the top, fresh primary rock surfaces. The higher result found on Bot 1 was an indication of heterogeneity present in the primary rock: a stronger grain structure was seen to exist at the location of this bottom surface.
SP61B1-Bot 1	The TM20 value found on the first bottom surface was larger with a comparable standard deviation to the adjacent surfaces. Further impacts on that surface were predicted to produce similar values. Thus, a second bottom surface was prepared by grinding. A hardness value consisting of 100 impacts met the same hardness as the top, fresh rock readings. This is believed to be an indication of innate grain structure heterogeneity in the primary rock.
SP61B2-Bot 1	Similar to the other block from this sample, the first bottom surface produced high results and is understandable as the blocks were extracted to the same thickness and were side-by-side, separated by a single cut at the time of extraction. One hundred impacts were conducted on this bottom surface but the overall result was that this surface comprised a grain structure that was stronger than seen on the top, fresh rock surfaces. A second surface was prepared by grinding and 100 impacts on this surface revealed a similar hardness to the top, fresh rock surfaces. This is believed to be an indication of innate grain structure heterogeneity in the primary rock.

SP69B1-Bot 1(1-2)	<p>With a comparable standard deviation found on the bottom surface (tested twice with 20 impacts) and a much higher hardness in comparison to the top surfaces, it was obvious that a discrepancy existed between the top and bottom of the block. Without grain structure heterogeneity being the cause for the increased value, this would seem that the top surfaces were not yet in the fresh rock. As the hardness variation was so large and with Hack et al., 1993 hardness versus depth result showing nearly a 20 mm thick weathered profile (Section 2.3.2, Figure 2-9) for sandstone, the block was flipped back over and grinding and hardness testing occurred for several more surfaces. It should be iterated that the bottom surface hardness was confirmed prior to ending testing on the specimen. It was understood that the result could be different, but if it was greatly different, the idea was that the fresh rock was not yet achieved from the top of the block. After achieving almost uniform results on the top of the block for various surfaces, it was obvious that the first and second bottom surfaces located in a stronger deposited layer in the sedimentary rock. The block was flipped back over and a third bottom surface was created after a deep grind was performed. Twenty impacts on this surface produced comparable results as was seen on the upper surfaces.</p>
-------------------	---

APPENDIX E – JRC SURVEY

Hello,

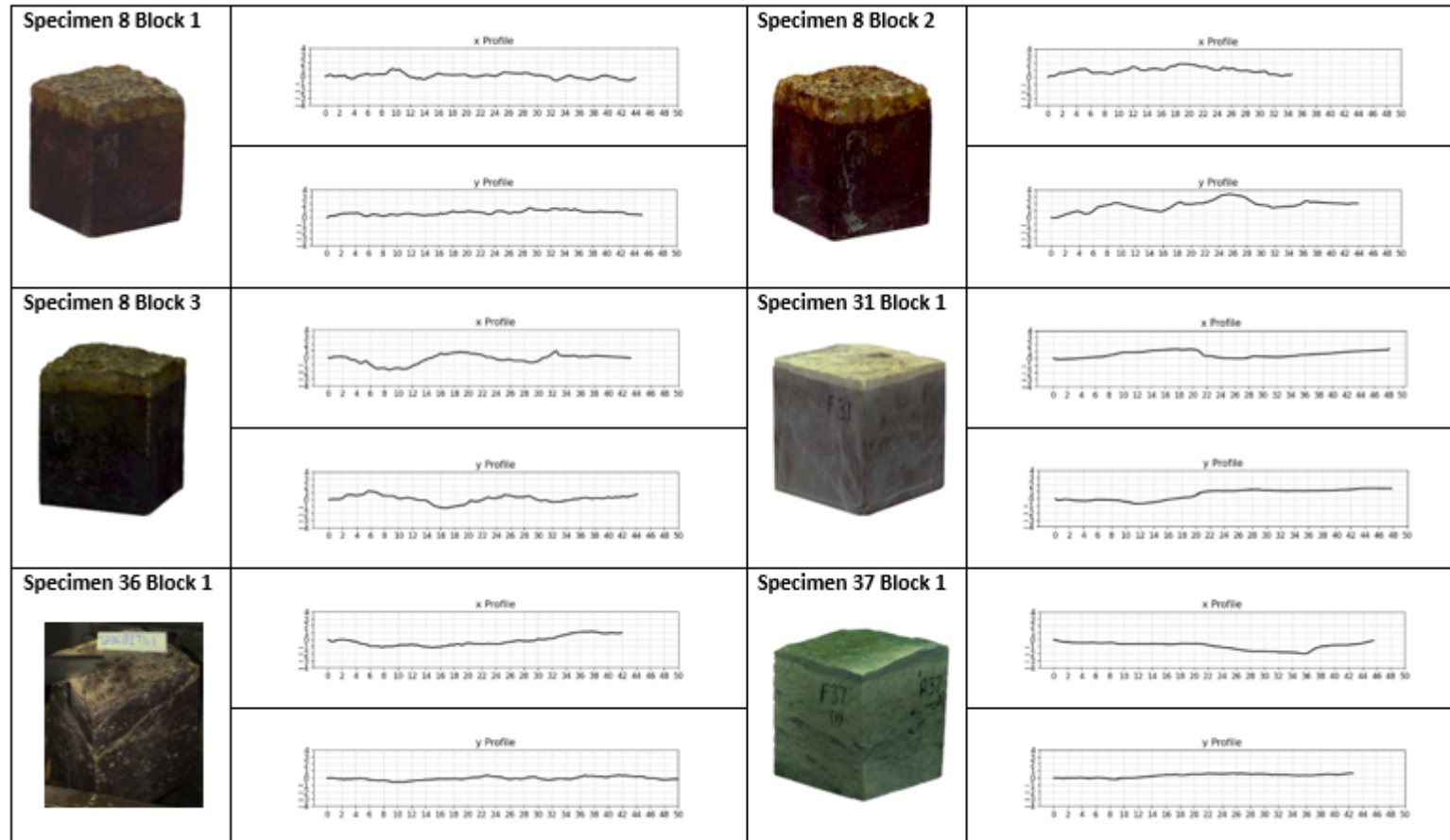
My name is Brock Jeans, I am a Master of Applied Science Student in Civil Engineering at Dalhousie University in the specialty of rock mechanics. As a component of my research, I performed 3D scanning of the natural rock surfaces of my specimens with the intention of predicting a Joint Roughness Coefficient (JRC) for each. We feel that we have the ability to predict JRC using Python using the point cloud data from the scans, however, we want to see how well this compares to selections made by industry professionals using the conventional Barton and Choubey (1977) charts.

In the attached document, two orthogonal profiles of 23 rock specimens are provided for this evaluation. These profiles have been approximately scaled to the same scale seen in the Barton and Choubey chart included on page 6. We are hoping that you would be willing to assist in providing an evaluation for us. If you are, please enter your information and predicted JRC values for each profile in the table provided on page 5 and return this to brock.jeans@dal.ca. I would like to note that your personal information entered on page 5 will be kept confidential. We appreciate your time and your contribution to our research project, and we look forward to your predictions!

Sincerely,

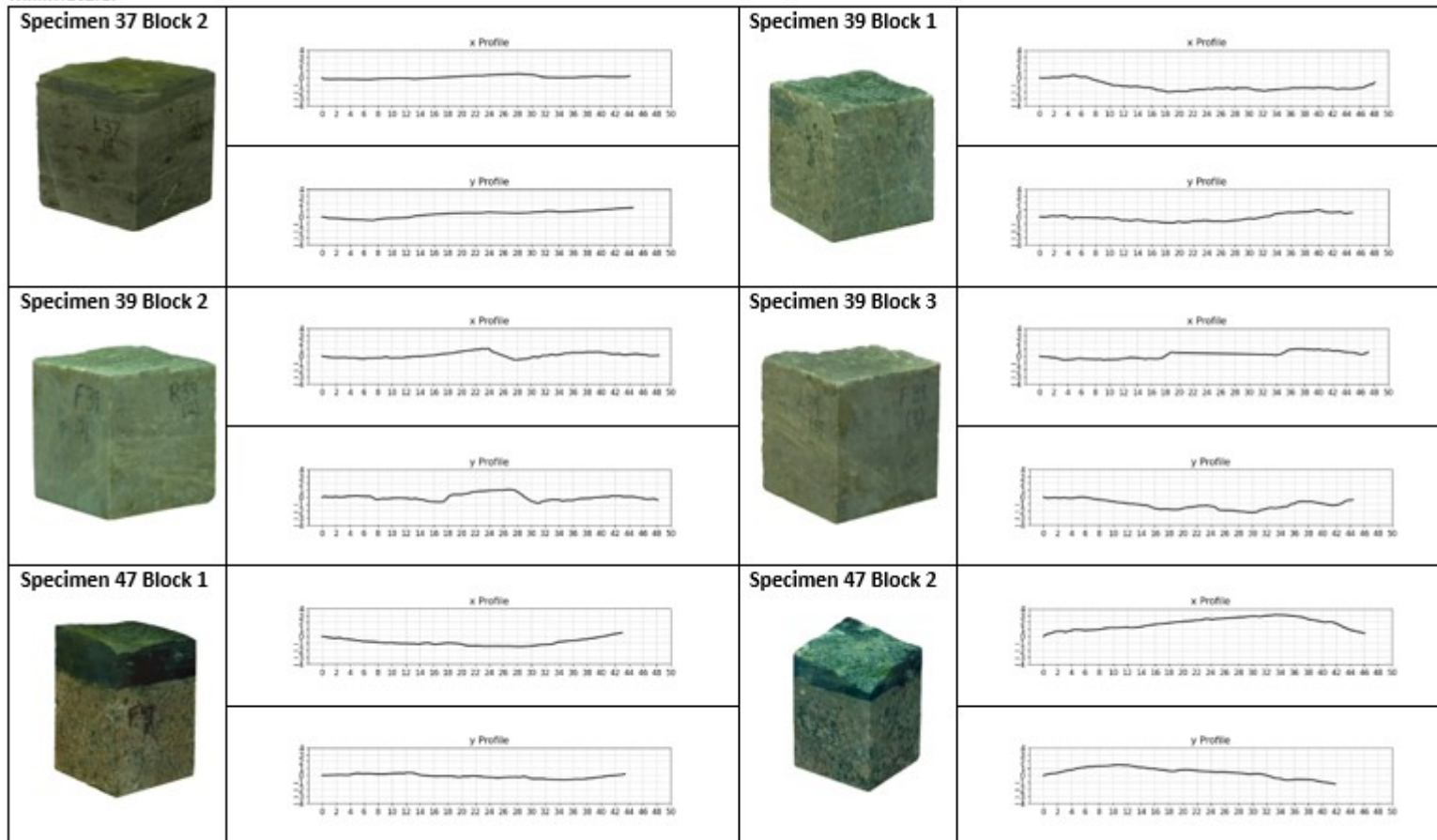
Brock Jeans
MAsc Student

The x and y profiles are at orthogonal orientations on the specimen surfaces. All profiles are shown with 1:1 (horizontal: vertical) ratio with all dimensions in millimeters.



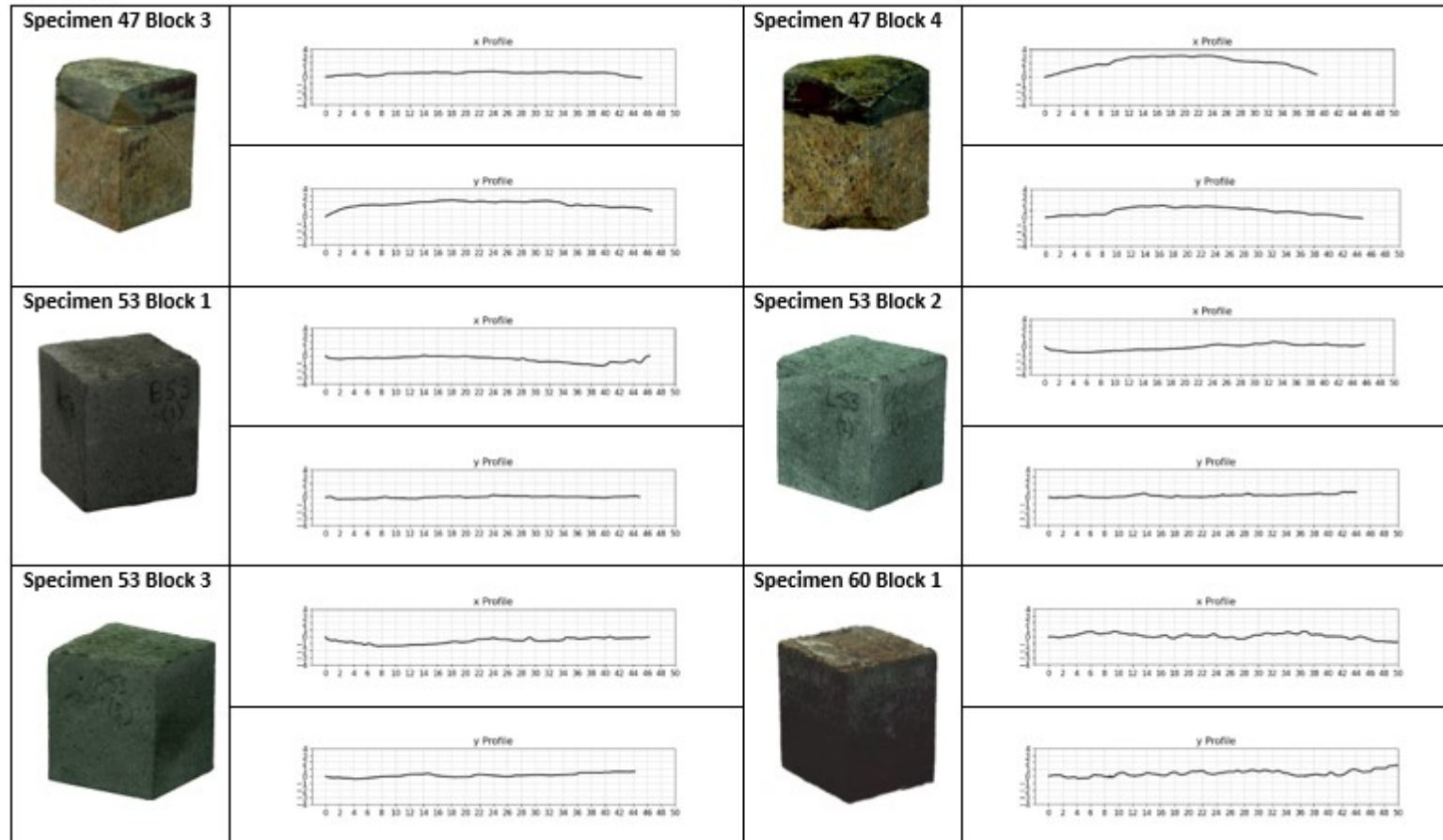
Note: The printed version is not to scale, but slightly exaggerated for visibility. Scale matches the JRC quantification chart scale on final page.

The x and y profiles are at orthogonal orientations on the specimen surfaces. All profiles are shown with 1:1 (horizontal: vertical) ratio with all dimensions in millimeters.



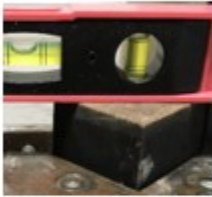
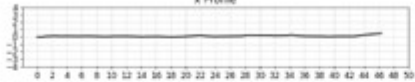

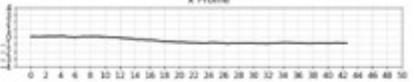
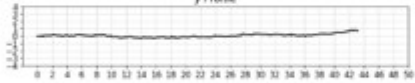


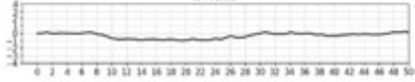

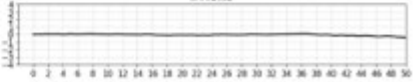
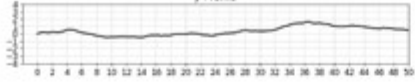
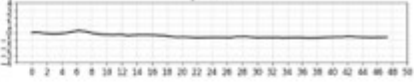

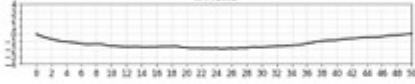
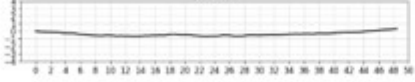
Note: The printed version is not to scale, but slightly exaggerated for visibility. Scale matches the JRC quantification chart scale on final page.

The x and y profiles are at orthogonal orientations on the specimen surfaces. All profiles are shown with 1:1 (horizontal: vertical) ratio with all dimensions in millimeters.



Note: The printed version is not to scale, but slightly exaggerated for visibility. Scale matches the JRC quantification chart scale on final page.

The x and y profiles are at orthogonal orientations on the specimen surfaces. All profiles are shown with 1:1 (horizontal: vertical) ratio with all dimensions in millimeters.

<p>Specimen 61 Block 1</p> 	<p>x Profile</p> 	<p>Specimen 61 Block 2</p> 	<p>x Profile</p> 
	<p>y Profile</p> 		<p>y Profile</p> 
<p>Specimen 62 Block 1</p> 	<p>x Profile</p> 	<p>Specimen 69 Block 1</p> 	<p>x Profile</p> 
	<p>y Profile</p> 		<p>y Profile</p> 
<p>Specimen 69 Block 2</p> 	<p>x Profile</p> 		
	<p>y Profile</p> 		

Note: The printed version is not to scale, but slightly exaggerated for visibility. Scale matches the JRC quantification chart scale on final page.

JRC Estimation Survey Form

-Your personal information will remain confidential-

Evaluator Name:

Firm/ Institution:











Position:

Experience Level as numerical value (1: no technical background, 2: no experience of JRC estimation, 3: some experience of JRC estimation or 4: very experienced at JRC estimation):

	JRC (x-profile)	JRC (y-profile)	Comments
S8B1			
S8B2			
S8B3			
S31B1			
S36B1			
S37B1			
S37B2			
S39B1			
S39B2			
S39B3			
S47B1			
S47B2			
S47B3			
S47B4			
S53B1			
S53B2			
S53B3			
S60B1			
S61B1			
S61B2			
S62B1			
S69B1			
S69B2			

Please return completed survey to Brock Jeans at brock.jeans@dal.ca

Thank you for your time and for contributing to our research project!

	<i>JRC</i> = 0 - 2
	<i>JRC</i> = 2 - 4
	<i>JRC</i> = 4 - 6
	<i>JRC</i> = 6 - 8
	<i>JRC</i> = 8 - 10
	<i>JRC</i> = 10 - 12
	<i>JRC</i> = 12 - 14
	<i>JRC</i> = 14 - 16
	<i>JRC</i> = 16 - 18
	<i>JRC</i> = 18 - 20
